INTERFACES AND INFORMATION IN GAUGE/GRAVITY DUALITY

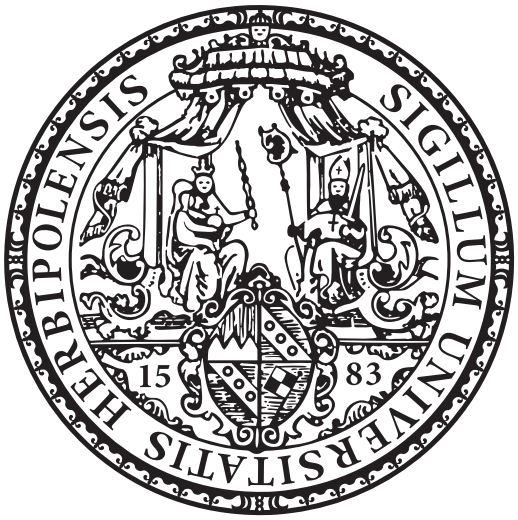

Dissertation zur Erlangung des naturwissenschaftlichen Doktorgrades der Julius-Maximilians-Universität Würzburg

Vorgelegt von
CHRISTIAN NORTHE

aus Mexiko-Stadt

Würzburg, 2019

Eingereicht am: 11.09.2019

bei der Fakultät für Physik und Astronomie

1. Gutachter: Prof. Dr. Johanna Erdmenger .....

2. Gutachter: Prof. Dr. Ewelina Hankiewicz .....

3. Gutachter: .....

der Dissertation

Vorsitzende(r): Prof. Dr. Raimund Ströhmer .....

1. Prüfer: Prof. Dr. Johanna Erdmenger .....

2. Prüfer: Prof. Dr. Ewelina Hankiewicz .....

3. Prüfer: Prof. Dr. Friedrich Reinert .....

im Promotionkolloquium

Tag des Promotionskolloquiums: 18.10.2019

Doktorurkunde ausgehändigt am: .....

Dedicado a mis padres

María Socorro Sylvia Montes de Northe & Dankwart Georg Northe

y a

Leila Rocio Field Slade

ABSTRACT

This dissertation employs gauge/gravity duality to investigate features of $(2+1)$-dimensional quantum gravity in Anti-de Sitter space (AdS) and its relation to conformal field theory (CFT) in $1+1$ dimensions. Concretely, we contribute to research on the frontier of gauge/gravity with condensed matter as well as the frontier with quantum information.

The first research topic of this thesis is motivated by the Kondo model, which describes the screening of magnetic impurities in metals by conduction electrons at low temperatures. This process has a description in the language of string theory via fluctuating surfaces in spacetime, called branes. At high temperatures the unscreened Kondo impurity is modelled by a stack of pointlike branes. At low temperatures this stack condenses into a single spherical, two-dimensional brane which embodies the screened impurity.

This thesis demonstrates how this condensation process is naturally reinvoked in the holographic D1/D5 system. We find brane configurations mimicking the Kondo impurities at high and low energies and establish the corresponding brane condensation, where the brane grows two additional dimensions. We construct supergravity solutions, which fully take into account the effect of the brane on its surrounding spacetime before and after the condensation takes place. This enables us to compute the full impurity entropies through which we confirm the validity of the g-theorem.

The second research topic is rooted in the connection of geometry with quantum information. The motivation stems from the "complexity equals volume" proposal, which relates the volume of wormholes to the cicruit complexity of a thermal quantum state. We approach this proposal from a pragmatic point of view by studying the properties of certain volumes in gravity and their description in the CFT.

We study subregion complexities, which are the volumes of the regions subtended by Ryu-Takayanagi (RT) geodesics. On the gravity side we reveal their topological properties in the vacuum and in thermal states, where they turn out to be temperature independent. On the field theory side we develop and proof a formula using kinematic space which computes subregion complexities without referencing the bulk. We apply our formula to global AdS_3, the conical defect and a black hole. While entanglement, i.e. minimal boundary anchored geodesics, suffices to produce vacuum geometries, for the conical defect we also need geodesics windings non-trivially around the singularity. The black hole geometry requires additional thermal contributions.

ZUSAMMENFASSUNG

In dieser Dissertation geht es um die Beziehung zwischen Quantengravitation im (2+1)-dimensionalen Anti-de Sitter-Raum und konformer Feldtheorie in 1+1 Dimensionen. Insbesondere stellt diese Arbeit neue Zusammenhänge her zwischen der Eichtheorie/Gravitationsdualität oder *Holographie* einerseits und der Festkörperphysik sowie auch der Quanteninformationstheorie andererseits.

Das erste Thema dieser Arbeit ist inspiriert durch den Kondo-Effekt. Dieser beschreibt die Abschirmung magnetischer Störstellen in einem Metall durch Leitungselektronen bei tiefen Temperaturen. Die String-Theorie kann diesen Prozess mittels fluktuierender Flächen in der Raumzeit, sogenannten Branen, beschreiben. Bei hohen Temperaturen modelliert die String-Theorie die magnetische Störstelle als Stapel punktförmiger Branen. Bei tiefen Temperaturen kondensiert dieser Stapel zu einer einzelnen zwei-dimensionalen, sphärischen Brane. Diese Kondensation ist gleichbedeutend mit der magnetischen Abschirmung der Störstelle.

Ein Ziel dieser Dissertation ist es zu zeigen, dass diese Kondensation auf natürliche Weise im holographischen D1/D5-System implementiert wird. Hierzu beschreiben wir analoge Kondo-Störstellen als Stapel von Branen, die bei sinkenden Energien zu einer sphärischen Brane kondensieren, welche zwei extra Dimensionen besitzt. Hiernach konstruieren wir die Supergravitationslösungen, welche den vollständigen Einfluss der Branen-Störstelle auf die umgebende Raumzeit vor und nach der Kondensation berücksichtigt. Diese Lösungen erlauben es die Entropien der Störstellen zu bestimmen, womit wir die Gültigkeit des g-Theorems bestätigen.

Als nächstes widmet sich diese Arbeit der Beziehung zwischen Geometrie und Quanteninformation. Die Motivation stammt vom "complexity equals volume"-Vorschlag, welcher das Volumen eines Wurmloches mit der Schaltkreis-Komplexität eines thermischen Zustandes verbindet. Um solche Zusammenhänge zu untersuchen, wählen wir einen pragmatischen Zugang, indem wir uns den Eigenschaften bestimmter Volumina zuwenden.

Wir untersuchen sogenannte Teilregionskomplexitäten. Diese sind Volumima von Regionen, die durch Ryu-Takayanagi-Flächen berandet werden. Auf der Gravitationsseite enthüllen wir deren topologische Eigenschaften im Vakuum und in thermischen Zuständen. In Letzteren zeigen wir, dass Teilregionskomplexitäten temperaturunabhängig sind. Zuletzt untersuchen wir Teilregionskomplexitäten im Rahmen der Feldtheorie. Unter Verwendung des kinematischen Raumes entwickeln und beweisen wir eine Formel zur Berechnung von Teilregionskomplexitäten in der CFT ohne auf die Gravitationsseite Bezug nehmen zu müssen.

Als Beispiele für die Anwendung unserer Formel betrachten wir globales AdS_3, Kegelgeometrien und schwarze Löcher. Um Vakuum-Geometrien zu beschreiben, reicht Verschränkung in ihrer Darstellung als minimale Geodäten aus. Doch bereits für die Kegelgeometrien werden Geodäten benötigt, die sich nicht-trivial um die Singularität winden. Geometrien mit schwarzen Löchern beinhalten darüber hinaus noch thermische Beiträge.

PUBLICATIONS

The material in Part iii is published in two publications:

Topological Complexity in AdS_3/CFT_2 [2]

Abstract:
We consider subregion complexity within the AdS_3/CFT_2 correspondence. We rewrite the volume proposal, according to which the complexity of a reduced density matrix is given by the spacetime volume contained inside the associated Ryu-Takayanagi (RT) surface, in terms of an integral over the curvature. Using the Gauss-Bonnet theorem we evaluate this quantity for general entangling regions and temperature. In particular, we find that the discontinuity that occurs under a change in the RT surface is given by a fixed topological contribution, independent of the temperature or details of the entangling region. We offer a definition and interpretation of subregion complexity in the context of tensor networks, and show numerically that it reproduces the qualitative features of the holographic computation in the case of a random tensor network using its relation to the Ising model. Finally, we give a prescription for computing subregion complexity directly in CFT using the kinematic space formalism, and use it to reproduce some of our explicit gravity results obtained at zero temperature. We thus obtain a concrete matching of results for subregion complexity between the gravity and tensor network approaches, as well as a CFT prescription.

Holographic Subregion Complexity from Kinematic Space [3]

Abstract:
We consider the computation of volumes contained in a spatial slice of AdS3 in terms of observables in a dual CFT. Our main tool is kinematic space, defined either from the bulk perspective as the space of oriented bulk geodesics, or from the CFT perspective as the space of entangling intervals. We give an explicit formula for the volume of a general region in the spatial slice as an integral over kinematic space. For the region lying below a geodesic, we show how to write this volume purely in terms of entangling entropies in the dual CFT. This expression is perhaps most interesting in light of the complexity=volume proposal, which posits that complexity of holographic quantum states is computed by bulk volumes. An extension of this idea proposes that the holographic subregion complexity of an interval, defined as the volume under its Ryu-Takayanagi surface, is a measure of the complexity of the corresponding reduced density matrix. If this is true, our results give an explicit relationship between entanglement and subregion complexity in CFT, at least in the vacuum. We further extend many of our results to conical defect and BTZ black hole geometries.

CONTENTS

LIST OF FIGURES

LIST OF TABLES

ACRONYMS

AdS Anti-de Sitter Space

BPS Bogomol'nyi–Prasad–Sommerfield

BCFT Boundary Conformal Field Theory

CFT Conformal Field Theory

CS Chern-Simons

CV Complexity Equals Action

DBI Dirac-Born-Infeld

DD Dirichlet-Dirichlet

DN Dirichlet-Neumann

EHT Event Horizon Telescope

EPR Einstein-Podolsky-Rosen

ER Einstein-Rosen

LHS Left Hand Side

LIGO Laser Interferometer Gravitational-Wave Observatory

ND Neumann-Dirichlet

NN Neumann-Neumann

NS Neveau-Schwarz

QCD Quantum Chromodynamics

QFT Quantum Field Theory

R Ramond

RG Renormalization Group

RHS Right Hand Side

RR Ramond-Ramond

RT Ryu-Takayanagi

SYM Super Yang-Mills Theory

vev Vacuum expectation value

WZW Wess-Zumino-Witten

1 INTRODUCTION

Amongst all fundamental forces of nature, gravity is the first that we come to accept as children and yet it is the most elusive of all when we study it as adults. It has been a little over a hundred years since Albert Einstein demonstrated that – classically – gravity emerges through the curvature of spacetime [103–105]. Nevertheless, while electromagnetism, the weak and the strong force have all successfully been described in the quantum realm via the *standard model*, gravity has withstood any attempt at quantization. It actually gets worse! Gravity cannot simply be cast into the language of quantum field theory (QFT) as it stands, because it is not renormalizable [217]. Therefore a unification of gravity with quantum mechanics á la standard model is a dead end.

It takes the development of new concepts providing new ways of understanding gravity. And these are in high demand since interesting times lie ahead! Recent progress in experiment has impressively demonstrated that black holes are more palpable than ever before. Indeed, it is precisely a black hole, where the effects of gravity become important at the quantum scale.

In September of 2015 scientists of the Laser Interferometer Gravitational-Wave Observatory (LIGO) collaboration witnessed the merger of two black holes through the measurement [1] of its emanating *gravitational waves*. Einstein had predicted the existence of gravitational waves himself [106], but excluded the possibility of ever detecting them, since their effect is so unfathomably small – praise for the scientists at LIGO.

While the gravitational waves provide indirect proof of the existence of black holes, earlier this year we finally obtained direct evidence: The Event Horizon Telescope (EHT) managed to image [12] the supermassive black hole at the center of the supergiant elliptical galaxy Messier 87* – a galaxy over 50 million light years away! Again, Einstein is proven wrong about his own theory, since he discarded black holes as a mathematical artifact not realized in nature. Yet, he concluded correctly that these mysterious regions in spacetime entailed his general theory of relativity did not paint the full picture and had to be replaced one day...

Any successful quantization of gravity is bound to reproduce general relativity in its classical limit. More hints for a theory of quantum gravity come from considering black holes as thermodynamic systems [44–46, 153]. These ideas culminated in the statement that black holes carry their own entropy, called the *Bekenstein-Hawking entropy*,

$$S_{\mathrm{BH}} = \frac{k_{\mathrm{B}} c^3 \mathcal{A}}{4\hbar G}, \tag{1.1}$$

and radiate at *Hawking temperature*

$$T_{\mathrm{H}} = \frac{\hbar c^3}{8\pi G M k_{\mathrm{B}}}, \tag{1.2}$$

The non-extensiveness of S_{BH} is traced back to the long range nature of the gravitational force.

where we have employed the speed of light c, Planck's constant $\hbar$, Newton's constant G, Boltzmann's constant k_{B}, the mass of the black hole M and the area of the event horizon $\mathcal{A}$. The surprise here was that the thermodynamic entropy does not scale with volume V of the black hole as one might expect, since usually entropy is an extensive quantity. Rather it scales "just" with the surface area of the event horizon, $\mathcal{A}$. In particular this provides upper bounds on the amount of entropy, or equivalently information, that can be stored inside a black hole [47].

One decisive element in discovering the holographic principle was the black hole information paradox. We describe it below.

Gerard 't Hooft and Leonard Susskind elevated the validity of these bounds to *any* system which combine the rules of gravity and the quantum realm. They argued that that the amount of information that can be stored in a designated region of spacetime always scales with the region's surface area, not its volume [156, 157, 222]. Any attempted violation of this bound by accumulating more information in said spacetime region, is immediately stifled by nature through the formation of a black hole. Similarly to a hologram, which is able to capture three-dimensional information even though it is a two-dimensional photograph, this feature has come to be known as the *holographic principle*: the degrees of freedom of a $(d+1)$-dimensional gravitational system are stored in only d dimensions. Generally we refer to applications of the holographic principle simply as *holography*.

One candidate for a theory of quantum gravity is string theory. The reader will be pleased to hear that string theory does indeed abide by the holographic principle via Juan Maldacena's *Anti-de Sitter/Conformal Field Theory correspondence* (AdS/CFT) [179]. In fact, it is the only explicit realization of the holographic principle to date. This correspondence relates a gravitational theory on Anti-de Sitter space to a (quantum) conformal field theory living on the conformal boundary of AdS. The CFT has one dimension less and is the "hologram" of the gravity theory. We speak of a *duality* in the sense that any object in one theory has a counterpart in the other. Building on AdS/CFT, many more holographic examples with less symmetry have been studied. They all have in common that they link gauge theories to gravity so that in general we refer to these correspondences as *gauge/gravity duality*.

The true marvel of AdS/CFT is that it relates a theory of gravity to a quantum field theory *without* gravity usually employed to describe elementary particles. This clearly intermingles our traditional views on what physics our theories truly represent. Moreover, it is an example of a weak/strong coupling duality, that is, if for instance the CFT is strongly coupled, the gravity theory is weakly coupled. Strongly coupled field theories are notoriously hard to control, because of the breakdown of perturbation theory. Yet, in AdS/CFT we gain access to quan-

tities of interest through the weakly coupled dual, where computations are practicable.

Through these properties AdS/CFT has opened an avenue to investigate strongly coupled systems. For instance, it is possible to extract advanced and retarded Greens functions from the causality structure of a black hole. These in turn gave rise to the perhaps most prominent trademark of the gauge/gravity duality: the computation of the ratio of shear viscosity η to entropy density s,

$$\frac{\eta}{s} = \frac{1}{4\pi}\frac{\hbar}{k_{\mathrm{B}}}, \tag{1.3}$$

applicable to strongly coupled fluids [175, 220]. In fact, this holographic result is assumed to provide a lower bound for realistic systems. Indeed, so far no violation of it was detected experimentally, not even with strongly coupled quark-gluon plasmas [73, 178].

Equation (1.3) describes a transport coefficient, which is most relevant in the study of liquids or solids. This takes us into the realm of condensed matter physics. It examines collective phenonema and many-body interactions in phases of matter. Importantly for us, it enables scientists to engineer strongly correlated systems, which may provide an arena to test the gauge/gravity duality experimentally. At the least AdS/CFT grants conceptual insight into the possible mechanisms at strong coupling, aside from making certain computations analytically tractable in the first place, as corroborated by (1.3). In this vein condensed matter physicists gain access into the study of strongly coupled electron systems through the gauge/gravity duality. The present thesis pursues a similar goal through the study of holographic models of the *Kondo effect* – more on this below.

Mostly, we use the correspondence to learn something about quantum field theories through gravity. A different reading of AdS/CFT follows by turning the crank around and using the algebraic structure on the field theory side to learn how it (re-)organizes on the gravity side in order to extract clues on the quantization of gravity. For instance, it has been investigated how microstates in the CFT average into ensembles, which have effective black hole descriptions in gravity [36]. These studies suggest that black holes are in fact coarse-grained descriptions of microstate geometries. Other examples are the computation of ergoregion emissions of a specific class of black holes through CFT amplitudes [22–28].

Our discussion makes clear that gauge/gravity, derived from string theory, provides a strong and flexible formalism to investigate a wide range of physical phenomena. Recent advances from the realm of *quantum information* suggest however that gauge/gravity duality is a more general concept, applicable also outside the string theory framework. The kickoff for this development was Ryu's and Takayanagi's groundbreaking paper [212], which introduced a holographic notion of entan-

glement entropy. This discovery has given rise to a thriving economy interested in the connection of quantum physics with geometry. Its perhaps most notable result is the equivalence of linearized Einstein equations and the first law of entanglement [86, 119].

By now it is clear that holography inevitably intermingles our concepts of gravity and quantum theory. Thus, it almost certainly will produce more loose threads, whose resolution bring us closer to the unification of gravity and quantum mechanics. Thus it provides clues to find a theory of everything, which is certainly in the spirit of Einstein...

This thesis takes us into two of the aforementioned fields of research, each of which gets its own introduction momentarily.

- The first topic is motivated by condensed matter and is concerned with the modelling of a holographic Kondo effect. We motivate this venture thoroughly in Section 1.1.
- The second topic is geared towards quantum information and investigates the role of geometry in the dual field theory. This is motivated in-depth in Section 1.2.

1.1 HOLOGRAPHIC BOUNDARY RG FLOWS AND THE KONDO EFFECT

A large part of this thesis is dedicated to the construction of RG flows in holography by drawing inspiration from the *Kondo model* [171, 172], which describes the screening of magnetic impurities by conduction electrons in a metal at low temperatures. An obvious motivation to study Kondo physics in holography is finding systems of strongly correlated electrons coupled to magnetic impurities. Another intriguing characteristic of the model is that it displays a dynamically generated scale, turning it into a toy model for quantum chromodynamics. Our particular interest aims at a better understanding of interfaces in holographic theories and their RG flows. Moreover, it is desirable to have explicit holographic systems, which obey the g-*theorem* [131].

The Kondo Effect

Few phenomena have had such a long-standing and malleable impact on physics as the Kondo model, which is underpinned by the following historical outline. Originally, the Kondo effect dates back to 1964. It then resurged in the 1970s in the development of the renormalization group [231] and Fermi liquid descriptions [193], followed in the 1980s by the Bethe Ansatz [19, 20] or large-N limits [52]. The 1990s introduced the Kondo effect to conformal field theory, where it had notable impact in the development of *boundary RG flows* [4, 7–10]. Taking this as a base in the 2000s, the formal CFT community generalized the findings

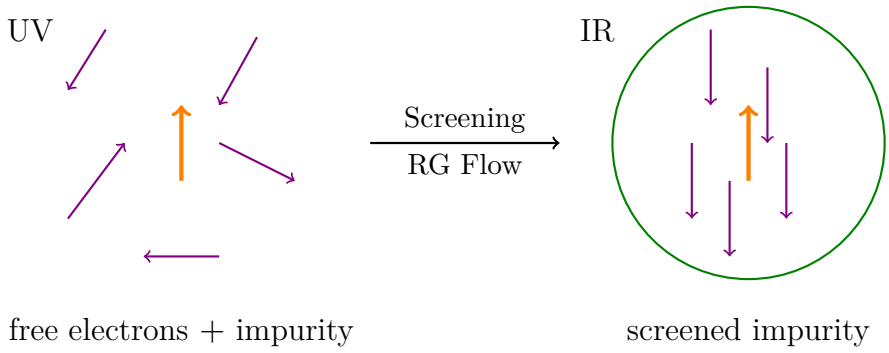

Figure 1: UV: Free electrons and uncoupled impurity. IR: Conduction electrons screen the impurity by forming a bound state with the impurity.

of the 90s to more abstract CFTs [13, 123, 127–130, 142, 143] and *interfaces* [33, 173]. This provides the viewpoint we want to assume in this thesis, namely we think of the Kondo effect as a *defect RG flow* – but more on that in due time. Tracing the Kondo effect back to the 60s, it is in fact the very first occurence of such a flow in theoretical physics! The 2010s then finally acquaint the Kondo model with holography [109, 110, 113–117, 150, 194]. Our interest lies as well in such setups. Other contemporary activity concerning the Kondo model is geared towards *nanotechnology* [174] and *quantum dots* [218, 219].

In Chapter 4 we will discuss the CFT description of the Kondo model as defect RG flow in detail.

The Kondo effect describes the rise in resistivity with decreasing temperature for conductors, which are doped with low concentrations of localized magnetic impurity atoms. The example discussed in the original source [171] is that of gold containing iron impurities. Suppose we have such a probe at hand and start to lower the temperature. Then the resistivity will decrease. Unlike undoped conductors or superconductors, the resistivity of the gold probe will hit a minimum at a sufficiently low temperature, T_{min}, before rising again. This effect is proportional to the impurity concentration. It was Kondo's insight to attribute this increase in resistivity to the spin-spin interaction of the conduction electrons and the magnetic impurity. Indeed, by going to second order in perturbation, he confirmed the increase theoretically [171]. Being perturbative, Kondo's result breaks down at a designated temperature $T_{\text{K}} < T_{\text{min}}$, called the *Kondo temperature*. The swell of non-perturbative methods outlined in the preceeding paragraph aimed at understanding impurity systems at temperatures below T_{K}.

The modern viewpoint describes the Kondo effect as an RG flow. At high energies, the kinetic energy of the conduction electrons outweighs the impact of the impurity by far, resulting in a free theory. At low energies the electrons begin to notice the presence of the magnetic impurity and shield it off by forming a cloud surrounding the impurity, see Figure 1.

All that changes in a boundary RG flow is truly the boundary condition. The bulk of the field theory remains unchanged.

More abstractly the impurity provides a conformal boundary condition in the UV, a distinct one in the IR and the Kondo effect has the former RG-flow into the latter. This has a description in the formal language of boundary conformal field theory (BCFT). The boundary condition in the UV is realized by a stack of pointlike objects, called D0-branes, while the boundary condition in the IR is realized by a single extended, two-dimensional object, called D2-brane. The Kondo RG flow then has the stack of D0-branes flow, or *condense*, into the single spherical D2-brane. Let us stress that in this formalism the (multi-channel) Kondo effect is equivalent to the emergence of two extra dimensions of an abstract object, the brane!

Processes of this kind have been investigated before and are called *non-abelian brane polarization* or *Myers effect* [190]. In this way the Kondo model unites impurity physics in condensed matter and D-brane dynamics in string theory, a feature certainly unexpected at its time. It is this beautiful behavior that we draw inspiration from in our search for RG flows in holography, with the intend to mimic Kondo physics as accurately as possible in strongly coupled environments.

Why is this useful?

The insights gained by studying Kondo physics have successfully been abstracted into a solution generating technique, which provides boundary RG flows for a variety of BCFTs [128, 130]. Ideally, holographic Kondo-like flows provide fertile soil in similar spirit. That is, given one holographic Kondo-like flow, we also gain insight into the construction of a multitude of analogous flows in various holographic systems, thereby shedding light on the interrelation of holographic systems in general. Indeed, this appears to be the case.

See [124–126, 208–210] for modern advances in non-rational CFTs.

Moreover, the flows of [128, 130] have one important restriction: they pertain to rational CFTs. After free theories, these are the tamest CFTs of all, and in fact, the majority of all CFTs is non-rational. CFTs are an indispensable part in the analysis of the general space of QFTs – they are the fixed points of RG flows. Thus it is important to get a good hold on non-rational CFTs. Holography provides an excellent playground in that respect, since these CFTs are non-rational by default. Extra bonus comes from the fact that these theories hand us strongly coupled electron systems, all through the study of a weakly coupled gravity dual.

Interfaces are prominent tools to study conformal field theories in general [29, 43, 61, 132, 198]. Holographic interfaces appeared in [11, 32, 53, 90, 111, 167, 168, 185].

More motivation for our work comes from the desire to understand interfaces and defects in holography and their RG flows. *Interfaces* are extended objects separating two possibly distinct QFTs, for us CFT_1 and CFT_2. They act as maps between the two theories. If $\mathrm{CFT}_1 = \mathrm{CFT}_2$, we speak of a *defect*. Boundaries and interfaces enjoy a close connection via the *folding trick*, which turns an interface between CFT_1

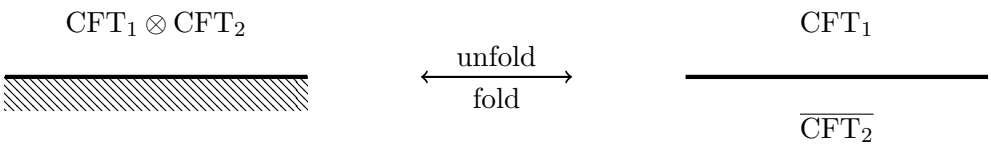

Figure 2: The BCFT of the combined system $\mathrm{CFT}_1 \otimes \mathrm{CFT}_2$ (left) is unfolded along the boundary into an interface theory between CFT_1 on the upper half-plane and $\overline{\mathrm{CFT}_2}$ on the lower half-plane (right). Similarly, interface theories can be folded along the interface into boundary theories.

and CFT_2 into a tensor product theory product theory with a boundary and vice versa, as exemplified in Figure 2.

The Kondo model, being a boundary theory can also be unfolded; it turns into a defect theory. The Kondo RG flow then turns one defect into another, hence it is a *defect RG flow*. Our objective will be to go one step further and construct interfaces, not just defects, in holography. Just as the Kondo impurity can be modelled with branes, the natural candidate for our holographic interfaces will again be branes. Once these interfaces are at hand, we look for RG flows á la Kondo, i.e. flows which realize a non-abelian brane polarization giving rise to two extra dimensions on the interface brane.

In fact, interfaces provide a natural framework for the study of impurities [16, 170, 186, 202, 203, 214, 233].

The final incentive for studying holographic Kondo flows concerns the concept of *fusion* between interfaces and boundaries. It was again the Kondo model, which served as orientation in setting up the general concept [33]. Specifically this means that one can construct interfaces, called *conformal defect lines*, which can be moved on top of a boundary – without generating singularities – in order to change its boundary condition. In particular, such defect lines implement the Kondo flow. These operators define universal RG flows in the sense that they are independent of the boundary condition in the UV. Holography then opens the door for an intriguing question: what is the meaning of this kind of fusion in gravity? Unfortunately, our interfaces will not satisfy the right criteria to answer this question. Nevertheless, it appears that our flows can be generalized to a different holographic system with more structure, where a good chance exists to find appropriate interfaces; see the outlook in Chapter 11.

We now turn our attention to the other topic studied in this the thesis: the investigation of volumes in gravity and quantum information.

1.2 GRAVITY, QUANTUM INFORMATION AND VOLUMES

Information and black holes lie at the heart of the reconciliation of gravity with quantum physics. In fact, they might represent the loose thread, whose resolution leads to a theory of everything. One aspect of this thread carries its own name, the “black hole information paradox”.

A black hole devoures everything in its vicinity, thereby piling up more and more information. Hawking taught us that a black hole radiates, ever so slightly, with temperature (1.2). Here is where the paradox is rooted, since the temperature depends only the mass of the black hole, not on the details of the information that fell into it. After some (excruciatingly long) time period, the black hole evaporates completely, leaving no trace of its contend. This stands in severe conflict with the foundations of quantum physics, which posit that quantum information is eternally preserved. Given perfect knowledge of the wavefunction of the universe at some point in time it should be possible to trace the universe arbitrarily into the future and past.

In 1997 the paradox instigated a famous wager with Preskill on one side vs. Hawking & Thorne on the other [154]. Hawking conceded in 2004 [204].

Even though it is not resolved to date, the black hole information paradox has already had important impact on theoretical physics. In fact, its most famous consequence is non other than the holographic principle [156, 157, 222]. The role of AdS/CFT in this regard was investigated early on in [177]. See [155, 197, 201] for more recent accounts and [183] for a summary of possible resolutions.

Geometrization of Information through Holography

Despite its enormous importance, the activity on the interface of quantum information and gravity was rather moderate up to a decade after AdS/CFT and the black hole information paradox. Scientists simply lacked a concrete tool to probe the existing concepts. The long awaited game changer came in the form of holographic entanglement entropy [212]. Its advent in 2006 triggered an explosion of ideas unveiling a profound connection between quantum information and gravity, again resting on the shoulders of holography. Most notable are the observations that geometry arises through entanglement [228], which is impressively backed up by the equivalence of linearized Einstein's equations with the first law of entanglement [86, 119].

Entanglement entropy of a subregion A of the field theory's spacetime is computed through the von Neumann entropy of a reduced density matrix ρ_A. While computing this in the field theory is very involved, entanglement entropy lends itself naturally to a geometric picture in the dual gravity theory. It is computed through

$$S_A = \frac{k_{\mathrm{B}} c^3 \mathcal{A}_A}{4\hbar G}, \tag{1.4}$$

where $\mathcal{A}_A$ is the area of a certain codimension-two surface, called Ryu-Takayanagi (RT) surface. It is anchored at the boundary of the spacetime region A of the CFT and reaches into the gravitational bulk in a special way, which separates the subregion A from its complement in the dual gravity theory – details will be spelled out in Chapter 8. The similarity with the Bekenstein-Hawking entropy, (1.1), is overwhelming. In fact, it is incorporated as special case of (1.4). It is striking

over and over that it is precisely this combination of prefactors of the Bekenstein-Hawking entropy through which (1.4) reproduces the CFT result on the nose, with barely any effort.

The geometrization of entanglement has sparked many interesting mechanisms for long-standing controversies. One notable instance is the Einstein-Podolsky-Rosen (EPR) paradox [107] from 1935: an attempt to prove that the world is specified entirely by *hidden variables*, contrary to quantum physics lore. Einstein, Podolsky and Rosen proposed a quantum scenario which forced one to abandon locality – a sacred concept back in the day – upon discarding hidden variables. This inspired the famous quote "spooky action at a distance". In hindsight this paradox can be seen as introducing quantum entanglement in the first place.

It was only in 1964 that John Bell proposed a set of inequalities to settle the debate [48], in favor of entanglement and non-locality and against hidden variables. Modern approaches originating in holography now explain the communication between an entangled pair of particles via small, non-traversable wormholes, which connect the pair [41, 108, 164, 165, 181]. These wormholes are called *Einstein-Rosen bridges* (ER) after their discoverers. Thus, the geometrization of entanglement via wormholes has come to be known as "ER=EPR".

Information and Volumes

In a similar vein, it was realized that one could use holographic entropy to probe what is literally invisible to the naked eye: the *inside* of a two-sided black hole, or a wormhole [152]. Susskind delved deeper into the implications and found that the *volume* of this wormhole has to increase over time [224]. This must have some dual in the field theory and Susskind argues in favor of *complexity* of the state dual the two-sided black hole geometry. This notion comes from computer science and measures how difficult it is to construct the state in question using unitary operations. For obvious reasons, this conjecture has come to be known as "complexity equals action" proposal, or "CV" proposal for short.

Unfortunately, this proposal is very difficult to test, since there is no satisfactory notion of complexity in strongly coupled field theories yet, as is required for AdS/CFT. Even though progress in the implementation of complexity has been made in free QFTs [76, 77, 149, 163], this program is still in its infancy and it remains to be seen whether Susskind's proposal can be tested rigourously in the near future.

Recently defects debuted in the investigation of complexity [75].

This provides the stepping stone for the work in this thesis. We think about a complementary question first: Can we make sense of the "bulk volume" with available tools in the field theory? This question can be more basic than Susskind's, because it does not a priori involve black holes. Of course our question can also be posited for the interior of

black holes, in which case it rivals Susskind's problem. In any event, the resolution of our question will eventually produce indications on how to tackle the inside of a black hole.

In order to approach our question, we concentrate on a certain class of promising volumes called *subregion complexities* [14]. These are the volumes of the regions enclosed by RT surfaces and their boundary region A and have been conjectured to compute the complexity of the traced out state of the subregion.

Even though we will refer to this volume as subregion complexity, we will not insist on it truly being a complexity. Rather, we take a pragmatic approach here. Mainly, we are interested in unveiling the properties of this object. Any proposed field theory dual will have to satisfy our findings and thus our work provides important clues. In fact, we develop a formalism, which computes these volumes for us solely through field theory data! One result is that entanglement is actually sufficient to compute bulk volumes at will in vacuum states. However, we will confirm Susskind's opinion that "entanglement is not enough" as soon as we investigate excitations. These require extra ingredients, which we discuss soon enough. In order to tease, we anticipate one observation: Even though entanglement is geometry, not all of geometry is entanglement.

1.3 RESULTS AND OUTLINE OF THIS THESIS

Based on the general considerations above, this thesis pursues two goals:

- The construction of Kondo-like RG flows within the framework of the gauge/gravity duality. The importance of this comes from several angles. For one, it realizes strongly coupled fermions coupled to impurities. In particular, we aim for a holographic description, with access to a lagrangian – this is a shortcoming of previous holographic descriptions of Kondo physics. Another motivation comes from the formal development of a class of interfaces in CFT and their RG properties. This provides a new playground for the investigation of a multitude of concepts or techniques, for instance, entanglement entropy and complexity.

- The other goal lies on the interface of gauge/gravity with quantum information and aims at understanding the properties of spacetime regions in gravity. We focus on the most obvious notion: their volumes. This is essential in understanding the CV proposal. Should this proposal be correct, the properties of volumes in gravity imply constraints on complexity, which are otherwise hard to derive in field theory. Moreover, we learn about the building blocks of geometry in terms of the field theory. In the cases of

interest we learn that these are entanglement, entwinement and thermal contributions.

We now summarize the content:

1.3.1 *Preliminaries, Part i*

The first part of this thesis reviews general preliminary material necessary to understand the reasoning in the remainder of this thesis.

Chapter 2 contains an introduction to branes and conformal field theory. Both topics are particularly relevant in our discussion of holographic flows in Part ii. The material covered is quite extensive since the author hopes to invite readers not familiar with string theory to keep reading. Readers who are already familiar with these concepts can still skim through this chapter in order to get acquainted with our notation.

Chapter 3 provides an introduction to the gauge/gravity duality. The concept behind the AdS/CFT correspondence is explained through use of Juan Maldacena's original example $\mathrm{AdS}_5/\mathrm{CFT}_4$. This thesis focuses on the case $\mathrm{AdS}_3/\mathrm{CFT}_2$ derived from the D1/D5 system. We give a description of its gravity side, which is central to the RG flows presented in this thesis, and we explain how the field theory is organized.

1.3.2 *Holographic Kondo-Like Flows, Part ii*

The second part of this thesis discusses holographic Kondo RG flows. We focus on the D1/D5 CFT, whose holographic gravity dual lives in $\mathrm{AdS}_3 \times S^3 \times T^4$. Choosing this theory is advantageous when looking for Kondo physics for several reasons. Firstly, it is a (1+1)-dimensional CFT just as is the case for the Kondo model. Secondly, the Kondo impurities enjoy SU(2) symmetry, which is naturally realized in the D1/D5 CFT due to the S^3 factor in the gravity dual. Thirdly, it is an exceptionally well studied example of a holographic theory. In particular, we have access to the lagrangian of the theory, which is a tremendous advantage over previous holographic Kondo models [109, 110, 113–117, 194].

When we speak of the D1/D5 CFT we actually mean an entire family of theories controlled by a twenty-dimensional parameter space [22].

Results of Part ii

We construct two classes of interfaces, or, in Kondo-speak, impurities with two possibly distinct D1/D5 CFTs to either side. The first class of interfaces is given by (p, q)-strings, while the second class is given by D3-branes charged in the same manner. We establish an RG flow of Kondo-type between these two classes of interfaces. For the RG fixed points we construct supergravity solutions which fully include the back-reaction of the interfaces in the gravity dual. Using these solutions we

(p, q)-strings are (1+1)-dimensional surfaces charged under p units of D-string charge and q units of F-string charge. D3-branes are (3+1)-dimensional.

compute the exact impurity entropies and confirm that they decrease along the RG flow, just as in the original Kondo model. Our model allows for two types of Kondo flows analogous to over-screened and exactly screened impurities. We show that the perturbing operator is marginally relevant.

Outline of Part ii

Chapter 4 reviews the Kondo model's description as two-dimensional CFT. After introducing the Kondo model and its relevance in physics, we discuss the commonly used depiction of the fixed points as Wess-Zumino-Witten (WZW) models. Thereafter, we briefly explain the relationship of the Kondo flow and fusion rules and move toward a description at home in the more formal language of BCFT. This rephrases the Kondo flow as non-abelian brane polarization and provides the blueprint for the holographic flows put forth in this thesis.

Chapter 5 implements Kondo-like flows in AdS_3/CFT_2. Our interfaces are the (p, q)-strings and D3-branes, charged with p units of D-string charge and q units of F-string charge, appearing already as probe branes in [33]. We establish the former as the UV fixed point and the latter as the IR fixed point of our Kondo flows. The main result of this chapter is the calculation of the profile of the RG flow using the techniques from [64]. Moreover, using the non-abelian DBI action [190] we show that the perturbing operator is marginally relevant. In this chapter we work in the probe brane approximation.

When we neglect the effect that a brane has on its surroundings, we speak of the probe brane approximation. Otherwise we say that we include backreaction.

Chapter 6 constructs the fully backreacted supergravity solutions dual to the RG fixed points using the setup of [79]. In other words, the main result of this chapter is the construction of supergravity solutions corresponding to (p, q)-string interfaces and D3 interfaces with $AdS_3 \times S^3 \times T^4$ asymptotics. Both classes of solutions are a priori independent and we connect them through charge matching as fixed points of an RG flow. Through comparison with the results of Chapter 5, we identify our supergravity solutions as the correct RG fixed points of our Kondo-like flows. The supergravity framework allows us to investigate interfaces with charges of the order of the background charge. In particular, we realize critical screening of the impurity, which follows the same pattern as in the original Kondo flow. The full analysis is done once in the F1/NS5 S-duality frame and thereafter in the D1/D5 frame.

When the impurity disappears completely in the IR, we say that it is critically screened.

Chapter 7 directs our attention to the interface entropy of the UV and IR impurities. Following [78], we compute the g-factor for both RG fixed points using our supergravity solutions in the F1/NS5 and D1/D5 S-duality frames. Crucially, they contain more information than the g-factors of the probe brane construction, as we confirm by explicitely taking the appropriate limit. Furthermore, we confirm that the interface entropies decrease along the RG flow giving the main result of

The g-factor is the exponential of the interface entropy.

this chapter. This instates the validity of the g-theorem, thereby fully legitimizing our flow's existence. We conclude with a brief outlook on the field theory side.

A short version of our discussion here will appear in an upcoming publication, together with details on the field theory, which are currently under inspection. This publication is written in collaboration with Johanna Erdmenger and Charles Melby-Thompson [112].

1.3.3 *Quantum Information and Volumes, Part iii*

The third part of this thesis investigates properties of bulk volumes within the context of AdS_3/CFT_2 and their connection to quantum information. The object of interest is subregion complexity. These are the volumes of regions in spacetime that are bounded by RT geodesics and its entangling interval on the boundary. We work with the standard geometries available in this dimensionality. These are AdS_3 in global and Poincaré patch coordinates, conical defects, dual to primary states, and BTZ black holes, dual to thermal states. The central tool is holographic entanglement entropy.

In contrast to the previous part, the work here will not rely on the D1/D5 system, even though one could certainly use that system as an example.

Results of Part iii

We derive topological properties of subregion complexities in AdS_3/CFT_2 in gravity. Given a disconnected entangling region with several components in the vacuum, we compute its subregion complexity. Such configurations have multiple entanglement phases. At transition points subregion complexity is discontinous and we demonstrate that the jump is determined solely by the topology of the participating entanglement phases. We repeat the analysis for a single interval in the BTZ geometry, which has two entanglement phases. First we demonstrate that subregion complexity is, contrary to entanglement entropy, temperature independent in both entanglement phases. Then we show that the jump in subregion complexity is again dictated by topology. The subregion complexity of conical defects is shown to interpolate between the two phases of the black hole.

Moving on to the field theory we derive and proof a formula, which computes subregion complexities in the CFT without referencing the bulk. This involves designing a new regularization scheme. We apply our formula to the vacuum state, to primary states of the CFT and thermal states. We conclude that entanglement entropy suffices to construct vacuum geometries, while conical defects also require entwinement. Black hole geometries are shown to include further thermal contributions. Through this we establish a lower bound for subregion complexities in generic states, given by the entanglement contributions.

Outline of Part iii

Chapter 8 starts out with lightning introductions to the key notions necessary at all times in this part. The first is entanglement entropy and its holographic realization through the RT-proposal. The second is complexity along with a mention of Susskind's "complexity=volume" proposal. We end with an explanation of subregion complexity. The latter is the focus of this part of the thesis.

In Chapter 9 we compute subregion complexity for arbitrary subregions via the Gauss-Bonnet theorem in gravity. Our procedure lays bare the topological properties of subregion complexity, which is the first main result. In particular, we discover that the difference in subregion complexity, when transitioning between entanglement phases is topological. Moreover, after repeating our analysis in thermal states with a single entangling interval, we confirm that the jump in subregion complexity between the entanglement phases is again topological and, moreover, temperature independent. This work is published in [2].

In Chapter 10 we compute subregion complexity in the field theory. The framework of choice is *kinematic space*, whose necessary details are reviewed at the beginning of this chapter. As main result, we present and proof a formula which computes bulk volumes purely from the field theory. The virtue of this lies in the fact that subregion complexity is inherently defined through gravity so far and the field theory dual is unknown. This gives a notion of what "bulk volume" means in the field theory for all cases studied in the following. These are vacuum states, primary states of the CFT and thermal states. The main ingredient is entanglement, which suffices to construct vacuum geometries. For primary states we additionally need entwinement and with thermal states also find extra thermal contributions. Our construction provides a lower bound for subregion complexity, which any candidate for a field theory dual has to satisfy. This work is published in [3].

The papers [2, 3] were written in collaboration with R. Abt, J. Erdmenger, M. Gerbershagen, H. Hinrichsen, C. Melby-Thompson, R. Meyer and I. Reyes.

For the convenience of readers, who are not familiar with supersymmetry, we have gathered some introductory material in Appendix A.

1.4 CONVENTIONS

This thesis is written in units, where the speed of light c, the reduced Planck constant $\hbar$ and Boltzmann's constant k_B all equal unity,

$$c = \hbar = k_B = 1 \tag{1.5}$$

Furthermore, all metrics carry the "mostly plus" signature.

Part I

PRELIMINARIES

Habe nun, ach! Philosophie,
Juristerei und Medizin,
Und leider auch Theologie
Durchaus studiert, mit heißem Bemühn.
Da steh' ich nun, ich armer Tor,
Und bin so klug als wie zuvor!
Heiße Master, eventuell Doktor gar,
Und ziehe schon an die zehen Jahr'
Herauf, herab und quer und krumm
Meine Schüler an der Nase herum -
Und sehe, daß wir nichts wissen können!
Das will mir schier das Herz verbrennen.
[...]
Mich plagen keine Skrupel noch Zweifel,
Fürchte mich weder vor Hölle noch Teufel -
[...]
Auch hab' ich weder Gut noch Geld,
Noch Ehr' und Herrlichkeit der Welt;
Es möchte kein Hund so länger leben!
Drum hab' ich mich den Strings ergeben,
Ob mir durch Geistes Kraft und Mund
Nicht manch Geheimnis würde kund;
Daß ich nicht mehr mit sauerm Schweiß
Zu sagen brauche, was ich nicht weiß;
Daß ich erkenne, was die Welt
Im Innersten zusammenhält...

Angepasst von Goethes Faust [139]

2

D-BRANES AND CFT

The gauge/gravity duality emerged within the context of string theory. This chapter is an introduction to the required facets of string theory, aimed at the non-expert reader. It touches upon two topics

A. Dp-branes,

B. Conformal field theory.

Both are everpresent in string theory and are vast subjects of their own.

Dp-branes are the backbone of the AdS/CFT correspondence and this thesis heavily exploits their characteristics. Time is therefore well invested in understanding their features so that Dp-branes fill the better part of this chapter. Branes have two faces and both are essential in reading this thesis. Firstly, branes may be seen as giving rise to gauge theories on their worldvolume and secondly they may be seen as heavy objects curving their surrounding spacetime. Section 2.1 conveys the material of interest in a self-contained manner, while pointing the reader to complementary sources whenever adequate. The journey starts with a study of boundary conditions of a free boson theory, whereafter we explain how these give rise to Dp-branes. Then we argue that branes are charged objects. Lastly, we discuss the description of Dp-branes in terms of the Dirac-Born-Infeld (DBI) action.

Dp-branes have developed into a rich subject and it is impossible to do it justice here. As a matter of fact entire books have been filled with Dp-branes [166].

Conformal field theory is not only a vital ingredient in string theory; despite its tremendously constraining symmetry, it also appears in condensed matter physics, where it models critical phenomena [92] and, particularly important for us the Kondo effect [5]. Section 2.2 begins with a review of the conformal algebra, explains how the spectra in two-dimensional CFTs are organized and introduces fusion rules. This provides the prerequisites to discuss boundaries and interfaces in CFT, which in turn is the basis to understand the Kondo effect and our holographic analogs below.

At times, a basic understanding of supersymmetry and supergravity comes in handy and the author has composed a introductory material in Appendix A.

2.1 DP-BRANES

We begin our exposition in Section 2.1.1 with the study of boundary conditions, their interpretation in string theory as Dp-branes, T-duality and charges of D-branes. Then, in Section 2.1.2, we restrict to the most common low energy effective description of a Dp-brane in terms of the Dirac-born-Infeld (DBI) and Chern-Simons (CS) actions.

2.1.1 *Features of D-branes*

Boundary Conditions

Let us begin with the simple action of a single scalar $X(\tau,\sigma)$ on a $(1+1)$-dimensional manifold Σ with boundary coordinatized by space σ and time τ[1],

$$S = \frac{1}{4\pi}\int d\sigma d\tau \left[\Big(\partial_\sigma X\Big)^2 + \Big(\partial_\sigma X\Big)^2\right]. \tag{2.1}$$

We choose $\tau \in (-\infty,+\infty)$ and $\sigma \in (0,\pi)$ so that we are situated on the strip. The distance between its boundaries is parametrized by σ. Varying this action leads to

$$\delta S = \frac{1}{\pi}\int d\sigma d\tau \left[-\Big(\partial_\sigma^2+\partial_\tau^2\Big)X\cdot\delta X + \partial_\tau\Big(\partial_\tau X\cdot\delta X\Big) + \partial_\sigma\Big(\partial_\sigma X\cdot\delta X\Big)\right]. \tag{2.2}$$

If it were not for the boundary, the vanishing of this action would simply imply the well known equations of motion, $\Big(\partial_\sigma^2+\partial_\tau^2\Big)X = 0$. Since there is no boundary in the time direction, we simply have the fields fall off sufficiently fast at $\tau = \pm\infty$ so as to have the second summand vanish. The last term is more interesting. Its vanishing reads,

$$\frac{1}{\pi}\int d\tau\Big(\partial_\sigma X\Big)\delta X\Big|_{\sigma=0}^{\sigma=\pi} = 0 \tag{2.3}$$

It vanishes for two distinct types boundary conditions

$$\partial_\sigma X\Big|_{\sigma=0,\pi} = 0, \qquad \text{Neumann condition,} \tag{2.4}$$

$$\delta X\Big|_{\sigma=0,\pi} = 0 = \partial_\tau X\Big|_{\sigma=0,\pi}, \qquad \text{Dirichlet condition.} \tag{2.5}$$

A detailed discussion within the framework of CFT can be found in chapter six of [55].

Boundary Conditions and D-branes

In order to assign an interpretation let us carry these boundary conditions over to string theory. In string theory we have ten such scalars X^μ with $\mu = 0,\ldots,9$. Each is interpreted as a coordinate of the string parameterizing the string's embedding into a ten-dimensional *target space*, which is usually spacetime itself. The zeroth scalar, X^0 is the string's time coordinate, the remaining scalars describe nine spatial coordinates. The values $X|_{\sigma=0,\pi}$ then indicate the open string's endpoints.

1 Here we are not yet concerned with string theory, so we omit all factors of α' etc.

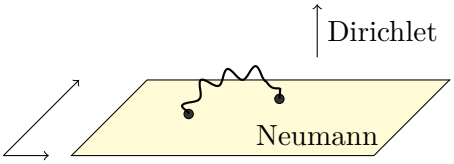

Figure 3: Open string ending on Dp-brane. We have $p+1$ Neumann boundary conditions giving rise to the worldvolume of the brane, while the remaining $10-(p+1)$ transverse coordinates have Dirichlet boundary conditions.

$\mathcal{M}_{10}$	0	1	2	3	4	5	6	7	8	9
N D5	•	•	•	•	•	•	-	-	-	-

Table 1: An exemplary brane configuration. A "•" indicates Neumann coordinates meaning that the brane is extended in these directions. A "-" indicates Dirichlet directions meaning that the brane is pointlike in these directions. Here we have six Neumann directions, $p=5$, referred to as a D5-brane. The table describes a stack of N such branes embedded into a lorentzian tenfold $\mathcal{M}_{10}$.

When a coordinate has Neumann boundary conditions, the string's end moves freely in target space. One can show that it does so at the speed of light. This may happen for a set X^a of coordinates simultaneously, with $a=0,\dots,p$. When a coordinate X has Dirichlet boundary conditions, (2.5), the strings end is constrained to a fixed position in target space, $X^i|_{\sigma=0,\pi}=c^i$. This may happen for some number of coordinates X^i simultaneously, with $i=p+1,\dots 9$. Then the string is attached to a $(p+1)$-dimensional hypersurface in target space, called *Dp-brane*. A simple visualization is given in Figure 3.

Dp-branes are hypersurfaces in target space (usually spacetime), where open strings can end.

The "D" stands for Dirichlet and the specifier p indicates the spatial dimensions of the Dp-brane. When the dimensionality of the hypersurface is not of import one oftentimes simply refers to them as D-branes. Later on, we will discuss that D-branes are charged objects under certain fields. Under that aspect we will discover even other kinds of branes charged under different fields. In fact, the *fundamental string* itself, the string of string theory, is referred to as a brane in the below, because it is an extended object.

The $(p+1)$-dimensional hypersurface is also referred to as the *worldvolume* of the theory. This is in analogy to the worldline of a particle in relativistic mechanics. Actually for $p=0$, i.e. for no spatial extension, we have a particle at hand, called the *D-particle*. We will make use of this analogy below, when discussing charges. When $p=1$, that is when the worldvolume is comprised of one spatial direction and the time direction, we call it a *worldsheet*. Note that this terminology is used as well for the fundamental string, which is not however a D-brane and so a D1-brane is often called a *D-string*.

In this thesis the time coordinate X^0 has always Neumann boundary conditions, since otherwise the worldvolume would live only at an instant in time. Configurations where all directions including the time coordinate satisfy Dirichlet boundary conditions, i.e. $p = -1$ can, nevertheless, also be studied and go by the name *instantons*.

We may also consider multiple branes of the same type stacked on top of each other. In this thesis we will always be considering coinciding branes. In the literature it is common however, to also consider seperated branes. This leads for instance for occurences of quarks on within the framework of string theory. Brane configurations are often summarized in tables such as Table 1 for a stack of N exemplary D5-branes embedded into a lorentzian tenfold $\mathcal{M}_{10}$ as target space. When considering only a single brane the fundamental string can only attach to said brane. When dealing with a stack of N branes however the fundamental strings may start on one brane and end on another. It is important to keep track of this and so we assign labels $m = 1, \ldots, N$ to the starting point and $n = 1, \ldots, N$ to the endpoints. Together, m and n are called *Chan-Paton* factors.

For simplicity we take $\mathcal{M}_{10}$ to be ten-dimensional Minkowski-space, which has an $SO(1,9)$ Lorentz symmetry. This is broken by the presence of the Dp-brane,

$$SO(9,1) \longrightarrow SO(1,p) \times SO(10-p). \tag{2.6}$$

The first factor on the RHS is the surviving Lorentz symmetry on the brane worldvolume, while the second factor describes rotations about the brane in the transverse directions, given by the Dirichlet directions, where the brane appears to be a dot. Moreover, a single D-brane or a stack of coincident D-branes of the same type break half of the 32 supersymmetries of type II string theory. States of string theory, which preserve half of the supersymmetries are called $\frac{1}{2}$-BPS. If the stack is not coincident more supersymmetry is broken.

When branes of different sizes are at play, we can encounter strings with mixed boundary conditions as exemplified in Table 2. The common worldvolume directions have Neumann boundary conditions at both ends; they are called Neumann-Neumann directions (NN). The common non-worldvolume directions have Dirichlet boundary conditions at both ends; they are called Dirichlet-Dirichlet directions (DD). NN and DD directions are what we dealt with above when discussing a single type of brane; we just did not specify that they had the same boundary conditions at both of the string's ends. The new ingredients here are the Neumann-Dirichlet[2] (ND) and Dirichlet-Neumann (DN) coordinates.

What about the preserved supersymmetries in the case of two distinct types of D-branes? It turns out that if the combined number of ND

2 We arbitrarily announce the $D5$-branes in the example of Table 2 to be the "first" branes and the D1-branes to be the "second" branes. This determines whether it is an ND or DN coordinate.

$\mathbb{R}^{1,9}$	0	1	2	3	4	5	6	7	8	9
N_5 D5	•	•	•	•	•	•	-	-	-	-
N_3 D3	•	•	-	-	-	-	-	-	•	•

Table 2: Example of mixed boundary conditions: Black indicates NN coordinates, green indicates DD coordinates, red indicates ND coordinates and blue indicates DN coordinates.

$\mathbb{R}^{1,9}$	0	1	2	3	4	5	6	7	8	9
N_5 D5	•	•	•	•	•	•	-	-	-	-
N_1 D1	•	•	-	-	-	-	-	-	-	-

Table 3: The D1/D5 system: Black indicates NN coordinates, green indicates DD coordinates, red indicates ND coordinates and blue indicates DN coordinates. This system plays a major role in this thesis.

and DN directions is a multiple of four. The D1/D5 brane system from the main text is presented in Table 3. It showcases two NN directions, four DD directions, four ND directions and no DN directions. So its combined number ND and DN directions is four and it can be shown that this brane configuration preserves a total of 8 supersymmetries out of the 32 of the type IIB string – precisely a quarter. Hence their name, $\frac{1}{4}$-BPS states of string theory.

Type II String Theory and T-Duality

When we say type II string theory we mean one of two possible theories: type IIA or type IIB. For reading this thesis the most relevant difference between the two is that they can harbor distinct types of branes. This is traced back to the different chiralities of the supersymmetry generators in the two theories, but we do not really need these (interesting) details. We content ourselves with acknowledging that both, IIA and IIB, have 32 supersymmetries, which are then broken to some extend by the introduction of branes. In IIA theories we can have Dp-branes with p even, while IIB can only accomodate Dp-branes with p odd. We exclusively work with IIB theory in this thesis.

There exists a natural mapping between the two theories called *T-duality*. We only touch upon it briefly in the main part of this thesis and so we point the reader to chapter six of [42] for a more detailed account. Here, we restrict to a single feature of T-duality. It acts on individual directions and turns Neumann into Dirichlet boundary condidions and vice versa. This implies that, if we take a Dp-brane and act with a T-duality on a direction X^a along the worldvolume, then this direction becomes a transverse direction and the brane turned into a D$(p-1)$ brane. It turns a worldvolume coordinate X^a into a direction, which is

$\mathbb{R}^{1,9}$	0	1	2	3	4	5	6	7	8	9
N_5 D5	•	•	-	-	-	-	-	-	-	-
N_1 D1	•	•	•	•	•	•	-	-	-	-

Table 4: D1/D5 system after applying T_{2345}. The D5 branes turned into D1 branes and vice versa. The numbers N_5 and N_1 remind us of what used to be fivebranes and onebranes.

transverse to the D$(p-1)$-brane. Similarly, if we apply a T-duality on a direction X^i transverse to a Dp-brane we obtain a D$(p+1)$-brane.

We can apply multiple T-dualities on several coordinates at a time. Important for the main text is the quadruple T-duality, T_{2345}, acting on the 2, 3, 4, 5 direction of the D1/D5 system outlined in Table 3. It exchanges the D5 and D1 branes leading to the configuration given in Table 4.

Charges

Now we turn our attention to the charges that the branes carry. To that end we digress briefly into electromagnetism in four spacetime dimensions governed by Maxwell's equations,

$$dF = \star J_m, \qquad d\star F = \star J_e. \tag{2.7}$$

Here $F = dA$ is the field strength, J_e is the familiar electric current one form and J_m is its (not so familiar) cousin responsible for magnetic charge, which we call g. Consider an electron of charge e, which couples to the gauge field one form $A = A_\mu dx^\mu$ via the interaction term

$$S_{int} = e\int A = \int d\tau A_\mu \frac{dX^\mu}{d\tau}, \tag{2.8}$$

where the integral is carried out over the worldline of the electron parametrized by τ. The second line carries out the pullback of the gauge field A to the worldline. The electric and magnetic charges my be extracted through

Generically, branes without charges decay for reasons that we will not delve into in this thesis. Charges stabilize the brane and are therefore a crucial aspect of branes.

$$e = \int_{S^2} \star F, \qquad g = \int_{S^2} F, \tag{2.9}$$

where the S^2 surrounds the source, either the electron or the magnetic monopole. These charges are related by Dirac's quantization condition,

$$e \cdot g \in 2\pi\mathbb{Z}. \tag{2.10}$$

In order to make contact with D-branes in string theory, we think of the electron or the magnetic monopole as D0-like particles[3] and generalize what we found to extended objects embedded in ten spacetime dimensions. Much as the electron ("$p = 0$"[4]) of charge e couples to a one-form A_1, a Dp-brane couples to a $(p+1)$-form gauge field C_{p+1} via

$$\begin{aligned} S_{int} &= \mu_p \int C_{p+1} \\ &= \frac{\mu_p}{(p+1)!} \int C_{\mu_1 \dots \mu_{p+1}} \frac{\partial X_1^\mu}{\partial \xi^0} \dots \frac{\partial X^{p+1}}{\partial \xi^p} d^{p+1}\xi. \end{aligned} \tag{2.11}$$

F_{p+2} is the gauge field strength related to C_{p+1}. μ_p is the charge of the D-brane. The integral is carried out over the worldvolume of the D-brane parametrized by ξ^a, $a = 0, \dots, p$. The second line carries out the pullback of the gauge field C_{p+1} to the worldvolume. The electric and magnetic charges may be extracted through

In d spacetime dimensions the Hodge star operation $\star$ turns an n-form into a $(d-n)$-form.

$$\mu_p = (-1)^p \int_{S^{d-p-2}} (\star F)_{d-p-2}, \qquad \mu_{d-p-4} = \int_{S^{p+2}} F_{p+2} \tag{2.12}$$

Here, we have chosen use arbitrary spacetime dimensions in order to highlight the connection with (2.9), where we have $p = 0$ and $d = 4$. Of course, we are interested in type II string theory with $d = 10$ and p between zero and nine.

In contrast to (2.9), in (2.12) the spheres engulfing the branes are of different dimensionality. This is traced back to the fact that the magnetic dual of any electrically charged object in arbitrary spacetime dimensions d does not share the dimensionality of its electric pendant. For a Dp-brane in with electric charge μ_p the magnetic dual assumes the structure of a $(d-p-4)$ brane with magnetic charge μ_{d-p-4}. Again the charges satisfy Dirac's quantization condition,

$$\mu_p \mu_{6-p} \in 2\pi\mathbb{Z}. \tag{2.13}$$

The fields C_{p+1} and F_{p+2} are known as Ramond-Ramond (RR) gauge fields and corresponding RR fields strengths, respectively. Dp-branes are always charged at least under the gauge fields C_{p+1}. Below we discuss how Dp-brane can couple to RR fields of other form degree.

We already mentioned that IIA theory can only accomodate Dp-branes with p even, while IIB theory harbors branes with p odd. This implies also that each theory only incorporates the corresponding RR gauge fields C_{p+1}. Of course, since both theories feature fundamental strings they also have the NS two-form and $F5$ branes.

3 They are not D0-branes for reasons that will become obvious in the next section.

4 The electron has no spatial extend and thus it would have $p = 0$, if it were a brane. It is not a brane however, since it harbors no gauge theory on its worldline; hence the quotes on $p = 0$.

(p,q)-Strings and (p,q)-Fivebranes

We conclude by pointing out that fundamental strings do not couple any RR form (C_2 would have the appropriate form degree). Fundamental strings couple to the NS two-form B, which we mentioned in passing above. Within the context of branes one often refers to the fundamental strings as $F1$- or $NS1$-branes, where the F stands for fundamental and the NS for Neveau-Schwarz, while the 1 just counts the spatial extension as for the D-string. Of course there is also a magnetic dual, whose dimensionality can be determined as for magnetic D-branes, via $(d-p-4)$ giving 5 in the case at hand. Hence they are six-dimensional branes and they go by the name $NS5$-brane. In this thesis we will mostly refer to them as $F5$s.

It is possible to write down bound states, charged with p[5] units under C_2 and q units under B. If the object is two-dimensional, it is called a (p,q)-string and if it is six-dimensional is a (p,q)-fivebrane. A single fundamental string is in this notation a $(0,1)$-string and a D-string is a $(1,0)$-string.

When discussing IIB supergravity we will encounter *S-duality*, which exchanges B and C_2 turning fundamental strings into D-strings and vice versa, or more generally (p,q)-strings into (q,p)-strings.

2.1.2 *Low Energy Effective Worldvolume Theory*

The discussion here follows [54]. We have introduced D-branes as hypersurfaces on which fundamental strings can end. They are not just that, however. One of their most crucial aspects is that they have dynamics of their own! They harbor entire (gauge) theories on their worldvolume. This is a drastic conceptual leap. Generally one has to refrain to the framework of BCFT to study honestly the dynamics of D-branes. This is in general very complicated. For our purposes it suffices to consider a class of low energy effective theories

$$S_{eff} = S_{DBI}[G,\phi,B] + S_{CS}[C_p] \tag{2.14}$$

governed by so-called Dirac-Born-Infeld (DBI) action and Cherns-Simons (CS) type actions. The DBI summand depends on the metric G, the dilaton ϕ and the NS two-form B, while the CS piece depends on the RR gauge fields C_p. String theory knows two expansion parameters, α' and the string coupling g_s. Our effective action is to leading order in g_s and to all orders in α'. We begin with the case of a single brane and thereafter we discuss its generalization to multiple branes.

5 This p is not related to the p indicating a dimensionality of a brane.

Dirac-Born-Infeld for a Single Brane

Let us first state the Dirac-Born-Infeld action before making some remarks on it,

$$S_{DBI} = -T_p \int_{\mathcal{W}} d^{p+1}\xi e^{-\phi(X)} \sqrt{-\det(P[G+\mathcal{F}])}, \tag{2.15}$$

$$\mathcal{F} = B + 2\pi\alpha' F. \tag{2.16}$$

T_p is the Dp brane's tension

$$T_p = \frac{2\pi}{l_s^{p+1}}, \qquad \alpha' = l_s^2. \tag{2.17}$$

$\mathcal{W}$ is the branes worldvolume and $P[-]$ denotes the pullback from ten-dimensional target space, coordinatized by X^μ, to $\mathcal{W}$, coordinatized by ξ^a. Exemplified with the metric we have,

$$P[G]_{ab} = \frac{\partial X^\mu}{\partial \xi^a}\frac{\partial X^\nu}{\partial \xi^b} G_{\mu\nu}, \qquad \mu,\nu = 0,\dots 9, \quad a,b = 0,\dots,p. \tag{2.18}$$

In the main text, (3.5), we split of the asymptotic part of the dilaton, $\phi(X) = \phi_0 + \phi(X)$, which gives rise to the string coupling $g_s = e^{\phi_0}$. The low-energy excitations (the massless excitations) of open strings ending on the brane give rise to $U(1)$ gauge fields. F_{ab} is the corresponding gauge field strength. Unlike G and B the field strength lives only on the worldvolume and not on the full ten-dimensional target space. Hence it need not be pulled back. It turns out that by itself F is not gauge invariant and needs to be accompanied by the the NS two-form B. The gauge invariant field strength is then the combination in (2.16).

When dealing with a stack of N branes below, the low-energy excitations of open strings give rise to $U(N)$ gauge fields on the brane.

The coordinates $X\mu(\xi)$ describe the embedding of the brane into ten-dimensional target space $\mathcal{M}_{10}$. We have mentioned that open strings give rise to gauge fields on the brane. To be more precise, we are referring to the $p+1$ coordinates of the string parallel to the worldvolume, inducing a gauge field $A_a(\xi)$. The remaining coordinates, $X^i(\xi)$ with $i = p+1,\dots,9$ transverse to the brane describe fluctuations of the brane inside $\mathcal{M}_{10}$. Together the gauge field and the transverse fluctuation comprise the massless bosonic degrees of freedom of the open string on the D-brane.

We like to employ *static gauge*, where we just identify the coordinates the $p+1$ coordinates parallel the worldvolume with the worldvolume coordinates themselves and decompose the remaining embedding functions, X^i, into a constant piece and a fluctuation about it,

$$X^a = \xi^a, \qquad X^i = x^i + 2\pi\alpha'\chi^i(\xi) + \dots \tag{2.19}$$

A prototype of the Dirac-Born-Infeld action, the *Born-Infeld* action was considered a long time before the advent of string theory as non-

linear generalization of Maxwell's theory, that is $U(1)$ gauge theory in flat space. It corresponds to choosing flat target space $\mathbb{R}^{1,9}$ in (2.15). That is set $G_{\mu\nu} = \eta_{\mu\nu}$, $B = 0$ and have the fluctuating piece of the dilaton vanish $e^{\phi} = g_s$,

$$S_{BI} = -T_p \int_{\mathcal{W}} d^{p+1}\xi \, g_s^{-1} \sqrt{-det(P[\eta + 2\pi\alpha' F])}. \tag{2.20}$$

If we then restrict to powers of small field strength F, we recover familiar electrodynamics plus free fields,

$$S_{DBI} = -(2\pi\alpha')^2 \, T_p \, g_s^{-1} \int d^{p+1}\xi \left[1 + \frac{1}{4} F_{ab} F^{ab} + \frac{1}{2} \partial_a \chi^i \partial^a \chi^i + \dots \right]. \tag{2.21}$$

The prefactor can then be identified with the coupling of the gauge theory, g_{YM}^{-2}, which we know to be the Yang-Mills coupling in Chapter 3,

$$g^2_{YM,p} = \frac{g_s}{T_p (2\pi\alpha')^2} = g_s (2\pi)^{p-2} \alpha'^{\frac{p-3}{2}}. \tag{2.22}$$

When introducing the AdS/CFT correspondence, we were concerned with the case $p = 3$, in which case we reproduce one statement in (3.1), i.e. $g^2_{YM,3} = 2\pi g_s$. When discussing $\mathrm{AdS}_3 \times \mathrm{S}^3 \times T^4$ we contemplated D1- and D5-branes for which we get $g^2_{YM,1} = g_s/(2\pi\alpha') = g_s/(2\pi l_s^2)$ and $g^2_{YM,5} = 2\pi g_s \alpha' = 2\pi g_s l_s^2$, respectively.

Chern-Simons for a Single Brane

The Chern-Simons terms parallel the couplings we considered when discussing the charges of a brane, (2.11). Indeed, such terms are present here, they are not the full story however. The complete set of couplings to the brane reads,

$$S_{CS} = \mu_p \int_{\mathcal{W}} P\Big[\sum_n C_n \wedge e^{\mathcal{F}} \Big]. \tag{2.23}$$

Out front we find again the charge, μ_p of the Dp-brane and the integral is carried out over the worldvolume $\mathcal{W}$. We reencounter the two-form gauge invariant field strength $\mathcal{F} = B + 2\pi\alpha'$ and the reader is reminded that F lives only on $\mathcal{W}$ and need not be pulled back. The sum is over all possible RR potentials. This differs depending on whether we consider IIA or IIB theory. The former harbors only D-branes with even p, while the latter only has odd p. The guideline to single out the contributing RR potentials is the dimension of $\mathcal{W}$, since the form-degree of the

integrand must match it; otherwise the integral is ill-defined. To clarify, let us consider the case $p = 5$ in IIB string theory,

$$S_{CS} = \mu_5 \int_{\mathcal{W}} P\left[C_5 + C_3 \wedge \mathcal{F} + C_1 \wedge \mathcal{F} \wedge \mathcal{F}\right]. \tag{2.24}$$

As promised we have a term of the form (2.11), but we see that also RR potentials with $p < 5$ couple to the brane. Hence we can also find D1-brane and D3-brane charge on a D5-brane. This is an important feature and the lower dimensional D-brane charge is interpreted as *dissolved* charge on the brane. Note that through B in $\mathcal{F}$ we not only have dissolved RR charge, but also dissolved fundamental string charge. In the main text we describe the dissolution of D1- and F1-brane charge on a D3-brane. When discussing the CS term for the stack of branes below, we will discover that then also RR-potentials corresponding to branes of higher dimension than the brane under consideration can couple.

Dirac-Born-Infeld for a Stack of Branes

We now go on to discuss the DBI action for a stack of N coinciding Dp-branes. The material in this section is taken from Myers' seminal paper [190] and the reader is directed to it for more information. The first main difference to the single brane case is that the gauge theory on the brane is no longer a $U(1)$ gauge theory, but a $U(N)$ theory. This is precisely what we have in the AdS/CFT correspondence.

One might expect that the gauge group is $U(1)^{\otimes N}$ rather than $U(N)$. When the branes' loci do not coincide this is in fact the case.

The gauge field and the coordinate fluctuations, (2.19), become $\mathfrak{u}(N)$ valued, $A_\mu = A_\mu^a T^a$ and $\chi^i = \chi^{i,a} T^a$, respectively. T^a are $U(N)$ generators and $i = p+1, \ldots, 9$ labels the directions transverse to the stack of branes. We need to introduce the two tensors

$$E_{\mu\nu} = G_{\mu\nu} + B_{\mu\nu}, \tag{2.25}$$

$$Q^i_{\ j} = \delta^i_{\ j} + 2i\pi\alpha'[\chi^i, \chi^k]E_{kj}. \tag{2.26}$$

Lower case greek letters run over ten-dimensional target space. The part of E lying on the transverse directions, E_{ij}, is promoted to be the isomorphism between tangent space of target space and its dual. This implies that in those directions indices are no longer raised and lowered by G_{ij} but E_{ij}. The DBI action is then expressed as

$$S_{DBI} = -T_p \int_{\mathcal{W}} d^{p+1}\xi \mathrm{Tr}\left(e^{-\phi}\sqrt{-\det(P[D]_{ab} + 2\pi\alpha' F_{ab})\det(Q^i_{\ j})}\right) \tag{2.27}$$

$$D_{ab} = E_{ab} + E_{ai}(Q^{-1} - \delta)^{ij}E_{jb}. \tag{2.28}$$

The trace is over the gauge group. The prescription for evaluating this trace is not yet completely clear. It is ambiguous because the entries of

the included tensors are themselves non-abelian. Usually one uses the symmetric trace prescription, even though it is known to break down at sixth order. In the main text we can circumvent this issue and hence do not discuss it any further here; the reader is directed to [190] for further comments.

Let us now consider the relevant case for the AdS/CFT correspondence. In Chapter 3 we will mention without detailed explanation how the action for a single D3-brane is enhanced to that of a stack of D3-branes. In particular, this gives rise to an extra non-commutative potential term, which is required to find SYM theory. Let us go over the details now. As appropriate for the discussion below we approach flat target space with $B = 0$ and $G_{\mu\nu} = \eta_{\mu\nu}$. To dig up the desired term, it suffices to consider the second determinant in (2.27). In an expansion about flat target space it gives to leading order

$$\sqrt{\det Q^i_{\ j}} = 1 - \frac{(2\pi\alpha')^2}{4}[\chi^i, \chi^j][\chi^i, \chi^j] + \dots \tag{2.29}$$

As promised we obtain a potential term suited for the $\mathcal{N} = 4$ SYM action. These are only the leading order terms and corrections arise also from the first determinant in (2.27).

Chern-Simons for a Stack of Branes

Lastly, we turn to the CS term for a stack of N branes; again we draw from [190]. We need to introduce one technicality from differential geometry: the *interior product* ι [191]. Consider a p-form ω on a manifold M. Then one can feed a vector V into the first entry of ω via the interior product with V

$$\iota_V \omega(V_1, \dots, V_{p-1}) := \omega(V, V_1, \dots, V_{p-1}), \tag{2.30}$$

where the V_i are some vectors. The crucial point for us is that the form $\iota_V\omega$ is only a $(p-1)$-form. As an example consider a two-form ω and two vectors V, W,

$$\begin{aligned} \omega =& \frac{1}{2}\omega_{\mu\nu} dx^\mu dx^\nu \\ \iota_V\omega =& V^\mu \omega_{\mu\nu} dx^\nu \\ \iota_W\iota_V\omega =& W^\nu V^\mu \omega_{\mu\nu} = -\iota_V\iota_W\omega \end{aligned} \tag{2.31}$$

The last equatity follows from antisymmetry of the two-form. It implies that the interior product is a nilpotent operation $\iota_V^2 = 0$ if V is an ordinary vector. For us, this won't be the case. We use the matrix-valued fluctuations $\chi = \chi^i \partial_i = \chi^{i,a} T^a \partial_i$, which we introduced in (2.19) and hence antisymmetry only produces the commutator,

$$\iota_\chi \iota_\chi \omega = \chi^j \chi^i \omega_{ij} = \frac{1}{2}[\chi^j, \chi^i]. \tag{2.32}$$

Now let us turn our attention to CS term. It reads

$$S_{CS} = \mu_p \int_{\mathcal{W}} \mathrm{Tr}\left(P\left[e^{2i\pi\alpha' \iota_\chi \iota_\chi} \left(\sum_n C_n \, e^B \right) \right] e^{2\pi\alpha' F} \right). \tag{2.33}$$

The trace is again over the gauge group, $U(N)$. If we have the number of branes N shrink to one, the χ^i become abelian and due to $\iota_\chi^2 = 0$ we recover (2.23). In the abelian case we observed that, if we consider a D5-brane, not only the RR form of degree six couples to the brane, but also all RR with lower degree could couple. Here, due to the interior product ι_χ^2, which basically counts as form-degree -2, also RR forms of degree higher than six can couple. This features in the RG flow of Chapter 5, where we have a stack of D1-branes which can couple to the RR potential of a D3-brane. The RG flow eventually truly turns the stack of D1-branes into a single D3-brane.

2.2 CONFORMAL FIELD THEORY

This last section is concerned mainly with two dimensional CFT. Ocassionally, we will comment on adaptations to the higher dimensional case. In contrast to the previous sections, here we have more material to cover. Thus, this section is steeper in character. It will mostly compile the necessary tools required in future sections and not give complete derivations. There are several accessible references, from where we draw the material presented here, e.g. [55, 92, 138, 207].

We begin with a lightning introduction to conformal symmetry and quickly specify to $(1+1)$-dimensions and its field theoretic formalism. Thereafter we present a brief survey of boundary conditions in Section 2.2.2. We close with general remarks on interfaces in $(1+1)$-dimensional CFT in Section 2.2.3.

2.2.1 *Conformal Field Theory on the Plane*

Conformal Algebra

We are concerned with conformal transformations in flat space of mostly plus signature. A conformal transformation preserves angles locally, which is expressed through

$$\eta_{\rho\sigma} \frac{\partial x'^\rho}{\partial x^\mu} \frac{\partial x'^\sigma}{\partial x^\nu} = \Lambda(x) \eta_{\mu\nu}. \tag{2.34}$$

$\Lambda(x)$ is a real function of spacetime. Setting $\Lambda = 1$ we observe that ordinary Poincaré transformations form a subset of the conformal transformations. More precisely, they form a subgroup of the conformal group, which in $\mathbb{R}^{1,d-1}$ is $\mathrm{SO}(2,d)$. This may be seen via use of infinitesimal

transformations $x' = x + \epsilon$ in (2.34). One can then group all possible transformations according to four types of generators

A. Translations generated by a vector

$$P_\mu = -i\partial_\mu$$

B. Rotations generated by an antisymmetric tensor

$$L_{\mu\nu} = i\left(x_\mu \partial_\nu - x_v \partial_\mu\right)$$

C. Dilations generated by scalar

$$D = -ix^\mu \partial_\mu$$

D. Special conformal transformations generated by a vector

$$K_\mu = -i\left(2x_\mu x^v \partial_v - (x\cdot x)\partial_\mu\right)$$

In total these give $N = d + \frac{d(d-1)}{2} + 1 + d = \frac{(d+2)(d+1)}{2}$ generators. Precisely the required amount for the Lorentz group on $\mathbb{R}^{1,d-1}$. The isomorphism is given by

$$\begin{aligned} J_{\mu,v} &= L_{\mu v}, \quad J_{-1,\mu} = \tfrac{1}{2}\left(P_\mu - K_\mu\right) \\ J_{-1,0} &= D, \quad J_{0,\mu} = \tfrac{1}{2}\left(P_\mu + K_\mu\right) \end{aligned} \tag{2.35}$$

These indeed generate $\mathfrak{so}(2,d)$,

$$[J_{mn}, J_{rs}] = i\left(\eta_{ms}J_{nr} + \eta_{nr}J_{ms} - \eta_{mr}J_{ns} - \eta_{ns}J_{mr}\right). \tag{2.36}$$

In two dimensions the situation is more interesting. The global conformal group $\mathrm{SO}(2,2)$ is only a subgroup of the group of conformal transformations. Let us Wick rotate onto the Euclidean plane; more precisely we work with its compactification, the Riemann sphere $\mathbb{C}\cup\infty$. Then, *all* holomorphic and anti-holomorphic functions are angle preserving and therefore conformal transformations. These are obviously infinite dimensional vector spaces and so the conformal group is infinite in two dimensions. It is generated by operators $L_n, \overline{L}_n$ with $n \in \mathbb{Z}$, which form two commuting copies of the *Virasoro algebra*

Actually, the angle preserving maps are all meromorphic functions. However, we will stick to the CFT literature where this is tacitly implied when we say holomorphic.

$$[L_m, L_n] = (m-n)L_{m+n} + \frac{\mathsf{c}}{12}\left(m^3 - m\right)\delta_{m+n,0} \tag{2.37}$$

$$\left[\overline{L}_m, \overline{L}_n\right] = (m-n)\overline{L}_{m+n} + \frac{\overline{\mathsf{c}}}{12}\left(m^3 - m\right)\delta_{m+n,0} \tag{2.38}$$

$$\left[L_n, \overline{L}_m\right] = 0 \tag{2.39}$$

It can be shown that only six out of all these generators are well-defined everywhere on the Riemann sphere, namely $L_0, L_{\pm 1}$ and their anti-holomorphic counterparts. It is these six, which generate the subgroup

$\mathrm{SO}(2,2)$. The *central charges* c and $\overline{\mathsf{c}}$ commute with all other generators. Thus, by Schur's Lemma, on irreducible representations it assumes a fixed value. In fact, in a given theory it will always assume the same value on all of the occuring representations. For instance the free boson has $\mathsf{c} = \overline{\mathsf{c}} = 1$, while the free fermion has $\mathsf{c} = \overline{\mathsf{c}} = 1/2$. In this work we will only be concerned with theories, which have $\mathsf{c} = \overline{\mathsf{c}}$. Moreover, the value of the central charge is large in holographic theories. To abbreviate (2.37) we oftentimes write $\mathsf{Vir} \times \overline{\mathsf{Vir}}$. Let us point out that the Virasoro generators are the modes of the energy momentum tensor of the CFT

$$T(z) = \sum_{n\in\mathbb{N}} z^{-n-2} L_n, \quad \overline{T}(\overline{z}) = \sum_{n\in\mathbb{N}} \overline{z}^{-n-2} \overline{L}_n. \tag{2.40}$$

The Spectrum

Now that we have the Virasoro algebra at our disposal we can organize the spectrum according to its representations. Firstly, choose a basis in which L_0 and $\overline{L}_0$ are diagonal. Then we introduce a specific set of states called *primary states*, which satisfy

$$L_0|\phi\rangle = h|\phi\rangle, \tag{2.41}$$
$$\overline{L}_0|\phi\rangle = \overline{h}|\phi\rangle \tag{2.42}$$
$$L_n|\phi\rangle = \overline{L}_n|\phi\rangle = 0, \qquad n > 0. \tag{2.43}$$

The eigenvalue h is called the *conformal weight*, $\overline{h}$ is the anti-conformal weight while their sum, $\Delta = h + \overline{h}$, is called *conformal dimension* and their difference, $s = h - \overline{h}$ is the *conformal spin*. Primaries lie at the heart of the description of conformally invariant theories, because they are highest weight states of the Virasoro algebra. When there is a finite amount of primary states, the theory is called *rational*, and *irrational*, when there is an infinite amount of primaries. The former class of CFTs is understood to a large degree, while for the latter class only few examples exist, which are under good control. Most of the discussion from here on out is analogous for the holomorphic and anti-holomorphic sector, so that we discuss mostly only the former and comment on the latter when necessary.

Observe that due to

$$[L_0, L_{-m}] = mL_{-m} \tag{2.44}$$

the application of Virasoro modes with negative subscript increments the conformal weight. Each primary gives rise to an infinite tower of *descendants*,

$$L_{-k_1} L_{-k_2} \cdots L_{-k_n} |\phi\rangle \quad (1 \leq k_1 \leq \cdots \leq k_n)\,, \tag{2.45}$$

with conformal dimensions

$$h' = h + k_1 + k_2 + \cdots + k_n \equiv h + N. \tag{2.46}$$

Any state in a conformal field theory is either a primary or a descendant. A *conformal family* $[\phi]$ is simply the collection of a single primary and all of its descendants. Be aware that a conformal transformation will never mix different conformal families. Note that (2.45) are only the holomorphic descendants and each primary has an analogous set of anti-holomorphic descendants where L_n is replaced by $\overline{L}_n$. Of course, we have to also replace h by $\overline{h}$ in (2.46).

There are important caveats about reducibility of the conformal representations leading to constraints on correlation functions, which we will not discuss here. These arise when a state is simultaneously primary and descendant. Such states are called null.

Let us call the set of all primaries of the theory I. Its elements consist of tupels $(i, \bar{\imath})$, where i labels the holomorphic piece of the primary with conformal weight h_i and $\bar{\imath}$ labels the antiholomorphic piece with conformal weight $h_{\bar{\imath}}$. When we wish to be specific we write $|\phi_{i,\bar{\imath}}\rangle$ for a primary state.

In generality, covariance of a quantum field theory under some symmetry algebra $\mathcal{W} \times \overline{\mathcal{W}}$ means that its spectrum carries an action of this algebra. In our case $\mathcal{W} = \mathsf{Vir}$ and $\overline{\mathcal{W}} = \overline{\mathsf{Vir}}$. We are concerned with theories, whose state space consists of superselection sectors,

$$\mathcal{H} = \bigoplus_{(i,\bar{\imath})\in I} M_{i,\bar{\imath}}\, \mathcal{H}_i \otimes \mathcal{H}_{\bar{\imath}}, \tag{2.47}$$

where $\mathcal{H}_i$ and $\mathcal{H}_{\bar{\imath}}$ are irreducible representations of the conformal algebra. They are synonymous with conformal families. The reason we do not write $[\phi_{(i,\bar{\imath})}]$ in (2.47), however, is that $[\phi]$ is usually reserved for the *fields* rather than the states. We have not properly introduced fields, but let us briefly mention that in a CFT there is an isomorphism between fields and states called the *operator state correspondence*. Lastly, $M_{i,\bar{\imath}}$ counts the multiplicity of each primary field in the theory at hand.

Every unitary CFT contains one primary state with conformal weights $h = \overline{h} = 0$. From (2.41) it is clear that it is annihilated also by L_0, $\overline{L}_0$. It is not difficult to show that this state is also annihilated by L_{-1}, $\overline{L}_{-1}$, which generate translations, and so this state is invariant under the global conformal group $\mathrm{SO}(2,2)$. In fact this state is unique. This is enough to identify it as the vacuum of the theory. Let us label it by $i = \bar{\imath} = 0$. Then we can concisely capture this in $M_{0,0} = 1$.

The vacuum corresponds to the identity field $\mathbb{1}$, which is the only field in a CFT without boundary condition which has a non-vanishing one-point function.

The partition function is then given by

$$Z(\tau, \overline{\tau}) = \sum_{(i,\bar{\imath})\in I} M_{i,\bar{\imath}}\, \chi_i(q)\, \chi_{\bar{\imath}}(\overline{q}), \tag{2.48}$$

where $q = e^{2\pi i \tau}$ and $\overline{q}$ its complex conjugate. The *modular parameter* τ is itself complex. The *characters*,

$$\chi_i(q) = \mathrm{Tr}_{\mathcal{H}_i} q^{L_0 - \frac{c}{24}}, \tag{2.49}$$

count the states in the irreducible conformal representation $\mathcal{H}_i$.

Wess-Zumino-Witten Models

We will mostly be interested in theories, which obey more symmetry than just conformal invariance. Among all such theories Wess-Zumino-Witten (WZW) are, perhaps, understood best. The literature on them is vast and we will only summarize the necessary elements here. Excellent introductions can be found in [55, 92, 137], which are all rooted in the seminal work [232].

The spectrum of Wess-Zumino-Witten models carries, additonally to $\mathsf{Vir} \times \overline{\mathsf{Vir}}$, an action of a *Kac-Moody algebra* $\hat{\mathfrak{g}}_k$,

$$\left[J_n^a, J_m^b\right] = i f^{abc} J_{n+m}^c + kn\delta^{ab}\delta_{n,-m}. \tag{2.50}$$

As in the Virasoro algebra, we have a central element, k, which commutes with all other generators of the algebra. Note also the appearance of the structure constants f^{abc} of the underlying Lie algebra $\mathfrak{g}$ and thus a, b, c run over its adjoint representation. In fact, we can identify the Lie bracket of $\mathfrak{g}$ by fixing $n = m = 0$ in (2.50). The relation of the Kac-Moody modes to the Virasoro modes is

$$[L_n, J_m^a] = -mJ_{n+m}^a. \tag{2.51}$$

This is implies that the Kac-Moody generators are modes of current fields with (anti-) conformal weight one

$$J^a(z) = \sum_{n\in\mathbf{Z}} z^{-n-1} J_n^a \tag{2.52}$$

Both, (2.50) and (2.52) have an anti-holomorphic counterpart. The energy momentum tensor is given by currents through the so-called *Sugawara construction*,

$$T(z) = \frac{1}{2(k+g)} \sum_a \left(J^a J^a\right)(z). \tag{2.53}$$

Here, the parentheses enclosing the currents indicate a normal ordered product and g is the dual coxeter number. In the case of our interest, $\hat{su}(N)_k$ we have $g = N$. Whenever there is an extended symmetry, it is sensible to classify the state space according to the highest weight states of the extended symmetry algebra, instead of the Virasoro algebra. For this a thorough analysis of the representation theory of affine Lie algebras is required. This would take us too far affield and thus we contend ourselves with the example most relevant to the original Kondo problem, $\hat{\mathfrak{su}}(2)_k$. It has $k+1$ highest weight states also termed *WZW-primaries* each labelled by a half integer $j = 0, 1/2, 1, \ldots k/2$, which

carries the interpretation of spin. We can write down this model's partition function,

$$Z(\tau,\overline{\tau}) = \sum_{j=0}^{k/2} |\chi_j(\tau)|^2, \tag{2.54}$$

where the sum runs over half-integers. In this model the characters in the holomorphic and anti-holomorphic sector turn out to be complex conjugates of each other leading to the absolute value. Furthermore, this model has an infinite amount of Virasoro primary states, which, remarkably, are repackaged into a finite number of WZW primaries.

It can be shown that all WZW-primaries are also Virasoro primary, while the converse is not true. We will not always indicate with respect to which algebra a state is primary. However, in the presence of an extended symmetry we will always mean the primaries of the extended algebra. Similarly, the symbol $[\phi_i]$ will stand for a *WZW family* corresponding to the i-th WZW primary, whose descendants can be computed analogously to (2.45) with the L_n replaced by J_n. We call the set of WZW primaries $I_{\mathcal{W}}$.

Fusion Rules

Whenever representations are at hand, we may ask what their tensor products are, which should decompose into a sum of irreducible representations of the algebra, weighted by Clebsch-Gordan-type coefficients. In our case the representations are infinite dimensional and the regular tensor product developes unwanted properties. However, an appropiate tensor product can be defined [133, 189]. It is called the *fusion product*,

$$[\phi_i] \times [\phi_j] = \sum_k N_{ij}^k \, [\phi_k]. \tag{2.55}$$

Here, $[\phi_i]$ stands for a representation of the chiral algebra, which in the case of an Kac-Moody symmetry algebra corresponds to a WZW family. When there is no extended symmetry $[\phi_i]$ labels conformal families (we omit the anti-holomorphic label $\bar{\imath}$). The coefficients N_{ij}^k, which are the analogue of the Clebsch-Gordan coefficients, are called *fusion rules*. They are symmetric in the lower two indices,

$$N_{ij}^k = N_{ji}^k \tag{2.56}$$

and satisfy an associativity relation

$$\sum_m N_{im}^l \, N_{jk}^m = \sum_n N_{ij}^n \, N_{nk}^l. \tag{2.57}$$

The vacuum representation, which we have labeled $i = 0$, behaves like a unit under fusion, $N_{0j}^{k} = \delta_{i,k}$. Moreover, we can introduce the conjugate representation, i^{+}, of i via the relation,

$$N_{ij}^{0} = \delta_{j,i^{+}}. \tag{2.58}$$

We are most interested in the algebra $\hat{\mathfrak{su}}(2)_k$, for which each representation associated with a primary field is its own conjugate, i.e., $N_{ii}^{0} = 1$. This model's full fusion rules are

$$N_{j_1 j_2}^{j_3} = \begin{cases} 1 & \text{if } |j_1 - j_2| \leq j_3 \leq \min(j_1 + j_2, k - j_1 - j_2) \text{ and } j_1 + j_2 + j_3 \in \mathbb{Z}, \\ 0 & \text{otherwise.} \end{cases} \tag{2.59}$$

2.2.2 *Boundary Conformal Field Theory*

We are now set to introduce boundaries to a CFT. This program was single-handedly invoked by Cardy in [67] and many good reviews can be found [68, 134, 207]; we draw mainly from the latter.

Gluing Conditions and Boundary Spectra

While ordinary CFT is defined on the entire complex plane, we now introduce a boundary with boundary condition α along the real line. The theory is then defined only on the upper half plane $\Im z \geq 0$. Translational invariance perpendicular to the boundary is broken and we must secure that no energy nor momentum leak through the boundary to the lower half plane. This is accomplished by

$$T(z) = \overline{T}(\overline{z}) \quad \text{for } z = \overline{z}. \tag{2.60}$$

Relations, which relate holomorphic to antiholomorphic fields at the boundary are called *gluing conditions*. Any boundary condition α which respects (2.60) is a *conformal boundary condition*. They have one crucial implication. Recall that CFTs on the entire plane are governed by two *independent* copies of the Virasoro algebra. Introducing a boundary relates the two copies via (2.60), so that the theory carries an action of only a single Virasoro algebra. Thus the spectrum is no longer organized in terms of products of representations of the chiral algebra, (2.47), but only single copies

$$\mathcal{H}_{\alpha} = \bigoplus_{i} \mathcal{H}_{i}^{n_{\alpha}^{i}}, \tag{2.61}$$

where i labels again representations of the chiral algebra and α a conformal boundary condition. The n_{α}^{i} account for possible multiplicities of one representation.

Extended symmetries must also be glued and we will restrict to the case of a Kac-Moody algebra and rational CFT. If we are interested only in conformal boundary conditions, we may impose any gluing,

$$J(z) = \Omega[\overline{J}(\overline{z})] \quad \text{for } z = \overline{z}, \tag{2.62}$$

so long as we respect (2.60). Ω is a local automorphism of the chiral algebra $\hat{\mathfrak{g}}_k$ and must satisfy $\Omega[T] = T$.

We will stick to the simplest case, $\Omega = \mathbb{1}$, known as the *Cardy case*. In this case Cardy [67] taught us that there is a finite set of conformal boundary conditions, each labelled by one primary of the chiral algebra. This prompts us to label the conformal boundary conditions by the set of primaries I, i.e., $\alpha = i$. Furthermore, Cardy managed to show that the multiplicities in (2.61) are in fact given by the fusion rules $n^i_\alpha \equiv n^i_j = N^i_{jj}$. We can then write down the partition function of the theory

$$Z_{\alpha=j}(\tau) = \sum_{i \in I_{\mathcal{W}}} N^i_{jj}\, \chi_i(\tau) \tag{2.63}$$

The subscript on Z declares, which boundary condition the theory is concerned with.

An Example

For our guinea pig, $\hat{\mathfrak{su}}(2)_k$, we straightforwardly get

$$Z_{\alpha=j}(\tau) = \sum_{i=0}^{k/2} N^i_{jj}\, \chi_i(\tau). \tag{2.64}$$

This is to be contrasted with (2.54). In string theory BCFT describes open strings, i.e. branes. In that context (2.63) (and thus (2.64)) count the field content on the worldvolume of a brane.

Let us go on to assign a geometric interpretation to the specific boundary conditions of $\hat{\mathfrak{su}}(2)_k$ as branes. This is essential in the Kondo effect. WZW models are conformal field theories with group target, that is, they map the complex plane or the upper half plane into the group manifold. In the case at hand this is $\mathrm{SU}(2) \simeq S^3$. Each boundary condition corresponds to a conjugacy class on $\mathrm{SU}(2)$. There are two distinct types of boundary conditions for $\mathrm{SU}(2)$

POINTLIKE (D0) The conjugacy classes of the two center elements $\pm e$, with e the group unit. These are zero dimensional sets. We call these D0-branes because they occupy no spatial direction. Their spectrum is given by (2.64) with $j = 0$ for the north and $j = k/2$ for the south pole.

SPHERICAL (D2) All other conjugacy classes are two dimensional and known to coincide with two spheres wrapping $\mathrm{SU}(2) \simeq S^3$.

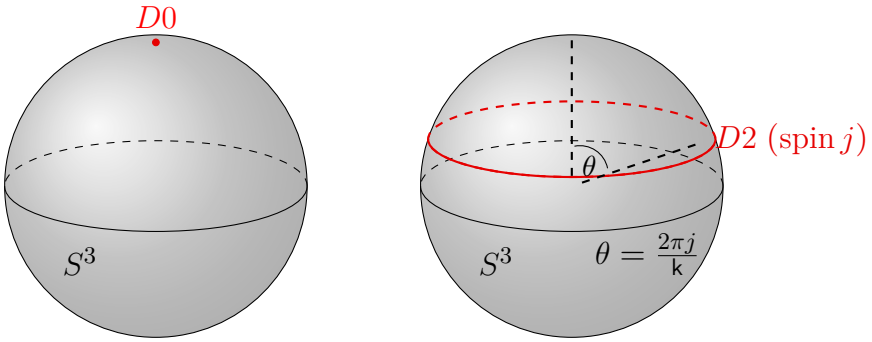

Figure 4: Left: D0-brane boundary condition. These correspond to spin $j = 0$ and $j = k/2$. Right: D2-brane boundary condition. These correspond to spin $j = 1/2, 1, \ldots k$

> Once a Cartan torus is chosen, one still has half a $U(1)$'s worth of these conjugacy classes to choose from. We call these D2-branes, because they occupy two spatial directions. Their spectrum is given by (2.64) with $j \neq 0$ and $j \neq k/2$.

Now, since there is only a finite set of primaries and hence only a finite set of boundary conditions, not every conjugacy class can correspond to a boundary condition. Let us choose a Cartan torus. This amounts to choosing spherical coordinates and labelling a north and south pole. The pointlike conjugacy classes sit at these poles. The north pole corresponds to the primary of the vacuum, $j = 0$, while the south pole corresponds to $j = k/2$. Introduce a polar angle $\theta \in [0, \pi]$, say. The remaining $k - 1$ boundary conditions correspond to conjugacy classes, which are equally spaced on the polar angle $\theta = \frac{2\pi j}{k}$. This is illustrated in Figure 4.

Boundary States

The data of each BCFT can be captured elegantly in *boundary states* $\|\mathcal{B}\rangle\rangle$. These are built from objects availale in the CFT without boundary, and are thus not elements of (2.63). The reason we can construct these states anyway is traced back to worldsheet duality. The basis for constructing the boundary states is (2.60), which instates that no energy-momentum leaks through to the lower half plane. Via worldsheet duality this condition maps into an operator $(L_n - \overline{L}_{-n})$, which in turn defines the boundary states

$$(L_n - \overline{L}_{-n})\|\mathcal{B}\rangle\rangle = 0, \qquad n \in \mathbb{Z} \tag{2.65}$$

Any solution $\|\mathcal{B}\rangle\rangle$ to this infinite amount of linear equations gives rise to a sensible BCFT. It can be shown that for a rational CFT on the full plane with p primaries, there are exactly p solutions $\|\mathcal{B}\rangle\rangle$. This

means that for this CFT we only have p admissible conformal boundary conditions.

Whenever extended symmetries are present we get another set of equations of similar type for the currents of this extra symmetry. Kac-Moody symmetries, for instance, were glued according to (2.62). This maps into

$$(J_n + \Omega[\overline{J}_{-n}])\|\mathcal{B}\rangle\rangle = 0 \tag{2.66}$$

We will make no explicit use boundary states in our calculations below, which is why we keep our discussion on boundary states at a minimum. Nevertheless, anybody who wishes to seriously work with BCFT should however take a closer look either at the original source [162, 195] or the reviews [55, 68, 134, 207]. For our purposes boundary states provide an excellent vantage point to introduce interfaces.

2.2.3 *Interfaces in Conformal Field Theory*

Interfaces provide mappings between theories through generalized boundary conditions. This turns them into rich playgrounds for a great host of ideas For instance they are of interest when studying the interplay of (conformal) field theories [29, 43, 61, 132, 198], in holography [11, 32, 53, 90, 111, 167, 168, 185], in impurity problems [16, 170, 186, 202, 203, 214] and entanglement [51, 58]. The Kondo effect, to be discussed in Chapter 4, is one such example and a great portion of this thesis is dedicated to studying Kondo analogues in holography. In this section we follow [32].

Folding Trick

Let us consider tensor products of two possibly distinct CFTs, $\text{CFT}_1 \otimes \text{CFT}_2$. The findings of this chapter are straightforwarldy generalized to an arbitrary number of CFTs, but for the purposes of this thesis, two suffice. We confine $\text{CFT}_1 \otimes \text{CFT}_2$ to the upper half-plane, $\Im(z) \geq 0$, as in the previous section. The obvious question is: What are the allowed boundary states of this new system? The formal answer is given by the analogue of (2.65),

$$(L_n^{(1)} + L_n^{(2)} - \overline{L}_{-n}^{(1)} - \overline{L}_{-n}^{(2)})\|\mathcal{B}\rangle\rangle = 0, \qquad n \in \mathbb{Z}, \tag{2.67}$$

where $L_n^{(i)}$ and $\overline{L}_n^{(i)}$ are the Virasoro modes of CFT_i, with $i = 1, 2$. Now comes a conceptual leap: we unfold CFT2 onto the lower half plane with $\Im(z) \leq 0$. Note that the relative orientation of CFT_2 towards the boundary changes under this operation. To correct for that we

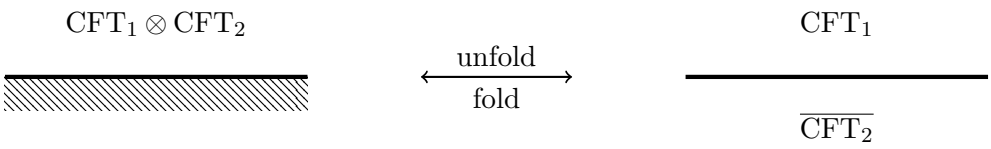

Figure 5: The BCFT of the combined system $\mathrm{CFT}_1 \otimes \mathrm{CFT}_2$ (left) is unfolded along the boundary into an interface theory between CFT_1 on the upper half-plane and $\overline{\mathrm{CFT}_2}$ on the lower half-plane (right). Similarly, interface theories can be folded along the interface into boundary theories.

have to exchange the holomorphic and antiholomorphic sectors; this is indicated by

$$\mathrm{CFT}_2 \to \overline{\mathrm{CFT}_2} \tag{2.68}$$

The picture at hand is now that we have CFT_1 on the upper half-plane and $\overline{\mathrm{CFT}_2}$ on the lower half-plane, separated by the real line; see Figure 5. The separation line is called an *interface* or a *domain wall*. When we have $\mathrm{CFT}_1 = \mathrm{CFT}_2$ we speak of *defects* rather than interfaces.

When working with a boundary on the real line line, i.e. before unfolding, condition (2.67) prohibited energy-momentum flow across the boundary. After unfolding we get

$$(L_n^{(1)} + \overline{L}_n^{(2)} - \overline{L}_{-n}^{(1)} - L_{-n}^{(2)})\|\mathcal{B}\rangle\rangle = 0, \qquad n \in \mathbb{Z}, \tag{2.69}$$

and its interpretation changes. It now implies continuity of $T - \overline{T}$ along the real line, with $T = T^{(1)} + T^{(2)}$ [32]. The deep insight here is that we can speak of boundaries of tensor product theories and interfaces interchangeably.

The next step is to analyze some possible solutions to (2.69) (equivalently we could stick with (2.67)). One possible solution is for instance

$$\|\mathcal{B}\rangle\rangle_{\text{Reflect}} = \|\mathcal{B}_1\rangle\rangle \otimes \|\mathcal{B}_2\rangle\rangle. \tag{2.70}$$

The fact that the state factorizes implies that $(L_n^{(1)} - \overline{L}_{-n}^{(1)})$ and $(\overline{L}_{-n}^{(1)} - L_n^{(2)})$ individually annhilate the boundary state $\|\mathcal{B}\rangle\rangle$. While the former is equivalent to (2.65) for the upper half-plane, the latter is too, but after application of (2.68). This means that there is no energy-momentum leak across the interface neither from above, nor from below. CFT_1 and CFT_2 do not communicate and one is urged to say that both theories decouple. This is true, up to the subtlety that the boundary conditions on the lower half-plane and the upper half-plane may be correlated. Nevertheless, we speak of *factorizable* boundary states whenever (2.70) holds.

We have more options than this, since now we could for instance also consider the possibility where the interface simply glues $T^{(1)} = \overline{T}^{(2)}$ and $\overline{T}^{(1)} = T^{(2)}$ at $z = \overline{z}$ (in the boundary theory these correspond to $T^{(1)} = T^{(2)}$ and $\overline{T}^{(1)} = \overline{T}^{(2)}$ respectively). This corresponds to the operator relations

$$\left(L_n^{(1)} - \overline{L}_{-n}^{(2)}\right) \|\mathcal{B}\rangle\rangle_{\text{transmit}} = 0 \tag{2.71}$$

$$\left(L_n^{(2)} - \overline{L}_{-n}^{(1)}\right) \|\mathcal{B}\rangle\rangle_{\text{transmit}} = 0 \tag{2.72}$$

These interfaces are totally transmissive, letting through all information across the real line. The simplest case of this scenario occures when $\text{CFT}_1 = \text{CFT}_2$. The theories must not be identical however. For instance, the upper theory could be a free scalar compactified at radius R, while the lower theory is again a free scalar, but now compactified at radius $r \neq R$.

Totally reflective boundary states, (2.70) and totally transmissive boundary states, (2.71), lie at the two extremes of possible boundary states for interfaces. Generic interfaces will lie somewhere in between and in general will be described by some entangled boundary state. These boundary states are in general difficult to find. Quantitative statements on how close they are to either the reflective or transmissive extreme are captured by the reflection and transmission coefficients [184, 205]. This concludes our preliminary material.

s

3

THE GAUGE/GRAVITY CORRESPONDENCE

This chapter contains a lightning introduction to the celebrated AdS/CFT correspondence following [18, 54, 216]. Since its discovery in 1997 by Juan Maldacena [179], it has reshaped the way we think about gravity and gauge theories. We mention right off the bat that there is no mathematically rigorous proof of this correspondence. Moreover, it is not clear whether, with the current mathematical vantage point, there can be a proof at all, since there is no clear-cut definition of the theories in question. Nevertheless over the years an overwhelming amount of evidence in its favor has been gathered by theoretical physicists so that it is widely believed to be true. It has become an integral part of modern theoretical physics and has found its way into almost any branch of physics including gravity, condensed matter theory and quantum information theory.

In physics *dualities* relate seeminingly different concepts to one another and often lead the way to novel insights. More precisely, the Hilbert spaces and the dynamical data of two distinct theories are equated and thus dualities furnish mathematical equivalences between these theories. Usually dualities connect theories with the same type of degrees of freedom. For instance in string theory we like to use the so-called T- and S-duality, mapping one string theory into another string theory. What is remarkable about the gauge gravity correspondence is that it links two theories, which traditionally were thought to describe two completely different types of degrees of freedom, namely gauge field theories and string theories. While the former is thought of as a theory of elementary particles, the latter is a candidate for quantum gravity.

It becomes even more intriguing: the gravity theory is at home in one dimension higher than the gauge theory. The gauge/gravity correspondence is therefore a concrete manifestation of the *holographic principle* [156, 157, 222]. This notion arose in the context of semi-classical gravity, when people realized that the information stored in a volume V_{d+1} can be read off of its boundary area A_d. Examples of this are black holes, whose entropy is given by the area of its event horizon. For a certain class of supersymmetric black holes this analogy could be succesfully carried to the quantum level [221]. This is in fact one of string theory's unrivaled merits.

Let us state the correspondence before motivating it:

$\mathcal{N} = 4$ Super Yang-Mills theory with gauge group $SU(N)$

is *dynamically equivalent* to

type IIB string theory compactified on $\mathrm{AdS}_5 \times \mathrm{S}^5$.

The super Yang-Mills (SYM) theory is conformally invariant, hence it is the CFT, or gauge side of the correspondence. It has two free parameters: the gauge rank N and the Yang-Mills coupling constant g_{YM}. Obviously, the $\mathrm{AdS}_5 \times \mathrm{S}^5$ lends its name to the gravity side of the correspondence. Both metric factors have constant curvature, and, while it is negative on the first factor, it is positive on the second. Moreover, due to supersymmetry they are set by the same number L, which we call the AdS radius. The gauge rank in the field theory is mirrored on the gravity side as N units of Ramond-Ramond (RR) four-form flux contained on S^5. We will lay down more details below. The string theory is controlled by two perturbation parameters, the string coupling constant g_s and the string length $l_s = \sqrt{\alpha'}$. In fact, it is not quite the string length, which is physically important here. Rather, its relation to the curvature scale of the geometry L/l_s is meaningful, since it informs us whether the strings are "small".

Much as electrons are charged under a gauge field, in string theory we have higher-dimensional objects called D-branes charged under RR gauge fields, each with an associated field strength.

The coupling constants on the two sides of the correspondence are identified as follows:

$$g_{YM}^2 = 2\pi g_s, \qquad 2g_{YM}^2 N = \frac{\mathsf{L}^4}{l_s^4}. \tag{3.1}$$

On the LHS we have written the field theory parameters, while the RHS displays the gravity parameters. Soon we will be interested in the large N limit, in which the field theory becomes semiclassical and its effective coupling constant is the combination $\lambda = g_{YM}^2 N$, called the *'t Hooft coupling*. As stated in the box, the correspondence is in its *strongest* form and conjectures the field theory and the string theory to be equivalent for arbitrary values of parameters in (3.1). Below we will motivate only its *weak* form, which imposes $N \to \infty$, $g_s \to 0$, $\lambda = g_{YM}^2 N \to \infty$. We emphasize that this maps a weakly coupled string theory into a strongly coupled field theory.

Being a duality, all objects of one theory have a pendant in the other. Empty $\mathrm{AdS}_5 \times \mathrm{S}^5$, for instance, is dual to the vacuum state in the field theory and we sometimes refer to the latter as the hologram. We may also consider excitations such as thermal states. They correspond to black holes in the interior of $\mathrm{AdS}_5 \times \mathrm{S}^5$, whose energy is determined by the Hawking temperature. Of course, the geometry is then no longer globally $\mathrm{AdS}_5 \times \mathrm{S}^5$, but only asymptotically so.

This chapter is organized as follows. We begin by introducing D3 branes and thereafter discuss their physics in two possible ways: (a) as a gauge theory in Section 3.1.1 and (b) as a solution to supergravity

$\mathbb{R}^{9,1}$	0	1	2	3	4	5	6	7	8	9
N $D3$	•	•	•	•	-	-	-	-	-	-

Table 5: A "•" indicates a brane extended in this direction, while a "-" means that the brane is pointlike in this direction.

Section 3.1.2. The combination of both viewpoints motivates the AdS/CFT conjecture as originally posed by Maldacena in [179] and we discuss it in Section 3.2. Subsequently, we give further evidence for the correspondence in Section 3.2.1 and relate the partition functions of the CFT and AdS sides of the correspondence in Section 3.2.2. For the purposes of this work we need a cousin of the correspondence which is situated in $\mathrm{AdS}_3 \times \mathrm{S}^3 \times T^4$ and we dedicate the rest of this chapter to reviewing this case.

3.1 TWO PERSONALITIES, ONE HOST: D3 BRANES

Prior to the discovery of the gauge/gravity correspondence physicists were studying black holes in string theory in an effort to understand their microscopic features. It is therefore no surprise that the central objects are branes, i.e. solutions of string theory, which produce geometries with event horizons[1]. The magic and appeal of these objects lie in that they not only give rise to black geometries, but also harbor gauge field theories on their worldvolume. This is in sharp contrast to ordinary black holes in general relativity and it is this feature which gives rise to the AdS/CFT correspondence.

For our immediate purposes we restrict ourselves to D3 branes, i.e. (3+1)-dimensional surfaces on which fundamental strings may end. Other realizations of the gauge/gravity correspondence in different dimensions can be found by considering different kinds and combinations of branes. Readers unfamiliar with these concepts from string theory are invited to look into Chapter 2, where we compile the required information for this work.

We study type IIB string theory in flat, ten-dimensional Minkowski spacetime $\mathbb{R}^{9,1}$ and we embed N flat and parallel D3 branes along the directions $x^0, \ldots, x^3$ as indicated in Table 5. In the transverse directions we conveniently place the brane at the origin, $x^4 = \cdots = x^9 = 0$.

Type IIB string theory has 32 supersymmetries and, remarkably, a D3 breakes just one half thereof. It is therefore $\frac{1}{2}$-BPS; see Section A.1 for the terminology. When considering a stack of *coincident* D3 branes we again only break 16 out of the 32 supersymmetries. Of course, ten-dimensional Poincaré symmetry is also broken into smaller pieces. Along the brane we preserve four-dimensional Poincaré symmetry, while in the six transverse directions, where the brane appears to

Type IIB string theory has $\mathcal{N} = 2$ supersymmetry in $d = 10$. This means its supersymmetries organize into two Majorana-Weyl spinors, each with 16 components.

1 Our D3 brane is an example of an extremal charged black hole. This means it has two horizons whose loci coincide.

be a point, we are left with an $SO(6)$ worth of rotations about the brane.

The next two subsections present the possible ways in which we can can now describe this physical system i.e. as a gauge theory in Section 3.1.1 and as a supergravity solution in Section 3.1.2. Both descriptions are valid in *different* regimes of the parameters in (3.1). Before delivering the details however, let us anticipate the idea behind the AdS/CFT correspondence: Both descriptions model the same physical system albeit being analytically tractable only in a specific regime. We will spell this out more clearly in Section 3.2.

A Remark for Non-String-Theorists

In string theory we have two basic types of strings, *closed strings* and *open strings*. The former give rise to the graviton, the dilaton ϕ and an antisymmetric two-form B called the Kalb-Ramond field or Neveu-Schwarz (NS) two-form. For now we set $B = 0$; it will only become important in later chapters. Its role is laid out more explicitly in Chapter 2. The second kind of string, open strings, end on extended objects, called Dp-branes, where they give rise to gauge degrees of freedom. String theory possesses a mapping called open-closed duality, which relates descriptions in terms of either string type to the other. This lies at the heart of the AdS/CFT correspondence. Hence we will lay down a description in terms of open strings and follow up by one in terms of closed strings in the next two sections.

3.1.1 *Open String Picture*

Our discussion here follows closely that of [18]. D-branes are surfaces in space on which fundamental strings may end. On this worldvolume, here the four-manifold parametrized by $x^0, \ldots, x^3$, the string excitations give rise to gauge degrees of freedom. This picture is however only reliable when the string is perturbative, i.e. $g_s \ll 1$. Since we are dealing with a stack of branes the strings may start on one brane but end on another. This implies that the effective coupling constant for string perturbation theory is now $g_s N$ and it is rather this combination which has to be small. Observe using (3.1) that it is proportional to $\lambda = g_{YM}^2 N$. Incidentally the limit $g_s N \ll 1$ ensures that the branes do not backreact on the ambient geometry $\mathbb{R}^{9,1}$. Hence we may think of the D3-branes as probes inside ten-dimensional Minkowski space. In later sections we will be forced to take N to be a large number. To draw a connection to the current discussion we will also assume this to be the case here, but only such that $g_s N \ll 1$ is not violated. Hence we can then safely take g_s to be small, at least parametrically in N.

We take $N \gg 1$ and $g_s \ll 1$ such that the limit $g_s N \ll 1$, in which the open string picture is reliable, is not violated.

In this weak coupling limit the system is described by open strings, interpreted as excitations of the (3+1) dimensional plane, closed strings

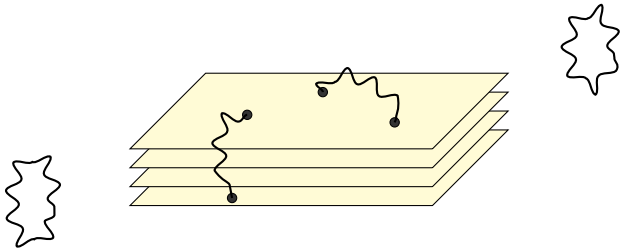

Figure 6: Open strings, governed by S_{open}, attach to a stack of D3-branes. Closed strings, governed by S_{closed}, surround the stack of D3-branes in (9+1)-dimensional spacetime. Both types of string can interact via S_{int}.

surrounding the brane, interpreted as excitations of the (9+1)-dimensional geometry, and their interactions

$$S = S_{\text{closed}} + S_{\text{open}} + S_{\text{int}}. \tag{3.2}$$

This is depicted in Figure 6. Both, the open and closed strings, have massless states as well as infinite towers of massive relativistic excitations with energies $M^2 \sim 1/l_s^2$. Since the string length is very small, already the low lying massive states are very energetic. It is convenient to integrate these excitations out. That is to say that we are taking the "low energy limit"

$$E^2 \ll \frac{1}{l_s^2}. \tag{3.3}$$

In this case we gain access to "low energy effective actions", which capture the dynamics of the massless states of the string theory only, which are, in contrast to the full string theory, tractable.

In our setup S_{closed} corresponds to closed strings in type IIB string theory, whose low energy limit is type IIB supergravity. On $\mathbb{R}^{9,1}$ the low-energy excitations are the fields of the graviton super- multiplet, i.e. the graviton h, the dilaton ϕ, the RR-forms and their superpartners respectively. Schematically we have

$$\begin{aligned} S_{\text{closed}} &= \frac{1}{2\kappa^2}\int d^{10}x\sqrt{-g}e^{-2\Phi}(R + 4\partial_M\phi\partial^M\phi) + \dots \\ &\simeq -\frac{1}{2}\int d^{10}x\partial_M h\,\partial^M h + \mathcal{O}(\kappa). \end{aligned} \tag{3.4}$$

Capital latin letters denote ten-dimensional spacetime indices and the ten-dimensional gravitational constant can be expressed in terms of string parameters $2\kappa^2 = (2\pi)^7\alpha'^4 g_s^2$. In going to the second line we expanded the metric in fluctuations around flat space $g = \eta + \kappa h$. The explicit appearance of κ is to ensure canonical normalization of the kinetic terms in the second line. The dots refer to kinetic terms for the RR forms and all superpartners. All of their interactions scale with $\kappa^2 E^8 \propto g_s^2 l_s^8 E^8$, which is small due to (3.3) and since we have

taken $g_s \ll 1$. Therefore, S_{closed} reduces to free supergravity in flat ten-dimensional Minkowski space, describing the strings surrounding the D3 brane.

We now turn our attention to $S_{\text{open}} + S_{\text{int}}$, which at low energies is given in terms of the DBI lagrangian on which details can be found in Section 2.1.2. It is simplest to study it first for a single D3 brane and then mention the adaptations for larger N. It reads

In contrast to the expressions in Section 2.1.2 we have pulled out the constant asymptotic value of the dilaton $\exp\phi = \exp(\phi_0 + \phi(x)) = g_s \exp\phi(x)$.

$$S_{\text{DBI}} = -\frac{1}{(2\pi)^3 l_s^4 g_s} \int d^4x e^{-\phi} \sqrt{-\det(\hat{g} + 2\pi l_s^2 F)} \tag{3.5}$$

Since we have embedded our brane into flat space there is no Kalb-Ramond B-field. The hat on the metric g_{MN} indicates its pullback onto the worldvolume $x^0, \ldots, x^3$ (static gauge) , which we will indicate by greek indices μ, ν. The gauge field strength $F = dA$ corresponds to a gauge connection $A = A_\mu dx^\mu$ living on the worldvolume. There is one scalar field for each transverse direction $x^{i+3} = 2\pi l_s^2 \chi^i$ describing the fluctuations of the brane in the transverse directions. Performing the pullback and expanding $e^{-\phi}$, $g = \eta + \kappa h$ to leading order in $l_s^2 = \alpha'$ gives

$$S_{\text{open}} = -\frac{1}{2\pi g_s} \int d^4x \left(F_{\mu\nu} F^{\mu\nu} + \frac{1}{2} \partial_\mu \chi^i \partial^\mu \chi_i + \mathcal{O}(\alpha') \right), \tag{3.6}$$

$$S_{\text{int}} = -\frac{1}{8\pi g_s} \int d^4x \phi F_{\mu\nu} F^{\mu\nu} + \ldots. \tag{3.7}$$

Of course this is only for a single brane; we are interested in a stack of N D3-branes. Details for the generalization are laid out in (2.27) and (2.29). The upshot is that all derivatives have to covariantized and we have to add the potential term,

$$V = \frac{1}{2\pi g_s} \sum_{i,j} \text{Tr} \left([\chi^i, \chi^j]^2 \right) + \mathcal{O}(\alpha'). \tag{3.8}$$

Given the identification of coupling constants in (3.1) we find that to lowest order in α' the action S_{open} is in fact the bosonic part of $\mathcal{N} = 4$ SYM with gauge group $\text{SU}(N)$ in four dimensions!

Finally, we turn to the interactions, (3.7), They are secretely also of order α'. The reason is that the form as stated above is not canonically normalized and we have to rescale ϕ by $\kappa \propto \alpha' g_s$. Thus there are no interaction terms to lowest order between the open string excitations, i.e. the gauge field, and the closed strings, in this case the dilaton. In contrast to (3.4), where we found a free theory, here we recover a *fully interacting*, albeit weakly coupled QFT, because $\lambda \propto g_s N \ll 1$.Since we agreed on large N above this theory is in a semiclassical limit.

To sum up, a large number N of D3 branes embedded into $\mathbb{R}^{9,1}$ in the limit where they do not backreact, $g_s N \ll 1$, and at low energies $E^2 \ll 1/\alpha'$ (or $\alpha' \ll 1$) can be reliably described by

$$\Big(\text{free supergravity on } \mathbb{R}^{9,1}\Big) \oplus \Big(\mathcal{N} = 4\,\text{SYM theory}\Big) \tag{3.9}$$

within the context of type IIB string theory.

3.1.2 *Closed String Picture*

Our exposition here follows that of [54, 216]. We now turn our attention to a different description of a stack of N D3 branes, one that contains no signs of open strings nor gauge theory and arises purely from considering closed strings; hence the name. The description is in terms of black D3 brane solutions to type IIB supergravity carrying N units of Ramond-Ramond four-form charge. This is a charged black hole solution, albeit instead of spherical geometry it is an extended object (black brane) in spacetime. That this picture is in fact accurate is a conjecture itself [200], but over the years it has passed all tests at our disposal and is therefore believed to be true.

Type II supergravity is a low energy approximation to type II string theory and – before we give the concrete D3 brane solution – we need to understand in what regime we may reliably replace the latter by the former. It will *not* be the same weak coupling limit as in Section 3.1.1. As we will see in Section 3.2 this discrepancy lies at the heart of the AdS/CFT conjecture.

If we were to embed supergravity into string theory, the required corrections would be organized in powers of l_s/L. Here L is a characteristic scale set by the parameters in the supergravity solution as will be shown below and will coincide with the AdS radius in (3.1). In the "point-particle limit", where the string length is much smaller than the characteristic scale,

$$\mathsf{L} \gg l_s \qquad \overset{(3.1)}{\longrightarrow} \qquad g_s N \gg 1, \tag{3.10}$$

corrections to supergravity are safely discarded. Note that this is again a low energy limit in string theory, where we neglect excitations with masses $M \sim 1/l_s^2$. In contrast to our discussion in the gauge theory picture in Section 3.1.1, where we required $g_s N \ll 1$, we find that the supergravity picture is valid at the opposing extreme.

In principle supergravity is a quantum theory of gravity and, if we want to accurately describe it via a classical solution, we have to turn off all quantum fluctuations. This is achieved by tuning the characteristic scale to be much larger than the Planck length l_P,

$$\mathsf{L} \gg l_P \sim (l_s^4 g_s)^{1/4} \qquad \overset{(3.1)}{\longrightarrow} \qquad N \gg 1. \tag{3.11}$$

Supergravity yields a good description of string theory when $N \gg 1$ and $g_s N \gg 1$. Further we restrict to the regime of perturbative string theory $g_s \ll 1$.

This justifies taking the large N limit in the open string picture, since it will have to be the same number when combining the two pictures in Section 3.2. While in the gauge theory picture it encodes the number of D3 branes, we will shortly see that in the supergravity picture it also informs us about the charge of the black brane. In conclusion, supergravity gives a good portrayal of N D3 branes within type IIB string theory when $N \gg 1$ and $g_s N \gg 1$. As long as we do not violate these conditions we are free to take $g_s \ll 1$ and we will choose so in order to be in the regime of perturbative string theory.

Let us now discuss the three-brane solution in question. Apart from the metric it is given by the dilaton and antisymmetric Ramond-Ramond four-form

$$ds^2 = H^{-1/2}\eta_{\mu\nu}dx^\mu dx^\nu + H^{1/2}(dr^2 + r^2 d\Omega_5^2) \tag{3.12a}$$

$$e^\Phi = g_s, \tag{3.12b}$$

$$F_5 = (1+\star)\epsilon_{\mathbb{R}^{1,3}} \wedge dH^{-1}, \tag{3.12c}$$

$$H = 1 + \frac{\mathsf{L}^4}{r^4}, \qquad \mathsf{L}^4 = 4\pi g_s \alpha'^2 N, \quad r^2 = \sum_{i=4}^{9} x^i x^i. \tag{3.12d}$$

The dilaton is constant throughout the solution and is therefore given by its asymptotic value, which we choose to be small, $g_s \ll 1$. The first piece in the metric is four-dimensional Minkowski space and the remainder is six-dimensional Euclidean space written in polar coordinates. Obviously, this solutions carries the expected $SO(1,3) \times SO(6)$ symmetry. This is a fully backreacted solution, which encodes the distortion of spacetime by the presence of the D3 branes. Instead of the Ramond-Ramond four form C_4 we have listed its field strength $F_5 = dC_4$ using the volume form $\epsilon_{\mathbb{R}^{1,3}}$ on the flat worldvolume of the branes. Given this form, we are in a position to confirm the claim we made earlier that this solution has N units of flux,

$$\int_{\mathrm{S}^5} \star F_5 = N, \tag{3.13}$$

through a five-sphere engulfing the branes in the transverse directions, i.e. S^5 is given by $\sum_{i=4}^{9} x^i x^i = 1$. This is possible since the branes appear as points in the transverse directions. We see that we are dealing with a charged black hole and only state without proof that this black hole is in fact extremal.

Charged black holes have two event horizons. When the locations of both horizons coincide, we speak of an extremal charged black hole.

Let us now take a closer look at the (harmonic) function H. Far away from the brane, $r \gg \mathsf{L}$, we have $H = 1$ and the geometry (3.12a) turns into ten-dimensional Minkowski space[2]. The components of F_5 vanish as r^{-5} in this limit. The event horizon is located at the other extreme,

2 In fact, in order to reach (3.12), integration constants were chosen such that this was the case.

$r = 0$, and we zoom into its surroundings – referred to as *near-horizon region* or *throat-region* – via $r \ll \mathsf{L}$,

$$ds^2 = \frac{r^2}{\mathsf{L}^2}\eta_{\mu\nu}dx^\mu dx^\nu + \frac{\mathsf{L}^2}{r^2}(dr^2 + r^2 d\Omega_5^2). \tag{3.14}$$

The first two summands constitute AdS_5 and the last summand is an S^5 of unit radius. Observe that even though the harmonic function H is not regular close to the horizon, $r = 0$, the near-horizon region shows no signs of irregularity.

To sum up, we may think of the D3 solution of supergravity as interpolating between Minkowski space and $\mathrm{AdS}_5 \times \mathrm{S}^5$,

$$ds^2_{\mathrm{AdS}_5\times\mathrm{S}^5} \quad \overset{r\to 0}{\longleftarrow} \quad ds^2_{D3} \quad \overset{r\to\infty}{\longrightarrow} \quad ds^2_{\mathbb{R}^{9,1}}, \tag{3.15}$$

and, almost delightfully, both asymptotic regions feature more symmetry. Recall that the D3 brane solution supports 16 supercharges, which is only half as much as the 32 of either $\mathbb{R}^{9,1}$ or $\mathrm{AdS}_5 \times \mathrm{S}^5$. Even though both asymptotic regions preserve the same amount of supersymmetry, their bosonic symmetries and therefore also the corresponding supersymmetry algebras differ substantially. Poincaré supersymmetry governs Minkowski space $\mathbb{R}^{9,1}$, while $\mathrm{AdS}_5 \times \mathrm{S}^5$ is invariant under the anti-de-Sitter supergroup $PSU(2,2|4)$. We will return to this in Section 3.2.1.

Moreover, to all orders in α' and g_s we know how to quantize string theory on Minkowski space and we say that it is an exact "perturbative ground state" of type IIB string theory. It is not clear on the other hand, how to quantize string theory on $\mathrm{AdS}_5 \times \mathrm{S}^5$. However, it can be shown that it is also an exact perturbative ground state of type IIB string theory [54]. This characteristic will come in handy soon, when we argue that the gauge/gravity duality involves all of string theory on $\mathrm{AdS}_5 \times \mathrm{S}^5$ and not just supergravity. It should be noted that the interpolating solution (3.12) does receive α' corrections when embedded into string theory, which makes the fact that it gives rise to exact perturbative ground states in the limits discussed even more remarkable.

Now that we have a feel for the solution at hand, let us ask what low energy excitations of IIB string theory are admitted on this background. There will be two types:

LONG WAVELENGTH GRAVITONS Gravitons with large wavelengths $\lambda \gg \mathsf{L}$, or equivalently low energies $E \ll 1/\mathsf{L}$ do not fit into the throat-region $r \sim \mathsf{L}$ and therefore occupy the flat asymptotic region $r \gg \mathsf{L}$ far away from the D3 brane. Their couplings to all other degrees of freedom scale to zero with energy and hence the long-wavelength gravitons at hand decouple. Once again we uncover free gravity in flat ten-dimensional Minkowski space!

NEAR-HORIZON STRINGS Normally black holes present us with a gravitational potential well and this solution is no different. Closed

strings near the horizon have fallen down into this well, $r \sim 0$. The required energy to excite a string theory state at small but fixed radius r is $E_r \sim 1/\sqrt{\alpha'}$, which is huge! However, an observer at infinity can only ever see red-shifted energies

$$E_\infty = \sqrt{-g_{00}} E_r = H(r)^{-1/4} E_r \sim \frac{r}{\mathsf{L}} \frac{1}{\sqrt{\alpha'}}, \tag{3.16}$$

and this may be arbitrarily small for small r Let us emphasize that also large energies E_r appear to be small in the throat-region. Thus we expect to find not only supergravity modes, but *all* IIB string theory excitations near the horizon, that is on $\mathrm{AdS}_5 \times \mathrm{S}^5$.

Our proclamation to find the full spectrum of IIB string theory on $AdS_5 \times \mathrm{S}^5$ and not just the IIB supergravity modes might appear a little rushed. Especially since we invested great effort to establish the low-energy limit, in which the supergravity solution (3.12) can be trusted, we would believe that all massive string excitations are not present from the get-go. Here is where the previously introduced fact that $AdS_5 \times \mathrm{S}^5$ is an exact perturbative ground state of IIB string theory saves the day. It implies that all corrections[3] occuring when embedding supergravity into string theory on this background vanish anyways.

Before concluding this section we clarify one aspect of the near-horizon limit. Since we want to be able to distinguish sensibly between small distances from the brane we have to be very careful about how we zoom into the throat-region. Therefore we cannot just naively take $r \to 0$, because this should have this coordinate dimension vanish. We will restore resolution at small values of r by combining small r with the other limit at play here: the decoupling limit $\alpha'/\mathsf{L} \ll 1$ or simply $\alpha' \to 0$. The correct limit,

$$\alpha' \to 0, \quad r \to 0 \quad \text{such that} \quad U \equiv \frac{r}{\alpha'} \quad \text{is fixed}, \tag{3.17}$$

is referred to as the *Maldacena limit*. The new coordinate U can be tuned at will and lets us explore the near horizon-region without ambiguity. It has units of Energy and, once we have established the correspondencewe may think of the radial direction U as an energy- or RG-scale for the CFT.

To sum up, a large number N of D3 branes embedded into $\mathbb{R}^{9,1}$ in the limit where they do backreact, $g_s N \gg 1$ (point-particle limit $l_s/\mathsf{L} \ll 1$), and at low energies $E^2 \ll 1/\alpha'$ (or $\alpha' \ll 1$) can be reliably described by

$$\Big(\text{free supergravity on } \mathbb{R}^{9,1}\Big) + \Big(\text{IIB string theory on } \mathrm{AdS}_5 \times \mathrm{S}^5\Big) \tag{3.18}$$

within the context of type IIB string theory.

3 they are organized in powers of l_s/L, which we argued to be small.

3.2 THE MALDACENA CONJECTURE

At last we are in a position to think about the AdS/CFT correspondence. In the previous two sections we described a system of N D3-branes embedded into ten-dimensional Minkowski space. We were careful to point out the regimes of validity of the gauge theory and supergravity descriptions. The duality arises from an order of limits issue. Indeed, both sides required low energies $E^2 \ll 1/\alpha'$ and a large number of branes, $N \to \infty$, while keeping $g_s N$ fixed. Thereafter, the gauge theory demands $g_s N \ll 1$, whereas the gravity description requires $g_s N \gg 1$.

The key leading to the AdS/CFT correspondence is that both are still describing the *same* dynamical system, albeit in distinct limits. Let us collect the tools employed by both descriptions. The open string picture led us to consider free gravitons propagating in flat space and four-dimensional $\mathcal{N} = 4$ SYM, (3.9). On the other hand the closed string picture features type IIB string theory on $\mathrm{AdS}_5 \times \mathrm{S}^5$ and, again, featured free gravitons in flat space, (3.18). We can identify a free gravity subsystem on both sides. Maldacena was daring enough to not stop there, but to also conjecture the (dynamical) equivalence of the other two subsystems at play,

$$\text{IIB string theory on } \mathrm{AdS}_5 \times \mathrm{S}^5 \;\sim\; \mathcal{N} = 4\, SYM \,\text{theory on } \mathbb{R}^{3,1} \quad (3.19)$$

The way of reading this is that both theories describe the same system, albeit each description being analytically tractable in a different regime and their defining parameters are matched as in (3.1). The claim is that every state, amplitude, etc. of the gauge theory has its own pendant in the string theory. It implies that an observer with access only to particle accelerators would think of his surroundings as filled with supersymmetric gauge fields and quarks in a four-dimensional world, while an observer equipped to measure gravitational waves, say, would perceive his surroundings as superstrings propagating in ten-dimensional $\mathrm{AdS}_5 \times \mathrm{S}^5$. In both worlds the t'Hooft coupling λ would be the same. If it were large, the string theorist could test detailed calculations to confirm his description of the system, whereas the particle physicist – rightfully confident that gauge theory is the correct device to describe his world – would have to overcome the major obstacle of large coupling, impeding his calculations [216].

3.2.1 *Symmetry Matching*

Let us gather further evidence in favor of the correspondence by comparing the symmetries of the theories. Recall that the a stack of D3 branes preserves sixteen out of thirty-two supersymmetries. The gauge theory living on the worldvolume repackages these into four supercharges Q^I_α, meaning $I = 1, 2, 3, 4$ – hence $\mathcal{N} = 4$ – which individually are spinors in four dimensions, i.e. $\alpha = 1, 2, 3, 4$. As anticipated above this theory is

more symmetric than the D3 branes themselves. It is also conformally invariant, meaning that its β function vanishes, and it has therefore another sixteen *superconformal* charges S^I_α replenishing the total number of supersymmetries to thirty-two. This concludes the analysis of all fermionic symmetry generators present in the gauge theory. Let us turn our attention to the bosonic generators. Obviously, being conformal implies the presence of the conformal group in four dimensions, which is $SO(4,2)$[4]. Lastly, remember the presence of an $SO(6)$ symmetry rotating the stack of D3 branes in the transverse directions. In the field theory it rotates the fluctuation fields $x^{i+3} = 2\pi\alpha'\phi^i$ into each other. Furthermore, the supercharges and superconformal charges each furnish a four-dimensional representation of this symmetry individually. That is to say the $SO(6) \simeq SU(4)$ acts on the label I. Groups, which shuffle supercharges into each other are referred to as $\mathcal{R}$ symmetry. Altogether the full theory enjoys invariance under the supergroup

$$PSU(2,2|4) \supset SO(4,2) \times SO(6)_{\mathcal{R}}, \tag{3.20}$$

where we have highlighted the discussed bosonic content on the RHS. Incidentally, these are the isometries of AdS_5 and S^5, respectively. It is an instructive exercise to work out the Killing vectors of AdS_5 in Poincaré patch coordinates and to confirm that they transform the conformal boundary into itself and act there as conformal transformations. Regarding the fermionic symmetries we only mention that the full IIB string theory on $\mathrm{AdS}_5 \times S^5$ can be shown to also have invariance group $PSU(2,2|4)$. Interested readers may consult [18] chapter 7.

3.2.2 *Partition Function*

Our discussion so far has been very qualitative. Let us see what we can say quantitavely. We cover only one aspect, the partition function. The discussion here is taken from [18] and we point the reader to chapter five and onward thereof for more details.

Consider the partition function of a d-dimensional gauge quantum field theory,

$$Z[\phi_0] = \left\langle \exp\left(i \int d^d x\, \phi_0^i(x) O_i(x) \right) \right\rangle. \tag{3.21}$$

The O_i comprise a set of gauge invariant operators, while ϕ_0^i are their corresponding sources. We can generate correlation functions from $Z[\phi_0]$ by taking functional derivatives with respect to the ϕ_0^i and subsequently setting $\phi_0^i = 0$.

That was for the CFT. If the AdS/CFT correspondence is to be taken seriously, then all we should be able to reproduce all correlators

4 They are the isometries of the lightcone in four-dimensional Minkowski space.

computed in this way from the gravity side. First, we have to identify which operator O_i in the gauge theory corresponds to what operator in the string theory. We say that they are *dual* to one another. Each meaningful object in one theory has a dual in the other description. The collection of all such identfications makes up the *holographic dictionary*. Finding these relations is in general not a trivial task. Useful guidelines are quantum numbers under the existing symmetries. Without derivation we state the most popular example of a duality: Fluctuations h of the metric about flat space, $g = \eta + \kappa\, h + \mathcal{O}(h^2)$, in the string theory are dual to the energy momentum tensor of the CFT,

$$h_{\mu\nu} \longleftrightarrow T_{\mu\nu}. \tag{3.22}$$

In general relativity we learn that fluctuations such as h give rise to spin-two particles and hence h carries the interpretation of the *graviton*, i.e. the boson which mediates gravity. Hence (3.22) relates the two protagonists on both sides of the correspondence.

Let us choose Poincaré coordinates on AdS_5,

$$ds^2 = \frac{dz^2 + \eta_{\mu\nu} dx^\mu dx^\nu}{z^2}, \qquad \mu, \nu = 0, \ldots, 3. \tag{3.23}$$

For $z \to 0$ this metric is conformally equivalent to flat space in four dimensions. In this limit we approach the boundary of AdS_5, where the CFT lives. In what follows x denotes the boundary coordinates. When refer to the interior of AdS_5 as the *bulk* and specify a point in it by the tuple (z, x).

In CFT we organize operators in terms of their conformal dimension, so let $O^i(x)$ have conformal dimension Δ_i. Furthermore assume that the $O^i(x)$ are dual to fields $\phi^i(z, x)$ on the gravity side,

$$\phi^i \longleftrightarrow O^i. \tag{3.24}$$

When approaching the boundary of AdS_5 the fields $\phi^i(z, x)$ assume a boundary value proportional to the source of the dual operator O^i, $\phi^i(z \to 0, x) \sim z^{4-\Delta_i} \phi_0^i(x)$. In generality $\Delta_i > 4$ and hence the power on the RHS is negative, The source is then extracted via

$$\lim_{z \to 0} z^{\Delta_i - 4} \phi^i(z, x) = \phi_0^i(x). \tag{3.25}$$

The strongest form of the AdS/CFT correspondence then equates the CFT partition function and the string partition function,

$$\left\langle \exp\left(i \int d^d x\, \phi_0^i(x) O_i(x) \right) \right\rangle_{CFT} = Z_{\mathrm{IIB}}\left[\phi_0^i(x)\right], \tag{3.26}$$

where the source on the RHS is understood as the limit (3.25). Unfortunately, the partition function of the string theory is not known.

The remedy lies in restricting to the weak form of the correspondence, where we may approximate the string partition function around solutions $\tilde{\phi}^i$ of IIB supergravity. The source is then extracted via

$$\lim_{z\to 0} z^{\Delta_i - 4}\tilde{\phi}^i(z,x) = \phi_0^i(x). \tag{3.27}$$

Then (3.26) simplifies to

$$\left\langle \exp\left(i \int d^d x\, \phi_0^i(x) O_i(x) \right) \right\rangle_{CFT} = \exp\Big(i S_{SUGRA}\Big[\phi_0^i(x)\Big]\Big), \tag{3.28}$$

where the source on the RHS is now understood as the limit (3.27). It is a very impressive test of the AdS/CFT conjecture that this RHS was indeed shown to act as generating functional for correlators of the CFT involving the operators O^i.

This concludes our introduction to the AdS/CFT correspondence. We point out that the correspondence as we have encountered it is not the only version of holography. We may encounter cousins of $\mathrm{AdS}_5 \times \mathrm{S}^5$ by varying the dimensionality of the AdS part of the ten-dimensional manifold. In fact, the content of this theses is not concerned with $\mathrm{AdS}_5 \times \mathrm{S}^5$, but with the case of $\mathrm{AdS}_3 \times \mathrm{S}^3 \times T^4$ to which we now turn.

3.3 ADS$_3$/CFT$_2$

The object of this thesis are largely two-dimensional field theories and so the candidate discussed above, $\mathrm{AdS}_5 \times \mathrm{S}^5$, is not a natural one, because the field theory is four-dimensional. The boundary of AdS_3 is two-dimensional and hence is a natural habitat for the field theory. Luckily, holographic correspondences are known for this case and this section reviews the necessary aspects for this thesis. Whenever the development parallels the $\mathrm{AdS}_5 \times \mathrm{S}^5$ scenario, we will only skim over the details. We begin with the supergravity description in Section 3.3.1 and then move on to the field theory in Section 3.3.2. Readers unfamiliar with branes are invited too consult Chapter 2 first. Most elements in this section are taken from the in-depth review [89].

The brane configuration is presented in Table 6. The D1-branes and D5-branes share the first two coordinates. It is here where we the gauge theory, to be described below, is situated. The directions $x^3, \ldots, x^5$, which are transverse to the D1-branes, but parallel to the D5-branes, are compactified on a four-torus T^4. Its size is of order of the string scale and we denote its volume

$$V_{T^4} = \alpha'^2 (2\pi)^4 v_4. \tag{3.29}$$

The remaining directions, $x^6, \ldots, x^9$, are transverse to both types of branes and give an $\mathbb{R}^4$ geometry.

	0	1	2	3	4	5	6	7	8	9
N_5 $D5$	•	•	•	•	•	•	-	-	-	-
N_1 $D1$	•	•	-	-	-	-	-	-	-	-

Table 6: The D1-branes intersect with the D5-branes on the first two coordinates. The remaining four coordinates of the D5-branes are compactified to a T^4 and the remaining overall transverse coordinates lie on an $\mathbb{R}^4$.

We go on to describe the low-energy descriptions of the closed strings, followed by the low-energy description of the open strings. As we have seen these two complementary pictures are what gives rise to the AdS/CFT correspondence. Actually, there is a deep reason for that called *open-closed string duality*. We will not go into the details of that however.

3.3.1 *AdS$_3$/CFT$_2$: Supergravity*

The story starts again with a choice of brane configurations. One major difference to AdS$_5$/CFT$_4$ is that we need two distinct kinds of branes instead of just one: D5-branes and D1-branes. We mentioned already that a stack of branes of a *single* kind of brane breaks half of the 32 supersymmetries of IIB string theory. When more types of branes are at play potentially all supersymmetry may be broken. In this case the branes are arranged such that 8 supersymmetries may be preserved altogether[5]. These correspond to the intersection of the preserved supersymmetries of each type of brane.

The solution to type IIB supergravity with N_5 D5-branes and N_1 D1-branes supported by RR two-form flux $F^{(3)}$ reads

$$ds^2 = (H_1 H_5)^{-1/2} ds^2_{\mathbb{R}^{1,1}} + (H_1 H_5)^{1/2} ds^2_{\mathbb{R}^4} + \left(\frac{H_1}{H_5}\right)^{1/2} ds^2_{T^4} \tag{3.30a}$$

$$F^{(3)} = 2r_1^2 g_s e^{-2\Phi} *_6 \omega_{S^3} + \frac{2r_5^2}{g_s}\omega_{S^3} \tag{3.30b}$$

$$e^{-2\phi} = \frac{1}{g_s^2}\frac{Z_5}{Z_1}\,. \tag{3.30c}$$

ω is the unit volume form on S^3, $*_6$ the Hodge dual in the $(\mathbb{R}^{1,1}, \mathbb{R}^4)$ plane and

$$H_1 = 1 + \frac{r_1^2}{r^2} \qquad r_1^2 = \frac{g_s N_1 \alpha'}{v_4} \tag{3.31}$$

$$H_5 = 1 + \frac{r_5^2}{r^2} \qquad r_5^2 = g_s N_5 \alpha'\,. \tag{3.32}$$

5 More details are found in Chapter 2

The length

$$r^2 = \sum_{i=6}^{9} x^i x^i \tag{3.33}$$

is actually only the transverse distance from the D5-branes. Observe that it features not only in the harmonic function H_5, where it appears naturally, but also in H_1, the harmonic function for the D1-branes. In H_1 one would usually expect to find the transverse distance to the D1-branes in all directions perpendicular to the D1 locus, which includes the directions $x^2, \dots x^5$. The fact that these directions do not appear in the harmonic function H_1, means that the D1-branes are not localized in that subspace. We say that they are *smeared* over the $x^2, \dots x^5$ directions.

As before, we have to secure that corrections to supergravity are neglible. Here it plays out analogous to before, (3.10),

$$g_s N_1 \gg 1, \qquad g_s N_5 \gg 1 \quad \text{and } N_1, N_5 \gg 1. \tag{3.34}$$

This parallels the discussion in the $\mathrm{AdS}_5/\mathrm{CFT}_4$ case. The spacetime symmetries of the solution (3.30) are

$$SO(1,1) \times SO(4)_E \times \text{“}SO(4)_I\text{”}. \tag{3.35}$$

The first factor is the Lorentz symmetry on the directions x^0, x^1, where the D1-branes are situated. The second factor is for the $\mathbb{R}^4$ of the overall transverse directions $x^6, \dots, x^9$. The subscript E stands for external. The last factor $SO(4)_I$ – the subscipt stands for internal – is not really a symmetry anymore, hence the quotations. It corresponds to the directions transverse to the D1-branes and parallel to the D5-branes $x^2, \dots x^5$. Those directions would feature a sound $SO(4)_I$ symmetry, were it not for our compactification to T^4. Nevertheless we may still classify supergravity fields according to the quantum numbers of this factor, so we keep it around. A clearer statement is that the $SO(4)_I$ still acts on the tangent space of the T^4.

Near-Horizon Limit

In this case the Maldacena limit is performed via [180]

$$\alpha' \to 0, \tag{3.36a}$$

$$\frac{r}{\alpha'} \equiv U = \text{fixed}, \tag{3.36b}$$

$$v_4 = \frac{V_{T^4}}{(2\pi)^4 \alpha'^2} = \text{fixed}, \tag{3.36c}$$

$$g_6 = \frac{g_s}{\sqrt{v_4}} = \text{fixed}. \tag{3.36d}$$

In this limit the solution (3.30) becomes

$$ds^2 = \mathsf{L}^2(ds^2_{\text{AdS}} + ds^2_{S^3}) + \left(\frac{N_1}{v_4 N_5}\right)^{1/2} ds^2_{M^4} \tag{3.37a}$$

$$F^{(3)} = 2\alpha' N_5(\omega_{\text{AdS}_3} + \omega_{S^3}) \tag{3.37b}$$

$$e^{-2\Phi} = \frac{1}{g_6^2}\frac{N_5}{N_1} \tag{3.37c}$$

where, $\mathsf{L}^2 = r_1 r_5$, and $ds^2_{\text{AdS}_3}$ and $ds^2_{S^3}$ are unit radius metrics. Observe that AdS_3 and S^3 have the same radius. We learn that in the near-horizon region the D1/D5 system turns into $\text{AdS}_3 \times \text{S}^3 \times T^4$ supported by RR three-form flux.

3.3.1.1 *Symmetries*

The isometries of AdS_3 comprise the non-compact group $SO(2,2)$, which is incidentally the global conformal group in two dimensions. The isometries of S^3 account for the $SO(4)_E = SU(2)_E \times \widetilde{SU(2)}_E$. Together these two comprise the bosonic symmetry content. In the near-horizon limit the eight supersymmetries of the D1/D5 system are enhanced by another eight superconformal symmetries giving a total of sixteen fermionic generators. Anti-de-Sitter supergroups have been classified in [144] and from amongst all candidates the full supergroup of the present model is made out to be

$$SU(1,1|2) \times SU(1,1|2) \tag{3.38}$$

3.3.2 *AdS$_3$/CFT$_2$: Field Theory*

Now we turn our attention to the gauge theory living on the branes. Itself is not conformally invariant. Only after going to low-energies, in correspondence with taking the near-horizon limit, conformal symmetry emerges. For our purposes the gauge theory is more useful, so that we will not discuss the CFT here. The material in this section is taken from chapter four of [89]. Readers interested in the CFT may consult chapter five of said reference. Another useful reference is [22].

Consider a stack of N_5 D5- and a stack of N_1 D1-branes in IIB string theory aligned as noted in Table 6. We need to make sure that the branes do not backreact on the background geometry and that the string is perturbative. This is the case in the regime,

$$g_s N_1 \ll 1, \qquad g_s N_5 \ll 1, \tag{3.39}$$

opposite to the supergravity limit (3.34). This parallels the discussion in the $\text{AdS}_5/\text{CFT}_4$ case.

Individually each stack would give rise to a $U(N_5)$ gauge theory or a $U(N_1)$ gauge theory. This section basically spells out what we obtain

when we combine these two theories. At our disposal we have four types of open strings:

A. **5-5 strings** start and end on the D5-branes.

B. **1-1 strings** start and end on the D1-branes.

C. **5-1 strings** start on a D5-brane and end on a D1-brane.

D. **1-5 strings** start on a D1-brane and end on a D5-brane.

We now deal with each of them in turn. The first two are similar in spirit to the open strings of Section 3.1.1. In the language of this section they are called 3-3 strings. The latter two are actually them same thing up to orientation, but we will come to that. The resulting theory has $\mathcal{N} = (4, 4)$ supersymmetry in two dimensions, i.e. eight supercharges. It is usefull to classify them according to multiplets of $\mathcal{N} = 4$ in four dimensions, which has the same amount of supersymmetry. Let us quickly recapitulate the relevant multiplets:

VECTOR MULTIPLET It contains a vector field A_μ, two Weyl fermions, a complex scalar and three real auxiliary fields D^a with $a = 1, 2, 3$.

HYPERMULTIPLET It contains two complex scalars, two Weyl spinors and two complex auxiliary fields called F^i with $i = 1, 2$.

On-shell the auxiliary fields are replaced through their equations of motion.

5-5 Strings

These are the open strings, which are present whenever there is a D5-brane. We have in fact N_5 of these so that we should find the content of a $U(N_5)$ gauge theory in $(5 + 1)$ dimensions. Moreover, D5-branes are $\frac{1}{2}$-BPS, so that their presence breaks the supersymmetry content of IIB string theory from 32 to 16 supercharges. In $(5 + 1)$ dimensions these decompose into $\mathcal{N} = 2$ Weyl-spinors. The Yang-Mills coupling of the $U(N_5)$ gauge theory is, according to (2.22), $g^2_{YM,5} = 2\pi g_s \alpha' = 2\pi g_s l_s^2$.

Recall that four of the directions of the D5-brane worldvolume have been compactified down to the size of the string scale[6], (3.29). This implies that we are actually dealing with a two-dimensional theory coordinatized by x^0, x^1. Moreover Kaluza-Klein modes become very massive and can be dropped when considering low energies.

The bosonic field content is organized into [89]

$$\begin{aligned} \text{vector}: &\quad A_0^{(5)}, A_1^{(5)}, \chi_i^{(5)} \\ \text{hyper}: &\quad \chi_I^{(5)} \end{aligned} \tag{3.40}$$

6 The coupling picks up a factor of v_4 from the dimensional reduction

The superscript indicates that these fields originate from the 5-5 strings and all fields are $N_5 \times N_5$ hermitian matrices transforming in the adjoint representation of the gauge group, $U(N_5)$. As usual in brane constructions the transverse directions, we label them by $i = 6, \ldots, 9$ describe the fluctuations of the brane in transverse space, cf. (2.19). The remaining fields, labelled by $I = 2, \ldots, 5$ stem from the directions compactified on the T^4 and comprise the hypermultiplet. $\mathcal{N} = 2$, $d = 2$ supersymmetry has an $SU(2)_{\mathcal{R}}$ symmetry which groups these components in pairs

$$N_\alpha^{(5)} = \begin{pmatrix} N_1^{(5)} \\ N_2^{(5)\dagger} \end{pmatrix} = \begin{pmatrix} \chi_5^{(5)} + i\chi_4^{(5)} \\ \chi_3^{(5)} - i\chi_2^{(5)} \end{pmatrix} \tag{3.41}$$

so that α transforms in the fundamental of the $\mathcal{R}$ symmetry.

1-1 Strings

The discussion for the 1-1 strings is analogous to that of the 5-5 strings. Whenever there are D1-branes we have 1-1 strings and they yield a $U(N_1)$ gauge theory in $(1+1)$ dimensions. D1-branes are $\frac{1}{2}$-BPS, so that their presence breaks the supersymmetry content of IIB string theory from 32 to 16 supercharges. However, as we they are not the same supersymmetries as preserved by the 5-5 strings. The Yang-Mills coupling of the $U(N_1)$ gauge theory is, according to (2.22),$g^2_{YM,1} = g_s/(2\pi\alpha') = g_s/(2\pi l_s^2)$.

The bosonic field content is organized into [89]

$$\begin{aligned} &\text{vector}: && A_0^{(1)}, A_1^{(1)}, \chi_i^{(1)} \\ &\text{hyper}: && \chi_I^{(1)} \end{aligned} \tag{3.42}$$

The superscript indicates that these fields originate from the 1-1 strings and all fields are $N_1 \times N_1$ hermitian matrices transforming in the adjoint representation of the gauge group, $U(N_1)$. Otherwise the labelling is as for the 5-5 strings. As before the $SU(2)_{\mathcal{R}}$ symmetry groups the hypermultiplet components in pairs

$$N_\alpha^{(1)} = \begin{pmatrix} N_1^{(1)} \\ N_2^{(1)\dagger} \end{pmatrix} = \begin{pmatrix} \chi_5^{(1)} + i\chi_4^{(1)} \\ \chi_3^{(1)} - i\chi_2^{(1)} \end{pmatrix} \tag{3.43}$$

with α transforming in the fundamental of the $\mathcal{R}$ symmetry.

5-1 and 1-5 Strings

By themselves the 5-5 strings and 1-1 strings preserve 16 out of 32 supercharges, which we call SUSY$_1$ and SUSY$_5$. While these two sets are distinct they have a non-vanishing intersection. It is these supercharges that are left unbroken by the presence of the 5-1 and 1-5 strings. They

are 8 supercharges in total, which are organized into $\mathcal{N} = (4,4)$ at $d = 2$.

The 5-1 strings sit in the fundamental representation of $U(N_5)$ and in the anti-fundamental representation of $U(N_1)$. At the massless level these strings give rise to two bosonic and two fermionic degrees of freedom. The 1-5 strings sit in the fundamental representation of $U(N_1)$ and in the anti-fundamental representation of $U(N_5)$. At the massless level these strings also give rise to two bosonic and two fermionic degrees of freedom [22]. Combined the massless content makes up a hypermultiplet, whose bosonic components we repackage into two complex scalars,

$$M^\alpha, \qquad M^\dagger_\alpha, \tag{3.44}$$

transforming in the same representation of $SU(2)_\mathcal{R}$ as the $N^{(p)}_\alpha$. The fields M^α are $N_5 \times N_1$ matrices transforming under gauge transformations as $M^\alpha \mapsto U_{\mathrm{D5}} M^\alpha U^\dagger_{\mathrm{D1}}$.

The 5-5 and 1-1 strings by themselves constitute independent $U(N_5)$ and $U(N_1)$ gauge theories, which are coupled by the 1-5 and 5-1 strings to give a $U(N_5) \times U(N_1)$ gauge theory.

Bosonic Lagrangian and Higgs Branch

For simplicity, we express the bosonic part of the lagrangian as the dimensional reduction of a 6d theory, with $m, n = 016789$ but $\partial_{6789} = 0$,

$$L = \sum_{p=D1,D5} L^{(p)} + L_M \tag{3.45}$$

The first two summands collect the bosonic pieces from the 5-5 and 1-1 strings,

$$L^{(p)} = \frac{1}{g^2_{YM,p}} \mathrm{Tr}_{N_p} \Big(-\frac{1}{2} F^{mn} F_{mn} + D^i D^i - \mathcal{D}^m N^\dagger_\alpha \mathcal{D}_m N^\alpha + F^\dagger_\chi F_\chi + N^\dagger_\alpha \sigma_i [D^i, N^\alpha] \Big), \tag{3.46}$$

while the last piece is the couples them via the 5-1 and 1-5 strings,

$$L_M = \mathrm{Tr}_{N_1} \Big(-(\mathcal{D}_m M^\alpha)^\dagger \mathcal{D}^m M^\alpha + F^\dagger_M F_M + M^\dagger \sigma_i (D^i_{(5)} M - M D^i_{(1)}) \Big), \tag{3.47}$$

We omitted the $(p) = (1), (5)$ superscript on the multiplets stemming from the 5-5 and 1-1 strings. D^i $(i = 1, 2, 3)$ are the three real auxiliary fields of the vector multiplets, while F_χ, F_M are the complex auxiliary

fields of the hypermultiplets. $\mathcal{D}_m$ are gauge covariant derivaties and σ_i are the Pauli matrices.

Finding a vev for a component of the vector multiplets, say $\chi_i^{(p)}$, is equivalent to having the Dp-branes separate in the i^{th} direction; the Chan-Paton factors encode which branes separate. When all branes have separated we say that the system is on the *Coulomb branch*. On the other hand, when all branes have the same locus in the overall transverse space we say that we are on the *Higgs branch*. In this case the hypermultiplets may acquire a non-zero vev. We are interested in the latter branch and we can forcefully place us there by turning on either a *Fayet-Iliopolis parameter* [89]

$$\frac{1}{g^2 N}\zeta_i \mathrm{Tr}_F(D^i_{(p)})\,, \qquad \zeta_i \in \mathbb{R} \tag{3.48}$$

or by turning on a *theta term*,

$$\frac{\theta}{2\pi}\mathrm{Tr}_F(F_{01})\,. \tag{3.49}$$

Integrating out the $D^i_{(p)}$ auxiliary fields in (3.45) yields the U(N_5) and U(N_1) D-term constraints

$$\sigma^{i\alpha}{}_\beta\Big(M^\beta M^\dagger_\alpha + [N^{(5)\beta}, N^{(5)\dagger}_\alpha]\Big) + \frac{\zeta^i_{(5)}}{N_5}\mathbb{1} = 0 \tag{3.50}$$

$$\sigma^{i\alpha}{}_\beta\Big(-M^\dagger_\alpha M^\beta + [N^{(1)\beta}, N^{(1)\dagger}_\alpha]\Big) + \frac{\zeta^i_{(1)}}{N_1}\mathbb{1} = 0 \tag{3.51}$$

respectively. When the ζ parameters are turned on, we can only satisfy the constraints by taking the Ms to be non-vanishing as promised. In particular, the eigenvalues of $N^{(5)}$ and $N^{(1)}$ should coincide. in the literature these equations are more commonly presented in terms of $A = M^1$, $\tilde{A}^\dagger = M^2$,

$$AA^\dagger - \tilde{A}^\dagger\tilde{A} + [N^{(5)}_1, N^{(5)\dagger}_1] - [N^{(5)\dagger}_2, N^{(5)}_2] + \frac{\zeta_{(5)}}{N_5}\mathbb{1} = 0 \tag{3.52a}$$

$$A\tilde{A} + [N_{\mathrm{D5}}, \tilde{N}_{\mathrm{D5}}] + [N^{(5)}_1, N^{(5)}_2] + \frac{\zeta^c_{(5)}}{N_5}\mathbb{1} = 0 \tag{3.52b}$$

$$AA^\dagger - \tilde{A}^\dagger\tilde{A} + [N^{(1)}_1, N^{(1)\dagger}_1] - [N^{(1)\dagger}_2, N^{(1)}_2] + \frac{\zeta_{(1)}}{N_1}\mathbb{1} = 0 \tag{3.52c}$$

$$\tilde{A}A + [N_{\mathrm{D1}}, \tilde{N}_{\mathrm{D1}}] + [N^{(1)}_1, N^{(1)}_1] + \frac{\zeta^c_{(1)}}{N_1}\mathbb{1} = 0\,, \tag{3.52d}$$

where $\zeta^c_{(p)} = \zeta^1_{(p)} - i\zeta^2_{(p)}$. The solution to these equations are supersymmetric minima of the D1/D5 system, that is they have vanishing potential, $V = 0$. All possible solutions to $V = 0$ constitute the *moduli space* of the theory. Our constraints (3.50) are not the most general solution, since we forcefully placed ourselves on the Higgs branch. To explore the full moduli space we must admit the full Coulomb branch

and all intermediary solutions between Coulomb and Higgs. For our purposes, we only require the Higgs branch and so from now on, when we say moduli space, we mean its Higgs branch.

CFT and Near-Horizon Limit

When making contact with supergravity we again have to make sure that the gauge ranks N_p are large. Zooming into the near-horizon region in supergravity is equivalent to taking the IR limit in the gauge theory. This implies that we intergrate out all massive degrees of freedom. In fact, this justifies restricting to the supersymmetric minima of the D1/D5 system, i.e. solutions to (3.52).

Since we flow to an IR fixed-point, the theory develops a two dimensional conformal symmetry generated by the *Virasoro algebra*, whose central charge can be computed through the Brown-Henneaux formula [60],

$$\mathsf{c} = \frac{3\mathsf{L}}{2G_N^{(3)}}, \tag{3.53}$$

where $G_N^{(3)}$ is Newton's constant in three dimensions. For the solution (3.37) the central charge is then

$$\mathsf{c} = 6N_1N_5 + \text{subleading} \tag{3.54}$$

Moreover the 8 supersymmetries that were already at play are supplemented by another 8 superconformal symmetries so that the resulting theory has $\mathcal{N} = (4,4)$ superconformal symmetry. This has the right amount of supersymmetry to be matched with the findings of Section 3.3.1.1. What about the bosonic symmetries? We observed that the near-horizon limit in supergravity had an

$$SO(2,2) \times SO(4)_E \simeq (SL(2,\mathbb{R}) \times SU(2)) \times (SL(2,\mathbb{R}) \times SU(2))$$

symmetry. $SL(2,\mathbb{R})$ generates one chiral half of the global part of the Virasoro algebra and $SU(2)$ is then identified with the $\mathcal{R}$ symmetry of that chiral half of the super Virasoro algebra.

This concludes our review of $\text{AdS}_3/\text{CFT}_2$ and our introduction to the AdS/CFT in general.

Part II

THE KONDO MODEL AND HOLOGRAPHIC INTERFACE RG FLOWS

This part is dedicated to a holographic realization of Kondo physics. Parts of the material presented here will appear in a reduced form in an upcoming publication [112].

We begin with a review of the Kondo effect in Chapter 4 with the aim of introducing the CFT description of the Kondo-flow: A stack of pointlike branes clustered at the north pole of a three-sphere condense at low energies into a single two-dimensional brane wrapping a two-sphere at constant polar angle.

It is this behavior that we aim to mimic within the realm of $AdS_3 \times S^3 \times T^4$ holography. And indeed, in Chapter 5 we confirm that such flows exist and give all details of their construction using probe branes.

Probe brane limits are inherently limited, since most quantities of interest depend on backreaction in the gravity dual. It is therefore desirable to have a fully backreacted gravity dual of the entire RG flow. In general this is a very difficult task and we lay its groundwork in Chapter 6 by constructing the fully backreacted gravity duals of the fixed points of our Kondo-like flows.

One important prerequisite of any interface RG flow in (1+1) dimensions is that the boundary entropies decrease along the flow. In Chapter 7 we compute the relevant g-factors at the fixed points and confirm that they satisfy the g-theorem. Crucially, we show that the g-factors in the probe limit miss important information, which is encoded in gravitational backreaction.

A conclusion and outlook of Part ii is found in Chapter 11.

4

KONDO EFFECT

The Kondo effect [171] describes the screening of heavy magnetic impurities by conduction electrons in a metal at low temperatures. It is an example of a quantum field theory with negative beta function. Thus, when renormalizing the theory it flows from a trivial UV to an interacting IR fixed point. From a high-energy physics point of view it therefore deserves special attention as a toy model for quantum chromodynamics, besides being the first appearance of a defect flow in physics.

Consider conducting materials at low temperatures. As we send the temperature to absolute zero, one of two scenarios typically arises:

1. The resistivity decreases monotonically to some finite non-zero value. This is depicted in yellow in Figure 7.

2. At some critical temperature the system enters a superconducting phase, where the resistivity drops to zero. This is depicted in green in Figure 7.

In the 1930s however, experimentalists observed that materials doped with impurities displayed an anomalous increase in resistivity when temperature was lowered sufficiently. It was only until the 1960s that this could be explained by Kondo [171]. He realized that the increase in question was due to the spin-spin interactions of conduction electrons with heavy magnetic spin impurities. At high energies – the UV fixed

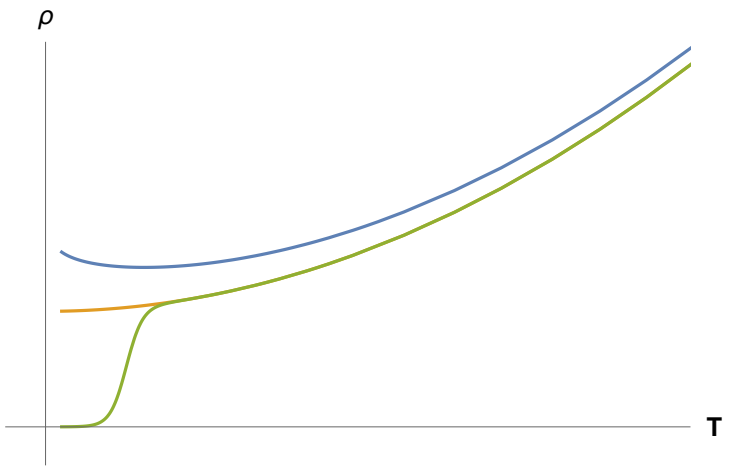

Figure 7: Resistivities against temperature for (1) normal conducting material drawn in yellow, (2) superconducting material drawn in green, (3) conductor with impurity drawn in blue. Figure by C. Melby-Thompson

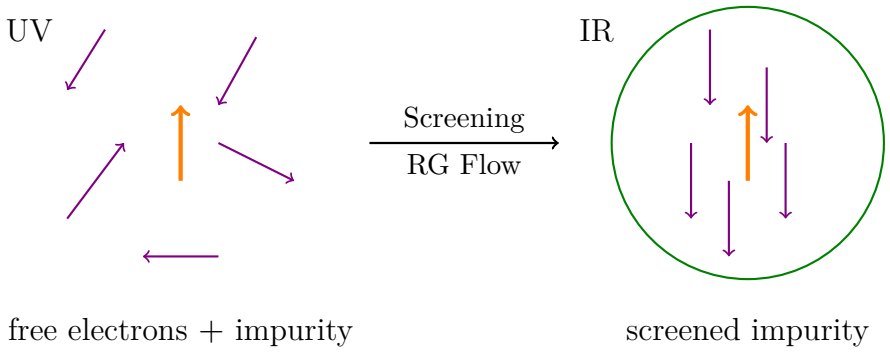

Figure 8: UV: Free electrons and uncoupled impurity. IR: Conduction electrons screen the impurity by forming a bound state with the impurity. In the original Kondo problem only a single electron couples to the impurity. When multiple channels are at play, more than one electron may couple to the impurity.

point of an RG flow – these impurites are basically ignored by the electrons. Yet, in the IR the tables turn:

3. At low energies the spin impurities form bound states with the conduction electrons, thereby screening the impurity; see Figure 8. As a consequence new contributions to scattering arise leading to an increase in resistivity. This is drawn in blue in Figure 7.

In the IR this model is described by a strongly interacting field theory Even though this picture originally emerged in 1964, the Kondo model accompanied theoretical physicists ever since contributing notably to distinct areas. To name a few, it has played a major role in the developement of Wilson's renormalization group (RG) [231], or presents fertile ground for techniques such as Fermi liquid descriptions [193], the Bethe Ansatz [19, 20] and large-N limits [52]. More importantly for this thesis, it has pushed our understanding of boundary conformal field theory (BCFT)[4, 7–10, 13, 123, 127–130] and of defect conformal field theory [33, 173]. Finally, variants of the Kondo model have been investigated holographically in [150] and later, in a series of papers [109, 110, 113–117, 194], a holographic dual of the entire RG flow linking the UV and IR fixed points was established. Other contemporary activity concerning the Kondo model is geared towards *nanotechnology* [174] and *quantum dots* [218, 219].

4.1 FIELD THEORY REVIEW OF THE KONDO EFFECT

In this section we present the common field theory lore of the Kondo effect following closely [5, 113]. We start with a system of free elec-

trons in $(3+1)$-dimensional flat spacetime and couple an impurity $\vec{S}$ as follows

$$H_K = \psi^\dagger_\alpha \frac{-\nabla^2}{2m}\psi_\alpha + \hat{\lambda}\delta(\vec{x})\vec{S}\cdot\psi^\dagger_{\alpha'}\frac{1}{2}\vec{\sigma}_{\alpha'\alpha}\psi_\alpha \tag{4.1}$$

The fermionic creation modes, $\psi^\dagger_\alpha$, and the annihilators, ψ_α, are valued in the fundamental representation of SU(2), that is, α may take two values: spin up, $\alpha = \uparrow$, or spin down, $\alpha = \downarrow$. The first term is the standard fermion kinetic term in three space dimensions and m is the electron's mass. The impurity $\vec{S}$ is localized at the origin and is also valued in the fundamental representation of SU(2). $\vec{\sigma}$ is the Pauli-matrix three-vector. When the coupling $\hat{\lambda}$ is positive we have anti-ferromagnetic coupling, while negative $\hat{\lambda}$ implies ferromagnetic coupling.

To leading order in perturbation the beta function of $\hat{\lambda}$ is negative. Hence, for negative $\hat{\lambda}$, the effective coupling at low energies vanishes. This case is harmless. If, however, $\hat{\lambda}$ is positive the consequences are more drastic: a dynamically generated scale emerges, T_K, which is called the *Kondo temperature*. Moreover, the system displays asymptotic freedom so that the effective coupling appears to diverge at low energies. This begs the question of the Kondo problem:

What is the ground state of the Kondo Hamiltonian (4.1)?

The heuristic answer is already given in Figure 8. Due to asymptotic freedom, at short wavelengths the system consists of free electrons and a decoupled spin. Now we drive the system to long wavelengths by lowering the temperature. Once we hit the Kondo temperature T_K, the ground state changes and a single electron forms an SU(2) singlet with the impurity, thereby screening it. Thus, in the IR, the impurity appears to be absent and the remaining electrons form a Landau Fermi liquid around it. The only remnant of the impurity is as boundary condition on the unbound electrons: their wavefunctions vanish at the locus of the bound state. The electrons cannot permeate the immediate surroundings of the bound state, unless they overcome the binding energy, which is proportional to $\hat{\lambda} \gg 1$. Hence, such occurences are highly improbable.

Both, the impurity and a single electron are spin-1/2. Their tensor product then decomposes into a symmetric triplet and an anti-symmetric singlet. The latter has lower energy.

The change of ground state also answers the issue of diverging coupling constant $\hat{\lambda}$. It is only an artifact from looking at the IR theory from a "UV perspective", while, as we have seen all that happens is that the IR degrees of freedom have rearranged into free electrons with a special boundary condition, ergo nothing dramatic.

The impurities that we will consider are in fact not valued in representations of SU(2), but in representations of SU(N) with large N. Moreover, we can consider multiple flavors of electrons, or in condensed

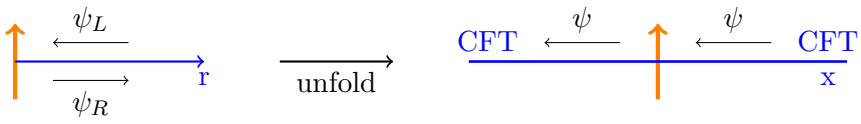

Figure 9: The Kondo model as $(1+1)$-dimensional system. On the left we have left and right moving fermions moving toward and away from the impurity and communicating via a boundary condition set by the impurity. On the right, after unfolding, only right moving fermions remain. The impurity presents no longer a boundary, but an defect.

matter language multiple channels k. The full symmetry of the theory is then

$$\mathrm{SU}(N) \times \mathrm{SU}(k) \times \mathrm{U}(1), \tag{4.2}$$

where $\mathrm{SU}(k)$ is the channel symmetry and $\mathrm{U}(1)$ is a charge symmetry. The electrons are valued the fundamental representation of $\mathrm{SU}(N) \times \mathrm{SU}(k)$, while the impurity is in some finite dimenstional representation of $\mathrm{SU}(N)$. Under $\mathrm{SU}(k) \times \mathrm{U}(1)$ the impurity transforms as a singlet. A Kondo system is then determined in terms of N, k and the representation of the impurity. The original Kondo problem discussed above has $N = 2$, $k = 1$ and the representation of the impurity is $\mathtt{s} = 1/2$ of $\mathrm{SU}(2)$.

4.1.1 *Kondo Model as CFT*

In the 1990s it was realized that the Kondo model could be rephrased as $(1+1)$-dimensional system [4, 7–10], where the remaining spatial dimension is the radial distance to the impurity. Firstly, we observe that the impurity term in (4.1) is spherically symmetric about the origin due to $\delta(x)$. What about the electrons? Affleck and Ludwig noted that the only contributions to scattering, were s-wave modes. Furthermore, if we deal with energies far below the fermi surface, we can linearize the dispersion relation of the system around the Fermi momentum k_F. Overall this leaves us with a description of the system using only a single spatial dimension, r, as promised. The in- and out-going s-waves are represented through left- and right-moving fermions, respectively. These fermions communicate with each other through a boundary condition imposed by the impurity, $\psi_L|_{r=0} = \psi_R|_{r=0}$. This is depicted in the LHS of Figure 9.

This description is in term of a boundary field theory. Via the "inverse" of the folding trick discussed in Section 2.2, the *unfolding trick*, we can turn this into a field theory with interface. All we have to do is to reflect the right moving fermions about the origin thereby turning them into left movers. This effectively extends the radial direction to negative values. What remains are left-moving s-wave fermions, which propagate toward the impurity, communicate with it and move past it.

To distinguish the boundary theory from the interface theory we call the spatial coordinate in the latter x. This is depicted in the RHS of Figure 9. The Hamiltonian for the left moving fermions ψ_L coupling to the impurity then reads

$$H = \frac{v_F}{2\pi}\psi_L^\dagger i\partial_x\psi_L + v_F\lambda\delta(x)\vec{S}\cdot\psi_L^\dagger\frac{\vec{\sigma}}{2}\psi_L, \tag{4.3}$$

where $v_F = k_F/m$ is the fermi velocity and we have suppressed $SU(N)$ indices on the fermions. The coupling here is related to the one in (4.1) via $\lambda = \frac{k_F^2}{2\pi^2 v_F}\hat{\lambda}$. For convenience we specify $v_F = 1$. The Kondo coupling is (classically) marginal since $\delta(x)$ and $\vec{S}$ have dimension zero, while ψ_L has dimension one-half.

The Kondo Model and CFT

Obviously, reducing the dimensionality of the problem from $(3+1)$ to $(1+1)$ dimensions simplifies the analysis, since we are left with only a single differential operator ∂_x instead of ∇ in (4.1). But this by itself is in fact not the real reason to go through all the trouble discussed above. The real reason is that (4.3) exhibits much more symmetry than (4.1), in fact, infinitely much more symmetry. Indeed, we encounter conformal symmetry, which has an infinite set of generators. Additionally, we find an extended symmetry under $\hat{\mathfrak{su}}(2)_1$. When studying generalized Kondo impurities with k channels, corresponding to the symmetry group (4.2), we obtain the affine algebra

$$\hat{\mathfrak{su}}(N)_k \times \hat{\mathfrak{su}}(k)_N \times \hat{\mathfrak{u}}(1). \tag{4.4}$$

The key observation is that we can use these emergent symmetries to determine the IR spectrum very elegantly.

Due to its holomorphic-anti-holomorphic factorization, $(1+1)$-dimensional CFT is most conveniently presented using complex coordinates $z = t + ix$. Let us first introduce the currents generating the symmetry algebra(4.4), starting with the $SU(N)_k$ factor,

$$J^a(z) = \left(\psi^{\alpha,i}(T^a)_\alpha{}^\beta\psi_{\beta,i}\right)(z) = \sum_{n\in\mathbb{Z}} z^{n-1}J_n^a. \tag{4.5}$$

T^a is a generator of SU(N), hence $a = 1,\dots N^2-1$, and it is represented in the fundamental of SU(N), meaning that α,β run (as before) from 1 to N. The index i is in the fundamental of SU(k), i.e. $i = 1,\dots,k$. Note that i cannot be contracted into the SU(N) generator T^a. We have an analogous set of currents for $\hat{\mathfrak{su}}(k)_N$

$$J^A(z) = \left(\psi^{\alpha,i}(T^A)_i{}^j\psi_{\alpha,j}\right)(z) = \sum_{n\in\mathbb{Z}} z^{n-1}J_n^A, \tag{4.6}$$

where T^A is a generator of $\mathrm{SU}(k)$ so that $A = 1, \dots, k^2 - 1$. Lastly, the algebra $\hat{\mathfrak{u}}(1)$ has rank 1 so that its only current is simply

$$J(z) = \left(\psi^{\alpha,i}\psi_{\alpha,i}\right)(z) = \sum_{n\in\mathbb{Z}} z^{n-1} J_n. \tag{4.7}$$

Note that we have chosen a slightly different normalization here than in (2.50), which is more in tune with spin. It highlights in a factor of two in the second summand of the RHS.

The currents (4.5) obey an $\hat{\mathfrak{su}}(N)_k$ Kac-Moody algebra,

$$\left[J^a_n, J^b_m\right] = i f^{abc} J^c_{n+m} + k\frac{n}{2}\delta^{ab}\delta_{n,-m}. \tag{4.8}$$

Here, f^{abc} are the structure constants of $\mathrm{SU}(N)$. Similarly, the $\hat{\mathfrak{su}}(k)_N$ currents, (4.6), obey (4.8) with k replaced by N and a, b replaced by A, B; the structure constants f^{ABC} are those of $\mathrm{SU}(k)$. Of course, the $\hat{\mathfrak{u}}(1)$ currents obey (4.8) as well. However, since $\mathrm{U}(1)$ is abelian its structure constants vanish and we are left only with the last term proportional to the level. Now, by rescaling the modes J_n we can rid ourselfs of said level, so that we do not assign any level to $\hat{\mathfrak{u}}(1)$. What remains in this case is then the *Heisenberg algebra*,

$$[J_n, J_m] = \frac{n}{2}\delta_{n,-m}. \tag{4.9}$$

The Heisenberg algebra may be though of as an infinite collection of the ordinary algebra of a single harmonic oscillator in quantum mechanics.

Let us now adress the spectrum of this theory. How many ground states are there? It suffices to restrict the discussion to $\hat{\mathfrak{su}}(N)_k$. The ground states are in one-to-one correspondence with the primaries of the extended symmetry, of which there are $k+1$. They are labelled by their spin $0, 1/2, \dots, k/2$. For $\hat{\mathfrak{su}}(k)_N$ the story is identical with k replaced by N. We will mainly be interested in studying the representation theory of just $\hat{\mathfrak{su}}(N)_k$ so that, in the following, by ground states we mean just the $k+1$ options provided by $\hat{\mathfrak{su}}(N)_k$. The remaining part of the algebra (4.4) will only become important when we match boundary conditions below. Now that we have the ground states, we can construct the spectrum using the modes J^a_n, J^A_n, J_n, which are creation operators if $n > 0$. Hence we act with arbitrary linear combinations of the creators – up to null vectors – thereby generating conformal towers on any ground state.

Absorption of Boundary Spin

In two-dimensional CFT the analysis is smoothest in terms of the energy momentum tensor. Consider therefore the Sugawara construction,

$$T = \frac{1}{2\pi(N+k)} J^a J^a + \frac{1}{2\pi(k+N)} J^A J^A + \frac{1}{4\pi N k} J^2 + \lambda\delta(x)\vec{S}\cdot\vec{J}. \tag{4.10}$$

Its main advantage over (4.3) is that the spin, channel and charge degrees of freedom can be treated separately. Let us now "complete the square" by defining a new current

$$\mathcal{J}^a \equiv J^a + \pi(N+k)\lambda\delta(x)S^a. \tag{4.11}$$

The energy momemtum tensor then takes the form

$$T = \frac{1}{2\pi(N+k)}\mathcal{J}^a\mathcal{J}^a + \frac{1}{2\pi(k+N)}J^AJ^A + \frac{1}{4\pi Nk}J^2, \tag{4.12}$$

after dropping a constant term $\propto \vec{S}\cdot\vec{S}$. This energy momentum tensor already looks like a Sugwara construction, but does it truly correspond to a Kac-Moody algebra (4.8)? In fact, it only does when the coupling assumes the special non-zero value

$$\lambda = \frac{2}{N+k}. \tag{4.13}$$

Together, (4.12) and (4.13) represent the IR fixed poiont of the RG flow [5]. This is the absorption of spin impurity explained heuristically above. We already discussed that the impurity features only implicitely in the IR as boundary condition on the fermions. What are the implications for the spectrum? Observe first that the symmetry algebra of the theory is again (4.4). Hence, the states have to organize themselves into representations of the same type as before. They are not the same as in the UV however.

Recall that the spin is valued in a representation of $\mathfrak{su}(N)$, which is the finite dimensional part of $\hat{\mathfrak{su}}(N)_k$. This inspired Affleck and Ludwig to propose that it is only the representations of the latter which take part in the RG flow [5], i.e. the representations of $\hat{\mathfrak{su}}(k)_N$ are just spectators. The process is that of fusion between the ground states of the UV theory and the representation of the impurity. Recall the fusion rules of $\hat{su}(N)_k$, which we introduced in Section 2.2 and reproduce here for convenience

$$N_{j_1j_2}^{j_3} = \begin{cases} 1 & \text{if } |j_1-j_2| \le j_3 \le \min(j_1+j_2, k-j_1-j_2) \text{ and } j_1+j_2+j_3 \in \mathbb{Z}, \\ 0 & \text{otherwise.} \end{cases} \tag{4.14}$$

Let us consider the simplest example: the original Kondo problem which has $N=2$, $k=1$ and $\mathsf{s}=1/2$. Start with the ground state of spin 0, i.e., we fuse $j_1=0$ and $j_2=\mathsf{s}$. This gives $j_3=1/2$ as only possible fusion product. Similarly if we choose the other ground state, $j_1=1/2$, we find $j_3=0$. In other words, in the original Kondo problem all that happens under the RG flow is that the two ground states are interchanged. How can we detect that the representations have indeed been interchanged, if the state content is identical to before? The answer lies,

of course, in the remaining symmetries which in the case at hand is just $U(1)$. In the UV the states build on the spin-zero ground state have odd $U(1)$ charge, while those build on the spin-$\frac{1}{2}$ ground state have even $U(1)$ charge. Since the $U(1)$ charges do not change under the RG flow, after interchanging the representations the spin-zero states have even $U(1)$ charge while the half-integer spin states have odd $U(1)$ charge.

The scenarios that arise when the level k is larger than one are as follows [6]:

CRITICAL SCREENING occures when $k = 2\mathsf{s}$. The system harbors sufficient channels to screen the impurity entirely. The IR physics is described by k free left-movers and no impurity. This happens by default in the original Kondo problem.

OVER-SCREENING occures when $k > 2\mathsf{s}$. The systems has too many channels trying to screen the impurity. The resulting bound state developes negative effective spin, which has then to be compensated for by more electrons of the surrounding fermi liquid. This game goes on giving rise to multiple layers surrounding the impurity.

UNDER-SCREENING occures when $k < 2\mathsf{s}$. The system harbors insufficient channels to screen the impurity completely. The IR physics is described by k free left-movers and an impurity of reduced spin $|\mathsf{s} - k/2|$.

In our holographic description we will only encounter the first two scenarios.

4.2 KONDO RG FLOW AS CONDENSATION PROCESS

We now turn to a description of the Kondo effect, which has been worked out by the string theory inclined CFT community [13, 123, 127–130]. It rephrases the Kondo effect as a condensation process between branes. The merit of this description is that it is applicable to other CFTs with group target (WZW models) and even coset models, thereby turning the Kondo effect into a solution generating technique for boundary conditions in BCFT. More immediate to our needs, it elicits the picture of the Kondo effect that we will pursue in holography: D-particles stacked at the north-pole of a three-sphere condense into a single two-sphere at fixed polar angle on said three-sphere. Our depiction is taken from the book [207].

Because the rule originates from the Kondo model it is generally called the "absorption of boundary spin" principle. Let us state the rule [9, 207] before applying it:

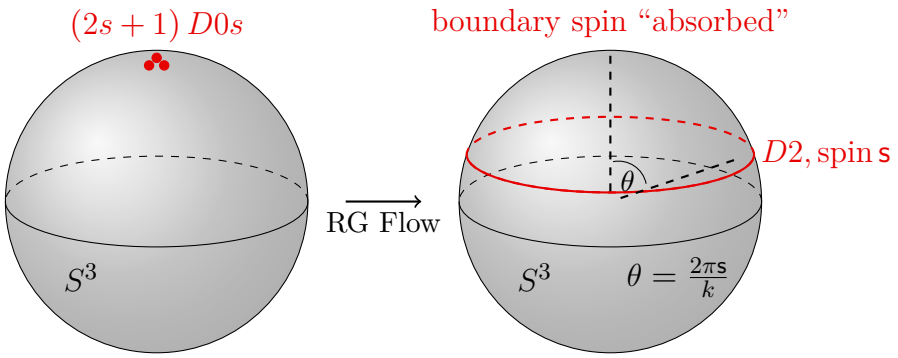

Figure 10: A stack of $(2\mathsf{s}+1)$ D0 branes condense into a single brane of spin s at fixed polar angle $\theta = 2\pi\mathsf{s}/k$. This process describes the absorption of an impurity by surrounding electrons in the Kondo model.

Given an impurity $\vec{S}$ in the spin-s irreducible representation of SU(2) the characters RG flow according to

$$(2\mathsf{s}+1)\chi_j(\tau) \longrightarrow \sum_l N^l_{j\mathsf{s}}\,\chi_l(\tau) \tag{4.15}$$

Characters, χ_j, were introduced in (2.49) and the fusion rules, N^k_{ij} were introduced in (2.55). The fusion rules of the model $\hat{\mathfrak{su}}(2)_k$, which are specific to the Kondo model, are found in (4.14). Consider the partition function of a single brane in the $\hat{\mathfrak{su}}(2)_k$ WZW model, (2.64). Generally, when considering a stack of M branes we have to take into account that the end of each open string may be attached to any of the M D0-branes. As a result the partition function of the stack of branes is M^2 times the partition function of the the single brane,

$$Z_{(M,\,j)} = M^2\, Z_{(1,\,j)} = M^2 \sum_{l=0}^{k/2} N^l_{j\,j}\,\chi_l(\tau). \tag{4.16}$$

The first subscript indicates the amount of stacked branes, while the second subscript labels the branes' type, in our case spin j. We are interested specifically in a stack of $M_\mathsf{s} = (2\mathsf{s}+1)$ pointlike branes located at the north pole, that is, branes of spin $j = 0$, with spectrum

$$Z_{(M_\mathsf{s},\,0)} = M_\mathsf{s}^2\, Z_{(1,\,0)} = M_\mathsf{s}^2\,\chi_0(\tau) \tag{4.17}$$

We now apply the "absorption of boundary spin" principle, (4.15), and we have to apply it twice, once for each end of an open string,

$$\begin{aligned} Z_{(M_\mathsf{s},\,0)} &= M_\mathsf{s}^2\, Z_{(1,\,0)} = M_\mathsf{s}^2\,\chi_0(\tau) \\ &\longrightarrow M_\mathsf{s}\,\chi_\mathsf{s}(\tau) \\ &\longrightarrow \sum_l N^l_{\mathsf{s}\mathsf{s}}\,\chi_l(\tau) = Z_{(1,\,\mathsf{s})}. \end{aligned} \tag{4.18}$$

We learn that the stack of pointlike branes with spin $j = 0$ has decayed into a *single* brane of spin $j = \mathsf{s}$! When $2\mathsf{s} < k$, i.e. overscreening, we obtain spherical brane wrapping the S^3 at constant polar angle $\theta = 2\pi\mathsf{s}/k$. When $2\mathsf{s} = k$, i.e. exact screening, the decayed brane is again pointlike and sits at $\theta = \pi$. This brane condensation is illustrated in Figure 10.

The objective of the next chapters is to carry this picture of the Kondo effect over into holography using a full string theory construction.

5

PROBE BRANES

In this chapter we begin our investigation of Kondo-like models withinthe realm of holography. The central element guiding us is the idea de-scribed towards the end of the previous chapter: A collection of point-like branes accumulated at the north pole of a three-sphere is unstableagainst decay into a single brane of dimension two wrapping a two-sphere at some constant polar angle.

As is appropiate for the Kondo model, we need a holographic setup incorporating a two-dimensional conformal field theory. The obvious candidate is type IIB string theory on $\mathrm{AdS}_3 \times \mathrm{S}^3 \times T^4$. Fortunately, it naturally incorporates a three-sphere on which to stage the RG flow of interest. Moreover, if we choose to realize this geometry as near-horizon limit of the F1/NS5 system, the S^3 has a description as a $\hat{su}(2)_\mathsf{k}$ WZW model, just as the Kondo model. To secure supersymmetry the brane configuration is not just purely situated on the three-sphere, but will also be extended on the AdS_3 part [31]. In both, the UV and IR, the extension into AdS_3 assumes the shape of an AdS_2 slice, whose isometries, $SO(2,1)$ match those of a $(0+1)$ dimensional defect theory. Precisely what is desired!

We begin this chapter with a recapitulation of AdS_2-branes inside AdS_3 in Section 5.1 and S^2-branes inside S^3 in Section 5.2. In Section 5.3, these two types of branes are combined into a D3-brane inside $\mathrm{AdS}_3 \times S^3$. Then come the news. We show that this D3-brane can be interpreted as the IR fixed point of an RG flow and compute the flow profile away from the UV fixed point. Lastly, in Section 5.4, we turn our attention to the UV fixed point. Using the corresponding non-abelian DBI action, we find the operator dimension of the perturbing operator. It is marginally relevant, thereby confirming that our flows are indeed tripped in the UV.

5.1 ANTI-DE SITTER BRANES

This section recapitulates the findings of [31] relevant to our work and is aimed at readers, who want to gather first experience with branes. The goal is to describe D1-branes embedded into AdS_3. We work with Poincaré patch coordinates

$$ds^2 = L^2 \frac{dz^2 - dt^2 + dx^2}{z^2} \tag{5.1}$$

where L is the AdS radius. When the branes do not backreact on the geometry, that is to say that the branes probe the geometry we can employ a DBI lagrangian to describe a single D-string,

$$\mathcal{L} = -T_{D1}\sqrt{-\det(\hat{g}+\mathcal{F})}, \qquad \mathcal{F} = \hat{B} + 2\pi\alpha' F, \tag{5.2}$$

Here, T_{D1} is the tension of the D1 brane and the field strength F corresponds to the $U(1)$ gauge field A. Unlike the Kalb-Ramond two-form B and metric g, which are present on all of AdS_3 the gauge field A is harbored on the worldvolume only. Hats indicate a pullback to the brane worldvolume, which we designate to have AdS_2 geometry[1], that is to say we lay the brane along the (z,t) subspace and choose static gauge such that these are indeed the worldvolume coordinates. The coordinate x is then cast into the role of a fluctuating field on this worldvolume, $x = x(z,t)$. All Ramond-Ramond fields vanish on AdS_3 in our duality frame and hence there are no Wess-Zumino terms so that the DBI action is complete as it stands.

AdS_3 is three-dimensional and thus its top-forms are three-forms, which all have to be proportional to the volume form $\omega = (L/z)^2 dz \wedge dt \wedge dx$. We can use this to narrow down the form of the Kalb-Ramond field by contemplating its exterior derivative $H = dB \propto \omega$. The proportionality constant can be shown to be $2/L$ and we can simply write

$$B = -\frac{L^2}{z^2} dt \wedge dx \qquad \Rightarrow \qquad \hat{B} = \frac{L^2}{z^2} x' dz \wedge dt. \tag{5.3}$$

Only the radial derivative $x' = \partial_z x$ appears in the pullback since antisymmetry of the forms eliminates the contribution from the time derivative $\dot{x}$. The gauge field $A = A_\mu\, dx^\mu$ has two components and we choose to gauge away $A_z = 0$, so that $F = F_{zt}\, dz \wedge dt = (\partial_z A_t - \partial_t A_z) dz \wedge dt = \partial_z A_t\, dz \wedge dt$. With this the gauge invariant field strength can be pieced together,

$$\mathcal{F} = \left(\frac{L^2}{z^2} x' + 2\pi\alpha' F_{zt}\right) dz \wedge dt = L^2 \left(\frac{x'}{z^2} + f\right) dz \wedge dt, \tag{5.4}$$
$$f \equiv \frac{2\pi\alpha' F_{zt}}{L^2}.$$

Lastly we can pull back the metric (5.1) to the worldvolume

$$\hat{g} = \frac{L^2}{z^2} \begin{pmatrix} 1 + x'^2 & x'\dot{x} \\ x'\dot{x} & \dot{x}^2 - 1 \end{pmatrix} \tag{5.5}$$

1 One of the results of [31] is that the only physical choices one has to embed a brane into AdS_3 are either hyperbolic branes (H_2) of anti-de Sitter branes (AdS_2)

and compute the lagrangian,

$$\mathcal{L} = -T_{D1}\frac{L^2}{z^2}\sqrt{M}, \qquad M \equiv 1 + x'^2 - \dot{x}^2 - (x' + z^2 f)^2. \tag{5.6}$$

In the following we are interested in static configurations and drop $\dot{x}$ already in the lagrangian. The equations of motion are then derivatives in z and we write them in their integrated form

$$x: \quad c = \frac{T_{D1}L^2 f}{\sqrt{M}}, \tag{5.7a}$$

$$A_t: \quad q = T_{D1}\, 2\pi\alpha' \frac{(x' + z^2 f)}{\sqrt{M}}, \tag{5.7b}$$

with two constants of integration k, q. The second equation is the Gauss constraint (in integrated form) and thus q is actually a charge. It counts the number of fundamental strings attached to our D-string and hence must be quantized. The other constant, c, will help us to distinguish two solutions to these equations and we start with the less interesting one for our purposes, namely $c \neq 0$. In this case we can, for instance, divide the A_t-equation by the x-equation to obtain

$$x' = \left(\frac{L^2}{2\pi\alpha'}\frac{q}{k} - z^2\right) f. \tag{5.8}$$

This can be plugged into the A_t equation, (5.7b), to solve for

$$\begin{aligned} \frac{\partial_z A_t}{T_{F1}L^2} = f = \pm \frac{1}{\sqrt{-(z^2 - y_+)(z^2 - y_-)}}, \\ y_\pm = \frac{L^2}{c}\left(qT_{F1} \pm T_{(1,q)}\right), \end{aligned} \tag{5.9}$$

where we have reinstated the tension of a fundamental string, $T_{F1} = (2\pi\alpha')^{-1}$ and that of a (p, q) string,

$$T_{(p,q)} = \sqrt{p^2 T_{D1}^2 + q^2 T_{F1}^2} \tag{5.10}$$

The gauge field strength has then a non-vanishing value at the conformal boundary of AdS_3, $f\big|_{z=0} = \pm c/(T_{D1}L^2)$.

Of course, the other type of solution to equations (5.7) corresponds to $c = 0$, which immediately implies a vanishing field strength, $f = 0$, and in turn the scalar x is found to have a linear dependence on the coordinate z,

$$A_t = a, \qquad x = q\frac{T_{F1}}{T_{D1}}z + x_0. \tag{5.11}$$

x_0 and a are integration constants. This is the solution presented in [31] and we will be concerned with it in the following. The solution describes

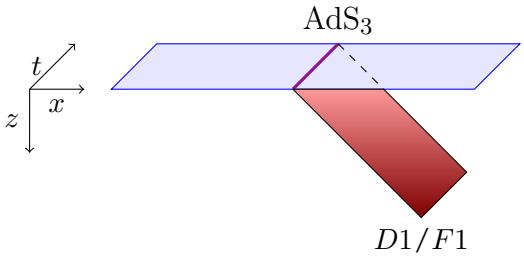

Figure 11: A (p,q) interface (shaded in red) hangs down with constant slope $x' = q\frac{T_{F1}}{T_{D1}}$ into AdS. In the CFT the interface is just the purple line, which splits the CFT spacetime in half. Two possibly distinct CFTs ar found to either side.

an AdS_2 brane hanging down from the boundary at position x_0 and reaching infinitely into the bulk of AdS_3. If there are no fundamental strings attached to the D string, $q = 0$, it simply falls down parallel to the z-coordinate, that is, it intersects the boundary perpendicularly. If there are fundamental strings attached to the brane, it stabilizes at an angle determined by the slope $x' = q\frac{T_{F1}}{T_{D1}}$ as can be seen in Figure 11.

This result applies bound state of a single D1-brane with q fundamental strings. What about about a bound state of p D1-branes and q fundamental strings, the (p,q) string? As explained in Section 2.1.2, whenever we treat stacks of D-branes, we have to resort to the non-abelian DBI action (5.49) in which all fields are in general non-commutative $p \times p$ matrices. This case will be considered below. Here we note, that we may also choose a configuration in which all fields are indeed commutative in (5.49). Then the non-abelian DBI action reduces to (5.2) multiplied by an overall factor of p stemming from the trace. In this case we can then adapt our result (5.11) by rescaling $T_{D1} \to pT_{D1}$,

$$A_t = a, \qquad x = \frac{qT_{F1}}{pT_{D1}} z + x_0. \tag{5.12}$$

Had we chosen a slicing of AdS_3 in terms of AdS_2 sheets, it would have become obvious that the brane is extended along one such AdS_2 slice. Further down we will prefer that description, because it highlights the $SO(2,1)$ conformal group of the defect, which appears naturally as isometries of AdS_2.

5.2 TWO-SPHERE BRANES

Ultimately we are interested in studying brane configurations inside of not only AdS_3, but $AdS_3 \times S^3$. We will treat the branes of the previous section as building blocks, which will be augmented in the S^3 directions by the branes discussed in the current section. Obviously, the AdS_2 brane by itself is a dot on S^3. Generally, we may have several such

dots on S^3 [2] and whenever we discuss these configuration we choose to locate these dots without loss of generality on the north pole. The more interesting option is that of an extra $S^2 \subset S^3$. These branes have been studied on their own as conformally invariant boundary conditions of the $\hat{\mathfrak{su}}(2)_k$ WZW model [30] and we recapitulate the necessary findings in this section.

The Lie group $SU(2)$ is isomorphic to S^3 and we choose spherical coordinates such that the metric assumes the form

$$ds^2 = L^2\Big[d\theta^2 + \sin^2\theta(d\phi^2 + \sin^2\phi\, d\chi^2)\Big]. \tag{5.13}$$

The naming of the sphere radius anticipates that it will be identified by supersymmetry with the AdS radius. It can be expressed through the string data

$$L^2 = k\alpha' . \tag{5.14}$$

We work in a duality frame where AdS_3 and S^3 have vanishing RR fields and non-trivial NS two form,

$$B = L^2\Big(\theta - \sin\theta\cos\theta\Big)\,\omega_{S^2}. \tag{5.15}$$

We have chosen a gauge where B is proportional to the volume form of the unit two-sphere $\omega_{S^2} = \sin\phi\, d\phi \wedge d\chi$.

Conformally invariant boundary conditions, i.e. branes, for CFTs with group target are conjugacy classes of the group, which in the case of the WZW model on $SU(2)$ are two-spheres. We choose worldvolume coordinates (ϕ, χ) for them so that they are distinguished by their value of polar angle θ. Furthermore, rational CFTs admit only a finite number of conformally invariant boundary conditions, each in one-to-one correspondence with one primary field of the chiral algebra. The $\mathfrak{su}(2)_k$ WZW model is no exception. It has $k+1$ WZW primaries and so from the $U(1)$'s worth of conjugacy classes of $SU(2)$ only $k+1$ give rise to conformally invariant boundary conditions. Let us label these by an integer $1 \le p \le k+1$.

There is a physical picture associated with this. Assume that we are embedding an S^2 brane into S^3. Since the homotopy group $\pi_2(S^3)$ is trivial all such two-spheres "have the urge" to shrink to zero size. What counteracts this is a worldvolume magnetic flux $F = dA$, where again A is a gauge field living on the brane. Only for specific, quantized values of flux will the brane be stabilized. As expected, this quantization ties in with the primary fields of the CFT and this is mirrored in the numeric value of the quantized worldvolume flux,

$$F = -\frac{p}{2}\,\omega_{S^2} \qquad \Leftrightarrow \qquad \int_{S^2} F = -2\pi p. \tag{5.16}$$

2 Of course then our DBI lagrangiang is not adequate anymore and must be replaced by its non-abelian cousin [190].

The smallest and largest value of the flux, $p = 1$ and $p = \mathsf{k} + 1$, correspond to D-particles, or if one wishes, two-spheres of zero size. In the CFT they represent the two conjugacy classes of the center elements $\pm\mathbb{1}$. All other values of p give rise to honest two spheres representing regular conjugacy classes. Pay attention however to the fact that the magnetic charges computed from $\int F$ or $\int \mathcal{F}$ are D-particle charges, because they are integrated two-forms. In other words, we can think of the stabilizing flux as arising from p D-particles dissolved on the two-sphere brane. Lastly, let us point out that flux coming from the gauge invariant combination

$$\mathcal{F} = \hat{B} + 2\pi\alpha' F = L^2\Big(\theta - \sin\theta\cos\theta - \theta_p\Big)\omega_{\mathrm{S}^2} \tag{5.17}$$

is *not* quantized. The quantity

$$\theta_p := \frac{\pi\alpha' p}{L^2} \overset{(5.14)}{=} \frac{\pi p}{\mathsf{k}} \tag{5.18}$$

is the value of the polar angle of the S^2 brane for fixed p and is a local minimum of the energy. We show in the following section that θ_p maintains this characteristic when we combine the S^2 branes of this section with the AdS_2 branes of the previous section into superssymmetric D3-branes. For now we just observe that the more D1-brane charge p is present on the S^2-brane, the further down it is stabilizes on the S^3.

5.3 SUPERSYMMETRIC $\mathrm{AdS}_2 \times S^2$ BRANES AS RG FIXED POINT

It is time to move towards Kondo-like flows in this geometric setting. As discussed in the CFT description of the Kondo effect, we are looking to have a collection of pointlike branes flow into a single spherical brane. The idea remains the same, however the S^2 brane of the Kondo effect is augmented by an AdS_2 piece inside AdS_3. The setting of our investigations is the near horizon region of the F1/NS5 system[3], which takes the shape $\mathrm{AdS}_3 \times \mathrm{S}^3 \times M_4$, with M_4 being a either T^4 or K_3; we choose the former.

Into this geometry we embed a D3= $\mathrm{AdS}_2 \times \mathrm{S}^2$ brane. Let us borrow one last piece of information. These branes have been shown in [31] to be supersymmetric. The angle at which the AdS_2 brane hangs into the bulk of AdS_3 is given by the slope of x in (5.12). The charge q still counts the number of fundamental strings attached to the brane, while the D1 charge p indicates the flux through the S^2. One is tempted to think it is the number of D1-branes in the system. This this not quite correct, because there are no D1-branes present in this setup. The correct way of thinking is that p counts the number of D1-branes *dissolved* into the

3 It can be reached from the more common D1/D5 system by an S-duality transformation.

D3-brane. This distinction is important since the RG flow we wish to describe is precisely the transition from a system

$$\text{UV: } p\ D1_q(\mathrm{AdS}_2) \qquad \longrightarrow \qquad \text{IR: } 1\ D3_{p,q}(\mathrm{AdS}_2 \times \mathrm{S}^2). \tag{5.19}$$

Subscript q indicates the units of attached fundamental strings, while subscript p indicates the dissolved D1 charge. The worldvolume geometry is indicated in parentheses. The UV fixed point involves multiple D1-branes and the discussion in Section 5.1 does not apply, because the lagrangian we used captures only the case of a single brane. It is possible to write down a DBI lagrangian using the more general non-abelian form presented in [190], and in Section 5.4 we will carry out such an analysis. Nevertheless, the results for a single AdS_2 brane can and will be put to use in the upcoming discussion of the D3= $\mathrm{AdS}_2 \times \mathrm{S}^2$. The main purpose of the current section is to establish that a D3= $\mathrm{AdS}_2 \times \mathrm{S}^2$ with p units of D1 charge dissolved in it indeed arises as IR fixed point and hence the proclaimed flow exists.

We choose coordinates on the constituents of $\mathrm{AdS}_3 \times \mathrm{S}^3$ as before,

$$ds^2 = L^2\left[\frac{dz^2 - dt^2 + dx^2}{z^2} + d\theta^2 + \sin^2\theta\left(d\phi^2 + \sin^2\phi\, d\chi^2\right)\right]. \tag{5.20}$$

The radii of AdS_3 and S^3 are forced by supersymmetry to coincide. For the worldvolume we choose coordinates

$$\xi^a = (z,\, t;\, \phi,\, \chi), \qquad \text{static gauge}, \tag{5.21}$$

which leaves us with two fluctuating fields, $x = x(\xi)$ and $\theta = \theta(\xi)$. Kondo-like physics should respect $SU(2)$ invariance and to achieve this we demand that all quantities be independent of the two-sphere coordinates $(\phi,\, \chi)$. Moreover, we are interested in static situations, which leaves us with $x = x(z)$ and $\theta = \theta(z)$. Recall that the holographic direction z prescribes an energy scale, so precisely this dependence determines how all fields change along the RG flow, in particular the polar angle $\theta(z)$. It corresponds to the S^2 part of the the D3-brane sliding down on the S^3. If it stops at some fixed value the flow exists. Indeed this will be the case and the polar angle will saturate at the obvious suspect θ_p, see (5.18).

As before we need to pull the metric back onto the worldvolume,

$$\hat{g} = L^2(z^{-2} + x'^2 + \theta'^2)dz^2 - \frac{L^2}{z^2}dt^2 + \sin^2\theta\left(d\phi^2 + \sin^2\phi\, d\chi^2\right). \tag{5.22}$$

The NS two-form can also be pieced together from the individual geometries, $B = B_{\mathrm{AdS}} + B_{\mathrm{S}}$. It's pullback to the worldvolume is

$$\hat{B} = \frac{L^2}{z^2}x'dz \wedge dt + L^2\Big(\theta - \sin\theta\cos\theta\Big)\sin\phi\, d\phi \wedge d\chi. \tag{5.23}$$

Of course we also have a $U(1)$ field strength, $F = F_{ab}\, d\xi^a \wedge d\xi^b$. Again we use the Kondo effect as guideline and demand $SU(2)$ invariance, which forbids crossterms between the AdS_2 and S^2 parts,

$$F = F_{zt}\, dz \wedge dt + F_{\phi\chi}\, d\phi \wedge \chi. \tag{5.24}$$

Here is where we employ the results of the Section 5.1 and Section 5.2 as an

$$\begin{aligned} \text{ansatz:} \qquad & x'(z) = \text{const}, \\ & F_{zt} = 0, \qquad F_{\phi\chi} = -\frac{p}{2}\sin\phi. \end{aligned} \tag{5.25}$$

The remaining component $F_{\phi\chi}$ is constrained by the Bianchi identity $dF = 0$ to be independent of z. Next, the gauge invariant field strength is also pieced together from the individual pieces (5.4) and (5.26),

$$\begin{aligned} \mathcal{F} =& \frac{L^2}{z^2} x' dz \wedge dt + L^2\Big(b(\theta) - \theta_p\Big)\sin\phi, \\ b(\theta) :=& \theta - \sin\theta\cos\theta, \end{aligned} \tag{5.26}$$

In the first line of (5.27) L means Lagrange function, while in the last line of the same equation it means the AdS *radius. Apologies for the overlap of notation.*

with θ_p as before, (5.18). At last we have assembled all ingredients for the DBI action of this system,

$$\begin{aligned} S_{DBI} &= \int dt\, L \\ &= -T_3 \int dz\, dt\, d\phi\, d\chi\, \sqrt{-\det(\hat{g} + \mathcal{F})} \\ &= -4\pi L^2\, T_3 \int dz\, dt\, \frac{L^2}{z^2}\sqrt{NP}, \end{aligned} \tag{5.27}$$

where

$$N = 1 + (z\theta')^2 - x'^2, \tag{5.28}$$

$$P = \sin^4\theta + (b(\theta) - \theta_p)^2. \tag{5.29}$$

Due to our requirements no quantity depends on the two-sphere coordinates (ϕ, χ), so that we could integrate out their contribution to the action leading to the prefactor $4\pi L^2$. Of course, the next step is to solve the equations of motion. Before we turn our attention to them however, it is instructive to sidestep into an investigation of the energy of the system. In particular, we are interested in configurations, which minimize the energy, while being constant in RG time z. If we think of the radial coordinate in AdS as energy scale, this implies that there is no (further) renormalization going on. We follow the treatment of [64], but stress that the case discussed here is genuinely new.

The hamiltonian H of the system, found as usual through a Legendre transformation of the Lagrange function L in (5.27), is

$$\begin{aligned} H =& \dot{\theta}\frac{\partial L}{\partial \dot{\theta}} + \dot{A}_z \frac{\partial L}{\partial \dot{A}_z} + \dot{A}_t \frac{\partial L}{\partial \dot{A}_t} - L \\ =& 4\pi L^2 T_3 \int dz \frac{L^2}{z^2}\sqrt{NP}. \end{aligned} \tag{5.30}$$

None of the first three momentum terms contribute, because we are static and we gauged $A_z = 0$ to begin with.

Our objective is a configuration where the polar angle $\theta(z)$ has stopped renormalizing, $\theta'(z) = 0$. Now that we have the hamiltonian at our disposal, we can easily inquire about such configurations which minimize the energy locally,

$$0 \overset{!}{=} \left.\frac{\partial H}{\partial \theta}\right|_{\theta'=0} = 4\pi L^2 T_3 \int dz \frac{L^2}{z^2}\sqrt{\frac{N}{P}}\, 2(\theta - \theta_p)\sin^2\theta. \tag{5.31}$$

In analogy with [64] we define[4]

$$\Lambda_p(\theta) := \theta - \theta_p. \tag{5.32}$$

It is then clear from (5.31) that the local energy minima are obtained for

$$\Lambda_p(\theta)\sin^2\theta = 0 \qquad \Rightarrow \qquad \theta = 0,\, \pi,\, \theta_p. \tag{5.33}$$

For $\theta = 0, \pi$ the brane has no extension on three-sphere, while the configuration corresponding to θ_p describes a $D3 = \mathrm{AdS}_2 \times \mathrm{S}^2$. In fact the latter is the global minimum. Indeed, straightforward evaluation of the energy (5.30) on these configurations ($\theta' = 0$) gives

$$H(\theta = 0) = H(\theta = \pi) = 4\pi L^2 T_3 |\theta_p| \sqrt{1 - x'^2} \int dz \frac{L^2}{z^2}, \tag{5.34}$$

$$H(\theta = \theta_p) = 4\pi L^2 T_3 |\sin\theta_p| \sqrt{1 - x'^2} \int dz \frac{L^2}{z^2}. \tag{5.35}$$

It is then simple to check that the non-trivial polar angle θ_p is the global energy minimum,

$$\frac{H(\theta_p)}{H(0)} = \left|\frac{\sin\theta_p}{\theta_p}\right| \leq 1. \tag{5.36}$$

This is the first important result. Not only does a $D3 = \mathrm{AdS}_2 \times \mathrm{S}^2$ appear as local minimum, but is also the global energy minimum. It is therefore a sensible candidate for the IR fixed point. In order to truly

4 Readers interested in comparing with [64] are advised that our p corresponds to their n.

establish it as the IR fixed point, we have to confirm that renormalization indeed stops at θ_p. To this end, we have to find solutions to the equations of motion.

Let us remark beforehand on saturation of (5.36), which is reached for $\theta_p = 0$. This is of course the situation where no D1-branes are dissolved. In Section 5.2 this case was out of the picture since we were using $SU(2)$ WZW model as guideline, which had as lowest value $p = 1$. Here we distance ourselves from this restriction a little and include the trivial case $\theta_p = 0$. A motivation to do so is the results from supergravity, which do admit $\theta_p \to 0$, however not because there are no D1 strings dissolved, but because that framework allows for multiple D3-branes. We will see that in that case the angle θ_p is controlled by the ratio of D1- and D3-branes and can be arbitrarily small if the D3-branes outnumber the D1-branes.

Now we return to the general situation, where the polar angle θ depends on the radial coordinate z. Determining the specific profile $\theta(z)$ requires an understanding of the equations of motion for the Lagrange function in (5.27). Even though it is just an ordinary differential equation, it turns out to be quite difficult to solve, as can be seen already for the simplest case $x' = 0$,

$$0 = \theta'' - z\theta'^3 - 2\Lambda_p(\theta)\sin^2\theta\frac{1+(z\theta')^2}{z^2(\sin^4\theta + (b(\theta)-\theta_p)^2)}. \tag{5.37}$$

Fortunately, there exists a very elegant approach to bypass solving the equations of motion, which was applied to a similar situation for higher-dimensional probe branes in RR backgrounds [64].

It is instructive to restrict to the case $x' = 0$ at first. The hamiltonian (5.30) can then be recast as

$$H = 4\pi L^4 T_3 \int dz\, \sqrt{\mathcal{Y}^2 + \mathcal{Z}^2}, \tag{5.38}$$

with the functions

$$z^2\mathcal{Y} = \Lambda_p \sin\theta + z\theta'(\sin\theta - \Lambda_p\cos\theta), \tag{5.39}$$

$$z^2\mathcal{Z} = z\theta'\Lambda_p\sin\theta - (\sin\theta - \Lambda_p\cos\theta) = z^2\frac{d}{dz}\frac{\sin\theta - \Lambda_p\cos\theta}{z}. \tag{5.40}$$

Writing the hamiltonian in this form grants easy access to the lower bound

$$H \geq 4\pi L^4 T_3 \int dz|\mathcal{Z}|. \tag{5.41}$$

Since $\mathcal{Z}$ is a total derivative the bound is easily integrated and found to depend only on the boundary values of $\theta(z)$. Hence any configuration $\theta(z)$ saturating the bound will automatically solve the equations of

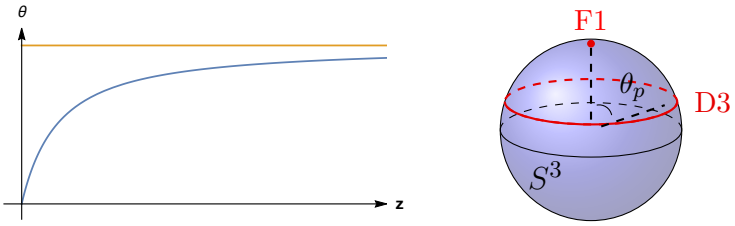

Figure 12: Left: Plot of the RG dependence of the polar angle θ given by (5.43). It saturates at the yellow line, which demarcates $\theta_p = \pi p/N_5$. Right: In the UV we have a stack of F1 strings, which condense in the IR into a single D3-brane at θ_p. Plot by Charles Melby-Thompson.

motion. From (5.38) it is evident that this happens when $\mathcal{Y} = 0$, which implies the first order differential equation,

$$z\theta' = -\frac{\Lambda_p \sin\theta}{\sin\theta - \Lambda_p \cos\theta}. \tag{5.42}$$

Which is, in contrast to the equation of motion (5.37), easily integrated to give

$$z = z_0 \frac{\sin\theta}{\theta - \theta_p}. \tag{5.43}$$

At best, we can invert this to give an implicit dependence $\theta(z)$. It is not necessary however to do so. In order to single out the fixed points, we have to look for values of θ for which the RG time, z, diverges and hence renormalization stops. This clearly happens for $\theta = \theta_p$. Note that $\theta = 0$ and $\theta = \pi$ do not fullfil this requirement giving definite evidence to rule out those two energy minima (recall (5.34)). A plot of (5.43) confirms that, as we move into the bulk with increasing z, the polar angle saturates at $\theta = \theta_p$, see Figure 12.

A different, and important, way of expressing the fact that renormalization stops is that the perturbing operator has become irrelevant, i.e. it no longer drives the system out of an RG fixed point. The defect field theory is in one dimension and hence "irrelevant" means that its dimension is bigger than one.

The last question we answer here is that of the preserved supersymmetries. In (5.42) we have found a first order differential equation, which generates solutions to the equations of motion (5.37). This feature is generally a hallmark of BPS equations and thus our flow preserves one half of the supersymmetries of the full system. Let us count how many those are. The near-horizon region of the F1/NS5 system featured sixteen superconformal symmetries. These are broken by the presence of the defect to eight superconformal symmetries. The flow, being BPS, then preserves only four supercharges. We emphasize that these are not superconformal. The fixed points of the flow on the other hand are conformal and hence they preserve eight superconformal sym-

metries. Along the flow, we loose conformality and with that also the superconformal generators. Certainly, there exist also other flows, which break all supersymmetry. Such are solutions to the equations of motion (5.37), but not (5.42). Altogether we have thus found a very special class of flows, namely those which preserve the maximal number of supercharges.

In an upcoming publication [112], together with my collaborators Johanna Erdmenger and Charles Melby-Thompson, we present the flows for interfaces with additional F1 charge. These are readily realized in the S-dual frame, the D1/D5 background, through use of *κ-symmetry*. If we think of reparametrizations in general relativity as bosonic symmetries, then κ-symmetry realizes their fermionic superpartners.

5.4 NON-ABELIAN BRANE POLARIZATION

The previous section was concerned with the describtion of the IR fixed point of the flow. Here we want to investigate the vicinity of the UV fixed point. The difficulty here lies in the fact that we need to describe multiple branes. They cannot be described by the same type of DBI action that we have used before, (5.2), which is valid only for a single D-string. Multiple D-branes are described by a non-abelian generalization, understood for the first time by Myers [190]. A review is found in Section 2.1.2.

We are interested in finding the dimension of the perturbing operator. In the IR we have already established that the perturbing operator becomes relevant. Otherwise, renormalization would not stop. In this section we will see that in the UV the perturbing operator does indeed drive the system out of the UV fixed point, i.e. it is relevant. As it turns out it is actually marginally relevant.

For our purposes it will be sufficient to evaluate this non-abelian DBI action to cubic order in the field θ. Again, we consider only the case of vanishing F-string charge on the interface. In this setup however this does not affect the result, since our considerations are entirely independent of the F-string charge, i.e. the results here are the same for any kind of (p, q)-string interface.

What are the relevant deformations of our brane configuration? Abelian deformations of our model induce a shift in the location of of the brane configuration on T^4 or S^3 and are all irrelevant operators. Fortunately, there is a natural relevant deformation, which is tripped by non-abelian polarization of our defect. This type of deformation is familiar from the SU(2) WZW model. Starting with the BCFT corresponding to p D0 branes on $\mathrm{SU}(2) \simeq S^3$, there exists for $p > 1$ a relevant boundary deformation. The deformation involves a maximally non-abelian deformation of the S^3 embedding coordinates. Because the H field is non-vanishing on S^3, a set of branes so polarized becomes

unstable toward flow to a single D2 brane wrapped stably on some $S^2 \subset S^3$.

The S^3 of our model is in fact described by just such a WZW sector. What has changed is that the string worldsheet theory in the presence of a deformation must remain conformal, so that the RG flow in the WZW model must now be realized as a "dynamical" process evolving in the direction of increasing z.

Let us examine briefly what happens when we first turn on the flow. To simplify matters, we switch to stereographic coordinates on S^3:

$$ds^2_{S^3} = \frac{(2\,d\vec{x})^2}{(1+r^2)^2}\,, \qquad \vec{x} \in \mathbb{R}^3\,. \tag{5.44}$$

Stereographic coordinates are related to polar coordinates by $r = \tan\frac{\theta}{2}$. The B-field on S^3 now takes the form

$$B_{S^3} = \ell^2 b\,\omega_{S^2} = \ell^2 b \frac{\epsilon_{ijk} x^i dx^j \wedge dx^k}{r^3}\,, \tag{5.45}$$

$$b = \theta - \sin\theta\cos\theta\,. \tag{5.46}$$

For convenience, we set $g(r) = \frac{4}{(1+r^2)^2}$ so that $g_{ij} = g(r)\delta_{ij}$.

We fix as the brane's worldsheet coordinates to be (t, z) and pick the pole $\vec{x} = 0$ to be the S^3 location of the D1-branes in the UV.

We study a deformation of the system in which the S^3 embedding coordinate matrix $\vec{\mathbf{x}}$ of the D1-branes in stereographic coordinates takes the form

$$\mathbf{x}^i = \lambda f(z) \mathbf{\Sigma}_i\,, \tag{5.47}$$

where the Hermitian matrices $\mathbf{\Sigma}_i$ satisfy the $\mathfrak{su}(2)$ commutation relations

$$[\mathbf{\Sigma}_i, \mathbf{\Sigma}_j] = i\epsilon_{ijk}\mathbf{\Sigma}_k\,. \tag{5.48}$$

We further assume that the fundamental of $\mathfrak{u}(k)$ is irreducible under $\mathfrak{su}(2)$, making it the spin $\frac{k-1}{2}$ representation. Then $\mathbf{r}^2 = \vec{\mathbf{x}}^2 = C_2(\Sigma)(\lambda f)^2 \mathbb{1}$, where $C_2(\Sigma) = \frac{k^2-1}{4}$ is the quadratic Casimir of $\mathfrak{su}(2)$ in the representation defined by $\vec{\mathbf{\Sigma}}$, making $r = \sqrt{C_2}\lambda f$ an abelian quantity. We further assume that the brane has a fixed location in the x^1 and M_4 directions[5].

The non-abelian DBI Lagrangian takes the form

$$I_{\text{DBI}} = -T_{\text{D1}}\text{Tr}\left(e^{-\Phi}\sqrt{-\det(E_{ab} + E_{ai}(Q^{-1}-\delta)^{ij}E_{jb} + \lambda F_{ab})\det(Q^i{}_j)}\right), \tag{5.49}$$

5 If we choose Janus coordinates on AdS_3 then the Janus coordinate ψ is also chosen to be an abelian constant in our ansatz.

where

$$E_{\mu\nu} = g_{\mu\nu} + B_{\mu\nu} \tag{5.50}$$
$$Q^i{}_j = \delta^i{}_j - i\lambda[\mathbf{x}^i, \mathbf{x}^k]E_{kj}\,. \tag{5.51}$$

In this expression, $\xi^a = (t, z)$ denote the worldsheet variables, while x^i denote the transverse variables.

Actually, we are only interested in finding the dimension of the perturbing operator θ. Since the perturbing operator will be the same for any kind of (p, q) string starting configuration, we simply restrict to the case of a pure F1 string defect, $F_{ab} = 0$, $\psi = 0$, $B_{\mathrm{AdS}_3} = 0$. The relevant components of $E_{\mu\nu}$ are then

$$\begin{aligned} E_{ij} &= L^2\left(g\,\delta^i{}_j + \frac{b(\theta(r))}{r^2}\epsilon_{ijk}\mathbf{\Sigma}^k\right), \\ E_{ab} &= g_{ab}, \\ E_{ia} &= 0 = E_{ai}, \end{aligned} \tag{5.52}$$

and we also have[6]

$$Q^i{}_j = \left(1 - \frac{2L^2 b}{\lambda\sqrt{C_2}}\right)\delta^i{}_j\mathbb{1} + \frac{2L^2 b}{\lambda(C_2)^{3/2}}\mathbf{\Sigma}^j\mathbf{\Sigma}^i + \frac{2L^2}{\lambda C_2}r^2\, g\,\epsilon_{ijk}\mathbf{\Sigma}^k \tag{5.53}$$

Then

$$-\det(E_{ab} + E_{ai}(Q^{-1} - \delta)^{ij}E_{jb}) = \frac{L^2}{z^2}\left(\frac{L^2}{z^2} + \frac{(\partial_z r)^2}{C_2}\mathbf{\Sigma}^i\left(Q^{-1}\right)_{ij}\mathbf{\Sigma}^j\right) \tag{5.54}$$

where $Q^{ij}(Q^{-1})_{jk} = \delta^i{}_k$ with $Q^{ij} = E^{ij} - i\lambda[\mathbf{\Sigma}^i, \mathbf{\Sigma}^j]$ and $E^{ij}E_{jk} = \delta^i{}_k$.

In order to extract the dimension of the perturbing operator it actually suffices to contemplate the potential generated by the action (5.49). Actually, we only require the mass term, $\mathcal{O}(\theta^2)$. We anticipate that it vanishes and hence we also compute the $\mathcal{O}(\theta^3)$ terms, which inform us whether we are dealing with a marginally relevant or marginally irrelevant operator.

Inspection of (5.54) together with $r = \tan\theta/2$ makes clear that this determinant contains no terms, which are purely powers of θ, but rather always feature derivatives in z. Hence, we content ourselfs with expanding its contributions to leading order, $\left(Q^{-1}\right)_{ij} = 4L^2\delta^i{}_k + \mathcal{O}(\theta)$ and $r = \theta/2 + \mathcal{O}(\theta^3)$. We get

$$-\det(E_{ab} + E_{ai}(Q^{-1} - \delta)^{ij}E_{jb}) = \frac{L^2}{z^2}\left(\frac{L^2}{z^2} + L^2(\partial_z\theta)^2\right) + \dots \tag{5.55}$$

6 We refrain from matching the indices on both sides of (5.53), because raising and lowering involves E^{ij}.

The important terms must then come from the other determinant in (5.49). Indeed, we find terms of the correct orders when expanding (5.53) ($r^2\, g = \sin^2\theta$)

$$Q^i{}_j = \delta^i{}_j + \theta^2 \frac{2L^2}{\lambda C_2}\epsilon_{ijk}\mathbf{\Sigma}^k + \theta^3 \frac{4}{3(C_2)^{3/2}\lambda}\Big(\mathbf{\Sigma}^j\mathbf{\Sigma}^i - C_2\delta^i{}_j\Big). \quad (5.56)$$

This yields

$$\sqrt{Q^i{}_j} = \left(1 - \theta^3 \frac{4}{3(C_2)^{1/2}}\right)\mathbb{1} + \mathcal{O}(\theta^4). \quad (5.57)$$

Overall we then get

$$e^{\Phi} I_{\mathrm{DBI}} = \frac{L^2}{z^2} + \frac{L^2}{2}(\partial_z\theta)^2 - \frac{L^2}{z^2}\frac{4L^2}{3\lambda\sqrt{C_2}}\,\theta^3 + \dots\,, \quad (5.58)$$

which carries no mass term and the cubic order is negative, i.e. the UV fixed point is repulsive. Therefore, we are dealing with a marginally relevant perturbation, as is the case in the actual Kondo model!

5.5 CONCLUSION

In this chapter we have described matters in a way, which emphasizes the mathematical connections between the brane constructions at work – at times at the expense of the physical picture. Let us therefore now gather all bits and pieces that we have accumulated in this chapter highlighting the physical process.

As explained before the Kondo model describes the screening of an impurity, which in the formal language of two-dimensional CFT is represented as a boundary RG flow. This RG flow can be recast into an appealing geometric form: a stack of pointlike branes condense into a bound state described by a two-dimensional brane wrapping a two-sphere inside an $\mathrm{S}^3 \simeq SU(2)$.

Our goal in this chapter was to find an analogous process within the realm of holography. As is appropiate for the Kondo model we need an avatar of AdS/CFT, which gives rise to a two-dimensional CFT at the conformal boundary. An obvious candidate is that of $\mathrm{AdS}_3 \times \mathrm{S}^3 \times T^4$. It naturally offers an S^3 to use as stage for the pointlike branes to condense into twobranes. Since we are dealing with string theory however, we have to secure supersymmetry. It implies that, in our case, the branes are of one dimension higher than in the actual Kondo model. This extra dimension is extended along the AdS_3 part of the ten-dimensional geometry.

For D-branes it is natural to have fundamental strings attach to it and so the impurity in the UV, that is before condensing, may generally be a (p, q) string. Likewise after condensing, that is in the IR, the three-brane carries the same units of onebrane charge; this time dissolved on

the threebrane. The first three sections of this chapter were dedicated to the construction of these charged D3-branes.

The RG flow starts with what was discussed last in this chapter: a stack of D1/F1 bound states extended along an AdS_2 sheet inside of AdS_3 and localized at the north pole of the S^3. Configurations of this type are known to be unstable to condensing into a different brane configuration, a process called non-abelian brane polarization. Our interest was to confirm this for our configuration. Indeed, we found that it is unstable! Moreover, the formalism handed us the dimension of the perturbing operator tripping the flow. It is marginally relevant, much to our delight since this is the case in the actual Kondo model.

As described in the second half of Section 5.3 the flow's IR fixed point[7] corresponds to a charged D3-brane with $AdS_2 \times S2$ geometry, just as desired.

We have worked in the probe brane approximation, that is we have readily neglected the backreaction of our interfaces on the F1/F5 background. In the next chapter we move the discussion into the realm of supergravity, where we do take the geometric influence of the interfaces into account. This moves us closer to the actual Kondo effect, since, among other things, we can then realize critical screening, which is inherently impossible with probe branes.

7 For simplicity we have restricted to a pure D1 charge on the D3-brane.

6

SUPERGRAVITY DUALS OF THE DEFECT FIXED POINTS

In the last chapter we learned that there are Kondo-like flows in holography. We treated the interface branes as probes without any influence on the F1/NS5 background, in which they move. This description is however only an approximation, because the interface branes actually do curve their environment. Only when the interface charge is much smaller than the background charge are we allowed to neglect the interface's backreaction, as was tacitly assumed above.

Of course, it is desirable to have a fully backreacted realization of the flows regardless how small the effect of the interface is for several reasons. The first is that AdS/CFT conjectures, in its weak form, a duality of a field theory with supergravity, not just the probe limit. Generally, quantities of interest require gravitational backreaction, expecially when we want to match with the CFT. This includes correlation functions, in particular one point functions, which measure the expectation values of fields in the presence of an interface, or reflection and transmission coefficients across the defect.

Having a fully backreacted supergravity solution dual to the RG flow in the field theory, is equivalent to having a geometry which smoothly deforms from the UV gravity dual to the IR gravity dual. This is in general a very difficult task and we install the first building blocks here, by presenting the gravity duals of the fixed points of the RG flow. Any gravity dual of the entire RG flow has to start and end with the solutions presented in the following. We rely on the general class of solutions to type IIB supergravity with $\mathrm{AdS}_3 \times S^3 \times T_4$ asymptotics presented in [79]. They are foliated by $\mathrm{AdS}_2 \times S^2$ submanifolds and preserve 8 super(conformal) symmetries, making them dual to superconformal defects in 2d CFT. These solutions include every geometry with these symmetries in which T_4 has no internal fluxes and has (aside from its size) constant moduli.

We begin with a review of these solutions in Section 6.1. In order to write down our solutions we relax the singularity constraints imposed in [79] in Section 6.2. We are then in good shape to determine all solutions required to make contact with the previous chapter in Section 6.3. First off, we construct the $\mathrm{AdS}_3 \times S^3 \times T^4$ solution arising from the F1/NS5 geometry. Into this solution we individually embed a D1/F1 interface as well as a D3 interface. Then we connect these interface solutions via the RG flow of the previous chapter. In Section 6.4 we repeat the same analysis in the D1/D5 duality frame in less detail, but still self-contained. It is the material of this section that will appear in reduced form in the upcoming publication [112]. Section 6.3 and Section 6.4 can

be read independently of each other so that readers interested only in one duality frame are free to skip the other.

6.1 SUPERGRAVITY DUALS OF CONFORMAL INTERFACES IN CFT_2

We wish to write down type IIB supergravity solutions incorporating Kondo-like RG flows. To that end, we consider the general class of half-BPS solutions, which are locally asymptotic to $\mathrm{AdS}_3 \times S^3 \times M_4$ worked out in [79]. A specific class of these solutions with multiple $\mathrm{AdS}_3 \times S^3 \times M_4$ asymptotic regions was later elaborated on in [78, 80].

The ten-dimensional geometries of interest to us are solutions to the Killing spinor equations based on the ansatz

$$ds_{10}^2 = f_1^2 ds_{\mathrm{AdS}_2}^2 + f_2^2 ds_{S^2}^2 + f_3^2 ds_{T_4}^2 + \rho^2\, dz\, d\bar{z}. \tag{6.1}$$

Here, $ds_{\mathrm{AdS}_2}^2$, $ds_{S^2}^2$, $ds_{T_4}^2$ are unit radius metrics for the indicated geometries. The last piece, $\rho^2\, dz\, d\bar{z}$, is the metric of a Riemann surface Σ with boundary over which the other geometries are fibered, i.e. $f_i = f_i(z, \bar{z})$ with $i = 1, 2, 3$. Positive definiteness of the metric requires the metric factors f_i and ρ to be real and positive-definite functions on Σ.

The metric factors

$$f_1^2 = \frac{e^{\phi}}{2f_3^2}\frac{|v|}{u}(a\,u + \tilde{b}^2), \tag{6.2a}$$

$$f_2^2 = \frac{e^{\phi}}{2f_3^2}\frac{|v|}{u}(a\,u - b^2), \tag{6.2b}$$

$$f_3^4 = e^{-\phi}\frac{u}{a}, \tag{6.2c}$$

$$\rho^4 = 4e^{-\phi}u\left|\frac{\partial_z v}{B}\right|^4 \frac{a}{v^2} \tag{6.2d}$$

are given in terms of four harmonic functions[1]

$$\begin{aligned} a &= A + \bar{A}, \qquad & b &= B + \bar{B}, \\ u &= U + \bar{U}, \qquad & v &= V + \bar{V} \end{aligned} \tag{6.3}$$

and their duals

$$\begin{aligned} \tilde{a} &= -i(A - \bar{A}), \qquad & \tilde{b} &= -i(B - \bar{B}), \\ \tilde{u} &= -i(U - \bar{U}), \qquad & \tilde{v} &= -i(V - \bar{V}). \end{aligned} \tag{6.4}$$

We have written the harmonic functions in terms of four holomorphic functions $A(z)$, $B(z)$, $U(z)$, $V(z)$ and their anti-holomorphic counter-

1 [79] uses supergravity conventions in which the RR four-form is a factor 4 to small. We rescale to string theory conventions, by setting $\mathrm{Hol}(\hat{h}) = U/4$ and shift $B \to B/2$. Since we use capital letters for meromorphic functions we write $V = \mathrm{Hol}(H)$.

parts $\bar{A}(\bar{z})$, $\bar{B}(\bar{z})$, $\bar{U}(\bar{z})$, $\bar{V}(\bar{z})$. Any solution to the setup of [79] is specified by these eight functions.

The expressions for the dilaton, axion χ and RR four form are

$$e^{-2\phi} = \frac{1}{4u^2}(a\,u - b^2)(a\,u + \tilde{b}^2), \tag{6.5a}$$

$$\chi = \frac{1}{2u}(b\,\tilde{b} - \tilde{a}\,u), \tag{6.5b}$$

$$C_K = \frac{1}{2a}(b\,\tilde{b} - a\,\tilde{u}). \tag{6.5c}$$

Here, C_K is the component of $C_{(4)}$ along the T^4 directions. The ansatz allows for one more component along the combined directions of S^2 and AdS_2, $C_{(4)} = C_K\,\omega_{T^4} + C_{\mathrm{AdS}_2,S^2}\,\omega_{\mathrm{AdS}_2} \wedge \omega_{S^2}$, which is related to C_K via self-duality of $F_{(5)}$. Here and below, all ω denote unit volume forms on the indicated geometries.

When discussing the defect RG flow below, we rely on matching the charges of the UV and IR defect. Choosing the correct notion of charge[2] is therefore imperative. For our purposes this is the Page charge, which is conserved, localized and quantized. The first two properties enable us to associate the correct amount of charge with points on Σ, corresponding either to the defect or CFT loci. The third property renders them useful for characterizing the dual CFT in terms of the quantized number of one- and five-branes. Note that the Page charges are not gauge invariant.

The Page charges differ from the commonly used Maxwell charges. For instance, the D1-brane Page charge reads

$$Q_{D1} = -\int_{S^7}\left(e^{\phi}\star\left(dC_{(2)} - \chi H_{(3)}\right) - C_{(4)}\wedge H_{(3)}\right). \tag{6.6}$$

Due to the symmetry of the ansatz (6.1) the three-forms are organized according to

$$H_{(3)} = dB_{(2)} = (\partial_a b^{(1)})da\wedge\omega_{\mathrm{AdS}_2} + (\partial_a b^{(2)})da\wedge\omega_{S^2}, \tag{6.7a}$$

$$F_{(3)} = dC_{(2)} = (\partial_a c^{(1)})da\wedge\omega_{\mathrm{AdS}_2} + (\partial_a c^{(2)})da\wedge\omega_{S^2}, \tag{6.7b}$$

2 A useful introduction to all notions of charge occuring in supergravity is presented in [182].

with $a = z, \bar{z}$. The dependence of $b^{(i)}$ and $c^{(i)}$ on the harmonic functions (6.3) is given by

$$b^{(1)} = -\frac{2v\,b}{a\,u - b^2} - h_1, \qquad h_1 = \int \frac{\partial_z v}{B} + c.c., \tag{6.8a}$$

$$b^{(2)} = \frac{2v\,\tilde{b}}{a\,u + \tilde{b}^2} + \tilde{h}_1, \qquad \tilde{h}_1 = \frac{1}{i}\int \frac{\partial_z v}{B} + c.c., \tag{6.8b}$$

$$c^{(1)} = -v\frac{a\,\tilde{b} - \tilde{a}\,b}{a\,u - b^2} + \tilde{h}_2, \qquad \tilde{h}_2 = \frac{1}{i}\int A\frac{\partial_z v}{B} + c.c., \tag{6.8c}$$

$$c^{(2)} = -v\frac{a\,b + \tilde{a}\,\tilde{b}}{a\,u + \tilde{b}^2} + h_2, \qquad h_2 = \int A\frac{\partial_z v}{B} + c.c. \tag{6.8d}$$

Full details on the derivation of the Page charges used in this paper can be found in the appendix of [80]; here we only collect the final expressions. The Page one-brane charges are

$$\begin{aligned} Q_{D1} = 4\pi\Bigg[&\int_{\mathcal{C}} \frac{u}{a}\frac{a\,u - b^2}{a\,u + \tilde{b}^2}\, i(\partial_z c^{(1)} - \chi\partial_z b^{(1)})dz \\ &+ \int_{\mathcal{C}} C_K \partial_z b^{(2)} dz\Bigg] + c.c. \end{aligned} \tag{6.9a}$$

$$\begin{aligned} Q_{F1} = 4\pi\Bigg[&\int_{\mathcal{C}} \frac{(a\,u - b^2)^2}{4a\,u} i\partial_z b^{(1)} dz - \int C_K \partial_z c^{(2)} dz \\ &- \int_{\mathcal{C}} \frac{u}{a}\frac{a\,u - b^2}{a\,u + \tilde{b}^2}\,\chi\, i(\partial_z c^{(1)} - \chi\partial_z b^{(1)})dz\Bigg] + c.c. \end{aligned} \tag{6.9b}$$

The integration contour $\mathcal{C}$ is a semicirle anchored at the boundary $\partial\Sigma$ and stems from partitioning the integration domain in (6.6) as $S^7 = T^4 \times S^2 \times \mathcal{C}$. The Page five-brane charges are[3]

$$Q_{F5} = 4\pi\left(\int_{\mathcal{C}} dz\,\partial_z b^{(2)} + c.c.\right) \tag{6.10a}$$

$$Q_{D5} = 4\pi\left(\int_{\mathcal{C}} dz\,\partial_z c^{(2)} + c.c.\right). \tag{6.10b}$$

The contour $\mathcal{C}$ is again a semicircle on the Riemann surface Σ located around poles on the boundary $\partial\Sigma$. Together with the fibered S^2, $\mathcal{C}$ yields an S^3, as is required to enclose a five-brane.

In analogy the Page D3-brane charge is given by

$$Q_{D3} = \oint_{\mathcal{C}}\left(\partial_z C_K\, dz + c.c.\right) \tag{6.11}$$

In this case the contour $\mathcal{C}$ is given by an S^1, which together with T^4 gives a five manifold as required for enclosing a three brane. In contrast

3 While the one-brane charges are electric charges, the five-brane charges are magnetic. To ease notation we refer to the NS5-brane as F5.

to the previous charges, this contour encloses a point in the interior of Σ.

This is the general solution for the ansatz (6.1).

6.2 REGULARITY CONSTRAINTS

In order to extract a class of Janus solutions the authors of [79] imposed a set of constraints, which turn out to be too strict for our purposes and hence in the this section we indicate our constraints. This exposition will appear in an upcoming publication [112].

The solutions studied in [79] admit only poles of order one in the functions A, B, U, V, and we will adopt this restriction. Furthermore, we will impose the following working assumptions

- The AdS_2 metric factor f_1 is finite and non-zero everywhere except at most at isolated singular points. Its poles designate the asymptotic $AdS_3 \times S^3 \times T^4$ regions.
- The S^2 metric factor f_2 is finite in the interior of Σ and vanishes on its boundary, except at most at isolated singularities.
- The metric factor f_3 of the T^4 and the dilaton are finite and non-zero *up to isolated points* on Σ.

The first two assumptions are also employed in [79]. In contrast to our third assumption, in [79] a finite and non-vanishing value for f_3 and the dilaton was demanded *everywhere* on Σ, which excludes the brane solutions of interest to us[4]. It is precisely these isolated points on Σ, which will be the loci of our defects, i.e. a fundamental string and a D3 brane. Our specific requirements and their consequences are detailed in the sections below.

We recapitulate three important consequences from the three items above worked out in [79] and adapt them to our case.

I. Vanishing harmonics on the boundary

The two requirements $f_2(\partial\Sigma) = 0$ and $f_1(\partial\Sigma) \neq 0$ impose

$$a(\partial\Sigma) = b(\partial\Sigma) = u(\partial\Sigma) = v(\partial\Sigma) = 0. \tag{6.12}$$

In Section 6.4.2 we will introduce the vacuum solution, which trivially satisfies (6.12). Below we will modify the vacuum so as to generate embedded defects. The constraint (6.12) presents a guideline for the specific shape of any modification. In particular it will become important when discussing the D3 solution.

II. Shared non-brane singularities

4 In particular, this forbids singularities in the interior of Σ and our D3 brane solution will be precisely of that type.

The functions a and u may have singularites away from the brane, which means that f_3 has to be finite at these locations. A look at (6.2c) reveals that, in order for this to be the case, a and u have to share these singularities. From (6.2b) we see that b has to feature this singularity as well. What is more, f_2 has to be non-negative everywhere, as is required for a reasonable metric factor, and thus[5]

$$a\,u - b^2 \geq 0. \tag{6.13}$$

At this singular non-brane locus, let us call it z_*, we can expand

$$A(z) = i\frac{a_*}{z - z_*} + \mathcal{O}(1), \tag{6.14a}$$

$$B(z) = i\frac{b_*}{z - z_*} + \mathcal{O}(1), \tag{6.14b}$$

$$U(z) = i\frac{u_*}{z - z_*} + \mathcal{O}(1), \tag{6.14c}$$

from which we learn

$$a_* u_* = b_*^2. \tag{6.15}$$

The location z_* may coincide with an asymptotic region, i.e. poles of f_1. However, in the solutions to come they will not correspond to any special point[6]. In the case where the dilaton and f_3 are finite and non-zero everywhere on Σ all singularities z_* are shared among A, B, U. We will add extra singularities to U, for which (6.15) does not hold, but nevertheless respect (6.13).

III. Shared zeroes among B and $\partial_z V$

The authors of [79] considered solutions for which the curvature scalar

$$R_\Sigma = -2\frac{\partial_z \partial_{\bar{z}} \log \rho^2}{\rho^2} \tag{6.16}$$

is non-singular everywhere on Σ, which forces $\partial_z V$ and B to have common zeroes. In order to generate our defects below, we will modify only the functions $U(z)$ and $\bar{U}(\bar{z})$, which does not affect this relation between $\partial_z V$ and B.

6.3 F1/F5 CASE

The previous two sections presented the general half-BPS solutions to the ansatz (6.1), which are asymptotically $\mathrm{AdS}_3 \times \mathrm{S}^3 \times T^4$. Now we make contact with our Kondo-like flows from the previous sections by

5 Of course, for all metric factors (6.2) to be non-negative we require also $a \geq 0$ and $u \geq 0$.

6 In the S-dual picture, where we embed defects into the $F1/NS5$ geometry, they do correspond to asymptotic regions

computing the supergravity solutions of the fixed points of the flow. The way to work in this formalism is via the asymptotic regions. Hence we begin by reducing all fields, charges and metric factors to the asymptotic regions in Section 6.3.1. We are then in good shape to construct the pure F1/F5 solution in Section 6.3.2 using the constraints presented in Section 6.2. Thereafter we can embed the relevant interfaces into the F1/F5 geometry. First up is the D1/F1 interface in Section 6.3.3; in contrast to before we carry out the analysis with arbitrary F1 charge on the interface. Thereafter, in Section 6.3.4, we present a D3 interface with dissolved F1 and D1 charge. Both solutions exist totally independent of each other and we connect them via our Kondo-like flows in Section 6.3.5. We find agreement with the results of the previous chapter.

The discussion here is very detailed. Readers who are not interested in too many fineprints are free to skip ahead Section 6.4, where they find the S-dual of the scenario here, that is the D1/D5 case. Our discussion there is less detailed, but still self-contained. A very short version of the D1/D5 scenario will appear in an upcoming publication [112] done in collaboration with Johanna Erdmenger and Charles Melby-Thompson.

6.3.1 *Asymptotic Regions*

The main tools in our analysis are the fields (6.5) and the charges (6.10), (6.9) evaluated at the asymptotic regions[7]. Since the Page charges in use are conserved and localized, knowledge of the charges at the asymptotic regions suffices to pin down the charges at another isolated point – spoilers, these special points will correspond to the interfaces.

Singularities in f_1 designate asymptotic $\mathrm{AdS}_3 \times S^3 \times T^4$ regions. In terms of the holomorphic functions the asymptotic regions are singled out as poles of V. Our defects glue (only) two CFTs and thus we are interested in solutions with two asymptotic regions, which we place at $z = 0$ and $z \to \infty$ in Σ. These regions are interchanged via inversion $z \to -1/z$. In the vicinity of $z = 0$ we expand the meromorphic functions to linear order

$$V(z) = iv_{-1}z^{-1} + iv_1 z + \dots \tag{6.17a}$$
$$A(z) = ia_{-1}z^{-1} + ia_0 + ia_1 z + \dots \tag{6.17b}$$
$$B(z) = ib_{-1}z^{-1} + ib_0 + ib_1 z + \dots \tag{6.17c}$$
$$U(z) = iu_{-1}z^{-1} + iu_0 + iu_1 z + \dots \tag{6.17d}$$

The coefficients v_j, a_j, b_j, u_j are real. Note that including a summand v_0 is obsolete, because it would only influence the harmonic dual $\tilde{v}$, which does not appear in any charge, field nor metric factor.

7 Unlike the D1/D5 case discussed below the expressions in this duality frame are not worked out in [80] so that we compute them ourselves here.

In coordinates $z = re^{i\theta}$ we obtain the leading order of the dilaton, axion and RR four form close to $z = 0$,

$$e^{-2\phi} = \frac{b_{-1}^2}{u_{-1}^2}\Big(2b_{-1}b_1 - a_1u_{-1} - a_{-1}u_1\Big) + \mathcal{O}(r), \tag{6.18a}$$

$$\chi = \frac{1}{b_{-1}}\Big(a_{-1}b_0 - a_0b_{-1}\Big) + \mathcal{O}(r), \tag{6.18b}$$

$$C_K = \frac{1}{b_{-1}}\Big(u_{-1}b_0 - u_0b_{-1}\Big) + \mathcal{O}(r). \tag{6.18c}$$

The metric factors are

$$f_1^2 = \frac{2}{r^2}\,\mathrm{sgn}(u_{-1})\,\frac{v_{-1}}{|b_{-1}|}\,a_{-1}^2\,e^{\frac{3}{2}\phi} \tag{6.19a}$$

$$f_2^2 = 2\sin^2\theta\,\mathrm{sgn}(u_{-1})\,\frac{v_{-1}}{|b_{-1}|}\,e^{-\frac{1}{2}\phi} \tag{6.19b}$$

$$f_3^4 = \frac{u_{-1}}{a_{-1}}\,e^{-\phi} \tag{6.19c}$$

$$\rho^2 = \frac{2}{r^2}\,\frac{|v_{-1}|}{|b_{-1}|}\,e^{-\frac{1}{2}\phi} \tag{6.19d}$$

These metric factors have to be, of course, positiv! Hence, this is a good place to stop and ponder on the signs that the various functions should have. To that end consider the harmonics

$$v = V + \bar{V} = 2\frac{\Im(z)}{|z|}\Big(v_{-1}|z|^{-1} - v_1|z|\Big) + \ldots, \tag{6.20a}$$

$$a = A + \bar{A} = 2\frac{\Im(z)}{|z|}\Big(a_{-1}|z|^{-1} - a_1|z|\Big) + \ldots, \tag{6.20b}$$

$$b = B + \bar{B} = 2\frac{\Im(z)}{|z|}\Big(b_{-1}|z|^{-1} - b_1|z|\Big) + \ldots, \tag{6.20c}$$

$$u = U + \bar{U} = 2\frac{\Im(z)}{|z|}\Big(u_{-1}|z|^{-1} - u_1|z|\Big) + \ldots \tag{6.20d}$$

Recall that the general prescribtions (6.2) forces a and u to be positive and we can choose $v > 0$ as well. This can be achieved for any value of $z \in \Sigma$ by choosing v_{-1}, a_{-1}, $u_{-1} > 0$ while v_1, a_1, $u_1 < 0$. The signs of b_{-1}, b_1 determine the sign of the various charges to be introduced below in (6.24) and are not fixed by general considerations. We anticipate here though that in the solutions that we study below, b_{-1} and b_1 will share their sign, in contrast to the other coefficient types.

Using coordinates $z = \exp(\psi + i\theta)$ the metric assumes the form ($\psi \to -\infty, r \to 0$)

$$ds_{10}^2 = \mathsf{L}^2\left(d\psi^2 + \frac{\mu}{4}e^{-2\psi}ds_{\mathrm{AdS}_2}^2 + d\theta^2 + \sin^2\theta ds_{S^2}^2\right) + \sqrt{\frac{u_{-1}}{a_{-1}}e^{-\phi}}ds_{T^4}^2$$

(6.21)

Here, we defined the ten-dimensional AdS radius L and a scale factor μ, which will become important when choosing a cutoff for AdS in later sections

$$\mathsf{L}^2 = 2\frac{v_{-1}}{|b_{-1}|}\, e^{-\frac{1}{2}\phi}, \qquad \mu = 4a_{-1}^2\, e^{2\phi} \tag{6.22}$$

The six-dimensional AdS radius $\mathsf{R} = \mathsf{L} f_3$ will be useful and appears in the scale factor,

$$\mu = \frac{(4v_{-1})^2}{\mathsf{R}^4}. \tag{6.23}$$

The five-brane Page charges (6.10) and the one-brane Page charges (6.9) are expressed through

$$q_{D5} \equiv \frac{Q_{D5}}{8\pi^2} = \frac{v_{-1}}{b_{-1}^2}\Big(a_0 b_{-1} - a_{-1} b_0\Big), \tag{6.24a}$$

$$q_{F5} \equiv \frac{Q_{F5}}{8\pi^2} = -\frac{v_{-1}}{b_{-1}}, \tag{6.24b}$$

$$q_{D1} \equiv \frac{Q_{D1}}{8\pi^2} = \frac{v_{-1}}{b_{-1}^2}\Big(u_0 b_{-1} - u_{-1} b_0\Big), \tag{6.24c}$$

$$q_{F1} \equiv \frac{Q_{F1}}{8\pi^2} = -\frac{v_{-1}}{b_{-1}}\Bigg(2b_{-1}b_1 - a_1 u_{-1} - a_{-1}u_1 - \frac{a_0 b_{-1} - a_{-1} b_0}{b_{-1}}\,\frac{u_0 b_{-1} - u_{-1} b_0}{b_{-1}}\Bigg). \tag{6.24d}$$

The ten-dimensional gravitational constant and the ten-dimensional Newton constant are

$$\kappa_{10}^2 = 8\pi G_N^{(10)}, \tag{6.25}$$

$$G_N^{(10)} = G_N^{(3)} \mathrm{Vol}(S^3_{\mathsf{L}}) \mathrm{Vol}(T^4_{f_3}) = G_N^{(3)}\, 2\pi^2 \mathsf{L}^3\, f_3^4, \tag{6.26}$$

where the subscripts in the volumes denote the respective radii[8]. The Brown-Henneaux formula then provides the central charge of the CFT at the asymptotic region,

$$\mathsf{c} = \frac{3\mathsf{L}}{2G_N^{(3)}} = \frac{96\pi^3}{\kappa_{10}^2}\left(\frac{v_{-1}u_{-1}}{b_{-1}^2}\right)^2 e^{-2\phi} \tag{6.27}$$

$$= \frac{96\pi^3}{\kappa_{10}^2}\Big(q_{D5}\, q_{D1} + q_{F5}\, q_{F1}\Big). \tag{6.28}$$

8 Whenever we omit the radius in Volume expression it implies unit radius, i.e. $\mathrm{Vol}(S^3) = 2\pi^2$

Lastly, the observation

$$\mathsf{R}^4 = 4\Big(q_{D5}\,q_{D1} + q_{F5}\,q_{F1}\Big) = \frac{4G_N^{(10)}}{\mathrm{Vol}(S^3)}\frac{\mathsf{c}}{6} \tag{6.29}$$

will be convenient. In the next section we proceed to write down the F1/F5 vacuum solution and will augment it in subsequent sections by a $(D1, F1)$ defect and a D3 defect.

6.3.2 *F1/F5 Vacuum*

The vacuum corresponds to the trivial interface in the CFT.

Since the pure F1/F5 geometry carries no interface we will also refer to this geometry as the vacuum, as in devoid of interfaces. At both asymptotic regions the geometry will have to look the same. In the CFT this is just is just the trivial interface, meaning that there will be only a single CFT on the entire conformal boundary of AdS_3. The practical consequence is that the inversion $z \to -\frac{1}{z}$ should not alter the shape of the meromorphic functions A, B, U, V. In other words, the expansions (6.17) are not expansions, but the full functions (no dots required). Note that all coefficients v_j, a_j, b_j, u_j are then truly constants for any $z \in \Sigma$.

This is not yet the F1/F5 and our next steps are concerned with changing this. First of all, the F5 charge (6.24b) should differ only in sign at the asymptotic regions, so as to fullfil charge conservation $q_{F5}^{(0)} + q_{F5}^{(\infty)} = 0$, which is equivalent to

One can read of the charges (6.24) at infinity via $v_{\pm 1} \to -v_{\mp 1}$ and similarly for a_j, b_j, u_j.

$$\frac{v_{-1}}{b_{-1}} = -\frac{v_1}{b_1} \tag{6.30}$$

Because, the signs of the v_j differ, those of b_j have to coincide and we choose them to be negative. The more crucial restrictions leading to the F1/F5 vacuum are of course the vanishing of D-brane charges. Consider first the D5 charge (6.24a),

$$q_{D5} = \frac{v_{-1}}{b_{-1}^2}\Big(a_0 b_{-1} - a_{-1} b_0\Big) \overset{!}{=} 0. \tag{6.31}$$

This can be solved in our case only if and only if $a_0 = 0 = b_0$. Indeed, if $\alpha_0 \neq 0 \neq \beta_0$ then (6.31) implies

$$\frac{a_{-1}}{a_1} = \frac{b_{-1}}{b_1}. \tag{6.32}$$

A non-vanishing value of u_0 an asymptotic region induces D1 charge at that region.

But this cannot be true since positivity of a fixes the LHS to be negative, while, as we just concluded, the RHS is positive. Similarly from the vanishing of the D1 charge (6.24c) is equivalent to $u_0 = 0$. In later sections we will be interested in generating D1 charge and it is now clear that this can be done by assigning an $\mathcal{O}(1)$ term to U.

At last we have the correct shape of the meromorphics corresponding to the vacuum,

$$V(z) = iv_{-1}z^{-1} + iv_1 z = i\nu\Big(z^{-1} - \hat{\nu}z\Big) \tag{6.33a}$$
$$A(z) = ia_{-1}z^{-1} + ia_1 z = i\alpha\Big(z^{-1} - \hat{\alpha}z\Big) \tag{6.33b}$$
$$B(z) = ib_{-1}z^{-1} + ib_1 z = -i\beta\Big(z^{-1} + \hat{\beta}z\Big) \tag{6.33c}$$
$$U_0(z) = iu_{-1}z^{-1} + iu_1 z = i\eta\Big(z^{-1} - \hat{\eta}z\Big), \tag{6.33d}$$

where the constants ν, α, β, η, $\hat{\nu}$, $\hat{\alpha}$, $\hat{\beta}$, $\hat{\eta}$ are chosen in anticipation of the computations below. They are all positive. As in the D1/D5 duality frame, the meromorphic U carries a subscript indicating the vacuum. It is only in U that modifications leading to defect solutions will occure.

Let us work out the implications of the constraints in Section 6.2.

I. Vanishing harmonics on the boundary

A glance at (6.20) (of course now we can forget about the dots) reveals that the constraint (6.12) is trivially satisfied.

II. Shared non-brane singularities

The meromorphic functions A, B, and U in (6.33) share their (non-interface) singularities lying at $z_* = 0$ and $z_* = \infty$, which coincides with the asymptotic regions and hence the coefficients in (6.15) become the coefficients appearing in (6.33),

$$z_* = 0: \qquad a_{-1}u_{-1} = b_{-1}^2 \quad \Rightarrow \quad \alpha\eta = \beta^2 \tag{6.34a}$$
$$z_* = \infty: \qquad a_1 u_1 = b_1^2 \quad \Rightarrow \quad \alpha\hat{\alpha}\eta\hat{\eta} = (\hat{\alpha}\beta)^2 \tag{6.34b}$$

Plugging the first into the second equation implies $\hat{\alpha}\hat{\eta} = \hat{\beta}^2$, which together with (6.34a) secures $a\,u_0 - b^2 \geq 0$ everywhere on Σ. These constraints will survive any modification, which induces an interface in later sections. In the rest of this section we will oftentimes write β, which is always going to be assumed to be determined by (6.34a).

The fact that these non-brane singularities lie at the asymptotic regions is an important feature[9] of the F1/F5 geometry, which actually makes the constraints (6.34) long overdue! Indeed, without it all expansions for the fields (6.18), the metric factors (6.19) and charges (6.24) would diverge and we tacitly employed it already in all those expressions.

III. Shared zeroes among B and $\partial_z V$

The last constraint,

$$\partial_z V = i\nu\Big(-z^{-2} - \hat{\nu}\Big) \stackrel{!}{=} 0 \tag{6.35a}$$
$$B = -i\beta\Big(z^{-1} + \hat{\beta}z\Big) \stackrel{!}{=} 0 \tag{6.35b}$$

9 This property is not shared by the D1/D5 geometry discussed below.

straightforwardly imposes $\hat{\beta} = \hat{\nu}$.

Out of the formerly eight parameters in (6.33) the constraints (6.34) and (6.35) remove three. The vacuum should however be given in terms of only three independent numbers, which are q_{F5}, q_{F1} and ϕ. So we still have to remove two parameters in (6.33). To that end we study the expressions for the charges at both asymptotic regions, which we label by superscripts (0) or (∞). Of course the charges should be related by charge conservation and the dilaton should coincide at both asymptotic regions. We commence to check these requirements with the F5 brane charges (6.24b), which are now expressed through

$$q_{F5}^{(0)} = \frac{\nu}{\beta} = -q_{F5}^{(\infty)}. \tag{6.36}$$

satsifying charge conservation. Similarly the fundamental string charges, (6.24d),

$$q_{F1}^{(0)} = q_{F5}^{(0)} \alpha\eta \Big(\sqrt{\hat{\alpha}} + \sqrt{\hat{\eta}}\Big)^2 = -q_{F1}^{(\infty)} \tag{6.37}$$

satisfy charge conservation identically. The missing constraint must come from the fixing the dilaton to assume the same value at both asymptotic regions. Indeed, the expression (6.18a) evaluated at both asymptotic regions gives

$$e^{-2\phi(0)} = \left(\frac{\beta}{\eta}\right)^2 \frac{q_{F1}^{(0)}}{q_{F5}^{(0)}}, \qquad e^{-2\phi(\infty)} = \left(\frac{\beta\hat{\beta}}{\eta\hat{\eta}}\right)^2 \frac{q_{F1}^{(\infty)}}{q_{F5}^{(\infty)}} \tag{6.38}$$

Requiring these expressions to be the same gives $\hat{\beta} = \hat{\eta}$. The result below (6.34), $\hat{\beta}^2 = \hat{\alpha}\hat{\eta}$ enforces then $\hat{\alpha} = \hat{\beta}$. Recalling what we learned in (6.35) we conclude that the hatted parameters all assume the same value, $\hat{\nu} = \hat{\alpha} = \hat{\beta} = \hat{\eta}$. We have one last freedom not mentioned so far, which is our last trump card: $SL(2,\mathbb{R})$ reparametrizations of Σ. We use those to scale the hatted parameters to unity, $\hat{\nu} = \hat{\alpha} = \hat{\beta} = \hat{\eta} = 1$.

Type IIB supergravity posseses, in contrast to its brother type IIA, an $SL(2,\mathbb{R})$ symmetry, which manifests itself in this setup through reparametrizations on Σ.

For later reference we present here the vacuum meromorphic functions

$$V(z) = i\nu\Big(z^{-1} - z\Big), \qquad v = 2\nu\frac{\Im(z)}{|z|}\Big(|z|^{-1} + |z|\Big), \tag{6.39a}$$

$$A(z) = i\alpha\Big(z^{-1} - z\Big), \qquad a = 2\alpha\frac{\Im(z)}{|z|}\Big(|z|^{-1} + |z|\Big), \tag{6.39b}$$

$$B(z) = -i\beta\Big(z^{-1} + z\Big), \qquad b = -2\beta\frac{\Im(z)}{|z|}\Big(|z|^{-1} - |z|\Big), \tag{6.39c}$$

$$U_0(z) = i\eta\Big(z^{-1} - z\Big), \qquad u = 2\eta\frac{\Im(z)}{|z|}\Big(|z|^{-1} + |z|\Big). \tag{6.39d}$$

Keep in mind that $\beta^2 = \alpha\eta$. The four meromorphics now depend only on three parameters. In order to elicit the physical significance of functions (6.39) we aim to express the ν, α, η in terms of the ex-

isting charges and the dilaton q_{F5}, q_{F1}, ϕ. This can be achieved by inspecting the charges (6.37), (6.37) and the dilaton (6.38), which after implementing all of our constraints assume the form

$$q_{F5}^{(0)} = \frac{\nu}{\sqrt{\alpha\,\eta}} = -q_{F5}^{(\infty)}, \tag{6.40a}$$

$$q_{F1}^{(0)} = 4\nu\sqrt{\alpha\,\eta} = -q_{F1}^{(\infty)}, \tag{6.40b}$$

$$e^{-2\phi(0)} = 4\alpha^2 = e^{-2\phi(\infty)}. \tag{6.40c}$$

The last equations hands us α on a silver platter. It is not difficult to solve for the remaining two parameters. The solution is

$$\nu = \frac{1}{2}\sqrt{q_{F5}^{(0)}\,q_{F1}^{(0)}}, \tag{6.41a}$$

$$\alpha = \frac{1}{2}e^{-\phi(0)}, \tag{6.41b}$$

$$\eta = \frac{1}{2}\frac{q_{F1}^{(0)}}{q_{F5}^{(0)}}e^{\phi(0)}. \tag{6.41c}$$

Given the functions (6.39) the combined metric factors (6.2) give rise to $\mathrm{AdS}_3 \times S^3 \times T^4$ for any point on Σ, i.e. not just asymptotically so (as given in (6.21)). In coordinates $z = \exp(\psi + i\theta)$ and employing (6.41) the metric reads

$$ds_{10}^2 = \mathsf{L}^2\left(d\psi^2 + \cosh^2\psi\, ds_{\mathrm{AdS}_2}^2 + d\theta^2 + \sin^2\theta ds_{S^2}^2\right) + \sqrt{\frac{q_{F1}^{(0)}}{q_{F5}^{(0)}}e^{\phi(0)}}ds_{T^4}^2, \tag{6.42}$$

with ten-dimensional AdS radius $\mathsf{L}^2 = 2q_{F5}^{(0)}e^{-\phi(0)/2}$ and scale factor $\mu = 1$. These are reproduced with the expression given in (6.22).

By comparison of (6.42) to the F1/F5 Einstein frame solution in the literature we can relate the Page charges to the integer valued charges N_1, N_5 as follows

$$Q_{F5} = 8\pi^2 q_{F5} = (2\pi)^2\alpha' N_5, \qquad Q_{F1} = 8\pi^2 q_{F1} = (2\pi)^6\alpha'^3 N_1, \tag{6.43}$$

and similarly for Q_{D5} and Q_{D1}. Plugged into the central charge (6.99) together with $4\pi\kappa_{10}^2 = (2\pi)^8\alpha'^4$ we obtain the well known result $\mathsf{c} = 6N_1N_5$.

In the following we will insert defects into this vacuum by modifying the function (6.39d). We will see that the expressions in (6.41) will be augmented by interface charges in such a way that they reduce to the vacuum solution when reducing the interface charge to zero. In particular we may think of the vacuum as the trivial or completely transmissive interface. We will abuse notation and refer to our interfaces

as defects, even though strictly speaking they map different theories into each other.

6.3.3 *D1/F1 Interface*

This section is dedicated to inserting a D1 defect into the vacuum of the previous section. Our arguments, even though taylored to produce "just" a D1 brane, will actually lead up to inserting a D1/F1 defect or (p, q) string. "Inducing a defect into the vacuum" means in practical terms that we keep supply some extra terms to the vacuum functions (6.41). We will now motivate that, in fact we only have to modify one of the four meromorphic functions, namely (6.39d).

In order to realize a D1 brane one has to impose a monodromy in the integrand of (6.9a) at the boundary of Σ. However, due to the simpler structure of (6.10b) it is simpler to T-dualize four times and look for D5 branes. Luckily, four T-dualities are realized via $A(z) \leftrightarrow U(z)$. D5 brane charge is then realized by implementing a pole in A. Back in the original picture, we obtain a D1 brane by adding a pole to $U(z)$ at $\xi \in \partial\Sigma = \mathbb{R}$,

$$U(z) = U_0 + \delta U^{D1}, \tag{6.44a}$$

$$\delta U^{D1} = ic\,\frac{\xi}{z-\xi}, \tag{6.44b}$$

$$\delta u^{D1} = \frac{2c\,\xi\,\Im(z)}{|z-\xi|^2}. \tag{6.44c}$$

The constant c will be tied to the D1 charge below. For a single stack of D1 branes we can, w.l.o.g., choose $\xi > 0$. Negative ξ would simply imply that the stack of branes lies on the upper boundary of the strip, which corresponds to $\theta = \pi$. The locus of the defect on Σ is depicted in Figure 13.

Actually, we are not interested in just a D1 brane defect. We are interested in one such defect which is smeared over the T^4 directions. Luckily for us, the formalism that we are using [79] achieves precisely that, which may be traced back to the fact that the ansatz described in Section 6.1 carries no fluxes on the T^4 manifold.

That the modification (6.44) indeed gives the correct behavior, i.e. a D1 brane smeared over the T^4 directions, can be checked by comparing to the supergravity solution of N_1 D1 and N_5 D5 branes in Einstein frame:

$$\begin{aligned} ds^2_{\mathrm{D1/D5}} = Z_1^{-3/4} Z_5^{-1/4} \eta_{\mu\nu} dx^\mu dx^\nu + Z_1^{1/4} Z_5^{3/4} dx^i dx^i \\ + Z_1^{1/4} Z_5^{-1/4} dx^m dx^m. \end{aligned} \tag{6.45}$$

The greek letters run over the directions parallel to the F1 and the F5 branes, i runs over the directions transverse to all branes and m runs

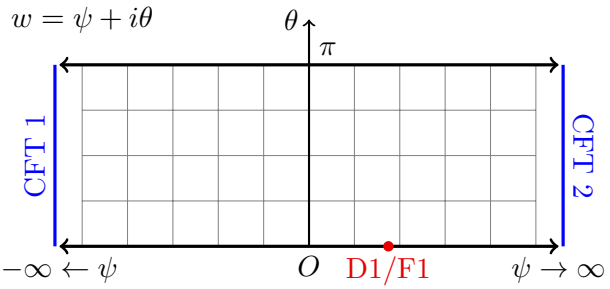

Figure 13: In strip coordinates $w = \psi + i\theta$ the two asymptotic regions, depicted by blue bars, lie at $\psi \to \pm\infty$. Each harbors a CFT and they typically differ due to the presence of the D1/F1 – we anticipate that generically the defect will carry both types of onebrane charge – defect located at $\xi \in \Sigma$ depicted as red dot. The lower boundary, $\theta = 0$, corresponds to the north pole of the S^3, while the upper boundary, $\theta = \pi$ corresponds to the southpole.

over the directions parallel to the D5 branes, but transverse to the F1 branes. The latter directions are compactified on a T^4 of volume V_4. The harmonic functions and the dilaton are

$$Z_1 = 1 + \frac{r_1^2}{r^2}, \quad r_1^2 = \frac{(2\pi)^4 g N_1 \alpha'^3}{V_4} \tag{6.46}$$

$$Z_5 = 1 + \frac{r_5^2}{r^2}, \quad r_5^2 = g N_5 \alpha' \tag{6.47}$$

$$e^{-2\phi} = \frac{1}{g^2}\frac{Z_5}{Z_1}. \tag{6.48}$$

g is the string coupling and α' its tension. Here $r^2 = x_i x^i$ is determined by the overall transverse directions only. This means that the D1 branes are not localized in the m directions, i.e. they are smeared over the T^4 directions.

We are interested in the near brane behavior of D1 branes smeared over the T^4 directions, so we set $N_5 = 0$ in (6.45) and perform the limit $r \to 0$. This gives

$$ds^2_{D1_{smeared}} \simeq \left(\frac{r}{r_1}\right)^{3/2} \eta_{\mu\nu} dx^\mu dx^\nu + \left(\frac{r_1}{r}\right)^{1/2} (dr^2 + r^2 d\Omega_3^2) + \left(\frac{r_1}{r}\right)^{1/2} dx^m dx^m. \tag{6.49}$$

We have written the overall transverse directions i in polar coordinates.

Now we are finally in a position to utter an expectation for the functions f_i in the ansatz (6.1). The prefactor of $\eta_{\mu\nu} dx^\mu dx^\nu$ gives the behavior of f_1, the prefactor of $d\Omega_3^2$ the behavior of f_2, and the prefactor of $dx^i dx^i$ the behavior of f_3. Thus we expect

$$f_1^2 \simeq r^{3/2}, \qquad f_2^2 \simeq r^{3/2}, \qquad f_3^2 \simeq r^{-1/2}, \qquad e^\phi \simeq r^{-1}. \tag{6.50}$$

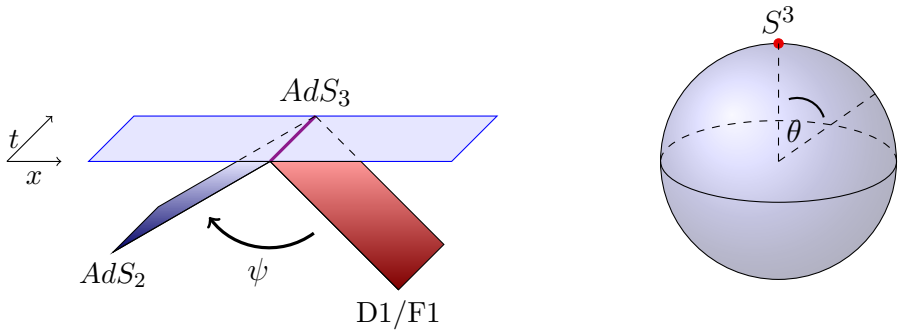

Figure 14: In coordinates $z = \exp(\psi + i\theta)$ AdS_3 is foliated by AdS_2 sheets shaded in dark blue and labelled by ψ. A D1/F1 string, shaded in red, is embedded into $AdS_3 \times S^3$ at $\xi = \exp \psi_\xi$, i.e. it sits at the north pole of S^3. The boundary of AdS_3, shaded in light blue, harbors the CFT and its intersection with the brane is the wordline of the field theory defect, colored in violet.

It can be readily checked that this is reproduced by (6.2) after plugging in the combination of (6.39) and (6.44). Set $z = \xi + ir$ and have r tend to zero.

The new pole in (6.44) is not shared by A and B and thus does not give rise to an extra constraint of type (6.15). Because the harmonic a is positive, the requirement (6.13) enforces

$$a\, u_0 - b^2 + a\delta\, u^{F1} \geq 0 \qquad \Rightarrow \qquad c\,\xi \geq 0 \tag{6.51}$$

Since we are building on the vacuum solution (6.101) the sum of the first two terms is positive by itself.Our choice $\xi > 0$ then renders c positive. The geometry is depicted in Figure 14 and we anticipate that the defect carries both types of onebrane charge, as we will see momentarily.

Now that we have convinced ourselves that the addition (6.44) to (6.39) generates a onebrane defect embedded into the F1/F5 geometry, we want to inquire about the physical significance of the involved parameters ν, α, η, c, ξ. This is achieved following the same philosophy as for the vacuum by expressing them in terms of the charges, which are now supplemented by defect charges, and the dilaton. Before we get to that, one remark is in order. Even though we use the same symbols ν, α, η as in the vacuum solution (6.39), these symbols will take a different form here due to the presence of the defect as we will see below. Nevertheless, they will reduce to their vacuum pendants (6.41) once the defect is removed.

Straightforward computation of the asymptotic charges (6.96) gives

$$q_{F5}^{(0)} = \frac{\nu}{\beta}, \qquad q_{F5}^{(\infty)} = -\frac{\nu}{\beta}, \tag{6.52a}$$

$$q_{F1}^{(0)} = \frac{\nu\alpha}{\beta}\left(4\eta + \frac{c}{\xi}\right), \qquad q_{F1}^{(\infty)} = -\frac{\nu\alpha}{\beta}\left(4\eta + c\,\xi\right), \tag{6.52b}$$

$$q_{D1}^{(0)} = c\frac{\nu}{\beta} = c\,q_{D5}^{(0)}, \qquad q_{D1}^{(\infty)} = 0, \tag{6.52c}$$

while q_{D5} still vanishes at both asymptotic regions. The constrained (6.34a) is still valid. Indeed, it arises from (6.15) at $z_* = \infty$.

As alluded to before, the defect, let us indicate it by superscript $\mathcal{D}$, carries D1 and F1 charge, which is fixed by charge conservation to be

$$q_{D1}^{\mathcal{D}} \equiv -q_{D1}^{(0)} - q_{D1}^{(\infty)} = -c\,q_{F5}^{(0)}, \tag{6.53a}$$

$$q_{F1}^{\mathcal{D}} \equiv -q_{F1}^{(0)} - q_{F1}^{(\infty)} = c\frac{\nu\alpha}{\beta}\left(\xi - \frac{1}{\xi}\right). \tag{6.53b}$$

For the particular value $\xi = 1$ corresponding to the AdS_2 sheet of smallest size, $q_{F1}^{\mathcal{D}}$ vanishes. In this case the F1 charges at both asymptotic regions differ only in sign.

The asymptotic values of the fields (6.91) are

$$e^{-2\phi(0)} = \frac{\beta^2\alpha}{\eta^2}\left(4\eta + \frac{c}{\xi}\right) = \frac{\beta^2}{\eta^2}\frac{q_{F1}^{(0)}}{q_{F5}^{(0)}}, \tag{6.54a}$$

$$e^{-2\phi(\infty)} = \frac{\beta^2\alpha}{\eta^2}\left(4\eta + c\xi\right) = \frac{\beta^2}{\eta^2}\frac{q_{F1}^{(\infty)}}{q_{F5}^{(\infty)}}, \tag{6.54b}$$

$$C_K(0) = -c = \frac{q_{D1}^{\mathcal{D}}}{q_{F5}^{(0)}}, \tag{6.54c}$$

$$C_K(\infty) = 0, \tag{6.54d}$$

while the axion χ still vanishes at both regions. This configuration features a jump in the dilaton, which is controlled by the discrepancy in F1 charge at the asymptotic regions,

$$e^{-2\phi(\infty)} = -e^{-2\phi(0)}\frac{q_{F1}^{(\infty)}}{q_{F1}^{(0)}}, \tag{6.55}$$

and is therefore not independent.

For the remainder of this article we drop the superscript on the F5 charge, $q_{F5} \equiv q_{F5}^{(0)} = -q_{F5}^{(\infty)}$. As with the vacuum we choose without loss of generality $\beta > 0$, which renders all charges at zero positive, while all charges at infinity and $q_{F1}^{\mathcal{D}}$ are then negative. For future reference we rewrite the F1 charges in (6.52) in the more suggestive form

$$q_{F1}^{(0)} = 4\nu\sqrt{\alpha\eta} - \frac{\alpha}{\xi}q_{D1}^{\mathcal{D}}, \qquad q_{F1}^{(\infty)} = -4\nu\sqrt{\alpha\eta} + \alpha\xi q_{D1}^{\mathcal{D}}, \tag{6.56}$$

which elicits that we recover the vacuum expression (6.40b) when $q_{D1}^{(0)}$ tends to zero. Thinking of the defect's F1 charge as difference of the absolute values of the F1 charges at the asymptotic regions suggests to also introduce their arithmetic mean,

$$q_{F1}^{\mathcal{D}} = |q_{F1}^{(\infty)}| - q_{F1}^{(0)} = -2\alpha q_{D1}^{\mathcal{D}} \sinh \psi_\xi, \tag{6.57a}$$

$$\overline{q_{F1}} \equiv \frac{|q_{F1}^{(\infty)}| + q_{F1}^{(0)}}{2} = 4\nu\sqrt{\alpha\eta} - \alpha q_{D1}^{\mathcal{D}} \cosh \psi_\xi \equiv \kappa\, 4\nu\sqrt{\alpha\eta}. \tag{6.57b}$$

Here, we have expressed the locus of the defect through its Janus coordinate $\xi = \exp \psi_\xi$. In the second equation we have introduced

$$\kappa := 1 + \frac{c}{4\eta} \cosh \psi_\xi, \tag{6.58}$$

and it quantifies how much the F1 charge differs from the vacuum case, (6.40b). For $c = 0$, i.e. when there is no defect, we have $\kappa = 1$ and (6.57b) reduces to the vacuum expression. Of course, the pairs $(q_{F1}^{(0)}, q_{F1}^{(\infty)})$ and $(q_{F1}^{\mathcal{D}}, \overline{q_{F1}})$ are linearly independent. In what follows we choose to use the latter unless stated otherwise.

Now we have all tools in hand to express the parameters ν, α, η, c, ξ in terms of the charges q_{F5}, $\overline{q_{F1}}$, $q_{F1}^{\mathcal{D}}, q_{D1}^{\mathcal{D}}$ and the dilaton at zero $\phi(0)$. In order to make out a strategy for inverting the equations (6.52), (6.57) and (6.54) let us for first specify to the case $q_{F1}^{\mathcal{D}} = 0$. In this case we learn from (6.57) and (6.56) that $\psi_\xi = 1$, or equivalently $\xi = 1$, and that $\overline{q_{F1}} = q_{F1}^{(0)} = -q_{F1}^{(\infty)} = \kappa 4\nu\sqrt{\alpha\eta}$. If it were not for κ, the situation would not differ from the vacuum case in Section 6.3.2. It turns out that we can actually form the same charge combinations as in the RHS of (6.41) leading to the set of relations

$$4\nu^2\kappa = q_{F5} q_{F1}^{(0)}, \tag{6.59a}$$

$$4\alpha^2\kappa = e^{-2\phi(0)}, \tag{6.59b}$$

$$4\eta^2\kappa = \left(\frac{q_{F1}^{(0)}}{q_{F5}} e^{\phi(0)}\right)^2. \tag{6.59c}$$

We could stick to this case and use the remaining equation at our disposal, (6.53a), to completely solve the equations for the charges and the dilaton. Instead, let us return to the general case $q_{F1}^{\mathcal{D}} \neq 0$. Then the F1 charge will again differ at both asymptotic regions and the mean is again an independent variable, $\equiv \overline{q_{F1}} \neq q_{F1}^{(0)} \neq -q_{F1}^{(\infty)}$. We will recover the scenario $q_{F1}^{\mathcal{D}} \neq 0$ in the appropiate limit later.

We can manipulate the equations using the same steps leading to (6.59) to obtain

$$4\nu^2\kappa = q_{F5}\overline{q_{F1}}, \tag{6.60a}$$

$$4\alpha^2\kappa = \frac{\overline{q_{F1}}}{q_{F1}^{(0)}} e^{-2\phi(0)}, \tag{6.60b}$$

$$4\eta^2\kappa = \frac{\overline{q_{F1}}\, q_{F1}^{(0)}}{q_{F5}^2}\, e^{2\phi(0)}. \tag{6.60c}$$

These reduce to (6.59) when turning off the defects F1 charge. We are intentionally using both pairs of F1 charges, $(q_{F1}^{(0)}, q_{F1}^{(\infty)})$ and $(q_{F1}^{\mathcal{D}}, \overline{q_{F1}})$. In the end we will eliminate the former by the latter. Once we express κ in terms of the charges we are done!

Note that we arrived at (6.60) without use of (6.78a). The latter equation can be reshaped to take the form

$$\cosh^2\psi_\xi = 1 + \frac{1}{(2\alpha)^2}\left(\frac{q_{F1}^{\mathcal{D}}}{q_{D1}^{\mathcal{D}}}\right)^2. \tag{6.61}$$

When plugged into (6.58) we find that, besides the charges, it depends only on α and η. To decide how to proceed it is wise to contemplate which equations in (6.60) depend on which parameters. The first of these equations carries information on (ν, α, η), the last two depend only on (α, η). Hence we should work with the latter two. They can be used to eliminate, for instance, α. The remainder is then a quadratic equation[10] in η purely in terms of the charges and the dilaton at zero – precisely what we want! With this in hand one can in particular solve for κ. The full solution is then

$$\nu = \frac{1}{2}\sqrt{\frac{q_{F5}\,\overline{q_{F1}}}{\kappa}}, \tag{6.62a}$$

$$\alpha = \frac{e^{-\phi(0)}}{2}\sqrt{\frac{1}{\kappa}\,\frac{2\overline{q_{F1}}}{2\overline{q_{F1}} - q_{F1}^{\mathcal{D}}}}, \tag{6.62b}$$

$$\eta = \frac{e^{\phi(0)}}{2}\sqrt{\frac{1}{\kappa}\,\frac{\overline{q_{F1}}\,(2\overline{q_{F1}} - q_{F1}^{\mathcal{D}})}{2q_{F5}^2}}, \tag{6.62c}$$

$$\sinh\psi_\xi = e^{\phi(0)}\sqrt{\kappa\,\frac{2\overline{q_{F1}} - q_{F1}^{\mathcal{D}}}{2\overline{q_{F1}}}}\,\frac{q_{F1}^{\mathcal{D}}}{|q_{D1}^{\mathcal{D}}|}, \tag{6.62d}$$

$$c = \frac{|q_{D1}^{\mathcal{D}}|}{q_{F5}} \tag{6.62e}$$

10 One of its two solutions is unphysical and we will simply discard it. The discussion here focusses on the physical solutions made out by demanding positivity of the metric η, which is required by the metric factors.

The proportionality factor κ is best expressed through (p,q) string tensions (Einstein frame),

$$T_{(q_{F1},q_{D1})} = \frac{1}{2\pi\alpha'}\sqrt{e^{\phi(0)}q_{F1}^2 + e^{-\phi(0)}q_{D1}^2}. \tag{6.63}$$

Then the proportionality factor reads

$$\kappa = \kappa(q_{D1}^{\mathcal{D}},\, q_{F1}^{\mathcal{D}}) \tag{6.64a}$$

$$= \frac{T^2_{\left(4\sqrt{q_{F1}q_{F1}^{(0)}},\, q_{D1}^{\mathcal{D}}\right)} - T^2_{\left(0,\, q_{D1}^{\mathcal{D}}\right)}}{\left(\sqrt{\sigma^2\left(q_{F1}^{\mathcal{D}}\right) + T^2_{\left(4\sqrt{q_{F1}q_{F1}^{(0)}},\, q_{D1}^{\mathcal{D}}\right)}} - T_{\left(0,\, q_{D1}^{\mathcal{D}}\right)}\right)^2 - \sigma^2\left(q_{F1}^{\mathcal{D}}\right)}$$

$$\sigma(q_{F1}^{\mathcal{D}}) = \frac{T_{\left(4q_{F1}^{(0)},0\right)}}{T_{\left(0,\, q_{D1}^{\mathcal{D}}\right)}} T_{\left(q_{F1}^{\mathcal{D}},0\right)} \tag{6.64b}$$

To avoid clutter we have employed $q_{F1}^{(0)} = \frac{1}{2}(2\overline{q_{F1}} - q_{F1}^{\mathcal{D}})$. The solution (6.62) embodies a natural cutoff for the defect's F1 charge, $|q_{F1}^{\mathcal{D}}| < 2\overline{q_{F1}}$, since otherwise the solution is no longer $\frac{1}{2}$-BPS. We could have guessed this threshold, because it is precisely where $2q_{F1}^{(0)}$ vanishes. Note that $\kappa > 0$ and that due to (6.62d) $\operatorname{sgn}(q_{F1}^{\mathcal{D}}) = \operatorname{sgn}(\psi_\xi)$. We go on to discuss two interesting limits.

Pure F1 Defect, $q_{D1}^{\mathcal{D}} \to 0$

When there is no D1 charge on the defect it is pushed to the boundary

$$\sinh\psi_\xi \to \operatorname{sgn} q_{F1}^{\mathcal{D}} \times \infty, \tag{6.65}$$

where it merges with the CFT. The triple in (6.62a)-(6.62c) assumes the shape of the vacuum expressions (6.41),

$$q^{\mathcal{D}}_{F1} > 0: \qquad \nu = \frac{1}{2}\sqrt{q_{F5}\, q^{(0)}_{F1}}, \tag{6.66a}$$

$$\alpha = \frac{e^{-\phi(0)}}{2}, \tag{6.66b}$$

$$\eta = \frac{e^{\phi(0)}}{2}\frac{q_{F5}}{q^{(0)}_{F1}}, \tag{6.66c}$$

$$q^{\mathcal{D}}_{F1} < 0: \qquad \nu = \frac{1}{2}\sqrt{q_{F5}\, |q^{(\infty)}_{F1}|}, \tag{6.66d}$$

$$\alpha = \frac{e^{-\phi(\infty)}}{2}, \tag{6.66e}$$

$$\eta = \frac{e^{\phi(\infty)}}{2}\frac{q_{F5}}{|q^{(\infty)}_{F1}|}, \tag{6.66f}$$

featuring the F1 charge of only one asymptotic region. The dilaton at $z \to \infty$ appears through virtue of (6.55). It cannot truly be the vacuum however, because the D1 charge differs at both asymptotic regions,

$$q^{\mathcal{D}}_{F1} > 0: \qquad q^{(0)}_{F1} = q^{bare}_{F1}, \qquad |q^{(\infty)}_{F1}| = q^{bare}_{F1} + q^{\mathcal{D}}_{F1}, \tag{6.67a}$$

$$q^{\mathcal{D}}_{F1} < 0: \qquad |q^{(\infty)}_{F1}| = q^{bare}_{F1}, \qquad q^{(0)}_{F1} = q^{bare}_{D1} + |q^{\mathcal{D}}_{F1}|, \tag{6.67b}$$

leading to disctinct central charges at both sides. Hence there is still an interface present. Obviously, reducing $q^{\mathcal{D}}_{D1} = 0$ leads exactly to the vacuum expressions (6.105).

Pure D1 Defect, $q^{\mathcal{D}}_{F1} \to 0$

The solution (6.62) confirms that a non-vanishing defect F1 charge $q^{\mathcal{D}}_{F1}$ stabilizes the defect at some non-trivial AdS_2 sheet $\psi_\xi \neq 0$. Let us now restrict to the AdS_2 sheet of smallest size

$$\sinh \psi_\xi = 0 \quad \Leftrightarrow \quad \xi = 1, \tag{6.68}$$

or in other words a pure D1 defect, $q^{\mathcal{D}}_{F1} = 0$. In this case we have $\sigma(0) = 0$ and the F1 charges coincide at both asymptotic regions so

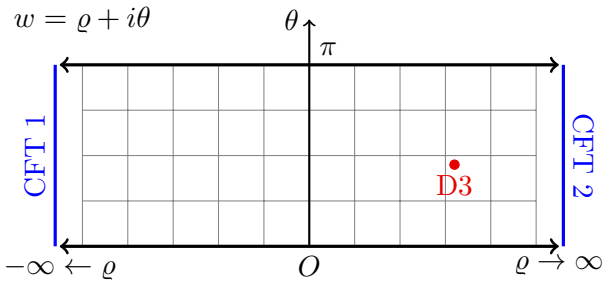

Figure 15: In contrast to the onebrane defect of the previous section, the D3 brane defect is located in the interior of Σ at $w = \psi_R + \Theta$, with $R = e_R^{\psi}$. Hence the defect is no longer located at the poles of the S^3, but wraps an S^2 at some constant value Θ.

that we drop the superscripts, $q_{F1} \equiv q_{F1}^{(0)} = -q_{F1}^{(\infty)} = \overline{q_{F1}}$. The solution (6.62) then reduces to

$$\nu = \frac{1}{2}\sqrt{\frac{q_{F5}\, q_{F1}}{\kappa_0}}, \tag{6.69a}$$

$$\alpha = \frac{1}{2\sqrt{\kappa_0}} e^{-\phi(0)}, \tag{6.69b}$$

$$\eta = \frac{1}{2\sqrt{\kappa_0}} \frac{q_{F5}}{q_{F1}} e^{\phi(0)}, \tag{6.69c}$$

$$c = \frac{|q_{D1}^{\mathcal{D}}|}{q_{F5}}, \tag{6.69d}$$

where the proportionality factor reduces considerably,

$$\kappa_0 \equiv \kappa(q_{D1}^{\mathcal{D}},\, 0) = \frac{T_{(4q_{F1}^{(0)},\, q_{D1}^{\mathcal{D}})} + T_{(0,\, q_{D1}^{\mathcal{D}})}}{T_{(4q_{F1}^{(0)},\, q_{D1}^{\mathcal{D}})} - T_{(0,\, q_{D1}^{\mathcal{D}})}}. \tag{6.70}$$

Lastly, we can perform the limit where the defect vanishes, $q_{D1}^{\mathcal{D}} \propto c \to 0$ leading to $\kappa_0 \to 1$ and therefore the triple (α, η, ν) reduces to the vacuum expressions (6.41).

6.3.4 *D3 Interface*

Next up is the D3 interface. We only motivate the it through D3 brane charge, (6.11), which is induced by monodromies of C_K. As is evident from (6.5c) the monodromy necessarily stems from $\tilde{u}$, since this building block appears in no other charge or field. If we denote by $w = R\, e^{i\Theta}$ the locus of a stack of D3 branes on Σ, we obtain monodromies by additions $\delta U \propto \log(z - w)$. This is depicted in strip coordinates in Figure 15.

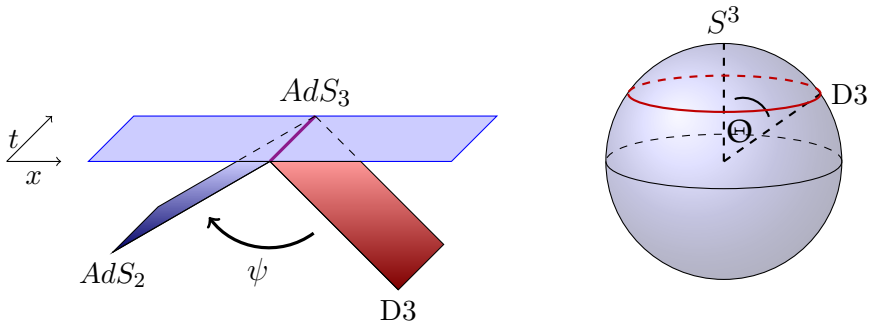

Figure 16: In coordinates $z = \exp(\psi + i\theta)$ AdS_3 is foliated by AdS_2 sheets shaded in dark blue and labelled by ψ. A D3 brane, shaded in red, is embedded into $AdS_3 \times S^3$ at $w = \exp(\psi_R + i\Theta)$, i.e. it wraps an S^2 on the S^3. The boundary of AdS_3, shaded in light blue, harbors the CFT and its intersection with the brane is the wordline of the field theory defect, colored in violet.

In order to respect point I in Section 6.2, i.e. $u(\partial\Sigma) = 0$, we employ the method of images and induce a mirror charge at $\bar{w}$ in the lower half plane. It can be readily checked that the modification

$$\delta U^{D3} = -\frac{q^{\mathcal{D}}_{D3}}{2} \log\left(\frac{z-w}{z-\bar{w}}\right), \tag{6.71a}$$

$$\delta u^{D3} = -\frac{q^{\mathcal{D}}_{D3}}{2} \log\left|\frac{z-w}{z-\bar{w}}\right|^2, \tag{6.71b}$$

$$\delta \tilde{u}^{D3} = i\frac{q^{\mathcal{D}}_{D3}}{2} \log\left[\frac{(z-w)(\bar{z}-w)}{(z-\bar{w})(\bar{z}-\bar{w})}\right] \tag{6.71c}$$

produces

$$Q^{\mathcal{D}}_{D3} = \pi\, q^{\mathcal{D}}_{D3}, \qquad q^{\mathcal{D}}_{D3} = \frac{(2\pi)^4 \alpha'^2}{\pi} N_3 \tag{6.72}$$

via (6.11). The second equation introduces the integer-valued D3-brane charge N_3. This is the same normalization as in the D1/D5 case. Since w lies on the upper half plane, Σ, we have $\Theta \in (0, \pi)$. Then the constraint $a\,u - b^2 \geq 0$ enforces positivity of $q^{\mathcal{D}}_{D3}$. The geometry is depicted in Figure 16 in coordinates $z = \exp(\psi + i\theta)$ with $R = \exp\psi_R$ and $\theta = \Theta$. As one might expect the polar angle will play an important role when making contact with the Kondo flows in Section 6.3.5.

Straightforward computation of the asymptotic charges (6.96) gives

$$q_{F5}^{(0)} = \frac{\nu}{\beta}, \qquad q_{F5}^{(\infty)} = -\frac{\nu}{\beta}, \tag{6.73a}$$

$$q_{F1}^{(0)} = \frac{\nu\alpha}{\beta}\left(4\eta + \frac{q_{D3}}{R}\sin\Theta\right), \qquad q_{F1}^{(\infty)} = -\frac{\nu\alpha}{\beta}\left(4\eta + q_{D3}\,R\sin\Theta\right), \tag{6.73b}$$

$$q_{D1}^{(0)} = c\frac{\nu}{\beta} = c\,q_{D5}^{(0)}, \qquad q_{D1}^{(\infty)} = 0, \tag{6.73c}$$

while q_{D5} still vanishes at both asymptotic regions. Again, the defect carries F1 and D1 charge,

$$q_{D1}^{\mathcal{D}} \equiv -q_{D1}^{(0)} - q_{D1}^{(\infty)} = -q_{D3}^{\mathcal{D}}\Theta\, q_{D5}, \tag{6.74a}$$

$$q_{F1}^{\mathcal{D}} \equiv -q_{F1}^{(0)} - q_{F1}^{(\infty)} = q_{D3}^{\mathcal{D}}\frac{\nu\alpha}{\beta}\left(R - \frac{1}{R}\right)\sin\Theta. \tag{6.74b}$$

The asymptotic values of the fields (6.91) are

$$e^{-2\phi(0)} = \frac{\beta^2\alpha}{\eta^2}\left(4\eta + \frac{q_{D3}}{R}\sin\Theta\right) = \frac{\beta^2}{\eta^2}\frac{q_{F1}^{(0)}}{q_{F5}^{(0)}}, \tag{6.75a}$$

$$e^{-2\phi(\infty)} = \frac{\beta^2\alpha}{\eta^2}\left(4\eta + q_{D3}R\sin\Theta\right) = \frac{\beta^2}{\eta^2}\frac{q_{F1}^{(\infty)}}{q_{F5}^{(\infty)}}, \tag{6.75b}$$

$$C_K(0) = -q_{D3}^{\mathcal{D}}\Theta = \frac{q_{F1}^{\mathcal{D}}}{q_{F5}}, \tag{6.75c}$$

$$C_K(\infty) = 0, \tag{6.75d}$$

while the axion χ still vanishes at both regions. As before the jump in the dilaton is not independent, cf. (6.55).

Let us define an effective D1 charge

$$q_{D1}^{\Theta} \equiv q_{D1}^{\mathcal{D}}\frac{\sin\Theta}{\Theta} \tag{6.76}$$

and use it to rewrite the F1 charges in (6.73),

$$q_{F1}^{(0)} = 4\nu\sqrt{\alpha\eta} - \frac{\alpha}{R}q_{D1}^{\Theta}, \qquad q_{F1}^{(\infty)} = -4\nu\sqrt{\alpha\eta} + \alpha R q_{D1}^{\Theta}. \tag{6.77}$$

Their linear combinations are ($R = e^{\psi_R}$)

$$q_{F1}^{\mathcal{D}} = |q_{F1}^{(\infty)}| - q_{F1}^{(0)} = -2\alpha q_{D1}^{\Theta}\sinh\psi_R, \tag{6.78a}$$

$$\overline{q_{F1}} \equiv \frac{|q_{F1}^{(\infty)}| + q_{F1}^{(0)}}{2} = 4\nu\sqrt{\alpha\eta} - \alpha q_{D1}^{\Theta}\cosh\psi_R \equiv \kappa^{(\Theta)}\,4\nu\sqrt{\alpha\eta}. \tag{6.78b}$$

In the second line we have again quantified the difference to the vacuum F1 charge (6.40b) via $\kappa^{(\Theta)}$. Evidently, the F1 charges (6.77) and their

linear combinations (6.78) look exactly like their counterparts (6.56) and (6.57), respectively, with the replacements $q^{\mathcal{D}}_{D1} \to q^{\Theta}_{D1}$ and $\xi \to R$ ($\psi_\xi \to \psi_R$). As the reader might have observed already the other relevant expressions, namely the F5 charge, (6.73a), and the dilaton in (6.75a) assume exactly the same form as their counterparts for the onebrane defect (6.52a) and (6.54). Therefore the result (6.62) of the previous section carries over with the adjustments $q^{\mathcal{D}}_{D1} \to q^{\Theta}_{D1}$, $\psi_\xi \to \psi_R$,

$$\nu = \frac{1}{2}\sqrt{\frac{q_{F5}\,\overline{q_{F1}}}{\kappa^{(\Theta)}}}, \tag{6.79a}$$

$$\alpha = \frac{e^{-\phi(0)}}{2}\sqrt{\frac{1}{\kappa^{(\Theta)}}\,\frac{2\overline{q_{F1}}}{2\overline{q_{F1}} - q^{\mathcal{D}}_{F1}}}, \tag{6.79b}$$

$$\eta = \frac{e^{\phi(0)}}{2}\sqrt{\frac{1}{\kappa^{(\Theta)}}\,\frac{\overline{q_{F1}}\,(2\overline{q_{F1}} - q^{\mathcal{D}}_{F1})}{2q^2_{F5}}}, \tag{6.79c}$$

$$\sinh\psi_\xi = e^{\phi(0)}\sqrt{\kappa^{(\Theta)}\,\frac{2\overline{q_{F1}} - q^{\mathcal{D}}_{F1}}{2\overline{q_{F1}}}\,\frac{q^{\mathcal{D}}_{F1}}{|q^{\Theta}_{D1}|}}, \tag{6.79d}$$

$$\Theta = \frac{1}{q_{F5}}\frac{q^{\mathcal{D}}_{D1}}{q^{\mathcal{D}}_{D3}}. \tag{6.79e}$$

The proportionality factor is the also the same as before, (6.64), again with the replacement $q^{\mathcal{D}}_{F1} \to q^{\Theta}_{F1}$,

$$\begin{aligned}\kappa^{(\Theta)} &= \kappa(q^{\Theta}_{D1},\, q^{\mathcal{D}}_{F1}) \\ &= \frac{T^2_{\left(4\sqrt{\overline{q_{F1}}q^{(0)}_{F1}},\, q^{\Theta}_{D1}\right)} - T^2_{\left(0,\, q^{\Theta}_{D1}\right)}}{\left(\sqrt{\sigma^2_\Theta\left(q^{\mathcal{D}}_{F1}\right) + T^2_{\left(4\sqrt{\overline{q_{F1}}q^{(0)}_{F1}},\, q^{\Theta}_{D1}\right)}} - T_{\left(0,\, q^{\Theta}_{D1}\right)}\right)^2 - \sigma^2_\Theta\left(q^{\mathcal{D}}_{F1}\right)}\end{aligned} \tag{6.80a}$$

$$\sigma_\Theta(q^{\mathcal{D}}_{F1}) = \frac{T_{\left(4q^{(0)}_{F1},0\right)}}{T_{\left(0,\, q^{\Theta}_{D1}\right)}}\, T_{\left(q^{\mathcal{D}}_{F1},0\right)}, \tag{6.80b}$$

Clearly $\kappa^{(\Theta=0)} = \kappa$. We remark that we still have $\kappa^{(\Theta)} > 0$. Similar to before (6.79d) implies $\mathrm{sgn}(q^{\mathcal{D}}_{F1}) = \mathrm{sgn}(\psi_R)$. Notice that we have not bothered to instate (6.79e) into the remaining entries of the solution. The system is described by three defect charges, $q^{\mathcal{D}}_{D1}$, $q^{\mathcal{D}}_{F1}$, $q^{\mathcal{D}}_{D3}$. Instead of using $q^{\mathcal{D}}_{D3}$ we can just as well use the ratio of charges $q^{\mathcal{D}}_{D1}/q^{\mathcal{D}}_{D3}$ or just as well Θ, which is the most convenient variable for our purposes.

Note that even though there are $q^{\mathcal{D}}_{D1}$ units of D1 strings present on the defect, in the solution this charge appears only in the diminished form $q^{\Theta}_{D1} = q^{\mathcal{D}}_{D1}\frac{\sin\Theta}{\Theta}$. Therefore there is a trade off between the effect of the D1 charge on the geometry and moving the defect away from the

boundary of Σ into its interior, as can be concluded from comparison with results of the previous section, (6.62) and (6.64).

The most important result is (6.79e), which conveys that the amount of D1 strings per D3 brane determines the value of the polar angle of the defect on the S^3. We will come back to this important point in the next section when we discuss in detail the RG flow. In contrast the defect's F1 charge has no influence on the polar angle.

In the limit where the D3 charge outweighs the D1 charge of the defect, the threebrane defect approaches the boundary of Σ, i.e. $\Theta \to 0$, or equivalently $q^{\Theta}_{D1} \to q^{\mathcal{D}}_{D1}$. This implies that all expressions in (6.79) and (6.80) reduce to those of the onebrane defect, (6.69) and (6.64), respectively. Similarly to before we can now study defects with only one type of one brane charge.

Pure F1 Defect, $q^{\Theta}_{D1} \to 0$

Since the threebrane defect cares only about the effective D1 charge (6.76) we have two options to remove the effect of D1 charge. The first is as before $q^{\mathcal{D}}_{D1} \to 0$. The second is when $\Theta = \pi$, which happens at a large value of D1 charge $q^{\mathcal{D}}_{D1} = \pi q_{F5} q^{\mathcal{D}}_{D3}$. Of course, the defect is again pushed to the boundary of AdS_3, $\sinh \psi_R \to \operatorname{sgn} q^{\mathcal{D}}_{F1} \times \infty$ and the triple (α, η, ν) behaves in the same way as before, (6.66).

Pure D1 Defect, $q^{\Theta}_{F1} \to 0$

As for the onebrane defect of the previous section the most notable impact of the defect's F1 charge is to stabilize the brane at some AdS_2 with non-minimal volume, $\psi_R \neq 0$, as can be seen in (6.79d). Let us now inspect the case of smallest size $\psi_R = 0$, i.e. a D3 brane with $q^{\mathcal{D}}_{D1}$ units of D1 strings dissolved and no attached F1 strings, $q^{\mathcal{D}}_{F1} = 0$. In this case we have $\sigma_{\Theta}(0) = 0$ and the F1 charges coincide at both asymptotic regions so that we drop the superscripts, $q_{F1} \equiv q^{(0)}_{F1} = -q^{(\infty)}_{F1} = \overline{q_{F1}}$. The solution (6.79) then reduces to

$$\nu = \frac{1}{2}\sqrt{\frac{q_{F5}\, q_{F1}}{\kappa_0^{(\Theta)}}}, \tag{6.81a}$$

$$\alpha = \frac{1}{2\sqrt{\kappa_0^{(\Theta)}}} e^{-\phi(0)}, \tag{6.81b}$$

$$\eta = \frac{1}{2\sqrt{\kappa_0^{(\Theta)}}} \frac{q_{F5}}{q_{F1}} e^{\phi(0)}, \tag{6.81c}$$

$$\Theta = \frac{1}{q_{F5}} \frac{q^{\mathcal{D}}_{D1}}{q^{\mathcal{D}}_{D3}} \tag{6.81d}$$

where we have, again, a considerable simplification,

$$\kappa_0^{(\Theta)} \equiv \kappa(q_{D1}^{\Theta}, 0) = \frac{T_{(4q_{F1}^{(0)}, q_{D1}^{\Theta})} + T_{(0, q_{D1}^{\Theta})}}{T_{(4q_{F1}^{(0)}, q_{D1}^{\Theta})} - T_{(0, q_{D1}^{\Theta})}}. \tag{6.82}$$

Lastly, we may turn the defect's effective D1 charge off, $q_{D1}^{\Theta} = 0$. Again we have two ways of doing so, either through $q_{D1}^{\mathcal{D}} = 0$ or $\Theta = \pi$. Both options remove the defect leading to a vacuum solution, (6.41). Indeed, $q_{D1}^{\mathcal{D}} = 0$ implies through (6.74) that $q_{D3}^{\mathcal{D}} = 0$, which in turn removes δU^{D3}, cf. (6.71). Moreover, δU^{D3} vanishes identically for $\Theta = \pi$.

6.3.5 *Solution Matching: the RG flow*

So far we have only described asymptotic $\mathrm{AdS}_3 \times S^3 \times T^4$ half BPS supergravity solutions, which harbor an extra D1/F1 or D3 defect. Both solutions can exist with complete disregard to one another. However, in this section we will interpret these solutions as endpoints of an RG flow, $D1/F1 \to D3$. Moreover, we establish that these RG flows are precisely our Kondo flows.

On the field theory side we describe a boundary RG flow implying that the ambient CFTs remain unchanged. They are characterized by the gauge rank $N_5 \propto q_{F5}$, the central charge $\mathsf{c} \propto q_{F5} q_{F1}$ and the dilaton, all of which remain unaffected by the boundary RG flow. Hence these charges and fields should remain unchanged under the flow,

$$Q_{brane}^{\mathrm{IR}} \stackrel{!}{=} Q_{brane}^{\mathrm{UV}}, \qquad \phi^{\mathrm{IR}} \stackrel{!}{=} \phi^{\mathrm{UV}}, \tag{6.83}$$

where these expressions refer to the values at either asymptotic region. The UV solution is the one-brane defect and the IR corresponds to the three brane defect discussed in Section 6.3.3 and Section 6.3.4 respectively. For the onebrane charges we will sometimes equivalently phrase this matching in terms of the arithmetic means (6.57b), (6.78b) and the defect charges (6.53), (6.74), which, due to charge conservation are identified as well. The goal of this matching is to relate the individual parameters in the onebrane solution (6.62) to those in the threebrane solution (6.79).

Let us start with the D1 charge. Identifying (6.53a) and (6.74a) tells us that

$$q_{D3}^{\mathcal{D}} \Theta = c. \tag{6.84}$$

Using this it is readily checked that for small Θ the threebrane modification (6.71) reduces to the onebrane modification (6.44), $\delta U^{D3} \simeq \delta U^{F1}$ if we fix $\xi = R$ meaning that the defect remains on the same AdS_2 sheet along the flow. This holds true only for small Θ or when the defect carries no extra F1 charge. Recall that the onebrane and the threebrane defect both occupy the AdS_2 sheet of smallest size, $x = 1$ ($\psi_\xi = 0$)

and $R = 1$ ($\psi_R = 0$) when $q^{\mathcal{D}}_{F1} = 0$. This property does not hold true when the defect is stabilized by extra F1 charge on a non-minimal AdS_2 slice. Indeed, by comparison of (6.62d) and (6.79d) we conclude that the defect moves inside of AdS_3,

$$\sinh\psi_R = \sqrt{\frac{\kappa^{(\Theta)}}{\kappa}}\,\frac{\Theta}{\sin\Theta}\,\sinh\psi_\xi . \tag{6.85}$$

Given the expressions (6.64) and (6.80) we can bound

$$1 \leq \frac{\kappa}{\kappa^{(\Theta)}} \leq \left(\frac{\Theta}{\sin\Theta}\right)^2 , \tag{6.86}$$

which saturates for $\Theta = 0$. Plugged into (6.85) this implies that the defect is pushed towards the boundary of AdS_3, $|\psi_R| \geq |\psi_\xi|$, along the RG flow when $q^{\mathcal{D}}_{F1} \neq 0$. Their sign is that of the defect's F1 charge, $\mathrm{sgn}(q^{\mathcal{D}}_{F1}) = \mathrm{sgn}(\psi_\xi) = \mathrm{sgn}(\psi_R)$.

Through comparison of (6.62) and (6.79) we can express the triple $(\alpha^{\mathrm{IR}}, \eta^{\mathrm{IR}}, \nu^{\mathrm{IR}})$ through their analogs in the one-brane defect

$$\nu^{\mathrm{IR}} = \sqrt{\frac{\kappa}{\kappa^{(\Theta)}}}\,\nu^{\mathrm{UV}}, \tag{6.87a}$$

$$\alpha^{\mathrm{IR}} = \sqrt{\frac{\kappa}{\kappa^{(\Theta)}}}\,\alpha^{\mathrm{UV}}, \tag{6.87b}$$

$$\eta^{\mathrm{IR}} = \sqrt{\frac{\kappa}{\kappa^{(\Theta)}}}\,\eta^{\mathrm{UV}}. \tag{6.87c}$$

Recall from our probe brane discussion that the angle Θ indicates the endpoint of the flow and (6.79e) now encapsules how it depends on the configuration of the defect in the UV,

$$\Theta = \frac{1}{q^{(0)}_{F5}}\frac{q^{\mathcal{D},\mathrm{UV}}_{D1}}{q^{\mathcal{D},\mathrm{IR}}_{D3}} = \frac{\pi}{N_5}\frac{p}{N_3}. \tag{6.88}$$

We have employed the integer valued charges given by (6.43) and (6.72). Also, we returned to the notation of the last chapter for the defect charge $q^{\mathcal{D},\mathrm{UV}}_{D1} = p$. In order to compare with (5.18) we recall that we only had a single D3 brane, $N_3 = 1$, in Chapter 5. Furthermore, the level of the $\hat{\mathfrak{su}}(2)_{\mathsf{k}}$ WZW model, is identified with the magnetic flux through the S^3, which is the number of F5 branes in our case. In short $N_5 = \mathsf{k}$. Together we obtain

$$\Theta = \frac{\pi p}{\mathsf{k}} = \theta_p\,, \tag{6.89}$$

exactly as desired. This confirms that the supergravity solutions studied in this chapter indeed correspond to the flows worked out in Chapter 5.

The defect charge in the UV is dissolved into the D3 brane defect in the IR. Moreover, the more units of D1 charge is dissolved into a single D3 brane, the further down the D3 branes slide on the S^3. This is in exact analogy with the mechanism in the original Kondo effect, where the amount of pointlike branes at the north pole of the S^3, that is boundary states corresponding to the vacuum representation in the UV, determines the representation corresponding to the final boundary state in the IR. Here we have the additional freedom to choose the number of D3 branes into which the D1/F1 defect dissolves and this diminishes the final value of the polar angle on the S^3. Recall that in the probe brane computation we also only considered a single D3 brane.

When Θ is small we have observed that the D3 solution, (6.79), is rather a onebrane defect, (6.62). In the RG flow picture this means that is is not energetically favorable for the defect to puff up into a D3-brane. In other words the UV onebrane defect does not carry enough charge to be stabilized at a macroscopically visible two-sphere on the S^3. There is basically no RG flow.

Lastly, we explore the other extreme where the D3 brane reaches the south pole, $\Theta = \pi$, which happens when $p/N_3 = \pi N_5$. For simplicity let us consider the case $q^{\mathcal{D}}_{F1} = 0$. We observed before that the defect vanishes in this limit. Crucially, this happens for a non-trivial number of fundamental strings p, did not vanish "on its own accord" – it got screened! If we recall our exposition in Section 4.2, we see that this is exactly what happens in the original Kondo flow! Note that we cannot observe this effect in the probe brane limit, because the defect charge reaches the order of the background charge and there is necessarily backreaction. Our supergravity solutions accurately account for this.

We now repeat the analysis in the D1/D5 case. Readers not interested in this scenario should feel free to skip ahead to Equation 6.4.5.

6.4 D1/D5 CASE

This section conducts the same analysis as its predecessor, albeit in the D1/D5 case. Both sections can be read independently of each other. Our discussion here is self-contained, yet less detailed as for the F1/F5 case. We follow the same logic as above beginning with the analysis of the asymptotic regions in Section 6.4.1 This is followed by the construction of the pure D1/D5 geometry in Section 6.4.2. Thereafter we explain how to induce a D1/F1 defect in Section 6.4.3 and a D3 defect in Section 6.4.4. These solutions may be considered entirely independent of each other. In order to make contact with the Kondo effect we connect these solutions in Section 6.4.5 by interpreting them as fixed points of an RG flow.

A short version of the exposition here will appear in an upcoming publication [112] in collaboration with Johanna Erdmenger and Charles Melby-Thompson.

6.4.1 *Asymptotic Regions*

The main tools in our analysis are the charges (6.10), (6.9) and fields (6.5) evaluated at the asymptotic regions. Even though, the D1/D5 solutions we are after are not included within the set of solutions studied in [79, 80] the explicit form of all required expressions at the asymptotic regions remains unchanged. This will be evident from the specific form of our modifications below. Thus, in this subsection, we cite all charges, fields and metric factors as computed in [80].

Singularities in f_1 designate asymptotic $\mathrm{AdS}_3 \times S^3 \times T^4$ regions. In terms of the holomorphic functions the asymptotic regions are singled out as poles of V. We are interested in solutions with two asymptotic regions, which we place at $z = 0$ and $z \to \infty$ in Σ. These regions are interchanged via inversion $z \to -1/z$. In the vicinity of $z = 0$ the meromorphic functions assume the form

$$V(z) = iv_{-1}z^{-1} + iv_1 z + \dots \tag{6.90a}$$
$$A(z) = ia_0 + ia_1 z + \dots \tag{6.90b}$$
$$B(z) = ib_0 + ib_1 z + \dots \tag{6.90c}$$
$$U(z) = iu_0 + iu_1 z + \dots \tag{6.90d}$$

All coefficients v_j, u_j, a_j, b_j in these expansions are real. Switching coordinates to $z = re^{i\theta}$ we find expressions for the dilaton, axion and RR four-form potential (see (6.5a)-(6.5c))

$$e^{-2\phi} = \frac{b_0^2}{u_1^2}(a_1u_1 - b_1^2) + \mathcal{O}(r), \tag{6.91a}$$
$$\chi = \frac{b_0 b_1}{u_1} - a_0 + \mathcal{O}(r), \tag{6.91b}$$
$$C_K = \frac{b_0 b_1}{a_1} - u_0 + \mathcal{O}(r). \tag{6.91c}$$

Similarly, the metric factors (6.2) become

$$f_1^4 = \frac{1}{r^4}\frac{4a_1b_0v_{-1}^2}{(a_1u_1 - b_1^2)^{3/2}} + \mathcal{O}(r^{-3}), \tag{6.92a}$$
$$f_2^4 = \sin^4\theta \frac{4a_1v_{-1}^2}{b_0^3}\sqrt{a_1u_1 - b_1^2} + \mathcal{O}(r), \tag{6.92b}$$
$$f_3^4 = \frac{b_0}{a_1}\sqrt{a_1u_1 - b_1^2} + \mathcal{O}(r), \tag{6.92c}$$
$$\rho^4 = \frac{1}{r^4}\frac{4a_1v_{-1}^2}{b_0^3}\sqrt{a_1u_1 - b_1^2} + \mathcal{O}(r^{-3}). \tag{6.92d}$$

Using coordinates $z = \exp(\psi + i\theta)$ the metric assumes the form ($\psi \to -\infty, r \to 0$)

$$ds_{10}^2 = \mathsf{L}^2\left(d\psi^2 + \frac{\mu}{4}e^{-2\psi}ds^2_{\mathrm{AdS}_2} + d\theta^2 + \sin^2\theta ds^2_{S^2}\right) + \sqrt{\frac{u_1}{a_1}e^{-\phi}}ds^2_{T^4}. \tag{6.93}$$

Here, we defined the ten-dimensional AdS radius L and a scale factor μ, which will become important when choosing a cutoff for AdS_3 in later sections,

$$\mathsf{L}^2 = 2\sqrt{\frac{a_1 v_{-1}^2 u_1}{b_0^4}}\, e^{-\frac{1}{2}\phi}, \qquad \mu = 4\frac{b_0^4}{u_1^2}\, e^{2\phi}. \tag{6.94}$$

The six-dimensional AdS radius $\mathsf{R} = \mathsf{L}f_3$ will be useful and appears in the scale factor,

$$\mu = \frac{(4v_{-1})^2}{\mathsf{R}^4}. \tag{6.95}$$

The five-brane Page charges (6.10) and the one-brane Page charges (6.9) are expressed through

$$q_{D5} \equiv \frac{Q_{D5}}{8\pi^2} = v_{-1}\frac{a_1 b_0 - a_0 b_1}{b_0^2}, \tag{6.96a}$$

$$q_{F5} \equiv \frac{Q_{F5}}{8\pi^2} = v_{-1}\frac{b_1}{b_0^2}, \tag{6.96b}$$

$$q_{D1} \equiv \frac{Q_{D1}}{8\pi^2} = -v_{-1}\frac{b_1 u_0 - b_0 u_1}{b_0^2}, \tag{6.96c}$$

$$q_{F1} \equiv \frac{Q_{F1}}{8\pi^2} = -v_{-1}\frac{b_0^2 b_1 + a_0 b_1 u_0 - a_1 b_0 u_0 - a_0 b_0 u_1}{b_0^2}. \tag{6.96d}$$

The ten-dimensional gravitational constant and the ten-dimensional Newton constant are

$$\kappa_{10}^2 = 8\pi G_N^{(10)}, \tag{6.97}$$

$$G_N^{(10)} = G_N^{(3)}\mathrm{Vol}(S^3_{\mathsf{L}})\mathrm{Vol}(T^4_{f_3}) = G_N^{(3)}\, 2\pi^2 \mathsf{L}^3\, f_3^4, \tag{6.98}$$

where the subscripts in the volumes denote the respective radii[11]. The Brown-Henneaux formula then provides the central charge of the CFT at the asymptotic region,

$$\mathsf{c} = \frac{3\mathsf{L}}{2G_N^{(3)}} = \frac{6}{4\pi\kappa_{10}^2}\left(Q_{D5}\, Q_{D1} + Q_{F5}\, Q_{F1}\right). \tag{6.99}$$

11 Whenever we omit the radius in Volume expression it implies unit radius, i.e. $\mathrm{Vol}(S^3) = 2\pi^2$

Lastly, the observation

$$\mathsf{R}^4 = 4\Big(q_{D5}\,q_{D1} + q_{F5}\,q_{F1}\Big) = \frac{4G_N^{(10)}}{\mathrm{Vol}(S^3)}\frac{\mathsf{c}}{6} \tag{6.100}$$

will be convenient. In the next section we proceed to write down the D1/D5 vacuum solution and will augment it in subsequent sections by a $(D1, F1)$ defect and a D3 defect.

6.4.2 *D1/D5 Vacuum*

We begin applying the formalism described to the simple case of a trivial defect, which is just the standard D1/D5 geometry. Sometimes we refer to it as the vacuum since it harbors no defect. It is devoid of NS fivebranes and fundamental strings and it can be checked using (6.96) that the assignments

$$A(z) = i\alpha\frac{z}{z^2-1}, \qquad a = \frac{2\alpha\Im(z)}{|1-z^2|^2}(1+|z|^2) \tag{6.101a}$$

$$B(z) = i\beta\frac{z^2+1}{z^2-1}, \qquad b = \frac{8\beta\Im(z)\Re(z)}{|1-z^2|^2} \tag{6.101b}$$

$$U_0(z) = i\eta\frac{z}{z^2-1}, \qquad u_0 = \frac{2\eta\Im(z)}{|1-z^2|^2}(1+|z|^2) \tag{6.101c}$$

$$V(z) = i\nu\left(\frac{1}{z}-z\right), \quad v = 2\nu\Im(z)(|z|^{-2}+1) \tag{6.101d}$$

secure $q_{F5} = 0 = q_{F1}$. The coefficients α, β, η, ν are chosen real. Due to the positivity of the metric factors (6.2), the numbers α and η not only share their sign, but are also both positive. Moreover ν is chosen to be positive. The meromorphic function U_0 will be modified later in order to induce the defects and thus it carries a subscript here indicating the vacuum. The remaining charges in (6.96) and the dilaton (6.91a) on both sides are not independent,

$$q_{D5}^{(0)} = \frac{\alpha\,\nu}{\beta} = -q_{D5}^{(\infty)}, \tag{6.102a}$$

$$q_{D1}^{(0)} = \frac{\eta\,\nu}{\beta} = -q_{D1}^{(\infty)}, \tag{6.102b}$$

$$e^{-2\phi(0)} = \frac{\alpha\,\beta^2}{\eta} = e^{-2\phi(\infty)}. \tag{6.102c}$$

Superscripts are used to indicate where this charge is evaluated, $z = 0$ or $z \to \infty$. Obviously, the first two equations are simply the expected charge conservation. The axion and the RR four-form, equation (6.91b) and (6.91c) respectively, vanish. We see that the sign of β determines the signs of the charges. In particular, the signs of both, D1 and D5 charges, coincide at one asymptotic region.

In accordance with the discussion in Section 6.2 the harmonics a, b, u_0, v vanish on the boundary $\partial\Sigma$, (6.12) and the meromorphics A, B, U share their singularites, (6.15), at $z = \pm 1$. The requirements (6.15) at these loci give rise to the same constraint and reduce the number of independent parameters in (6.101),

$$\beta^2 = \frac{\alpha\eta}{4}. \tag{6.103}$$

This identification will persist[12] through any modification that we will employ in order to give rise to defects later on. Also, B and $\partial_z V$ share their zeroes at $z = \pm i$ (point III). Moreover, it can be checked that

$$a\,u_0 - b^2 = \frac{4\alpha\eta\,\Im^2(z)}{|1-z^2|^4}\Big((1+|z|^2)^2 - 4\Re^2(z)\Big) \geq 0, \tag{6.104}$$

as desired by point II in Section 6.2.

It is useful to replace the three parameters (α, η, ν) by the physically meaningful charges and the dilaton. Therefore, we invert the system of equations (6.102),

$$\nu = \frac{1}{2}\sqrt{q_{D5}^{(0)}\,q_{D1}^{(0)}}, \tag{6.105a}$$

$$\alpha = 2e^{-\phi(0)}, \tag{6.105b}$$

$$\eta = 2\frac{q_{D1}^{(0)}}{q_{D5}^{(0)}}e^{-\phi(0)}. \tag{6.105c}$$

Given the functions (6.101) the combined metric factors (6.2) give rise to $\mathrm{AdS}_3 \times S^3 \times T^4$ for any point on Σ, i.e. not just asymptotically so. In coordinates $z = \exp(\psi + i\theta)$ and employing (6.105) the metric reads

$$ds_{10}^2 = \mathsf{L}^2\left(d\psi^2 + \cosh^2\psi\, ds_{\mathrm{AdS}_2}^2 + d\theta^2 + \sin^2\theta ds_{S^2}^2\right) + \sqrt{\frac{q_{D1}^{(0)}}{q_{D5}^{(0)}}e^{-\phi(0)}}ds_{T^4}^2, \tag{6.106}$$

with ten-dimensional AdS radius $\mathsf{L}^2 = 2|q_{D5}^{(0)}|e^{\phi(0)/2}$ and scale factor $\mu = 1$. These are reproduced with the expression given in (6.94). The metric (6.106) can be readily compared to the metric (6.42) of the F1/F5 vacuum.

By comparison of (6.106) to the D1/D5 Einstein frame solution in the literature we can relate the page charges to the integer valued charges N_1, N_5 as follows

$$Q_{D5} = 8\pi^2 q_{D5} = (2\pi)^2\alpha' N_5, \qquad Q_{D1} = 8\pi^2 q_{D1} = (2\pi)^6\alpha'^3 N_1, \tag{6.107}$$

12 In what follows we will sometimes keep the parameter β to avoid clutter in equations. Unless otherwise stated it will be determined by (6.103).

and similarly for Q_{F5} and Q_{F1}. Plugged into the central charge (6.99) together with $4\pi\kappa_{10}^2 = (2\pi)^8\alpha'^4$ we obtain the well known result $\mathsf{c} = 6N_1N_5$.

In the following we will insert defects into this vacuum by modifying the function (6.101c). We will see that the expressions in (6.105) will be augmented by defect charges in such a way that they reduce to the vacuum solution when setting the defect charge to zero. In particular we may think of the vacuum as the trivial or completely transmissive defect.

6.4.3 *F1/D1 Interface (UV)*

Our objective is to insert an F1 string into the vacuum solution, which is smeared over the T^4 directions. In order to find the behavior of the individual metric factors f_i and ρ near such a defect consider first the supergravity solution of N_1 F1 and N_5 F5 branes in Einstein frame[13]:

$$ds^2_{F1/F5} = Z_1^{-3/4}Z_5^{-1/4}\eta_{\mu\nu}dx^\mu dx^\nu + Z_1^{1/4}Z_5^{3/4}dx^i dx^i + Z_1^{1/4}Z_5^{-1/4}dx^m dx^m. \quad (6.108)$$

The greek letters run over the directions parallel to the F1 and the F5 branes, i runs over the directions transverse to all branes and m runs over the directions parallel to the F5 branes, but transverse to the F1 branes. The latter directions are compactified on a T^4 of volume V_4. The harmonic functions and the dilaton are

$$Z_1 = 1 + \frac{r_1^2}{r^2}, \quad r_1^2 = \frac{(2\pi)^4 N_1 \alpha'^3}{g_s V_4} \quad (6.109a)$$

$$Z_5 = 1 + \frac{r_5^2}{r^2}, \quad r_5^2 = \frac{N_5\alpha'}{g_s} \quad (6.109b)$$

$$e^{-2\phi} = \frac{1}{g_s^2}\frac{Z_1}{Z_5}. \quad (6.109c)$$

g_s is the string coupling and α' its tension. Here $r^2 = x_i x^i$ is determined by the overall transverse directions only. The fact that the harmonic function Z_1 corresponding to the F1 branes is independent of the T^4 directions implies that the fundamental strings are smeared over these directions, as desired.

13 It can be found starting from the D1/D5 metric after performing an S-duality. It inverts the dilaton, exchanges RR charges by NS charges, and leaves the Einstein frame metric invariant. Our expressions are adapted from [199].

We are interested in the near brane behavior of F1 branes smeared over the T^4 directions, so we get rid of the F5 branes, i.e. we set $N_5 = 0$, in (6.108) and perform the limit $r \to 0$. This gives

$$\begin{aligned} ds^2_{F1_{smeared}} \simeq & \left(\frac{r}{r_1}\right)^{3/2} \eta_{\mu\nu} dx^\mu dx^\nu \\ & + \left(\frac{r_1}{r}\right)^{1/2} (dr^2 + r^2 d\Omega_3^2) + \left(\frac{r_1}{r}\right)^{1/2} dx^m dx^m . \end{aligned} \tag{6.110}$$

We have written the overall transverse directions x^i in polar coordinates.

Now we are finally in a position to utter an expectation for the functions f_i in the ansatz (6.1). The prefactor of $\eta_{\mu\nu} dx^\mu dx^\nu$ gives the behavior of f_1, the prefactor of $d\Omega_3^2$ the behavior of f_2 and the prefactor of $dx^i dx^i$ the behavior of f_3. Thus we expect

$$f_1^2 \simeq r^{3/2}, \qquad f_2^2 \simeq r^{3/2}, \qquad f_3^2 \simeq r^{-1/2}, \qquad e^\phi \simeq r. \tag{6.111}$$

This behavior can also be reproduced in a different way by modifying the standard F1 solution. The harmonic function therein carries information on the number of transverse directions, i.e. eight. An F1 string smeared over the T^4 directions really only "has" four transverse directions, as if it were a five-brane. In order to elicit the asymptotic behavior, it then suffices to plug in the F5 harmonic function into the standard F1 string solution.

Another hint for the structure of an F1 brane solutions comes from considering the charges. In order to realize an F1 string one has to impose a monodromy in the integrand of (6.9b) at the boundary of Σ. Due to the complicated form of the F1 charge it is simpler to first S-dualize and to perform four T-dualities along the T^4 directions turning the F1 string into a D5 brane. From (6.10b) it is clear that one has to impose an extra pole in A at some location $\xi \in \partial\Sigma$ to produce a D5 charge. Negative values for x imply that the defect is localized at the south pole of the S^3 (in our coordinate system $z = re^{i\theta} = e^{\psi + i\theta}$). Thus we will choose without loss of generality $\xi > 0$. The insertion of this defect is visualized on Σ in strip coordinates $w = \log z$ in Figure 17.

Let us trace back what this implies for our F1 defect by undoing the duality transformations step by step. In our framework four T-dualities are realized via an exchange $A(z) \leftrightarrow U(z)$. Thus a D1 brane charge is imposed in place of the D5 charge by adding the pole not to A but U. S-duality acts on the meromorphic functions as follows [79]

$$A \to \frac{1}{A}, \qquad B \to i\frac{B}{A}, \qquad U \to U - \frac{B^2}{A}. \tag{6.112}$$

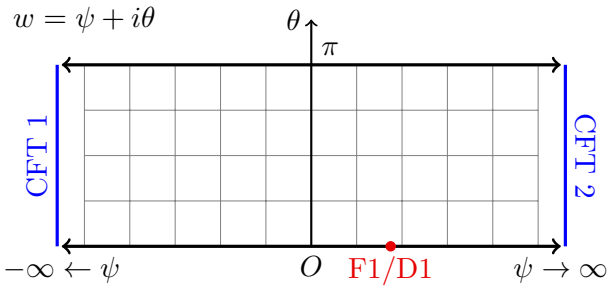

Figure 17: In strip coordinates $w = \psi + i\theta$ the two asymptotic regions, depicted by blue bars, lie at $\psi \to \pm\infty$. Each harbors a CFT and they typically differ due to the presence of the F1/D1 – we anticipate that the defect will carry both types of onebrane charge – defect located at $\psi_\xi \in \partial\Sigma$ depicted as red dot. The lower boundary, $\theta = 0$, corresponds to the north pole of the S^3, while the upper boundary, $\theta = \pi$ corresponds to the southpole.

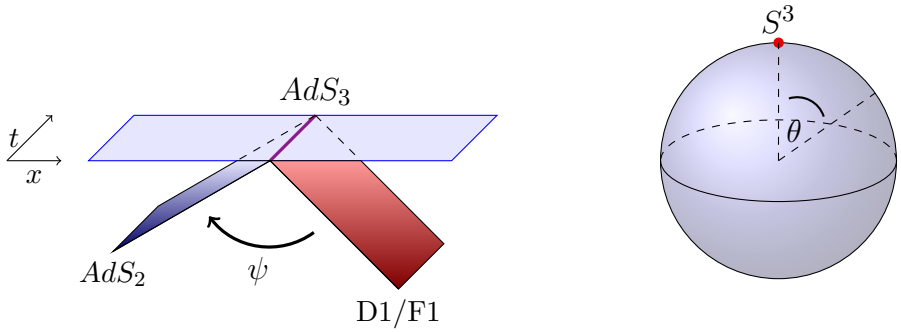

Figure 18: In coordinates $z = \exp(\psi + i\theta)$ AdS_3 is foliated by AdS_2 sheets shaded in dark blue and labelled by ψ. A D1/F1 string, shaded in red, is embedded into $AdS_3 \times S^3$ at $\xi = \exp\psi_\xi$, i.e. it sits at the north pole of S^3. The boundary of AdS_3, shaded in light blue, harbors the CFT and its intersection with the brane is the wordline of the field theory defect, colored in violet.

Contemplating the transformation of u we see that the extra pole for a D1 defect persists in the F1 case. Therefore we modify U_0 in (6.101),

$$U(z) = U_0 + \delta U^{D1}, \tag{6.113a}$$

$$\delta U^{D1} = ic\,\frac{z}{z-\xi}, \tag{6.113b}$$

$$\delta u^{F1} = \frac{2c\,\xi\,\Im(z)}{|z-\xi|^2}. \tag{6.113c}$$

The real constant c will be tied to the defect's F1 charge below.

As will become evident momentarily this modification does not give rise to a pure F1 string but a (p, q) string, and the defect's D1 charge is set by the value of ξ. The geometry is depicted in fig. 18 in coordinates $z = \exp(\psi + i\theta)$ with $\xi = \exp\psi_\xi$. Since the defect lies on $\partial\Sigma$ it sits at a pole of the S^3 and occupies one AdS_2 slice.

It is readily checked that for the special value $\xi = 1$, ($\psi_\xi = 0$) the asymptotic behavior (6.111) corresponding to a *pure* F1 string is reproduced. Indeed, plug the functions A, B, V of (6.101) together with (6.113) into (6.2a)-(6.2d), set $z = 1 + ir$ and have r tend to zero. In Figure 18 this corresponds to an F1 string intersecting the CFT spacetime orthogonally.

The new pole in (6.113) is not shared by A and B and thus does not give rise to an extra constraint of type (6.15). Since the harmonic a is positive, the requirement (6.13) enforces

$$a\,u_0 - b^2 + a\delta\,u^{F1} \geq 0 \qquad \Rightarrow \qquad c\,\xi \geq 0 \tag{6.114}$$

Since we are building on the vacuum solution (6.101) the sum of the first two terms is positive by itself, cf. (6.104). Our choice $\xi > 0$ then renders c positive.

Now that we have convinced ourselves that the addition (6.113) to (6.101) generates a onebrane defect embedded into the D1/D5 geometry, we want to inquire about the physical significance of the involved parameters ν, α, η, c, ξ. This is achieved following the same philosophy as before by expressing them in terms of the charges, which are now supplemented by defect charges, and the dilaton.

Straightforward computation of the asymptotic charges (6.96) gives

$$q^{(0)}_{D5} = \frac{\alpha\nu}{\beta}, \qquad q^{(\infty)}_{D5} = -\frac{\alpha\nu}{\beta}, \tag{6.115a}$$

$$q^{(0)}_{D1} = \frac{\nu}{\beta}\left(\eta + \frac{c}{\xi}\right), \qquad q^{(\infty)}_{D1} = -\frac{\nu}{\beta}\left(\eta + c\,\xi\right), \tag{6.115b}$$

$$q^{(0)}_{F1} = 0, \qquad q^{(\infty)}_{F1} = -c\frac{\alpha\nu}{\beta} = c\,q^{(\infty)}_{D5}, \tag{6.115c}$$

while q_{F5} still vanishes at both asymptotic regions. Even though we have used the same greek letters here as in (6.101) we emphasize that they will not take the same value as in (6.105). Their relation will become clear in (6.121). Their relation to their analogs in the vacuum solution will become clear at the end of this section. Nevertheless the parameters here still satisfy (6.103). Indeed, in the vacuum solution the requirements (6.15) at $z = \pm 1$ both gave rise to the same constraint. While at $z = 1$ we do not require regularity anymore due to the possibility $\xi = 1$, at $z = -1$ the constraint remains untouched yielding again $4\beta = \alpha\eta$.

As alluded to before, the defect, let us indicate it by superscript $\mathcal{D}$, carries D1 and F1 charge,

$$q^{\mathcal{D}}_{F1} \equiv -q^{(0)}_{F1} - q^{(\infty)}_{F1} = c\,q^{(0)}_{D5}, \tag{6.116a}$$

$$q^{\mathcal{D}}_{D1} \equiv -q^{(0)}_{D1} - q^{(\infty)}_{D1} = c\frac{\nu}{\beta}\left(\xi - \frac{1}{\xi}\right). \tag{6.116b}$$

For the particular value $\xi = 1$ corresponding to the AdS_2 sheet of smallest size, $q^{\mathcal{D}}_{D1}$ vanishes. In this case the D1 charges at both asymptotic regions differ only in sign.

The asymptotic values of the fields (6.91) are

$$e^{-2\phi(0)} = \frac{\beta^2\alpha}{\eta + c/\xi} = \frac{1}{\beta^2}\frac{q^{(0)}_{D5}}{q^{(0)}_{D1}}, \tag{6.117a}$$

$$e^{-2\phi(\infty)} = \frac{\beta^2\alpha}{\eta + c\,\xi} = \frac{1}{\beta^2}\frac{q^{(\infty)}_{D5}}{q^{(\infty)}_{D1}} \tag{6.117b}$$

$$C_K(0) = 0, \tag{6.117c}$$

$$C_K(\infty) = -c = -\frac{q^{\mathcal{D}}_{F1}}{q^{(0)}_{D5}}, \tag{6.117d}$$

while the axion χ still vanishes at both regions. This configuration features a jump in the dilaton, which is controlled by the discrepancy in D1 charge at the asymptotic regions,

$$e^{2\phi(\infty)} = -e^{2\phi(0)}\frac{q^{(\infty)}_{D1}}{q^{(0)}_{D1}}, \tag{6.118}$$

and is therefore not independent.

For the remainder of this article we drop the superscript on the D5 charge, $q_{D5} \equiv q^{(0)}_{D5} = -q^{(\infty)}_{D5}$. Without loss of generality we choose $\beta > 0$, which renders all charges at zero and $q^{\mathcal{D}}_{F1}$ positive, while all charges at infinity are then negative. For future reference we rewrite the D1 charges in (6.115) in the more suggestive form

$$q^{(0)}_{D1} = \frac{\nu\eta}{\beta} + \frac{1}{\alpha\xi}q^{\mathcal{D}}_{F1}, \qquad q^{(\infty)}_{D1} = -\frac{\nu\eta}{\beta} - \frac{\xi}{\alpha}q^{\mathcal{D}}_{F1}, \tag{6.119}$$

which elicits that we recover the vacuum expression (6.102b) when $q^{\mathcal{D}}_{F1}$ tends to zero. Thinking of the defect's D1 charge as difference of the absolute values of the D1 charges at the asymptotic regions suggests to also introduce their arithmetic mean,

$$q^{\mathcal{D}}_{D1} = |q^{(\infty)}_{D1}| - q^{(0)}_{D1} = \frac{q^{\mathcal{D}}_{F1}}{\alpha} 2\sinh\psi_\xi, \tag{6.120a}$$

$$\overline{q_{D1}} \equiv \frac{|q^{(\infty)}_{D1}| + q^{(0)}_{D1}}{2} = \frac{\nu\eta}{\beta} + \frac{q^{\mathcal{D}}_{F1}}{\alpha}\cosh\psi_\xi \equiv \kappa\frac{\nu\eta}{\beta}. \tag{6.120b}$$

Here, we have expressed the locus of the defect through its Janus coordinate $\xi = \exp\psi_\xi$. The second equation defines κ, which quantifies how much the D1 charge differs from the vacuum case, (6.102b). Of course, the pairs $(q^{(0)}_{D1}, q^{(\infty)}_{D1})$ and $(q^{\mathcal{D}}_{D1}, \overline{q_{D1}})$ are linearly independent. In what follows we choose to use the latter unless stated otherwise.

Overall we have added two new parameters, c and ξ to the system and obtained two new independent charges (6.116). Our next step is

to express the variables $(\alpha, \eta, \nu, c, \xi)$ in terms of the charges and the dilaton. In doing so it is useful to look for combinations of charges, which assume qualitatively the same shape as the right hand sides of (6.105),

$$\nu = \frac{1}{2}\sqrt{\frac{q_{D5}\,\overline{q_{D1}}}{\kappa}}, \tag{6.121a}$$

$$\alpha = 2e^{-\phi(0)}\sqrt{\kappa\,\frac{2\overline{q_{D1}} - q^{\mathcal{D}}_{D1}}{2\overline{q_{D1}}}}, \tag{6.121b}$$

$$\eta = 2\sqrt{\frac{1}{\kappa}\frac{\overline{q_{D1}}\,(2\overline{q_{D1}} - q^{\mathcal{D}}_{D1})}{2q^2_{D5}}}e^{-\phi(0)}, \tag{6.121c}$$

$$\sinh\psi_\xi = e^{-\phi(0)}\sqrt{\kappa\,\frac{2\overline{q_{D1}} - q^{\mathcal{D}}_{D1}}{2\overline{q_{D1}}}}\frac{q^{\mathcal{D}}_{D1}}{q^{\mathcal{D}}_{F1}}, \tag{6.121d}$$

$$c = \frac{q^{\mathcal{D}}_{F1}}{q_{D5}} \tag{6.121e}$$

The proportionality factor κ is best expressed through (p, q) string tensions (Einstein frame)

$$T_{(q_{D1},q_{F1})} = \frac{1}{2\pi\alpha'}\sqrt{e^{-\phi(0)}q^2_{D1} + e^{\phi(0)}q^2_{F1}}. \tag{6.122}$$

Then the proportionality factor reads

$$\kappa = \kappa(q^{\mathcal{D}}_{F1},\, q^{\mathcal{D}}_{D1}) \tag{6.123a}$$

$$= \frac{T^2_{\left(4\sqrt{\overline{q_{D1}}q^{(0)}_{D1}},\, q^{\mathcal{D}}_{F1}\right)} - T^2_{\left(0,\, q^{\mathcal{D}}_{F1}\right)}}{\left(\sqrt{\sigma^2\left(q^{\mathcal{D}}_{D1}\right) + T^2_{\left(4\sqrt{\overline{q_{D1}}q^{(0)}_{D1}},\, q^{\mathcal{D}}_{F1}\right)}} - T_{\left(0,\, q^{\mathcal{D}}_{F1}\right)}\right)^2 - \sigma^2\left(q^{\mathcal{D}}_{D1}\right)}$$

$$\sigma(q^{\mathcal{D}}_{D1}) = \frac{T_{\left(4q^{(0)}_{D1},0\right)}}{T_{\left(0,\, q^{\mathcal{D}}_{F1}\right)}}T_{\left(q^{\mathcal{D}}_{D1},0\right)} \tag{6.123b}$$

(6.123) and (6.64) are transformed into each other via an S-duality transformation S: $(q_{D1} \leftrightarrow q_{F1})$ and $S : e^{\phi} \leftrightarrow e^{-\phi}$. Since we treat the D1/D5 and F1/F5 cases separately in this chapter, we do not distinguish the two κs here.

To avoid clutter we have employed $q^{(0)}_{D1} = \frac{1}{2}(2\overline{q_{D1}} - q^{\mathcal{D}}_{D1})$. The solution (6.121) embodies a natural cutoff for the defect's D1 charge, $|q^{\mathcal{D}}_{D1}| < 2\overline{q_{D1}}$, since otherwise the solution is no longer $\frac{1}{2}$-BPS. We could have guessed this threshold, because it is precisely where $2q^{(0)}_{D1}$ vanishes. Note that $\kappa > 0$ and that due to (6.121d) $\mathrm{sgn}(q^{\mathcal{D}}_{D1}) = \mathrm{sgn}(\psi_\xi)$. We go on to discuss two interesting limits.

Pure D1 Defect, $q^{\mathcal{D}}_{F1} \to 0$

When there is no F1 charge on the defect it is pushed to the boundary

$$\sinh \psi_\xi \to \operatorname{sgn} q^{\mathcal{D}}_{D1} \times \infty, \tag{6.124}$$

where it merges with the CFT. The triple in (6.121a)-(6.121c) assumes the shape of the vacuum expressions (6.105),

$$q^{\mathcal{D}}_{D1} > 0: \qquad \nu = \frac{1}{2}\sqrt{q_{D5}\, q^{(0)}_{D1}}, \tag{6.125a}$$

$$\alpha = 2e^{-\phi(0)}, \tag{6.125b}$$

$$\eta = 2e^{-\phi(0)} \frac{q^{(0)}_{D1}}{q_{D5}}, \tag{6.125c}$$

$$q^{\mathcal{D}}_{D1} < 0: \qquad \nu = \frac{1}{2}\sqrt{q_{D5}\, |q^{(\infty)}_{D1}|}, \tag{6.125d}$$

$$\alpha = 2e^{-\phi(\infty)}, \tag{6.125e}$$

$$\eta = 2e^{-\phi(\infty)} \frac{|q^{\infty}_{D1}|}{q_{D5}}, \tag{6.125f}$$

featuring the D1 charge of only one asymptotic region. The dilaton at $z \to \infty$ appears through virtue of (6.118). It cannot truly be the vacuum however, because the D1 charge differs at both asymptotic regions,

$$q^{\mathcal{D}}_{D1} > 0: \qquad q^{(0)}_{D1} = q^{bare}_{D1}, \qquad |q^{(\infty)}_{D1}| = q^{bare}_{D1} + q^{\mathcal{D}}_{D1}, \tag{6.126a}$$

$$q^{\mathcal{D}}_{D1} < 0: \qquad |q^{(\infty)}_{D1}| = q^{bare}_{D1}, \qquad q^{(0)}_{D1} = q^{bare}_{D1} + |q^{\mathcal{D}}_{D1}|, \tag{6.126b}$$

leading to disctinct central charges at both sides. Hence there is still an interface present. Obviously, reducing $q^{\mathcal{D}}_{D1} = 0$ leads exactly to the vacuum expressions (6.41).

Pure F1 Defect, $q^{\mathcal{D}}_{D1} \to 0$

The solution (6.121) confirms that a non-vanishing defect D1 charge $q^{\mathcal{D}}_{D1}$ stabilizes the defect at some non-trivial AdS_2 sheet $\psi_\xi \neq 0$. Let us now restrict to the AdS_2 sheet of smallest size

$$\sinh \psi_\xi = 0 \quad \Leftrightarrow \quad \xi = 1, \tag{6.127}$$

or in other words a pure F1 defect, $q^{\mathcal{D}}_{D1} = 0$. In this case we have $\sigma(0) = 0$ and the D1 charges coincide at both asymptotic regions so

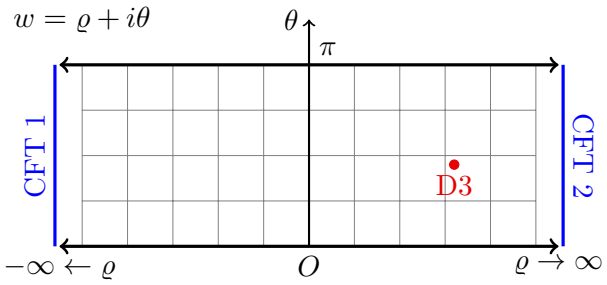

Figure 19: In contrast to the onebrane defect of the previous section, the D3 brane defect is located in the interior of Σ at $w = \psi_R + \Theta$, with $R = e^{\psi_R}$. Hence the defect is no longer located at the poles of the S^3, but wraps an S^2 at some constant value Θ.

that we drop the superscripts, $q_{D1} \equiv q_{D1}^{(0)} = -q_{D1}^{(\infty)} = \overline{q_{D1}}$. The solution (6.121) then reduces to

$$\nu = \frac{1}{2}\sqrt{\frac{q_{D5}\, q_{D1}}{\kappa_0}}, \tag{6.128a}$$

$$\alpha = 2\sqrt{\kappa_0} e^{-\phi(0)}, \tag{6.128b}$$

$$\eta = \frac{2}{\sqrt{\kappa_0}} \frac{q_{D1}}{q_{D5}} e^{-\phi(0)}, \tag{6.128c}$$

$$c = \frac{q_{F1}^{\mathcal{D}}}{q_{D5}}, \tag{6.128d}$$

where the proportionality factor reduces considerably,

$$\kappa_0 \equiv \kappa(q_{F1}^{\mathcal{D}}, 0) = \frac{T_{(4q_{D1}^{(0)}, q_{F1}^{\mathcal{D}})} + T_{(0, q_{F1}^{\mathcal{D}})}}{T_{(4q_{D1}^{(0)}, q_{F1}^{\mathcal{D}})} - T_{(0, q_{F1}^{\mathcal{D}})}}. \tag{6.129}$$

Lastly, we can perform the limit where the defect vanishes, $q_{F1}^{\mathcal{D}} \propto c \to 0$ leading to $\kappa_0 \to 1$ and therefore the triple (α, η, ν) reduces to the vacuum expressions (6.105).

6.4.4 *D3 Interface (IR)*

The second kind of defect that we want to discuss is that of a D3 brane inside the D1/D5 system. We will only motivate it through D3 brane charge, (6.11), which is induced by monodromies of C_K. As is evident from (6.5c) the monodromy necessarily stems from $\tilde{u}$, since this building block appears in no other charge or field. If we denote by $w = R\, e^{i\Theta}$ the locus of a stack of D3 branes on Σ, we obtain monodromies by additions $\delta U \propto \log(z - w)$. This is depicted in strip coordinates in Figure 19.

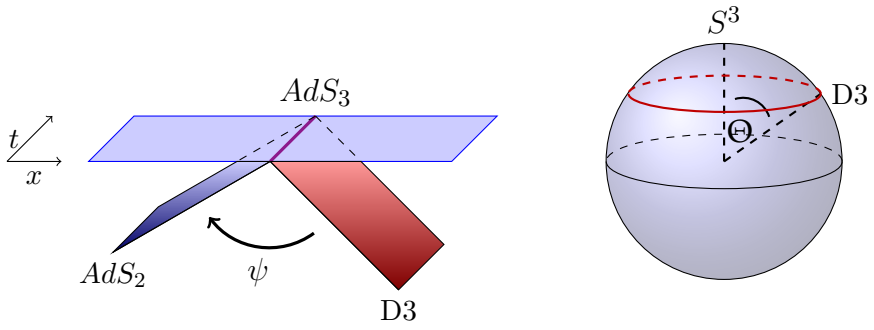

Figure 20: In coordinates $z = \exp(\psi + i\theta)$ AdS_3 is foliated by AdS_2 sheets shaded in dark blue and labelled by ψ. A D3 brane, shaded in red, is embedded into $AdS_3 \times S^3$ at $w = \exp(\psi_R + i\Theta)$, i.e. it wraps an S^2 on the S^3. The boundary of AdS_3, shaded in light blue, harbors the CFT and its intersection with the brane is the wordline of the field theory defect, colored in violet.

In order to respect point I in Section 6.2, i.e. $u(\partial\Sigma) = 0$, we employ the method of images and induce a mirror charge at $\bar{w}$ in the lower half plane. It can be readily checked that the modification

$$\delta U^{D3} = -\frac{q^{\mathcal{D}}_{D3}}{2} \log\left(\frac{z/w - 1}{z/\bar{w} - 1}\right), \tag{6.130}$$

$$\delta u^{D3} = -\frac{q^{\mathcal{D}}_{D3}}{2} \log\left|\frac{z - w}{z - \bar{w}}\right|^2, \tag{6.131}$$

$$\delta \tilde{u}^{D3} = i\frac{q^{\mathcal{D}}_{D3}}{2} \log\left[\left(\frac{\bar{w}}{w}\right)^2 \frac{(z - w)(\bar{z} - w)}{(z - \bar{w})(\bar{z} - \bar{w})}\right] \tag{6.132}$$

produces

$$Q^{\mathcal{D}}_{D3} = \pi\, q^{\mathcal{D}}_{D3}, \qquad q^{\mathcal{D}}_{D3} = \frac{(2\pi)^4 \alpha'^2}{\pi} N_3 \tag{6.133}$$

via (6.11). The second equation introduces the integer-valued D3-brane charge N_3. Since w lies on the upper half plane, Σ, we have $\Theta \in (0, \pi)$. Then the constraint $a\,u - b^2 \geq 0$ enforces positivity of $q^{\mathcal{D}}_{D3}$. The geometry is depicted in Figure 20 in coordinates $z = \exp(\psi + i\theta)$ with $R = \exp\psi_R$ and $\theta = \Theta$.

Straightforward computation of the asymptotic charges (6.96) gives

$$q_{D5} = \frac{\alpha\nu}{\beta}, \qquad q_{D5}^{(\infty)} = -\frac{\alpha\nu}{\beta}, \tag{6.134a}$$

$$q_{D1}^{(0)} = \frac{\nu}{\beta}\left(\eta + \frac{q_{D3}^{\mathcal{D}}}{R}\sin\Theta\right), \qquad q_{D1}^{(\infty)} = -\frac{\nu}{\beta}\left(\eta + q_{D3}^{\mathcal{D}} R\sin\Theta\right), \tag{6.134b}$$

$$q_{F1}^{(0)} = 0, \qquad q_{F1}^{(\infty)} = -q_{D3}^{\mathcal{D}}\Theta\frac{\nu\alpha}{\beta} = q_{D3}^{\mathcal{D}}\Theta\, q_{D5}^{(\infty)}, \tag{6.134c}$$

while q_{F5} still vanishes at both asymptotic regions. Again, the defect carries D1 and F1 charge,

$$q_{F1}^{\mathcal{D}} \equiv -q_{F1}^{(0)} - q_{F1}^{(\infty)} = q_{D3}^{\mathcal{D}}\Theta\, q_{D5}, \tag{6.135a}$$

$$q_{D1}^{\mathcal{D}} \equiv -q_{D1}^{(0)} - q_{D1}^{(\infty)} = q_{D3}^{\mathcal{D}}\frac{\nu}{\beta}\left(R - \frac{1}{R}\right)\sin\Theta. \tag{6.135b}$$

The asymptotic values of the fields (6.91) are

$$e^{-2\phi(0)} = \frac{\beta^2\alpha}{\eta + q_{D3}^{\mathcal{D}} R^{-1}\sin\Theta} = \frac{1}{\beta^2}\frac{q_{D5}}{q_{D1}^{(0)}}, \tag{6.136a}$$

$$e^{-2\phi(\infty)} = \frac{\beta^2\alpha}{\eta + q_{D3}^{\mathcal{D}} R\sin\Theta} = \frac{1}{\beta^2}\frac{q_{D5}^{(\infty)}}{q_{D1}^{(\infty)}} \tag{6.136b}$$

$$C_K(0) = 0, \tag{6.136c}$$

$$C_K(\infty) = -q_{D3}^{\mathcal{D}}\Theta = -\frac{q_{F1}^{\mathcal{D}}}{q_{D5}}, \tag{6.136d}$$

while the axion χ still vanishes at both regions. As before the jump in the dilaton is not independent, cf. (6.118).

Let us define an effective F1 charge

$$q_{F1}^{\Theta} \equiv q_{F1}^{\mathcal{D}}\frac{\sin\Theta}{\Theta} \tag{6.137}$$

and use it to rewrite the D1 charges in (6.134),

$$q_{D1}^{(0)} = \frac{\nu\eta}{\beta} + \frac{1}{\alpha R}q_{F1}^{\Theta}, \qquad q_{D1}^{(\infty)} = -\frac{\nu\eta}{\beta} - \frac{R}{\alpha}q_{F1}^{\Theta}. \tag{6.138}$$

Their linear combinations are

$$q_{D1}^{\mathcal{D}} = |q_{D1}^{(\infty)}| - q_{D1}^{(0)} = \frac{q_{F1}^{\Theta}}{\alpha}2\sinh\psi_R, \tag{6.139a}$$

$$\overline{q_{D1}} \equiv \frac{|q_{D1}^{(\infty)}| + q_{D1}^{(0)}}{2} = \frac{\nu\eta}{\beta} + \frac{q_{F1}^{\Theta}}{\alpha}\cosh\psi_R \equiv \kappa^{(\Theta)}\frac{\nu\eta}{\beta}. \tag{6.139b}$$

In the second line we have again quantified the difference to the vacuum D1 charge (6.102b) via $\kappa^{(\Theta)}$. Evidently, the D1 charges (6.138) and their linear combinations (6.139) look exactly like their counterparts (6.119) and (6.120), respectively, with the replacements $q^{\mathcal{D}}_{F1} \to q^{\Theta}_{F1}$ and $\xi \to R$ ($\psi_\xi \to \psi_R$). As the reader might have observed already the other relevant expressions, namely the D5 charge, (6.134a), and the dilaton in (6.136a) assume exactly the same form as their counterparts for the onebrane defect (6.115a) and (6.117). Therefore the result (6.121) of the previous section carries over with the adjustments $q^{\mathcal{D}}_{F1} \to q^{\Theta}_{F1}$, $\psi_\xi \to \psi_R$,

$$\nu = \frac{1}{2}\sqrt{\frac{q_{D5}\,\overline{q_{D1}}}{\kappa^{(\Theta)}}}, \tag{6.140a}$$

$$\alpha = 2e^{-\phi(0)}\sqrt{\kappa^{(\Theta)}\,\frac{2\overline{q_{D1}} - q^{\mathcal{D}}_{D1}}{2\overline{q_{D1}}}} \tag{6.140b}$$

$$\eta = 2\sqrt{\frac{1}{\kappa^{(\Theta)}}\,\frac{\overline{q_{D1}}\,(2\overline{q_{D1}} - q^{\mathcal{D}}_{D1})}{2q^2_{D5}}}\,e^{-\phi(0)}, \tag{6.140c}$$

$$\sinh\psi_R = e^{-\phi(0)}\sqrt{\kappa^{(\Theta)}\,\frac{2\overline{q_{D1}} - q^{\mathcal{D}}_{D1}}{2\overline{q_{D1}}}}\,\frac{q^{\mathcal{D}}_{D1}}{q^{\Theta}_{F1}}, \tag{6.140d}$$

$$\Theta = \frac{1}{q_{D5}}\frac{q^{\mathcal{D}}_{F1}}{q^{\mathcal{D}}_{D3}}. \tag{6.140e}$$

(6.141) and (6.80) are transformed into each other via an S-duality transformation S: $(q_{D1} \leftrightarrow q_{F1})$ and $S : e^{\phi} \leftrightarrow e^{-\phi}$. Since we treat the D1/D5 and F1/F5 cases separately in this chapter, we do not distinguish the two $\kappa^{(\Theta)}$s here.

The proportionality factor is also the same as before, (6.123), again with the replacement $q^{\mathcal{D}}_{F1} \to q^{\Theta}_{F1}$,

$$\begin{aligned}\kappa^{(\Theta)} &= \kappa(q^{\Theta}_{F1},\, q^{\mathcal{D}}_{D1}) \qquad\qquad (6.141a)\\ &= \frac{T^2_{\left(4\sqrt{\overline{q_{D1}}q^{(0)}_{D1}},\,q^{\Theta}_{F1}\right)} - T^2_{\left(0,\,q^{\Theta}_{F1}\right)}}{\left(\sqrt{\sigma^2_{\Theta}\left(q^{\mathcal{D}}_{D1}\right) + T^2_{\left(4\sqrt{\overline{q_{D1}}q^{(0)}_{D1}},\,q^{\Theta}_{F1}\right)}} - T_{\left(0,\,q^{\Theta}_{F1}\right)}\right)^2 - \sigma^2_{\Theta}\left(q^{\mathcal{D}}_{D1}\right)}\end{aligned}$$

$$\sigma_{\Theta}(q^{\mathcal{D}}_{D1}) = \frac{T_{\left(4q^{(0)}_{D1},0\right)}}{T_{\left(0,\,q^{\Theta}_{F1}\right)}}T_{\left(q^{\mathcal{D}}_{D1},0\right)}, \tag{6.141b}$$

Clearly $\kappa^{(\Theta=0)} = \kappa$. We remark that we still have $\kappa^{(\Theta)} > 0$. Similar to before (6.140d) implies $\mathrm{sgn}(q^{\mathcal{D}}_{D1}) = \mathrm{sgn}(\psi_R)$. Notice that we have not bothered to instate (6.140e) into the remaining entries of the solution. The system is described by three defect charges, $q^{\mathcal{D}}_{D1}$, $q^{\mathcal{D}}_{F1}$, $q^{\mathcal{D}}_{D3}$. Instead of using $q^{\mathcal{D}}_{D3}$ we can just as well use the ratio of charges $q^{\mathcal{D}}_{F1}/q^{\mathcal{D}}_{D3}$ or just as well Θ, which is the most convenient variable for our purposes.

Note that even though there are $q^{\mathcal{D}}_{F1}$ units of F1 strings attached to the defect, in the solution this charge appears only in the diminished

form $q_{F1}^{\Theta} = q_{F1}^{\mathcal{D}} \frac{\sin\Theta}{\Theta}$.Therefore there is a trade off between the effect of the F1 strings on the geometry and moving the defect away from the boundary of Σ into its interior, as can be concluded from comparison with results of the previous section, (6.121) and (6.123).

The most important result is (6.140e), which conveys that the amount of F1 strings per D3 brane determines the value of the polar angle of the defect on the S^3. We will come back to this important point in the next section when we discuss in detail the RG flow. In contrast the defect's D1 charge has no influence on the polar angle.

In the limit where the D3 charge outweighs the F1 charge of the defect, the threebrane defect approaches the boundary of Σ, i.e. $\Theta \to 0$, or equivalently $q_{F1}^{\Theta} \to q_{F1}^{\mathcal{D}}$. This implies that all expressions in (6.140) and (6.141) reduce to those of the onebrane defect, (6.128) and (6.123), respectively. Similarly to before we can now study defects with only one type of one brane charge.

Pure D1 Defect, $q_{F1}^{\mathcal{D}} \to 0$

Since the threebrane defect cares only about the effective F1 charge (6.137) we have two options to remove the effect of F1 charge. The first is as before $q_{F1}^{\mathcal{D}} \to 0$. The second is when $\Theta = \pi$, which happens at a large value of F1 charge $q_{F1}^{\mathcal{D}} = \pi q_{D5} q_{D3}^{\mathcal{D}}$. Of course, the defect is again pushed to the boundary of AdS_3, $\sinh\psi_R \to \operatorname{sgn} q_{D1}^{\mathcal{D}} \times \infty$ and the triple (α, η, ν) behaves in the same way as before, (6.126).

Pure F1 Defect, $q_{D1}^{\mathcal{D}} \to 0$

As for the onebrane defect of the previous section the most notable impact of the defect's D1 charge is to stabilize the brane at some AdS_2 with non-minimal volume, $\psi_R \neq 0$, as can be seen in (6.140d). Let us now inspect the case of smallest size $\psi_R = 0$, i.e. a D3 brane with $q_{F1}^{\mathcal{D}}$ F1 strings attached and no dissolved D1 strings, $q_{D1}^{\mathcal{D}} = 0$. In this case we have $\sigma_\Theta(0) = 0$ and the D1 charges coincide at both asymptotic regions so that we drop the superscripts, $q_{D1} \equiv q_{D1}^{(0)} = -q_{D1}^{(\infty)} = \overline{q_{D1}}$. The solution (6.140) then reduces to

$$\nu = \frac{1}{2}\sqrt{\frac{q_{D5}\, q_{D1}}{\kappa_0^{(\Theta)}}}, \tag{6.142a}$$

$$\alpha = 2\sqrt{\kappa_0^{(\Theta)}}\, e^{-\phi(0)}, \tag{6.142b}$$

$$\eta = \frac{2}{\sqrt{\kappa_0^{(\Theta)}}} \frac{q_{D1}}{q_{D5}} e^{-\phi(0)} \tag{6.142c}$$

$$\Theta = \frac{1}{q_{D5}} \frac{q_{F1}^{\mathcal{D}}}{q_{D3}^{\mathcal{D}}} \tag{6.142d}$$

where we have a considerable simplification,

$$\kappa_0^{(\Theta)} \equiv \kappa(q_{F1}^{\Theta}, 0) = \frac{T_{(4q_{D1}^{(0)}, q_{F1}^{\Theta})} + T_{(0, q_{F1}^{\Theta})}}{T_{(4q_{D1}^{(0)}, q_{F1}^{\Theta})} - T_{(0, q_{F1}^{\Theta})}}. \tag{6.143}$$

Lastly, we may turn the defect's effective F1 charge off, $q_{F1}^{\Theta} = 0$. Again we have two ways of doing so, either through $q_{F1}^{\mathcal{D}} = 0$ or $\Theta = \pi$. Both options remove the defect leading to a vacuum solution, (6.105). Indeed, $q_{F1}^{\mathcal{D}} = 0$ implies through (6.135) that $q_{D3}^{\mathcal{D}} = 0$, which in turn removes δU^{D3}, cf. (6.130). Moreover, δU^{D3} vanishes identically for $\Theta = \pi$.

6.4.5 *Solution Matching: the RG flow*

So far we have only described asymptotic $\mathrm{AdS}_3 \times S^3 \times T^4$ half BPS supergravity solutions, which harbor an extra D1/F1 or D3 defect and only alluded to in the respective section titles to its role in an RG flow. In this section we will manifestly interpret these solutions as endpoints of an RG flow, D1/F1→D3.

On the field theory side we describe a boundary RG flow implying that the ambient CFTs remain unchanged. They are characterized by the gauge rank $N_5 \propto q_{D5}$, the central charge $\mathsf{c} \propto q_{D5} q_{D1}$ and the dilaton, all of which remain unaffected by the boundary RG flow. Hence these charges and fields should remain unchanged under the flow,

$$Q_{brane}^{\mathrm{IR}} \stackrel{!}{=} Q_{brane}^{\mathrm{UV}}, \qquad \phi^{\mathrm{IR}} \stackrel{!}{=} \phi^{\mathrm{UV}}, \tag{6.144}$$

where these expressions refer to the values at either asymptotic region. The UV solution is the one-brane defect and the IR corresponds to the three brane defect discussed in Section 6.4.3 and Section 6.4.4 respectively. For the onebrane charges we will sometimes equivalently phrase this matching in terms of the arithmetic means (6.120b), (6.139b) and the defect charges (6.116), (6.135), which, due to charge conservation are identified as well. This matching is necessary in order to relate the individual parameters in the onebrane solution (6.121) to those in the threebrane solution (6.140).

We start with the F1 charge. Identifying (6.116a) and (6.135a) tells us that

$$q_{D3}^{\mathcal{D}} \Theta = c. \tag{6.145}$$

Using this it is readily checked that for small Θ the threebrane modification (6.130) reduces to the onebrane modification (6.113), $\delta U^{D3} \simeq \delta U^{F1}$ if we fix $\xi = R$ meaning that the defect remains on the same AdS_2 sheet along the flow. This is valid only for small Θ or when the defect carries no extra D1 charge. Recall that the onebrane and the threebrane defect both occupy the AdS_2 sheet of smallest size, $x = 1$ ($\psi_\xi = 0$) and $R = 1$ ($\psi_R = 0$) when $q_{D1}^{\mathcal{D}} = 0$. On the other hand,

when the defect does carry extra D1 charge, the defect stabilizes on a non-minimal AdS_2 slice, $x \neq 1$. Indeed, by comparison of (6.121d) and (6.140d) we conclude that the defect moves inside of AdS_3,

$$\sinh\psi_R = \sqrt{\frac{\kappa^{(\Theta)}}{\kappa}}\,\frac{\Theta}{\sin\Theta}\,\sinh\psi_\xi. \tag{6.146}$$

Given the expressions (6.123) and (6.141) we can bound

$$1 \leq \frac{\kappa}{\kappa^{(\Theta)}} \leq \left(\frac{\Theta}{\sin\Theta}\right)^2, \tag{6.147}$$

which saturates for $\Theta = 0$. Plugged into (6.146) this implies that the defect is pushed towards the boundary of AdS_3, $|\psi_R| \geq |\psi_\xi|$, along the RG flow when $q^{\mathcal{D}}_{D1} \neq 0$. Their sign is that of the defect's D1 charge, $\mathrm{sgn}(q^{\mathcal{D}}_{D1}) = \mathrm{sgn}(\psi_\xi) = \mathrm{sgn}(\psi_R)$.

The next step is to express the triple $(\alpha^{\mathrm{IR}}, \eta^{\mathrm{IR}}, \nu^{\mathrm{IR}})$ through their analogs in the onebrane defect through comparison of (6.121) and (6.140),

$$\nu^{\mathrm{IR}} = \sqrt{\frac{\kappa}{\kappa^{(\Theta)}}}\,\nu^{\mathrm{UV}}, \tag{6.148a}$$

$$\alpha^{\mathrm{IR}} = \sqrt{\frac{\kappa^{(\Theta)}}{\kappa}}\,\alpha^{\mathrm{UV}}, \tag{6.148b}$$

$$\eta^{\mathrm{IR}} = \sqrt{\frac{\kappa}{\kappa^{(\Theta)}}}\,\eta^{\mathrm{UV}}. \tag{6.148c}$$

Recall from our probe brane discussion that the angle Θ indicates the endpoint of the flow and (6.140e) now encapsules how it depends on the configuration of the defect in the UV,

$$\Theta = \frac{1}{q^{(0)}_{D5}}\frac{q^{\mathcal{D},UV}_{F1}}{q^{\mathcal{D},IR}_{D3}} = \frac{\pi}{N_5}\frac{p}{N_3}. \tag{6.149}$$

We have employed the integer valued charges given by (6.133) and (6.107) and returned to the notation of the last chapter for the defect charge $q^{\mathcal{D},\mathrm{UV}}_{F1} = p$. In order to compare with (5.18) first note that in Chapter 5 we restricted to a single D3 brane, $N_3 = 1$. Furthermore, by S-duality the D5 branes turn into F5 branes, and the number of F5 branes is identified with the level of the $\hat{\mathfrak{su}}(2)_{\mathsf{k}}$ WZW model, $N_5 = \mathsf{k}$. Together we obtain

$$\Theta = \frac{\pi p}{\mathsf{k}} = \theta_p, \tag{6.150}$$

exactly as desired. This confirms that the supergravity solutions studied in this chapter indeed correspond to the flows worked out in Chapter 5.

When Θ is small we have observed that the D3 solution, (6.140), is rather a onebrane defect, (6.121). In the RG flow picture this means that is is not energetically favorable for the defect to puff up into a D3-brane. In other words the UV onebrane defect does not carry enough charge to be stabilized at a macroscopically visible two-sphere on the S^3. There is basically no RG flow.

Lastly, we explore the other extreme where the D3 brane reaches the south pole, $\Theta = \pi$, which happens when $p/N_3 = \pi N_5$. In this limit the defect have the same effect on the geometry as the background. We can therefore not study this case with probe branes, since they do not backreact. In our supergravity setup this extra backreaction is accounted for. Now, for simplicity let us consider the case $q^{\mathcal{D}}_{D1} = 0$; it will be same reagardless of the location inside AdS_3, what matters is the behavior on S^3. We observed before that the defect vanishes in this limit. Crucially, this happens for a non-trivial number of fundamental strings p, therefore the interface does not vanish "on its own accord" – it gets screened! If we recall our exposition in Section 4.2, we see that this is exactly what happens in the original Kondo flow! This is not surprising in the S-dual frame, where the model on the S^3 is realized as an SU(2) WZW model. The importance of the S-dual motivates to repeat the entire analysis in the F1/F5 case.

This ends our general exposition of the D1/D5 case. A reduced version of our D1/D5 findings will appear in an upcoming publication [112].

SUMMARY

This chapter was by far the longest one, which is due to the fact that, even though supergravity is a beautiful concept, it is computationally involved. Our conclusion will be surprisingly short. "All" that happened here storywise, is that we computed supergravity solutions for the UV interface, the F1/D1 interface, and the IR, the D3 interface. As the reader may have noticed this was quite the challenge even though the general solution was at hand through [79]. Our supergravity solutions are a necessary stepping stone for future work, since any supergravity dual of the *entire* flow has to terminate at the solutions presented here. Moreover, most quantities of interest in the CFT require the details encoded in gravitational backreaction, such as correlators or reflection and transmission coefficients in the presence of the interfaces [205]. An explicit demonstration of the superiority of the supergravity solutions over the probe branes is given in the next chapter, where we compute boundary entropies at the fixed points. The supergravity expression contains more information, which drops out in the probe brane limit.

7

INTERFACE ENTROPIES

We dedicate a short chapter to the interface entropy S_{imp}, which is the logarithm of the so-called g-factor. We give its formal definition momentarily. Physically, it is the non-extensive – that is system size independent – contribution of the impurity to the full entropy of the system. Much as the central charge of the CFT gives a (rough) estimate of the degrees of freedom in the CFT, the g-factor counts boundary or interface degrees of freedom. Consider the original Kondo model for instance. At high energies, when the system is modelled by free electrons and a decoupled impurity, the g-factor simply counts the spin states of the impurity. Indeed, it is the logarithm of the dimension of impurity's representation [7]. At low energies the S_{imp} depends on the kind of screening. In the case of exact screening, it vanishes confirming that the impurity has vanished. In the case of overscreening a S_{imp} is non-vanishing, providing evidence of a non-trivial IR fixed point. In all cases it was shown in [7] that the number of degrees of freedom decreases along the RG-flow, i.e.

$$\lim_{T\to\infty} S_{\text{imp}} > \lim_{T\to 0} S_{\text{imp}} \tag{7.1}$$

This statement was generalized to all boundary RG flows in $(1+1)$-dimensional CFT and is known as the g-*theorem* [131].

In this chapter we compute the g-factor using the backreacted supergravity solutions and thereafter take the probe brane limit to elucidate the importance of backreaction. Moreover, we confirm the validity of the g-theorem for our flows, thus legitimating their existence fully. Parts of this chapter will appear in the upcoming publication [112].

Let us define the interface entropy using the folding trick through its its boundary analog. The *boundary entropy*, or g-*factor*, has several equivalent definitions. The original definition is as follows [7]. Place the CFT on a cylinder of radius β and length ℓ, with boundary states $\|\mathcal{A}\rangle\rangle$ and $\|\mathcal{B}\rangle\rangle$ at either end. In the limit $\ell \gg \beta$ of a unitary BCFT, the partition function has an expansion

$$\log Z = \frac{\pi \mathsf{c}}{6}\frac{\ell}{\beta} + (s_{\mathcal{A}} + s_{\mathcal{B}}) + O(\beta/\ell) \tag{7.2}$$

where $s_{\mathcal{A}}$ and $s_{\mathcal{B}}$ depend only on the choice of $\|\mathcal{A}\rangle\rangle$ and $\|\mathcal{B}\rangle\rangle$, respectively. The g-factor corresponding to boundary $\|\mathcal{A}\rangle\rangle$ is then $g_{\mathcal{A}} = e^{s_{\mathcal{A}}}$. Now comes a trick. We can write the same condition in terms of a single boundary state $\|\mathcal{A}\rangle\rangle$ by performing a conformal transformation to the

annulus, and then plugging the hole to produce a disk. In this case, the disk partition function becomes simply[1]

$$Z = g_{\mathcal{A}}\,. \tag{7.3}$$

It was proved in [63] that the g-factor for a boundary conformal field theory is encoded in the entanglement entropy as follows. Let the entangling region be an interval of length ζ_0 starting at the boundary. Then

$$S_{\zeta_0} = \frac{\mathsf{c}}{6}\log\frac{\zeta_0}{\epsilon} + s_{\mathcal{A}} + O(\epsilon)\,, \tag{7.4}$$

with central charge c, UV-cutoff ϵ, and conformal boundary condition $\mathcal{A}$. We can think of our interface theory as an unfolded BCFT with central charge $\mathsf{c} = \mathsf{c}^{(0)} + \mathsf{c}^{(\infty)}$. Since the fold is the locus of the interface, the entanglement interval reaches symmetrically into both sides of the interface.

We begin by computing the g-factors in Section 7.1 using our backreacted supergravity solutions of the previous chapter. First we present the F1/NS5 case and thereafter we S-dualize into the D1/D5 frame. In the latter we take the probe brane limit. Crucially, this will confirm that the supergravity solution contains more information thatn the probe brane picture. We conclude that backreaction plays an important role in the evaluation of the interface degrees of freedom.

7.1 SUPERGRAVITY COMPUTATION OF THE INTERFACE ENTROPY

This section is dedicated to the g-theorem in the backreacted supergravity solutions. First we explain how to deduce the g-factor from entanglement entropy in a holographic CFT in Section 7.1.1. Secondly, we apply this technique to the supergravity solutions of the previous chapter and discuss the g-theorem in Section 7.1.2.

7.1.1 *Interface Entropy in Asymptotically* $\mathrm{AdS}_3 \times S^3$ *Solutions*

A detailed account of how to compute boundary entropies for the solutions of [79] can be found in [78]. Here, we recapitulate the relevant ingredients.

In the beginning of this chapter we already concluded that we can extract the boundary entropy from the entanglement entropy if the entangling interval ends at the boundary. Moreover, using the doubling trick this procedure is also applicable to interfaces.

1 Technically speaking, Z can be multiplied by an arbitrary constant by including a conformally invariant counterterm. This can be eliminated by comparing $Z^2_{D_2}$ to Z_{S^2}, which is independent of renormalization scheme.

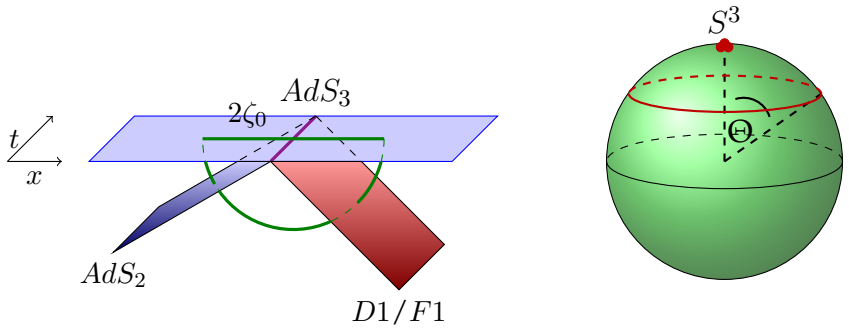

Figure 21: Entanglement minimal surface (depicted in green) wraps all of S^3 (and T^4) and is a geodesic inside AdS_3 anchored at a CFT space interval of size $2\zeta_0$

We are left with the task of computing the entanglement entropy in gravity. Fortunately, a very elegant answer to this question has been given by Ryu and Takayanagi (RT) when dealing with a holographic CFT[2]. They proposed [213] that the entanglement entropy for some entanglement region A in a d-dimensional CFT is computed as minimal area surface γ_A reaching into the bulk of AdS_{d+1} and anchored to A,

$$S_A = \frac{\mathrm{Area}(\gamma_A)}{4G_N}. \tag{7.5}$$

Newton's constant corresponds to the spacetime into which the minimal area surface is embedded. In our case this spacetime is ten-dimensional. Usually the minimal surface is codimension-2 in AdS_{d+1}. However, when dealing with product manifolds (which contain a copy of AdS_{d+1}) it is codimension-2 in the full manifold, i.e. in our case it is eight-dimensional.

Let us assign Poincaré patch coordinates (ζ, t) to a single AdS_2 sheet so that in the notation of (6.93) (with $r = e^{\psi}$)

$$ds^2_{\mathrm{AdS}_3} = \mathsf{L}^2\left(\frac{dr^2}{r^2} + \frac{\mu}{4}\frac{1}{r^2}\frac{d\zeta^2 - dt^2}{\zeta^2}\right). \tag{7.6}$$

This is valid at an asymptotic region ($r \to 0$) implying that this particular AdS_2 sheet approaches (one half of) the CFT spacetime and (ζ, t) may be identified with the CFT coordinates. We place one boundary of the entanglement interval at a distance ζ_0 from the defect locus ($\zeta = 0$). The entanglement interval extends an equal distance to the other side of the defect giving $A = 2\zeta_0$; see Figure 21.

At fixed time the minimal area surface pierces each AdS_2 sheet at the same position $z = z_0$. Otherwise the entangling interval would have no chance to lie symmetrically around the interface, which was one of our requirements for using the folding trick. Thus γ_A is a geodesic inside

2 Part iii contains a more detailed introduction to entanglement in gravity. Here we stick to a minimum in an effort to be self-contained.

of AdS_3 and wraps all of $S^2 \times T^4 \times \Sigma$. The pulled back metric has $ds^2_{AdS_2} = 0$ so that

$$S_A = \frac{1}{4G_N^{(10)}} \int_{S^2} d\Omega_2 \int_{T^4} d\Omega_4 \int_\Sigma \rho^2 \, f_2^2 \, f_3^4, \tag{7.7}$$

where $d\Omega_2$ and $d\Omega_4$ denote the volume elements of $S^2$and T^4, respectively, with unit radii. Recall that the metric functions depend only on the coordinates of Σ. Given the general form of the metric factors (6.2a)-(6.2d) we deduce

$$S_A = \frac{\mathrm{Vol}(S^2)}{4G_N^{(10)}} \int_\Sigma (a\,u - b^2) \left| \frac{\partial_z V}{B} \right|^2 . \tag{7.8}$$

This integral is divergent, as is appropiate for a boundary anchored geodesic in AdS_3. In coordinates $z = re^{i\theta}$ the cutoffs at $r \to 0$ and $r \to \infty$ are related to the UV cutoff ϵ in the CFT as follows

$$r_\infty = \frac{2\zeta_0}{\epsilon \sqrt{\mu^{(\infty)}}}, \qquad r_0^{-1} = \frac{2\zeta_0}{\epsilon \sqrt{\mu^{(0)}}}, \tag{7.9}$$

where the scale factors μ are given by (6.23) in the F1/F5 formalism and by (6.95) in the D1/D5 formalism. Note that the cutoffs are generally distinct for both asymptotic regions, which accounts for the fact that the CFTs on either side are not generally the same. This ends our recapitulation of [78].

7.1.2 *D1/F1 and D3 interface entropy*

In this section we compute the entanglement entropy via the formalism laid out in the previous section and from there we extract the boundary entropy for the D1/F1 and D3 defect according to (7.4). We perform the calculations in the F1/F5 case of Section 6.3 and thereafter we S-dualize to obtain the analogs in the D1/D5 frame. In fact the integrals are almost identical in the duality frames at hand.

It is convenient to define the abbreviation

$$q_{F1}^{bare} = 4\nu\sqrt{\alpha\eta} = \begin{cases} \frac{\overline{q_{F1}}}{\kappa}, & \text{UV}, \\ \frac{\overline{q_{F1}}}{\kappa^{(\Theta)}}, & \text{IR}, \end{cases} \tag{7.10}$$

which is motivated by (6.57b) and (6.78b). q_{F1}^{bare} would be the F1 charge, were it not for the modifications (6.44) and (6.71), as can be seen by recalling (6.40). Let us stress that by itself it is not a Page charge in the defect solutions and thus changes under the RG flow. Nevertheless it still contributes to the F1 charges, cf. (6.56) and (6.73). For us q_{F1}^{bare} is solely a book-keeping device.

Since $u = u_0 + \delta u$ the entanglement entropy splits into two pieces. The first is the contribution from the vacuum background into which the defects are embedded,

$$\begin{aligned}\mathcal{I}_0 =& \mathrm{Vol}(S^2) \int_\Sigma (a\, u_0 - b^2) \left|\frac{\partial_z V}{B}\right|^2 \\ =& 4\mathrm{Vol}(S^3)\, q_{F5}\, q_{F1}^{bare}\, \log \frac{r_\infty}{r_0}\end{aligned} \tag{7.11}$$

The second piece is determined by the defect deformations, (6.44) and (6.71), respectively,

$$\mathcal{I}_{\mathrm{UV,\,IR}} = \mathrm{Vol}(S^2) \int_\Sigma a\, \delta u^{D1,\,D3} \left|\frac{\partial_z V}{B}\right|^2 . \tag{7.12}$$

In evaluating (7.12) care has to be taken when approaching the defect loci. In polar coordinates, $z = re^{i\theta}$ they will produce a discontinuity for along $r = |\xi|$ or $r = R$, respectively. We find for the UV,

$$\begin{aligned}\mathcal{I}_{\mathrm{UV}} = 4\mathrm{Vol}(S^3)\, q_{F5} \Big[& - \left(q_{F1}^{(\infty)} + q_{F1}^{bare,\mathrm{UV}}\right) \log r_\infty \\ & + \left(q_{F1}^{(0)} - q_{F1}^{bare,\mathrm{UV}}\right) \log \frac{1}{r_0} \\ & + \overline{q_{F1}} - q_{F1}^{bare,\,\mathrm{UV}} - q_{F1}^{\mathcal{D}} \log |\xi| \Big],\end{aligned} \tag{7.13a}$$

and for the IR

$$\begin{aligned}\mathcal{I}_{\mathrm{IR}} = 4\mathrm{Vol}(S^3)\, q_{F5} \Big[& - \left(q_{F1}^{(\infty)} + q_{F1}^{bare,\mathrm{UV}}\right) \log r_\infty \\ & + \left(q_{F1}^{(0)} - q_{F1}^{bare,\mathrm{UV}}\right) \log \frac{1}{r_0} \\ & + \overline{q_{F1}} - q_{F1}^{bare,\,\mathrm{IR}} - q_{F1}^{\mathcal{D}} \log R \Big].\end{aligned} \tag{7.13b}$$

The divergent pieces contain the two summands of the asymptotic D1 charges (6.119), (6.138) and when combining the two integrals it is convenient to repackage them into the central charges via (6.100),

$$\begin{aligned}S_{2\zeta_0}^{\mathrm{UV,\,IR}} &= \frac{\mathcal{I}_0 + \mathcal{I}_{\mathrm{UV,\,IR}}}{4G_N^{(10)}} \\ &= \frac{\mathsf{c}^{(\infty)} + \mathsf{c}^{(0)}}{6} \log \frac{2\zeta_0}{\epsilon} + \log \mathsf{g}^{\mathrm{UV,\,IR}}.\end{aligned} \tag{7.14}$$

It is reassuring that the entanglement entropy assumes the desired form of a BCFT, cf. equation (7.4), with combined central charges. The sought after g-factors are

$$\log \mathsf{g}^{UV} = \frac{\mathsf{c}^{(\infty)} + \mathsf{c}^{(0)}}{12}\left(\log \kappa + 1 - \frac{1}{\kappa} - \frac{q^{\mathcal{D}}_{F1}}{\overline{q}_{F1}}\,\psi_\xi\right), \tag{7.15a}$$

$$\log \mathsf{g}^{IR} = \frac{\mathsf{c}^{(\infty)} + \mathsf{c}^{(0)}}{12}\left(\log \kappa^{(\Theta)} + 1 - \frac{1}{\kappa^{(\Theta)}} - \frac{q^{\mathcal{D}}_{F1}}{\overline{q}_{F1}}\,\psi_R\right), \tag{7.15b}$$

where we employed (7.10) and chose to express the loci of the defect through their Janus coordinate, $\log \xi = \psi_\xi$, $\log R = \psi_R$, which are to be found in (6.62d) and (6.79d), respectively. κ and $\kappa^{(\Theta)}$ are found in (6.64) and (6.80), respectively. If we first have $q^{\mathcal{D}}_{F1}$ vanish and subsequently remove $q^{\mathcal{D}}_{D1}$ we get $\kappa \to 1$ and $\kappa^{(\Theta)} \to 1$ as we concluded in the previous chapter. Then both g-factors vanish implying that there are no degrees of freedom on the interface. This is as it should since we have reduced the defect geometries to the vacuum, or, as we emphasized before, the trivial interface.

One crucial property of any boundary RG flow in a two dimensional CFT such as ours is a decreasing g-factor along the flow. This is the essence of the celebrated g-theorem. At last, we are now in a position to investigate this property by computing the difference in boundary entropies,

$$\log \frac{\mathsf{g}^{UV}}{\mathsf{g}^{IR}} = \frac{\mathsf{c}^{(\infty)} + \mathsf{c}^{(0)}}{12}\left(\log \frac{\kappa}{\kappa^{(\Theta)}} + \frac{1}{\kappa^{(\Theta)}} - \frac{1}{\kappa} + \frac{q^{\mathcal{D}}_{F1}}{\overline{q}_{F1}}\Big(\psi_R - \psi_\xi\Big)\right) \tag{7.16}$$

This expression has to be non-negative and the lower bound in (6.86) establishes this for all but the last term. It is also never negative. Indeed, through (6.85) we convinced ourselves that $|\psi_R| - |\psi_\xi| \geq 0$, which saturates either when both Janus coordinates vanish or when there is no flow $\Theta = 0$. Furthermore, recall from (6.62d) and (6.79d) that both Janus coordinates share the sign of $q^{\mathcal{D}}_{F1}$, which in turn provides $q^{\mathcal{D}}_{F1}\big(\psi_R - \psi_\xi\big) \geq 0$. Quot erat demonstrandum.

The non-negativity of (7.16) demonstrates that the g-factor decreases along the RG flow and fully legitimates the existence of our Kondo flows, even with strong backreaction!

Of course, (7.16) vanishes for $\Theta = 0$, since $\kappa^{(0)} = \kappa$ and $R = x$, simply because in that case the D3 defect reduces to the stack of D1 interfaces. More interestingly, and in tune with the original Kondo problem, for the case of critical screening, i.e. $\Theta = \theta_p = \pi$, we find that the g-factor, (7.15b), vanishes in the IR.

Boundary Entropy in D1/D5 System

Now we translate the our recent results into the D1/D5 frame via S-duality. It acts on the charges as [80]

$$S: \qquad \begin{pmatrix} q_{D1} \\ q_{F1} \end{pmatrix} \to \begin{pmatrix} 0 & 1 \\ -1 & 0 \end{pmatrix} \begin{pmatrix} q_{D1} \\ q_{F1} \end{pmatrix}, \tag{7.17}$$

$$\begin{pmatrix} q_{D5} \\ q_{F5} \end{pmatrix} \to \begin{pmatrix} 0 & 1 \\ -1 & 0 \end{pmatrix} \begin{pmatrix} q_{D5} \\ q_{F5} \end{pmatrix} \tag{7.18}$$

and does not alter q_{D3}. On the fields it acts as

$$S: \qquad C_K \to C_K, \qquad f_3^4 \to f_3^4, \qquad \tau \to -\frac{1}{\tau}, \tag{7.19}$$

where axion an dilaton have been combined in $\tau = \chi + ie^{-\phi}$. In our case the axion vanishes at the asymptotic regions and hence the last transformation flips the sign of the dilaton, $e^{\phi(0)} \to e^{-\phi(0)}$, as it should. Finding the g-factors in the S-dual picture is then a simple matter of applying the S-transformation to (7.15),

$$\log \mathsf{g}_S^{UV} = \frac{\mathsf{c}_S^{(\infty)} + \mathsf{c}_S^{(0)}}{12} \left(\log \kappa_S + 1 - \frac{1}{\kappa_S} - \frac{q_{D1}^{\mathcal{D}}}{q_{D1}} \psi_\xi^S \right), \tag{7.20a}$$

$$\log \mathsf{g}^{IR} = \frac{\mathsf{c}_S^{(\infty)} + \mathsf{c}_S^{(0)}}{12} \left(\log \kappa_S^{(\Theta)} + 1 - \frac{1}{\kappa_S^{(\Theta)}} - \frac{q_{D1}^{\mathcal{D}}}{q_{D1}} \psi_R^S \right), \tag{7.20b}$$

and their difference is

$$\log \frac{\mathsf{g}^{UV}}{\mathsf{g}^{IR}} = \frac{\mathsf{c}_S^{(\infty)} + \mathsf{c}_S^{(0)}}{12} \left(\log \frac{\kappa_S}{\kappa_S^{(\Theta)}} + \frac{1}{\kappa_S^{(\Theta)}} - \frac{1}{\kappa_S} + \frac{q_{D1}^{\mathcal{D}}}{q_{D1}} \left(\psi_R^S - \psi_\xi^S \right) \right) \tag{7.21}$$

Herein, the Janus coordinates are now those presented in D1/D5 duality frame, (6.121d) and (6.140d). The central charge c_S is given by (6.100) with the F1 and F5 charges turned off. Lastly, κ_S and $\kappa_S^{(\Theta)}$ are those given in (6.123) and (6.141).

Probe Brane Limit

We restrict to the D1/D5 frame, since the probe brane limit is taken simplest here. It amounts to having the dilaton shrink. Furthermore, in the probe brane flows we only considered the case where the defect carries no D1 charge (F1 charge before S-dualizing), $q_{D1}^{\mathcal{D}} = 0$, or equivalently $q_{D1}^{(0)} = -q_{D1}^{(\infty)} \equiv q_{D1}$. Hence the central charges (6.99) agree

on both asymptotic regions, $\mathsf{c}^{(0)} = \mathsf{c}^{(\infty)}$. We need only consider the simpler proportionality factors (6.129) and (6.143) in the present case.

The task is then to expand (7.20) for small dilaton $e^{\phi} \ll 1$,

$$\log \mathsf{g}^{UV} = \frac{Q_{D5} Q^{\mathcal{D}}_{F1}}{4\pi\kappa_{10}^2} e^{\phi} + \mathcal{O}(e^{2\phi}) = N_5\, p\, e^{\phi} + \mathcal{O}(e^{2\phi}), \tag{7.22a}$$

$$\log \mathsf{g}^{IR} = \frac{Q_{D5} Q^{\mathcal{D}}_{F1}}{4\pi\kappa_{10}^2} \frac{\sin\Theta}{\Theta} e^{\phi} + \mathcal{O}(e^{2\phi}) = N_5\, p\, \frac{\sin\Theta}{\Theta} e^{\phi} + \mathcal{O}(e^{2\phi}). \tag{7.22b}$$

We used the fact that the dilaton coincides on both regions, (6.118). It is clear that the probe brane expression carries less information than the full supergravity result. Thus we learn that crucial information on the interface degrees of freedom is encoded in gravitational backreaction!

Of course, the g-theorem is still satisfied

$$\log \frac{\mathsf{g}^{UV}}{\mathsf{g}^{IR}} = N_5\, p \left(1 - \frac{\sin\Theta}{\Theta}\right) e^{\phi} + \ldots, \tag{7.23}$$

unless there is no puffing up, but that is the case of no RG-flow.

This demonstrates that the probe brane limit does not account for all degrees of freedom captured on the interface.

7.2 A GLIMPSE AT THE FIELD THEORY

Our discussion focusses entirely on the gravity side and does not touch upon the other pillar of AdS/CFT: the field theory. This is simply due to the fact that the details are still under inspection at the writing of this text. Nevertheless we give a brief outline here.

We work with the gauge theory picture of the D1/D5 CFT, whose structure was laid out in Section 3.3.2. This is in contrast to the bulk of this thesis, where we worked with the F1/NS5 duality frame. We used conventional notation for the QFT as found in the literature. However, we want to highlight the SU(2) symmetry unbroken by the interface. Therefore, we need to rewrite the lagrangian in a form where all SU(2) symmetries are manifest, which to the author's knowledge has not appeared in the literature before. The desired symmetries are an $\mathrm{SU}(2)_- \times \mathrm{SU}(2)_+$ $\mathcal{R}$- symmetry and another SU(2) structure[3] on T^4, under which covariantly constant spinors are locally charged.

The D1/D5 brane configuration is found in Table 6.

Recall that the theory contains one vector multiplet and one hypermultiplet coming from the D1-branes and another such pair coming

3 This is a global symmetry before compactifying to obtain T^4 . It is broken by the imposed periodicity conditions, but we can still use it to organize the field content.

from the D5-branes. The two types of branes interact via D1-D5 strings giving rise to a bifundamental hypermultiplet. Overall, we have

$$L = L^{\text{vector}}_{\text{U}(N_1)} + L^{\text{vector}}_{\text{U}(N_5)} + L^{\text{hyper}}_{\text{D1}} + L^{\text{hyper}}_{\text{D5}} + L^{\text{hyper}}_{\text{D1-D5}} \tag{7.24}$$

The vector multiplets contain the fields $(A_\mu, A_I, \lambda_{+i\dot\alpha}, \lambda_{-i\dot\alpha})$, together with a symmetric doublet of auxiliary fields $D_{(ij)}$. Here, $\mu = (01)$, $I = (6789)$, $(\alpha, \dot\alpha)$ are doublet indices for the $\text{SU}(2)_- \times \text{SU}(2)_+$ $\mathcal{R}$-symmetry, and i is a doublet index for the SU(2) structure on T^4. The lagrangian of the vector multiplet is the dimensional reduction of six-dimensional SYM theory,

$$\begin{aligned} L^{\text{vector}} = \frac{1}{g^2}\text{Tr}\Big(&\frac{1}{2}(F_{01})^2 + \frac{1}{2}D_+A^I D_-A_I + \frac{1}{4}[A^I, A^J][A_I, A_J] \\ &+ \frac{1}{4}D^{ij}D_{ij} - \frac{i}{2}\lambda_-^{i\dot\alpha}D_+\lambda_{-i\alpha} - \frac{i}{2}\lambda_+^{i\alpha}D_-\lambda_{+i\alpha} \\ &+ \lambda_+^{i\alpha}\tau^I{}_\alpha{}^{\dot\alpha}[A_I, \lambda_{-i\alpha}]\Big)\,, \end{aligned} \tag{7.25}$$

where τ^I are the Weyl matrices for SO(4). The action is invariant under the supersymmetry variations

$$\begin{aligned} \delta A_+ &= 2i\epsilon_+^{i\alpha}\lambda_{+i\alpha} \\ \delta\lambda_{+i\alpha} &= F_{01}\epsilon_{+i\alpha} + D_+A_I(\tau^I\epsilon_-)_{i\alpha} \\ \delta A_- &= 2i\epsilon_-^{i\dot\alpha}\lambda_{-i\alpha} \\ \delta\lambda_{-i\dot\alpha} &= -F_{01}\epsilon_{-i\alpha} + D_-A_I(\overline{\tau}^I\epsilon_+)_{i\dot\alpha} \\ \delta A_I &= i(\epsilon_-\overline{\tau}^I\lambda_+) + i(\epsilon_+\tau^I\lambda_-) \\ \delta D_{ij} &= 2\epsilon^\alpha_{+(i}D_-\lambda_{+j)\alpha} + 2\epsilon^{\dot\alpha}_{-(i}D_+\lambda_{-j)\dot\alpha}\,. \end{aligned} \tag{7.26}$$

Since the lagrangian for the hypermultiplet is the same for all types ofhypermultiplets involved, we first turn to the hypermultiplet in generality. A hypermultiplet consists of a complex scalar doublet q_i and two complex Weyl fermion doublets $(\psi_{-\alpha}, \psi_{+\dot\alpha})$, all transforming in some representation of the gauge group. We set $\overline{q}^i = (q_i)^\dagger$ and similarly with $\psi_\pm$. The Lagrangian is

$$\begin{aligned} L = &- D^\mu\overline{q}^i D_\mu q_i + \bar q^i(D_i{}^j - A^IA_I\delta_i^j)q_j - \frac{i}{2}\overline{\psi}_-^\alpha\overleftrightarrow{D}_+\psi_{-\alpha} - \frac{i}{2}\overline{\psi}_+^{\dot\alpha}\overleftrightarrow{D}_-\psi_{+\dot\alpha} \\ &- \bar q^i(\lambda^\alpha_{+i}\psi_{-\alpha} + \lambda^{\dot\alpha}_{-i}\psi_{+\dot\alpha}) + (\overline{\psi}_-^\alpha\lambda^i_{+\alpha} + \overline{\psi}_+^{\dot\alpha}\lambda^i_{-\dot\alpha})q_i \\ &- \frac{1}{2}\overline{\tau}^I{}_\alpha{}^{\dot\alpha}(\overline{\psi}_-^\alpha A_I\psi_{+\dot\alpha}) - \frac{1}{2}\overline{\tau}^I{}_{\dot\alpha}{}^\alpha(\overline{\psi}_+^{\dot\alpha}A_I\psi_{-\alpha})\,, \end{aligned} \tag{7.27}$$

and is invariant under the transformations

$$\begin{aligned}
\delta q_i &= i\epsilon^{\alpha}_{+i}\psi_{-\alpha} + i\epsilon^{\dot\alpha}_{-i}\psi_{+\dot\alpha} \\
\delta\overline{q}^i &= i\epsilon^{i\alpha}_{+}\overline{\psi}_{-\alpha} + i\epsilon^{i\dot\alpha}_{-}\overline{\psi}_{+\dot\alpha} \\
\delta\psi_{-\alpha} &= 2D_- q^i\epsilon_{+i\alpha} + 2i\tau^I{}_{\alpha}{}^{\dot\alpha}A_I q^i\epsilon_{-i\dot\alpha} \\
\delta\overline{\psi}^{\alpha}_{-} &= 2D_-\overline{q}^i\epsilon^{\alpha}_{+i} - 2i\overline{q}^i A_I\tau^{I\alpha\dot\alpha}\epsilon_{-i\dot\alpha} \\
\delta\psi_{+\dot\alpha} &= 2D_+ q^i\epsilon_{-\dot\alpha} + 2i\overline{\tau}^{I\alpha}_{\dot\alpha}A_I q^i\epsilon_{+i\alpha} \\
\delta\overline{\psi}^{\dot\alpha}_{+} &= 2D_+\overline{q}^i\epsilon^{\dot\alpha}_{-i} - 2i\overline{q}^i A_i\overline{\tau}^{I\dot\alpha\alpha}\epsilon_{+i\alpha}\,.
\end{aligned} \tag{7.28}$$

We denote the D1-D1 and D5-D5 hypermultiplets as $(X_i, \eta_{-\alpha}, \eta_{+\dot\alpha})$. The D1-D5 hypermultiplets we call $(q_i, \psi_{-\alpha}, \eta_{+\dot\alpha})$, where q_i is an $N_5 \times N_1$ matrix transforming in the fundamental of $\mathrm{U}(N_5)$ and the antifundamental of $\mathrm{U}(N_1)$, while $\overline{q}^i = (q_i)^\dagger$ is its hermitian conjugate. We may still add Fayet-Iliopolis parameters, (3.48), and theta terms, (3.49), to the action (7.24).

So far, this is the system without interface, so that it preserves 16 superconformal symmetries. The interface will break the supersymmetryin half. and the surviving ones are parametrized by

$$\epsilon_{+i\alpha} = \tau^9{}_{\alpha}{}^{\dot\alpha}\epsilon_{-i\dot\alpha}\,. \tag{7.29}$$

Let us briefly sketch how the interfaces are constructed. This part is still under inspection, while this thesis is being typed. We begin with the simplest, which is a pure F1-string interface. It can be thought of as p F1-strings stretching between the D1/D5 system and a very distant D3-brane.

Naively, the realization of such a string in field theory is simple: it is a supersymmetric Wilson line of $\mathrm{U}(N_5)$ in the fundamental representation,

$$\mathcal{W} = \mathrm{Tr}_{N_5}\mathcal{P}\exp\left(i\int (A_0^{\mathrm{D5}} - X_9^{\mathrm{D5}})dt\right). \tag{7.30}$$

Because of the presence of light D1/D5 strings, however, a long string ending on the D1-branes can scatter into one ending on the D5 branes and this complicates the analysis. A similar situation is described in [226, 227] and remaining work is concerned with adapting this to our case. The setting is the instanton picture of the gauge theory [225]. The point is this: the scattering of D1-D3 strings into D5-D3 strings induces a mixing, after which the lowest lying fermions have a lagrangian description,

$$L_\varsigma = \varsigma^\dagger\left(i\partial_0 + \Omega_A\partial_t Z^A\right)\varsigma \tag{7.31}$$

where ς are fermionic degrees of freedom in the fundamental of $\mathrm{U}(N_5)$, Z^A is a coordinate on the moduli space of gauge instantons and Ω^A is

a $\mathrm{U}(N_5)$ connection, which is given to us by the ADHM construction. This provides interfaces of the type

$$\mathcal{W} = \mathrm{Tr}_F \, \mathcal{P} \exp\left(i \int dt \partial_t Z^A \Omega_A \left(y_0, Z \right) \right). \tag{7.32}$$

Our current task is to adapt this construction to the D1/D5 system above. To this end we conduct a thorough analysis of the possible boundary conditions preserving the correct supersymmetries (7.29) and work out the ADHM construction along the lines of [227]. This is the story in the UV. The interfaces in the IR are actually already at hand. They are the anologs of the Wilson lines studied in [140, 141].

SUMMARY

In this chapter we computed the g-factors for the fixed points of the flow holographically and confirmed the g-theorem. This fully legitimates the existence of our Kondo flows! Again, for critical screening the g-factors vanish in the IR, just as for the original Kondo model. Crucially, our g-factors contain important information, which is encoded in the backreaction of the gravity dual and cannot be reproduced by the probe brane limit. We concluded with a glimpse at the field theory picture.

This ends our discussion of holographic Kondo-like flows. A complete summary and an outlook are found in Chapter 11.

Part III

QUANTUM INFORMATION AND GRAVITY

In this part we investigate properties of volumes within the context of AdS_3/CFT_2 and their connection to quantum information.

We start in Chapter 8 by briefly introducing two notions from quantum information and their holographic realization. Namely, entanglement entropy and the Ryu-Takayanagi proposal, followed by complexity and the volume proposal. We end with Alishahiha's proposal to compute subregion complexity as volume enclosed by Ryu-Takayanagi surfaces.

In Chapter 9 we elegantly compute subregion complexity via the Gauss-Bonnet theorem in gravity. Our procedure lays bare the topological properties of subregion complexity when dealing with disconnected entangling intervals. In particular, we discover that the difference in subregion complexity, when transitioning between entanglement "phases" is topological. Moreover, after repeating our analysis in thermal states with a single connected entangling interval, we confirm that the jump in subregion complexity between entanglement plataeux is topological and temperature independent. This work is published in [2].

There is no sufficiently good handle on (subregion) complexity to test the complexity=volumes conjecture and its derivatives yet. We can address, however, a complementary question: What does "bulk volume" mean in the field theory? We give an answer to this in Chapter 10 for states sufficiently close to the vacuum, primary states and thermal states. The main ingredient is entanglement, which is completed by entwinement ant thermal contributions for excited states. In particular, we provide a lower bound for subregion complexity, which any candidate for a field theory dual has to satisfy. This work is published in [3].

lue

8

RESULTS FROM QUANTUM INFORMATION IN GRAVITY

In 2006 entanglement was introduced to the stage of the AdS/CFT correspondence [212, 213]. This work was literally groundbreaking since entanglement went completely unnoticed before, yet immediately after its inception it triggered a landslide of papers, by far too many references to list here. Evidence for this is that within only ten years an entire book had been crafted in [206]. Readers interested in the developement of the full story may consult references therein.

This chapter provides a heuristic introduction to holographic entanglement and complexity, covering the relevant facts for reading the following chapters. We begin in Section 8.1 with entanglement entropy and its holographic realization. Afterwards, in Section 8.3 we address complexity. We stress that this chapter will be very goal oriented and more complete accounts are found for instance in [206, 229, 234].

8.1 ENTANGLEMENT ENTROPY IN CFT

We are given a Hilbert space, which we assume to factorize into two sectors,

$$\mathcal{H} = \mathcal{H}_A \otimes \mathcal{H}_B. \tag{8.1}$$

Now, choose a pure bipartite state $|\Psi_{AB}\rangle \in \mathcal{H}$. If it *cannot* be written as a product state, i.e.

$$|\Psi_{AB}\rangle \neq |\Psi_A\rangle \otimes |\Psi_B\rangle \tag{8.2}$$

for $|\Psi_A\rangle \in \mathcal{H}_A$ and $|\Psi_B\rangle \in \mathcal{H}_B$ we say that the state is *entangled*.

Given some bipartite state, we can project onto the state in one sector, say A, by tracing the state's density matrix ρ over B, $\rho_A = \mathrm{Tr}_B \rho$. A standard measure for entanglement is then the *von-Neumann entropy* of the resulting density matrix ρ_A,

$$S(\rho_A) = -\mathrm{Tr}(\rho_A \log \rho_A). \tag{8.3}$$

This is nothing but the subsystem's entropy and thus it can be viewed as measuring the subsystems classical uncertainty. We will sometimes abreviate $S_A = S(\rho_A)$.

Of course nothing stops us from considering tripartite systems $\mathcal{H} = \mathcal{H}_A \otimes \mathcal{H}_B \otimes \mathcal{H}_C$ or any finite number of partitions of the Hilbert space. In this thesis we are interested in field theories living on some $(1+1)$-

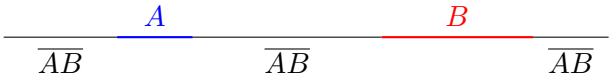

Figure 22: A single dimension of space is split according to the Hilbert space factorization $\mathcal{H} = \mathcal{H}_A \otimes \mathcal{H}_B \otimes \mathcal{H}_{\overline{AB}}$. The third partition is identified with the complement $\overline{AB}$ of the combined system AB.

dimensional spacetime. Moreover, in this chapter we always hold time fixed leaving just one dimension of space. Any multipartitioning then corresponds to splitting the spatial dimension into as many regions as partitions; see Figure 22 for a tripartite example.

Obviously this is a conceptual leap, since the Hilbert space factorization is now associated with regions in space itself. This is fine when working on a lattice, where each lattice point is assigned its own Hilbert space. In field theory however, this is in fact problematic, because fields are distributions and splitting space violently obstructs the smearing of the fields over some region. One has to appropiately regularize and one way of dealing with this issue is by imposing boundary conditions [69]. Here we will follow the standard approach in the literature and ignore this subtlety.

Evaluating (8.3) in a field theory is complicated in general. Good control over the situation is obtained when conformal symmetry is at play [62]. There are good reviews on that matter [63]. Since the technical details are not relevant to our story here, and since they would consume a lot of space, we only present the result here. For a single interval A of length a in an infinite 1D system at zero temperature the entanglement entropy reads,

$$S_A = \frac{\mathsf{c}}{3} \log \frac{a}{\epsilon}. \tag{8.4}$$

c is the central charge of the CFT and we are forced to introduce a UV cutoff ϵ. Its origin is made plausible by thinking of the spatial dimension as discretized with lattic spacing ϵ. Ultimately, the lattice spacing must be sent to zero in order to reach the continuum theory. Remarkably, this expression really only depends on two parameters, the subsystem size and the central charge c. Imagine taking different CFTs with identic central charge. Their entanglement entropy coincides for equal subsystem size a! In this sense the expression (8.4) is universal.

The reason lies in the fact that the entanglement entropy of n intervals can be traced back to correlators of $2n$ primary fields[1] When $n = 1$, i.e. in the case of a single interval, we require a two-point function, which is completely fixed by conformal invariance and thus universal. But already for $n = 2$, we deal with four-point functions. These consist of conformal blocks, which depend on the spectrum and

1 Had we gone through the trouble of reviewing the material of [63], we would have explicitly seen this. This would have been the only merit however, of an otherwise lengthy monologue.

the operator algebra. Hence already for two intervals entanglement entropy is non-universal. When discussing holography below, we will see that the large-c limit washes most of those fineprints away rendering entanglement entropy universal again.

The entanglement entropy of a single interval A of size a in a 1D system of finite size l_{CFT} at zero temperature reads

$$S_A = \frac{\mathsf{c}}{3} \log\left(\frac{2l_{\mathrm{CFT}}}{\epsilon} \sin\left(\frac{a}{l_{\mathrm{CFT}}}\right)\right). \tag{8.5}$$

For a single interval of size a in an infinite quantum system at finite temperature $T = \beta^{-1}$ the entanglement entropy is

$$S_A = \frac{\mathsf{c}}{3} \log\left(\frac{2\beta}{\epsilon} \sinh\left(\frac{a}{\beta}\right)\right) \tag{8.6}$$

Both (8.5) and (8.6) are again universal. It is in fact the same universality featuring in (8.4), because in $(1+1)$-dimensional CFT finite size or finite temperature are just one conformal transformation away from the infinite 1D system at zero temperature.

8.2 ENTANGLEMENT ENTROPY IN HOLOGRAPHY

Entanglement entropies are notoriously hard to compute in field theories. It comes as a surprise that they actually have a beautiful geometric realization within AdS/CFT. Again, we will only give heuristic arguments with the goal of introducing the vital objects for this part of the thesis. Here are a few pointers to the literature though: Holographic entanglement entropy was proposed in [212, 213] by Ryu and Takayanagi, and it therefore goes by the name RT-prescription. If one believes in the AdS/CFT correspodence, one can find a proof of the RT-prescription in [176], otherwise this paper still provides an explanation for its origin. These papers are all concerned with entanglement entropy in static situations. In order to study time dependence of entanglement entropy, the proposal was covariantized in [160].

We consider a state in a holographic CFT_d, dual to an asymptotically AdS_{d+1} spacetime. Let us state the RT-proposal:

Given an entangling region A with boundary ∂A in the CFT, the entanglement entropy associated to A is proportional to the area of a codimension-2 minimal surface γ_A – called the RT surface – embedded in AdS_{d+1} and anchored at ∂A. The minimal surface γ_A must be homologous to the entangling region A in the CFT. One example, that of an infinite 1D system in a CFT_2, is given in Figure 23. Concretely, the entanglement entropy is computed through

$$S_A = \frac{\mathrm{Area}\,(\gamma_A)}{4G_N^{(d+1)}}. \tag{8.7}$$

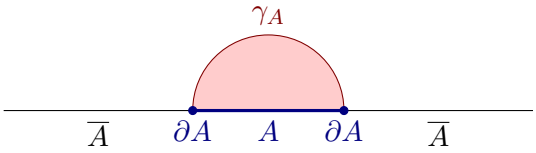

Figure 23: An example of an RT-surface γ_A in an infinite 1D system. The boundary ∂A of the entangling interval A consists of two points, demarcated by blue bullets. The RT surface γ_A ends on ∂A. We anticipate that it is a semicircle.

The difficulty lies in finding γ_A. Before we turn to an example however, let us briefly gain some insight into (8.7). Afficionados of general relativity will have spotted the resemblance with the Bekenstein-Hawking entropy (1.1) [45, 153]. In that case we would be measuring the thermal entropy of a black hole. It would again be given by an area, however, this time the surface in question would be the event horizon of the black hole. Newton's constant appears in identic fashion and it is almost eerie that it is precisely this prefactor, which leads in $(1+1)$-dimensions to the correct proportionality factor $\mathsf{c}/3$ encountered in (8.4). The necessary ingredient is the Brown-Hennaux formula for the central charge [60],

$$\mathsf{c} = \frac{3R}{2G_N^{(3)}}. \tag{8.8}$$

The analogy with black holes motivates a heuristic argument for the validity of (8.7). Consider again the reduced density matrix $\rho_A = \mathrm{Tr}_B \rho$. Since we have traced over B its degrees of freedom are essentially gone. Or are they? By varying B, we obtain different reduced density matrices ρ_A. So, in a sense, the traced out degrees of freedom excert their influence on ρ_A. Those degrees of freedom are just not accessible any longer, as if they were hidden behind a black hole horizon! Bigger black holes curve its surrounding geometry stronger than smaller black holes, thereby mimicking the influence of tracing out bigger or smaller regions B. Now, we can picture an observer located somewhere in the region shaded in red in Figure 23, that is between γ_A and the untraced (or accessible) boundary interval A. We can then think of γ_A as an event horizon, which shuts off our access to $B = \overline{A}$. Precisely the region we traced over.

Let us now confirm that RT-proposal indeed reproduces the entanglement entropy (8.4). The CFT state in question is the vacuum on an the complex plane, dual to the Poincaré patch

$$ds^2 = \frac{L^2}{z^2}\left(-dt^2 + dx^2 + dz^2\right). \tag{8.9}$$

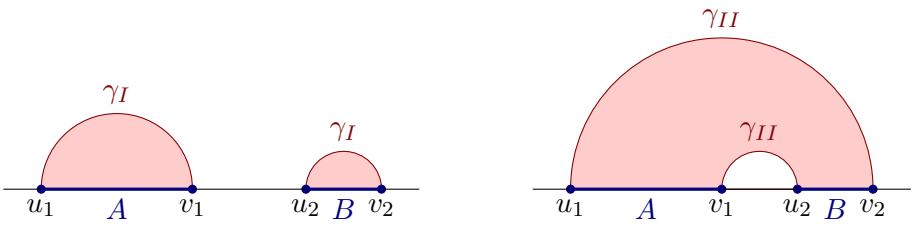

Figure 24: Two "phases" of entanglement entropy for two entangling intervals. In "phase I", on the left, the RT surface is disconnected. This happens when A and B are separated by a large distance. In "phase II", on the right, the RT surface connects interval A with B signaling entanglement between the two regions. Phase II dominates, when A and B are closeby.

A codimension-2 minimal surface in AdS_3 is a geodesic. Time is fixed, $dt = 0$, and we parametrize the embedding of the surface (it is not yet a geodesic!) by ξ. The pulled back metric onto this surface reads,

$$\hat{ds}^2 = \frac{L^2}{z^2}\left(x'(\xi)^2 + z'(\xi)^2\right) d\xi \tag{8.10}$$

As entangling interval we choose $A = [-a/2, a/2]$. The minimal curve attached to ∂A can be found by extremizing the area functional

$$\mathcal{S} = \frac{1}{4G_N^{(d+1)}} \int \sqrt{\hat{g}} d\xi = \frac{\mathsf{c}}{6} \int \frac{\sqrt{x'(\xi)^2 + z'(\xi)^2}}{z} d\xi \tag{8.11}$$

In the second line we used (8.8). Extremization with boundary conditions fixed at ∂A gives

$$x(\xi) = \frac{a}{2}\cos\xi, \quad z(\xi) = \frac{a}{2}\sin\xi. \tag{8.12}$$

Plugged back into (8.11) this gives

$$S_A = \frac{\mathsf{c}}{6} 2 \int_{\frac{2\epsilon}{a}}^{\frac{\pi}{2}} \frac{d\xi}{\sin\xi} = \frac{\mathsf{c}}{3} \log\frac{a}{\epsilon} \tag{8.13}$$

as desired. While in the CFT the cutoff ϵ appeared due to UV divergences, here it appears because AdS_3 is non-compact and thus the RT surface extends infinitely towards the (conformal) boundary. In order to get a finite result we have to cap the RT surface at some distance ϵ from the (conformal) boundary, which gives the lower bound in (8.13). Hence in the gravity picture ϵ arises due to IR divergences.

We now turn to two intervals A and B. Interestingly, in this case, there are two possible surfaces, γ_I and γ_{II}, satisfying the homology

constraint. They are shown in Figure 24. The selection criterion is minimal length. Repeating the above analysis gives

$$S_{AB} = \frac{\mathsf{c}}{3} \min \left(\log \frac{|u_1 - v_1|}{\epsilon} + \log \frac{|u_2 - v_2|}{\epsilon}, \log \frac{|u_1 - v_2|}{\epsilon} + \log \frac{|u_2 - v_1|}{\epsilon} \right). \tag{8.14}$$

For one specific choice of u_i, v_i the two options will yield the same entanglement entropy. In the next chapters we will treat these as "phases", which exchange dominance at this particular value of interval lengths. This transition will be of interest when we investigate the volumes enclosed by the RT-surfaces. The interesting feature to be discussed is that even though the entanglement entropy is constructed to be smooth at the transition, the enclosed volumes jump. Against naive intuition, this jump is topological.

More examples are found in chapter six of the textbook [206].

8.3 COMPLEXITY

Holographic entanglement entropy will be the main ingredient in our discussion below. However, we will oftentimes also encounter complexity. Even though we will never explicitely use the properties of this notion, here we give a very brief overview of complexity – just so the reader is eased in. There are good sources for interested readers, for instance [196].

The question we want to anser is:

How difficult is it to construct a state $|T\rangle$ of a given Hilbert space $\mathcal{H}$?

Of course, we have to start somewhere, and for us this is a *reference state* $|R\rangle \in \mathcal{H}$, chosen conveniently. We want to transform $|R\rangle$ into the state of our liking, the target state $|T\rangle$. In order to achieve that we are given a finite set of unitary transformations $\{U_i\}$ called *gates*. In equations, we ask whether

$$|T\rangle = U_{i_1} \dots U_{i_k} |R\rangle \tag{8.15}$$

is possible. Since the set of gates is finite, there is no guarantee that we can accomplish this task exactly. We can, however, get very close to $|T\rangle$. We thus allow for some tolerance ϵ. Once we reach the vicinity of $|T\rangle$, measured by ϵ, we declare (8.15) as satisfied. Now, there are certainly multiple combinations of gates, which will achieve this. We are interested in the optimal choice, so we look for the shortest string of gates $\{U_{\text{optimal}}\}$, which accomplishes (8.15). The length of this string, $\{U_{\text{optimal}}\}$ is defined to be the *complexity* of the state $|T\rangle$.

The notion of complexity, as we have defined it here, is naturally at home with finite dimensional Hilbert spaces $\mathcal{H}$. This thesis treats field

theories, which are inevitably based on infinite dimensional Hilbert spaces. First steps toward realizing complexity in this case were done in [192]. In this work the notion of complexity is assigned a geometric meaning as geodesics in Hilbert space. First advances in describing complexity in quantum field theory are presented in [76, 77, 149, 163]. Moreover, complexity was conjectured to measure the volume of wormholes in two sided black hole geometries [223].

It is this proposal that motivates the work presented in this part of the thesis. We are interested in a version of this proposal involving the RT proposal. It concerns holographic states traced over some subregion of Hilbert space. Then we can sensibly talk about RT surfaces providing the entanglement entropy of a subsystem. We may ask what the complexity of such states is. One proposal, very much inclined toward [223], is that this states' complexity is given holographically by the volume enclosed by the entangling region on the boundary and the RT surface. In Figure 23 and Figure 24 these are the volumes of the regions shaded in red. This proposal, first posed in [15], goes by the name of *subregion complexity* and triggered the work of the following two chapters. We always work with AdS_3/CFT_2. In Chapter 9 we deduce the topological properties of subregion complexity, and follow up in Chapter 10 with a prescription to compute subregion complexity purely from the field theory side.

A technicallity: the regions beneath the RT surfaces are two-dimensional and thus subregion complexities are given by areas in this case. We call it a volume still, since this generalizes to higher dimensions. Moreover, even though the RT surfaces are geodesics, we still speak of the "area of a surface" in this case.

9

TOPOLOGICAL COMPLEXITY

The success of entanglement entropy in guiding our understanding of geometry has paved the way for *complexity*, another quantity naturally at home in information science [196]. Given a desired *target state* and a *reference state* in a Hilbert space, complexity addresses the question of how difficult it is to construct the former out of the latter by use of a set of unitary transformations, called *gates*. The complexity of a pure quantum state is the minimal number of gates of any quantum circuit built from a fixed set of gates that produces this state from a given reference state. Complexity first entered the stage of AdS/CFT within the context of time-dependent thermal state complexity, where it was argued to be dual to either the volume of the Einstein-Rosen bridge [223], or the action of a Wheeler-DeWitt patch [59]. Recently, additional insight has been gained into both proposals from more detailed holographic studies [71, 72, 121, 122, 169].

The material we present here is found in [2] in joint collaboration with R. Abt, J. Erdmenger, H. Hinrichsen, C. Melby-Thompson, R. Meyer and I. Reyes. We will ocassionally reference this source again for emphasis.

9.1 SUBREGION COMPLEXITY FROM GRAVITY

Geometry and information are intimately related as was pointed out in a groundbreaking paper by Ryu and Takayanagi [213]. Their proposal was concerned in particular with areas. In this thesis we address a natural follow-up question: What about volumes of spacetime? There are already a few proposal in the air relating bulk volumes to *Fisher information* [40] and *fidelity susceptibility* [15, 120, 136, 188], or complexity [223]. This chapter takes us in a direction related to the latter. We study the *subregion complexity* of the reduced density matrix of a finite subregion A. This object was proposed in [14, 34, 211] that the subregion complexity should correspond to the volume of the co-dimension 1 region Σ enclosed by γ_{RT} and the cutoff surface (Figure 25).

Previous work [14] investigated subregion complexities in AdS_d with $d > 3$. The particular object of study of this chapter is the behavior of subregion complexity in $\mathrm{AdS}_3/\mathrm{CFT}_2$, for which [14] found unreasonable results. This motivates us to define subregion complexity of A in a slightly different way [2]:

$$\mathcal{C}(A) \equiv -\frac{1}{2}\int_{\Sigma} R\, d\sigma\,. \tag{9.1}$$

It is the integral over Σ of the scalar curvature R. The minus sign accounts for the negative curvature of asymptotically AdS spaces.

All examples studied here have constant spatial curvature, so that our definition coincides with Alishahiha's proposal [14]. Nevertheless, the definition in (9.1) has important advantages. Firstly, it is particularly natural in AdS_3, since the resulting quantity is dimensionless without introducing an *ad hoc* scale. Secondly, as will be detailed below, our prescription grants immediate access to a topological analysis. Finally, using our definition, one may think of the scalar curvature as a local *complexity density*. This is conceptually interesting on its own and lends itself naturally to geometric volumes.

The definition (9.1) is at home on the gravity side, where we can apply the Gauss-Bonnet theorem. It provides an elegant result, when the total length of the entangling region is held fixed: Any variation of the subregion complexity depend only on the Euler characteristic and are thus discrete. Interestingly, this property persists for any value of temperature. The aim of this chapter is to illustrate how to work with (9.1) in gravity.

It is instructive to compute the subregion complexity first in the simplest case: empty global AdS_3. In the first half of of this section we provide a simple formula for the subregion complexity of a disconnected entangling region A on the boundary of AdS_3. In the second half we compute the subregion complexity for a single interval at the boundary of the BTZ black hole geometry and thereafter for conical defects. All results can be conveniently related, when analytically continuing the mass parameter of the black hole to negative values. All these geometries are locally equivalent to AdS_3 and have constant spatial curvature.

First, we fix an entangling region A at the boundary. Its RT surface consists of geodesic(s) connecting the endpoints of A. Volumes anchored at the boundary of any asymptotically AdS geometry are divergent, so that we regularize by use of a cutoff slice γ_ϵ near the boundary. The result is a compact two-dimensional manifold Σ with boundary $\partial\Sigma = \gamma_{RT} \cup \gamma_\epsilon$. This is depicted in Figure 25.

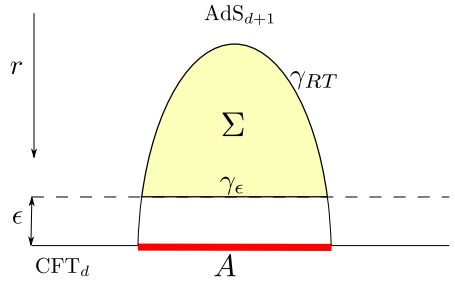

Figure 25: The subregion complexity is computed through the regularized volume of the region Σ, subtended by γ_{RT} and capped off by the cutoff surface γ_ϵ. Figure by Raimond Abt.

We use the Gauss-Bonnet theorem to unpack the subregion complexity (9.1) [2]:

$$\mathcal{C}(A) = -\frac{1}{2}\int_{\Sigma} R\, d\sigma = \int_{\partial\Sigma} k_g ds - 2\pi\chi(\Sigma)\ . \tag{9.2}$$

χ is the Euler characteristic of Σ and ds is the line element along $\partial\Sigma$. The geodesic curvature k_g will be defined properly below in (9.4). Here we point out that it measures how much the curve carved out by $\partial\Sigma$ deviates from a geodesic. In all cases of interest $\partial\Sigma$ is only piecewise smooth. Along the smooth portions of $\partial\Sigma$ we can still simply evaluate $\int_{\partial\Sigma} k_g ds$, while the turning points contribute with the value of their corner angles. This is because k_g has delta distribution singularities at these loci.

We now compute (9.2) for entangling regions on AdS_3, BTZ black holes and the conical defects. The time slices of these solutions have constant curvature $R = -\frac{2}{L^2}$, where L is the AdS radius.

9.1.1 *Zero temperature (AdS)*

Consider two entangling intervals of lengths x_1 and x_2 in the vacuum state of a CFT_2 on a circle of circumference $2\pi\, l_{\text{CFT}}$. Its metric is $ds^2_{\text{CFT}} = l^2_{\text{CFT}}(-L^{-2}\, dt^2 + d\phi^2)$ and the angular coordinate has periodicity $\phi \sim \phi + 2\pi$. This situation is dual to global AdS_3 (Figure 26) with metric

$$ds^2 = -f(r)dt^2 + \frac{dr^2}{f(r)} + r^2 d\phi^2\ , \tag{9.3}$$

where $f(r) = 1 + \left(\frac{r}{L}\right)^2$.

The entanglement entropy of the two subregions exhibits a transition between two "phases". The "order parameter" is the conformal ratio, which encodes the ratio of the sizes and separation of the two intervals x_1 and x_2 [118, 151]. On the CFT side, this transition has its origin in the exchange of dominance between the s and t channels in the four point function of twist fields. On the gravity side the two phases present themselves as the two different ways of connecting the interval endpoints by geodesics as is demonstrated in Figure 26, where we refer to them as phase I and phase II.

The reason that both phases cannot coexist lies in that the RT prescription qualifies only the geodesic of *minimal* length as entanglement entropy. At the transition point both phases have equal length. We observe that, even though the entanglement entropy is smooth across this transition point, the volume beneath the RT surface, i.e. the subregion complexity, is not. This discontinuity is the object of study here.

Let us now concretely compute the subregion complexity through (9.2), beginning with phase I. Σ composes of the two disjoint regions with boundary regions x_1 and x_2, each topologically a disk. Recall that

the Euler characteristic is additive, so that we obtain $\chi(\Sigma) = 2$. Next we turn to the integral of the geodesic curvature along the smooth parts of $\partial\Sigma$. The integrand, k_g vanishes on geodesics, so that γ_{RT} does not contribute. The only non-trivial piece comes from integrating along γ_ϵ, the circle segment at radius $r = Ll_{\text{CFT}}/\epsilon \equiv r_\epsilon$ with $\epsilon \ll l_{\text{CFT}}$. For metrics of the form (9.3), (which are at constant time) the geodesic curvature along a circle of radius r is simply

$$k_g = \left|\frac{Du}{ds}\right| = \frac{\sqrt{|f(r)|}}{r}\,, \tag{9.4}$$

where u is the unit vector tangent to the curve. We can specify this further to asymptotically AdS spaces, where $f(r) \to \left(\frac{r}{L}\right)^2$ as $r \to \infty$,

$$\int_{\gamma_\epsilon} k_g ds = \frac{\sqrt{|f(r_\epsilon)|}}{r_\epsilon}\int_{\gamma_\epsilon} ds = \frac{x_1 + x_2}{\epsilon} + \mathcal{O}(\epsilon)\,. \tag{9.5}$$

Of course, we should not forget the corner angles between γ_{RT} and γ_ϵ. Fortunately, no computation is needed, as it is known that γ_{RT} terminates perpendicularly at the conformal boundary of AdS [206]. Hence, any endpoint of the entangling region $A = x_1 \cup x_2$ provides a summand $\pi/2$ to the volume after sending $\epsilon \to 0$.

Summarizing all contributions, the subregion complexity for two disjoint intervals of length x_1 and x_2 is simply given by [2]

$$\mathcal{C}_I(\{x_1, x_2\}) = \frac{x_1 + x_2}{\epsilon} - 2\pi\ . \tag{9.6}$$

The subregion complexity in phase II works out analogously, the crucial difference being that the Euler characteristic is now $\chi(\Sigma) = 1$:

$$\mathcal{C}_{II}(\{x_1, x_2\}) = \frac{x_1 + x_2}{\epsilon}\,, \tag{9.7}$$

We see that both phases differ only by the constant topological term

$$\Delta\mathcal{C} = \mathcal{C}_{II} - \mathcal{C}_I = 2\pi\,, \tag{9.8}$$

and so the subregion complexity exhibits a discontinuous jump at the transition. This result was already computed in [49] by direct integration of the volume form, and in [136] using the Gauss-Bonnet theorem

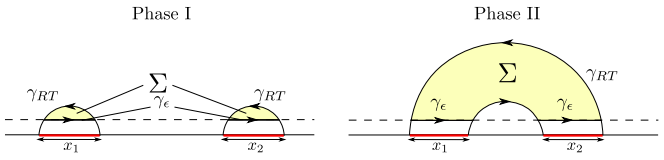

Figure 26: A system with two disconnected subsystems has two entanglement phases, I (left) and II (right). Figure by Raimond Abt.

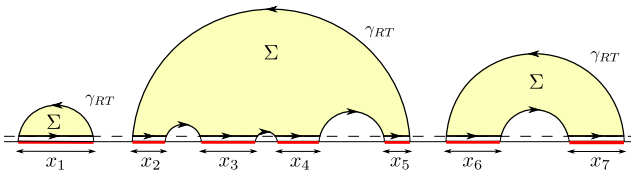

Figure 27: Example of a configuration of RT surfaces for several entangling intervals ($q = 7$) in the vacuum. Figure by Raimond Abt.

for intervals sharing one point. We now generalize our construction to an arbitrary number q of disjoint entangling intervals of length x_i, see Figure 27. Once we allow for more than two intervals, various different phases may arise, each with a specific form for γ_{RT}. When applying once again the Gauss-Bonnet theorem, the only extra we have to watch for is the larger number of corner angle contributes, each contributing $\pi/2$. The subregion complexity is then given by [2]

$$\mathcal{C}(\{x_i\}) = \frac{x}{\epsilon} + \pi q - 2\pi\chi\,, \tag{9.9}$$

We have abbreviated the total entangling length of the q intervals by $x = \sum_{i=1}^{q} x_i$ and χ the total Euler characteristic.

As before, when γ_{RT} undergoes a phase transition the only difference arises due to the Euler characteristic χ, thus

$$\Delta\mathcal{C} = -2\pi\Delta\chi\,. \tag{9.10}$$

We learn that, jumping from phase to phase while keeping the total length of the entangling intervals fixed, the subregion complexity varies discretely in multiples of 2π. This is the first main result in this chapter and we shall find below that the same is true of finite temperature states.

Lastly, when the entangling interval is the full boundary of global AdS_3, i.e. $A = 2\pi l_{\text{CFT}}$, we have no corner angles and $q = 0$. Plugged into the subregion complexity (9.9) we obtain the result

$$\mathcal{C}\,(\text{circle}) = 2\pi\left(\frac{l_{\text{CFT}}}{\epsilon} - 1\right)\,. \tag{9.11}$$

9.1.2 *Finite temperature (BTZ)*

States at finite temperature T in a CFT_2 on a circle are dual to BTZ black holes [39]. The state's temperature is encoded in the black hole's mass $T = L\sqrt{M}$, which we give in units where $8G_N = 1$. Their metric is of the form (9.3) with

$$f(r) = -M + \left(\frac{r}{L}\right)^2\,, \tag{9.12}$$

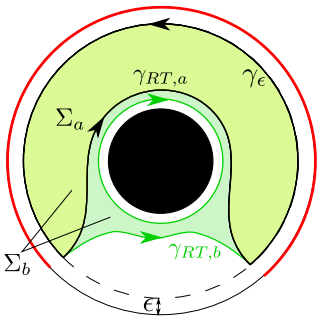

Figure 28: The RT surface γ_{RT} of a single interval, drawn in red, in the BTZ geometry has two phases, a and b. Figure by Raimond Abt.

It is well known that $M > 0$ corresponds to black holes while $M = -1$ reproduces AdS_3. The geometries for $-1 < M < 0$ correspond to conical defects in AdS, i.e. naked singularities without horizon.

Consider now a single entangling region of size x in this geometry. Its RT-surface, γ_{RT}, is known to exhibit two different phases a and b, as shown in Figure 28, provided that the entangling region is larger than half of the boundary perimeter. In phase b the geodesic γ_{RT} remains homotopic to the entangling region, while in phase a it is given by the geodesic of the complement plus a surface wrapping around the horizon of the black hole. Again the physically realized phase is picked out by minimality of of γ_{RT}. In contrast to before, in this case the transition cannot be controlled by a conformal ratio, since we consider only a single boundary interval. To find the order parameter, observe that for low temperatures the black hole is small so that $\gamma_{RT,b}$ is shorter than $\gamma_{RT,a}$ while for large temperatures the opposite is true. Thus, the phase transition is controlled by the mass of the black hole and they exchange dominance at $M = M^*$, where the entanglement in both phases coincides.

We can run through the same manipulations that produced (9.6) and (9.7) in the BTZ black hole. In fact, in phase a the result is identical to that of a single interval in the vacuum, namely

$$\mathcal{C}_a(x) = \frac{x}{\epsilon} - \pi \ , \tag{9.13}$$

Remarkably, this result is independent of the black hole's mass M! This provides the second main result of this chapter: the subregion complexity in a CFT_2 of a thermal state is "protected" against temperature variations. in spite of the fact that the entanglement entropy has a strong temperature dependence. γ_{RT} changes with the black hole size, and one may argue, that it changes in precisely such a way as to leave its enclosed volume constant. This result hinges on use of the Gauss-Bonnet theorem and the topological nature of the BTZ solution. Thus, this property is specific to three-dimensional gravity.

Let us again consider changes in the complexity. Imagine starting out in phase a at fixed entangling interval and tuning down the mass

M of the black hole, until we hit the phase transition and pass to phase b. This is shown in Figure 29. Fortunately, the geodesic curvature of the horizon vanishes so that the calculation of (9.2) follows the same recipe as before. The only difference between the phases lies again in the Euler characteristic, which is now $\chi(\Sigma_b) = 0$, as Σ_b is topologically an annulus. Therefore the corresponding complexities differ by [2]

$$\Delta\mathcal{C} = \mathcal{C}_b - \mathcal{C}_a = 2\pi\,, \tag{9.14}$$

as derived earlier in [49] by direct integration and [136] via Gauss-Bonnet. The topological nature is striking! Upon hopping between the phases changes by the same constant, irrespective of the entangling interval's size (so long as it is larger than half the boundary perimeter).

Now that we have a clear understanding of the BTZ black hole with positive mass, let us consider the case of lowering the mass below zero. It is known that for $M \in (-1, 0)$, the event horizon vanishes, leaving behind a naked singularity. These are termed "conical defects" in the literature, because they give rise to a deficit angle $2\pi(1 - \sqrt{-M})$ at the boundary. Conical defects carry a point particle in the center of the geometry giving rise to a Dirac delta peak; everywhere else the curvature is still $R = -\frac{2}{L^2}$.

Readers concerned with the violation of cosmic censorship, i.e., that singularities should never be naked, should find comfort in the fact that conical defects are perfectly sensible solutions Einstein's equations in three dimensions.

The entanglement entropy for conical defects in AdS_3 was studied in [38]. When computing the subregion complexity via (9.2), we have to pay attention to a subtlety: the topology of the conical defect is again that of an annulus. This is because the singularity at the center forces us to cut out an infinitesimal disk of radius ϵ surrounding it. Otherwise we cannot satisfy the homology constraint of the RT prescription. After computing the subregion complexity we take $\epsilon \to 0$. This introduces another boundary, whose geodesic curvature is again given by (9.4) but now with $f(r) = -M + \left(\frac{r}{L}\right)^2$. The integral around the disk is

$$\oint k_g ds = 2\pi\sqrt{f(r)} \underset{r\to 0}{\longrightarrow} 2\pi\sqrt{-M} \quad , \; M < 0\,. \tag{9.15}$$

All other contribution to (9.2) remain the same, hence we obtain for the conical defect [2]

$$\mathcal{C} = \frac{x}{\epsilon} + \pi - 2\pi\sqrt{-M} \quad , \; M < 0 \tag{9.16}$$

A consistency check is to have the mass shrink all the way to $M = -1$ in (9.16). This recover the AdS vacuum subregion complexity (9.13) as it should. Note that the subregion complexity approaches once more the same value as in phase a.

To summarize, for a single entangling region of fixed size, we find three different phases depicted in Figure 29. Even though the entanglement entropy varies non-trivially with temperature in all phases, the Gauss-Bonnet theorem guarantees that the subregion complexity in phase a and b are constant, exhibiting a topological jump of 2π at the

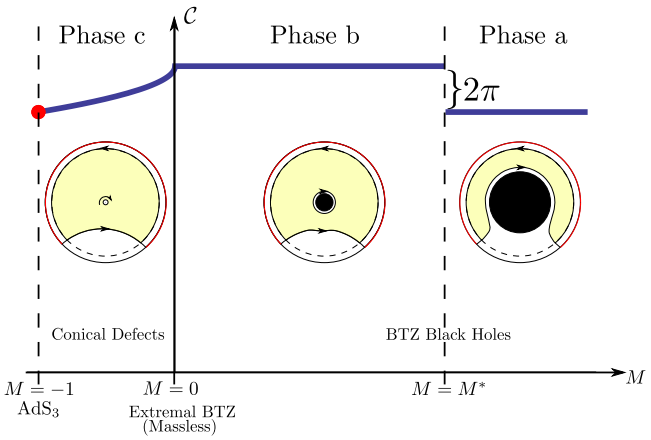

Figure 29: Subregion complexity as function of the black hole mass, for a fixed entangling region. Figure by Raimond Abt.

transition. This changes once we cross to the conical defect sector, in which a naked singularity appears causing the subregion complexity to vary smoothly over precisely the range of the jump, 2π.

Finally, it is simple to see that the subregion complexity for q intervals at finite temperature is analogous to (9.9), and the natural generalization of (9.16) for the conical defect case [2].

SUMMARY

In this chapter we outlined a relation between gravity and tensor networks within the framework $\text{AdS}_3/\text{CFT}_2$. Our particular interest lies on subregion complexity in light of the volume proposal. In AdS_3 the curvature is constantly $R = -2/L^2$, which inspired us to rewrite the volume proposal as an integral of the curvature scalar. This motivates us to think of the curvature scalar as a complexity density, which reflects the loss of degrees of freedom along an RG flow. In the case of $\text{AdS}_3/\text{CFT}_2$, this new form of the volume proposal is readily evaluated using the Gauss-Bonnet theorem. Interesting questions for the future are to consider higher dimensions in a similar way, to relate to the optimization approach of [65, 66, 187], to relate our approach with the holographic renormalization properties of the different proposals for complexity [70, 71], as well as to consider time-dependent situations [72].

Subregion complexity is particularly well suited to investigate the topological transitions described in this chapter. At these transitions, the subregion complexity changes by a contribution determined solely by the Euler characteristic of the minimal surface. This applies both at vanishing and at nonzero temperature. Remarkably, our result is independent of the temperature and thus of the size of the black hole even though the RT surface is highly temperature dependent.

A similar discontinuous jump of the subregion complexity is obtained in [2] via a numerical simulation, where we mapped a random tensor network to an Ising model. The numerics reproduce the discontinuous jump of subregion complexity, up to a numerical deviance: the simulation gives a jump of $\Delta\mathcal{C} = 4.0 \pm 0.3$ instead of the predicted $\Delta\mathcal{C} = 2\pi$ in the gravity picture.

The next chapter is dedicated to a study of subregion complexity in the the field theory.

10

BULK VOLUMES FROM CFT

In this chapter we carry the analysis of the topological complexity to the field theory. Before we can sensibly do that however, we need to answer a more basic question first:

What does "bulk volume" mean in the field theory?

In fact, this question is a little too ambitious for our current understanding and instead we take a more pragmatic approach here: we answer how to *compute bulk volumes* from the field theory. Remarkably, this can be done! The answer does, as of yet, not confirm nor deny the "complexity equals volume" proposal [223], since there is not yet a clear cut definition of complexity in interacting field theories. Nevertheless, building on the content of this chapter, future work might shed new light on any proposed volume dual.

Of course, we are particularly interested in subregion complexities, that is, volumes bounded by RT surfaces. Again there is no definition of these objects in the field theory currently. Yet, we provide a field theoretic formula, which computes volumes bounded by RT surfaces by purely accessing field theory data. This sheds light on the true nature of subregion complexity in the field theory, and ultimately any proposal for a subregion complexity will have to satisfy our formula.

Any volume will hence have two spatial dimensions and pedants would rightfully argue that these are surfaces. Nevertheless, we still call these surfaces volumes in analogy with the higher dimensional case, where we have RT *surfaces*, which enclose volumes.

In this chapter we make use of a novel tool, *kinematic space*, which we introduce in Section 10.1. Thereafter, in Section 10.2, we present a formula able to compute bulk volumes from the field theory and proof it. Only then are we in a position to apply it to subregion complexity. We demonstrate this procedure at length for the vacuum case in Section 10.3 and move on to excited states in Section 10.4.

The material presented here is drawn from [2, 3] in joint collaboration with R. Abt, J. Erdmenger, M. Gerbershagen and C. Melby-Thompson. We will occassionally reference these sources again for emphasis.

10.1 REVIEW OF KINEMATIC SPACE

Kinematic space was introduced as a tool for studying the AdS/CFT correspondence in [87] The utility of the kinematic space formalism lies in its ability to explicitly decode bulk geometry and as boundary information as we review in this section. Our aim of ultimately applying

this formalism to compute bulk volumes from field theory guides our presentation here and follows [3]. Kinematic space has however many more virtues such as applications to tensor networks [85], it clarifies the relation between bulk and boundary operators [56, 81, 84] and it handily turns the first law of entanglement into Einstein's equations [86] to name a few.

Even though the RT formula highlights a strong relationship between entanglement and geometry, it does not straightforwardly tell us how to construct the bulk geometry. First advances toward making this correspondence more precise were presented in [37]. Their approach was to construct the perimeter of a closed bulk curve from derivatives of the entanglement entropy in terms of a quantity called *differential entropy*. The continuation of this work produced the kinematic space formalism, which naturally incorporates these concepts [83, 85, 87]. Most of the objects discussed here have been worked out for compact manifolds by mathematicians, see e.g. [215]. However, to the author's knowledge, results on non-compact manifolds such as AdS are scarce and only the specific case of vacuum AdS_3 is treated by the mathematicians to some extend. Yet, as so often, physicists have a different focus than mathematicians.

Consider an asymptotically AdS_3 spacetime $\mathcal{M}$, that is, a spacetime, which mimics AdS_3 asymptotically:

$$ds^2 \sim -\frac{r^2}{L^2}dt^2 + L^2\frac{dr^2}{r^2} + r^2 d\phi^2 \qquad \text{as} \quad r \to \infty\,, \tag{10.1}$$

The angular coordinate is periodic, $\phi \sim \phi + 2\pi$, and L is the AdS radius.We consider the simplest case where $\mathcal{M}$ is static, with Killing time t.

Fix a spatial slice given by t = constant inside of . In this situation kinematic space $\mathcal{K}$ is the space of all oriented boundary-anchored geodesics that lying inside the time slice. We begin with the assumption that for any given pair of boundary points u, v there is a unique oriented geodesic running from u to v. This uniqueness is guaranteed in particular for geometries sufficiently close to pure AdS_3, but it will fail for thermal or primary states. We outline how to adjust kinematic space, when discussing these states below. A geodesic with endpoints in u, v on the boundary of AdS_3 is then synonymous with a single point in $\mathcal{K}$, making (u, v) a coordinate system on $\mathcal{K}$. Alternatively, we sometimes parametrize a geodesic through its midpoint θ of the interval $[u, v]$ together with its opening angle α as presented in Fig. 30. This simply amounts to the coordinate change

$$u = \theta - \alpha\,, \quad v = \theta + \alpha\,. \tag{10.2}$$

Of course, geodesics carry an orientation and kinematic space also accounts for that. For each geodesic (θ, α) we have the orientation inverse $(\theta + \pi, \pi - \alpha)$. This is depicted in Fig. 30.

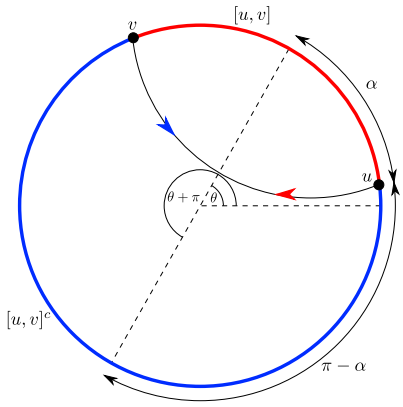

Figure 30: Parametrization of geodesics via their endpoints u and v or via the locus of their center θ and their opening angle α. The tuples (θ, α) and $(\theta+\pi, \pi-\alpha)$ correspond to the same geodesic, but with opposite orientation. The geodesic with the orientation of the red arrow is associated with the entangling interval $[u, v]$, while the geodesic with the orientation of the blue arrow is associated with the complement $[u, v]^c$. Figure by Raimond Abt from [3].

We understood that kinematic space naturally incorporates geodesics. What about points in AdS_3. It can also do that! Indeed, a bulk point p is encoded in $\mathcal{K}$ as the set of *all* geodesics running through p. This set is a curve in $\mathcal{K}$, the so-called *point curve* and one example is presented in Fig. 31.

Given our assumptions, the geodesics (u, v) are in one-to-one correspondence with the intervals $[u, v]$, so we may interpret $\mathcal{K}$ as the space of entangling regions of the CFT and consider the entanglement entropy $S(u, v)$ to be a function on it [87]. In case of a holographic CFT, this quantity is given at leading order in $1/N$ by the Ryu-Takayanagi formula:

$$S(u,v) = \frac{\ell(u,v)}{4G_N}\,. \tag{10.3}$$

Here $\ell(u, v)$ denotes the length of the geodesic (u, v), regularized for example by truncating at a large but finite value of r, and G_N is the bulk Newton's constant. The key observation of [83] was that S induces a natural metric $ds^2_{\mathcal{K}}$ on $\mathcal{K}$, along with a corresponding volume form ω:

$$ds^2_{\mathcal{K}} = \partial_u\partial_v S\, du\, dv = \frac{1}{2}(\partial_\theta^2 - \partial_\alpha^2) S\,(-d\alpha^2 + d\theta^2)\,, \tag{10.4}$$

$$\omega = \partial_u\partial_v S\, du \wedge dv = \frac{1}{2}(\partial_\theta^2 - \partial_\alpha^2) S\, d\theta \wedge d\alpha\,. \tag{10.5}$$

In integral geometry the volume form is known as the *Crofton form*. In this work we are only interested in geometries invariant under translations, implying that S depends only on the length $v - u = 2\alpha$ of

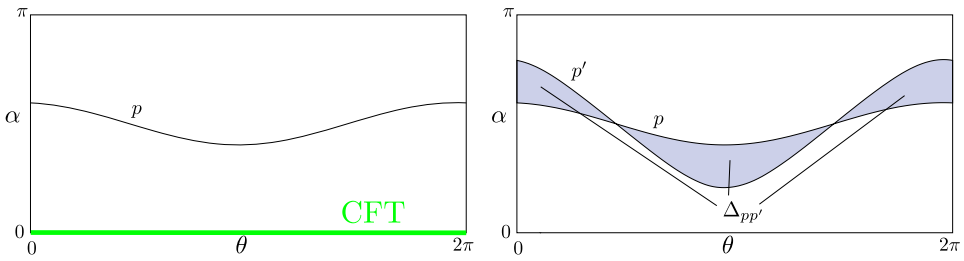

Figure 31: A point $p \in \mathrm{AdS}_3$ at constant time is associated with the set of all geodesics that intersect p (LHS). This set is a curve in $\mathcal{K}$, and is called the point curve of p. The geodesic distance of two points p and p' is proportional to the volume of the region $\Delta_{pp'}$ in $\mathcal{K}$ that is bounded by the point curves of p and p' (RHS). Any $(\theta, \alpha = 0)$ corresponds to boundary points of AdS_3. Hence the lower boundary of $\mathcal{K}$ is identified with the constant time slice of the CFT depicted in green (LHS). Figure by Raimond Abt from [3].

the entangling interval and not its particular position θ. This leads to simplifications in (10.4) and (10.5),

$$ds^2_{\mathcal{K}} = -\frac{1}{2}\partial^2_\alpha S(-d\alpha^2 + d\theta^2)\,, \qquad \omega = -\frac{1}{2}\partial^2_\alpha S d\theta \wedge d\alpha\,. \tag{10.6}$$

The metric $ds^2_{\mathcal{K}}$ is Lorentzian, and u and v are light-cone coordinates.

The geometric structure (10.4, 10.5) of $\mathcal{K}$ casts a new light on the bulk geometry in holography. For example, in pure AdS_3 point curves are known to be spacelike geodesics on $\mathcal{K}$ [87].[1] A central ingredient for us will be the geodesic distance $d(p, p')$ between two bulk points p and p', which can be expressed as an integral in kinematic space [87]:

$$\frac{d(p,p')}{4G_N} = \frac{1}{4}\int_{\Delta_{pp'}} \omega\,. \tag{10.7}$$

Here $\Delta_{pp'} \subset \mathcal{K}$ is the set of all geodesics separating p and p' in AdS_3. In $\mathcal{K}$ the set $\Delta_{pp'}$ is the region bounded by the point curves of p and p', as depicted in Fig. 31.

In all application below (θ, α) will also denote entangling intervals and we will view $\mathcal{K}$ as the space of these. With this nomenclature we can understand the causal structure of $\mathcal{K}$ in a natural way: Any interval (u_1, v_1) lies in the past of (u_2, v_2) if $[u_1, v_1] \subset [u_2, v_2]$. The orientation reversed geodesic $(\theta + \pi, \pi - \alpha)$ is spacelike related to the geodesic (θ, α); this is because $(\theta + \pi, \pi - \alpha)$ corresponds to the complement of the entangling interval (θ, α), as seen in Fig. 30. We constructed kinematic space with holographic theories in mind. Nevertheless, the same line of thought outlined here can be applied to non-holographic

1 In [87] it was shown that point curves are geodesics for several geometries, such as global AdS_3, conical defects and BTZ black holes.

theories. Again one obtains descriptions of geodesics in AdS_3. This time, however, AdS_3 does not carry an interpretation of a physical gravity theory, but is purely auxiliary.

Finally, as $\alpha \to 0$ the geodesic (α, θ) collapses to the boundary point $\phi = \theta$. Therefore, the lower boundary $\mathcal{K}$, $\alpha = 0$, can be identified with the CFT circle (see Fig. 31). This observation plays an important role in later sections.

For holographic theories the RT proposal is central in connecting kinematic space to quantum information. Equation (10.3) lets us compute the entanglement entropy of the interval $[u, v]$ through a length $\ell(u, v)$. This connection allows us to not only express bulk lengths, as in (10.7), but also volumes, which we study in Sec. 10.2, as integrals over derivatives of entanglement entropies. In this way, the information-theoretic properties of a constant time slice in the CFT encode the geometry of the corresponding constant time slice in the bulk.

Finally, let us argue that we can construct kinematic space without reference to the bulk. The Crofton form ω, for instance, can be recast as an infinitesimal version of the *conditional mutual information* of two intervals A and B with respect to a third interval C,

$$I(A, B|C) = S(AC) + S(BC) - S(ABC) - S(C)\,. \tag{10.8}$$

For neighboring infinitesimal intervals $A = [u - du, u]$, $B = [v, v + dv]$, $C = [u, v]$ we recover the crofton form [83]:

$$I(A, B|C) \approx \partial_u \partial_v S \, du \, dv \propto \omega\,. \tag{10.9}$$

The causal structure of $\mathcal{K}$ is motivated by requiring (u_1, v_1) to lie in the past of (u_2, v_2) if $[u_1, v_1] \subset [u_2, v_2]$. This immediately leads to

$$ds^2_{\mathcal{K}} \propto du \, dv\,. \tag{10.10}$$

The proportionality factor, $\partial_u \partial_v S$, is fixed by demanding that the volume form match the Crofton form. Thus, as claimed, the geometry of $\mathcal{K}$ can be constructed from the CFT side without reference to the bulk. This will be important for us when we construct a field theory expression for subregion complexity in the following.

10.2 THE VOLUME FORMULA

Let us begin by presenting the following formula [2, 3]

$$\frac{\mathrm{vol}(Q)}{4G_N} = \frac{1}{2\pi} \int_{\mathcal{K}} \lambda_Q \omega\,, \tag{10.11}$$

which computes the volume of a bulk region Q as a kinematic space integral. Here $\lambda_Q(\theta, \alpha)$ is the *chord length* of the geodesic (θ, α), defined to be the length of the intersection of the geodesic (θ, α) with Q; see

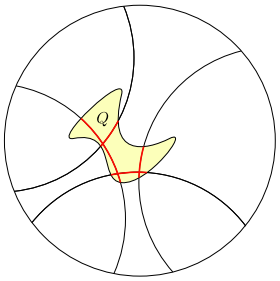

Figure 32: The volume of a region Q on the constant time slice is computed through an integral over the chord lengths of all geodesics. The chord length of a geodesic is the length of the segment of the geodesic that lies inside of Q, drawn in red. Figure by Raimond Abt from [3].

Fig. 32. The aim of this chapter is to establish that (10.11) indeed computes bulk volumes and to proof it. In the following sections we use it to derive an expression for holographic subregion complexity in the vacuum purely in terms of field theory quantities.

While formulae like this are known in integral geometry [215], we present here a simple proof of (10.11) for the kinematic space of a constant time slice of global AdS_3 with metric

$$ds^2_{\mathrm{AdS}_3} = -\frac{L^2+r^2}{L^2}dt^2 + \frac{L^2}{L^2+r^2}dr^2 + r^2 d\phi^2\,. \tag{10.12}$$

In this case the entanglement entropy is

$$S(\alpha) = \frac{\mathsf{c}}{3}\log\left(\frac{2l_{\mathrm{CFT}}}{\epsilon}\sin(\alpha)\right), \tag{10.13}$$

where $\mathsf{c} = \frac{3L}{2G_N}$ is the central charge, l_{CFT} is the radius of the CFT circle and ϵ is the UV cutoff. The corresponding metric and Crofton form are

$$ds^2_{\mathcal{K}} = \frac{\mathsf{c}}{6}\frac{1}{\sin^2\alpha}(-d\alpha^2 + d\theta^2)\,, \qquad \omega = \frac{\mathsf{c}}{6}\frac{1}{\sin^2\alpha}d\theta\wedge d\alpha\,. \tag{10.14}$$

Our strategy begins by verifying the volume formula for a disk D_R of radius R around the point $r = 0$ in a constant time slice of AdS_3. This computation was previously presented in [2]. We next show that the integral in (10.11) shares with volumes certain characteristic properties such as non-negativity and additivity, and use these properties to extend the volume formula to annular arcs. Using annular arcs it is possible to construct Riemann sums, which approximate the volume of Q arbitrarily well, proving the volume formula in the limit. This proof is taken from [3].

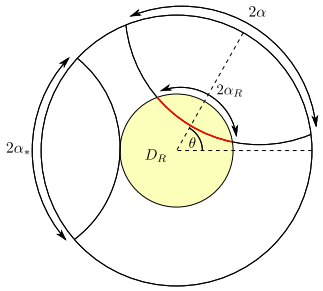

Figure 33: Each geodesic (θ, α) is assigned an opening angle α_R by the disk D_R. The angle α_* is the minimum opening angle a geodesic must have to contribute to D_R. Figure by Raimond Abt from [3].

We abbreviate the integral in 10.11 by

$$V(Q) \equiv \frac{2G_N}{\pi} \int_{\mathcal{K}} \lambda_Q \omega \,, \tag{10.15}$$

We need to show that then

$$V(Q) = \mathrm{vol}(Q) \,. \tag{10.16}$$

We now establish this for a disk D_R $(r \leq R)$ of radius R. The chord length of the geodesic (θ, α) for region D_R is

$$\lambda_{D_R}(\theta, \alpha) = \begin{cases} L \,\mathrm{arcosh}(1 + 2\frac{R^2}{L^2} \sin^2(\alpha_R)) \,, & \text{if } \alpha_* \leq \alpha \leq \pi - \alpha_* \\ 0 \,, & \text{otherwise.} \end{cases} \tag{10.17}$$

Here α_R is the opening angle of the geodesic (θ, α) on the boundary of the disk D_R (see Figure 33), and satisfies

$$\frac{R}{\sqrt{L^2 + R^2}} \cos(\alpha_R) = \cos(\alpha) \,. \tag{10.18}$$

The angle α_* is the minimus opening angle that a geodesic needs in order to be in contact with D_R. It is fixed by

$$\cos(\alpha_*) = \frac{R}{\sqrt{L^2 + R^2}} \,, \tag{10.19}$$

which specifies the family of geodesics (θ, α_*) tangent to D_R (Figure 33). Since λ_{D_R} vanishes for $\alpha \notin [\alpha_*, \pi - \alpha_*]$, as indicated in (10.17), $V(D_R)$ takes the form

$$V(D_R) = -\frac{1}{4\pi} \int_0^{2\pi} d\theta \int_{\alpha_*}^{\pi - \alpha_*} d\alpha \, \lambda_{D_R} \partial_\alpha^2 \ell \,. \tag{10.20}$$

We coordinate transform $V(D_R)$ into an integral over α_R and integrate by parts to find

$$\begin{aligned} V(D_R) &= \frac{1}{2}\int_0^\pi d\alpha_R (\partial_{\alpha_R}\lambda_{D_R})^2 = \int_0^\pi d\alpha_R \frac{2L^2R^2\cos^2(\alpha_R)}{L^2+R^2\sin^2(\alpha_R)} \\ &= 2\pi L^2\left(\sqrt{1+\frac{R^2}{L^2}}-1\right). \end{aligned} \tag{10.21}$$

This is indeed the volume of the disk D_R.

Our next step is to establish the following important properties of V:

1. $V(Q)\geq 0$, with equality only when $Q=\emptyset$. This holds because we deal with an integral of a non-negative function with a positive volume form.

2. V is additive,

$$V(Q\cup Q') = V(Q)+V(Q')-V(Q\cap Q')\,. \tag{10.22}$$

   Here, Q and Q' are any regions in the constant time slice of AdS_3 and the third term takes care of overcounting when considering $Q\cap Q'\neq\emptyset$. This property is a direct consequence of the additivity of chord lengths,

$$\lambda_{Q\cup Q'} = \lambda_Q+\lambda_{Q'}-\lambda_{Q\cap Q'}\,. \tag{10.23}$$

3. Non-negativity and additivity, together with $V(\emptyset)=0$, imply that V is monotonic,

$$V(Q)\leq V(Q') \quad \text{if } Q\subseteq Q'\,. \tag{10.24}$$

4. V is invariant under rotations around $r=0$. This follows from the rotational invariance of the vacuum state – which implies rotational invariance of the kinematic space measure – and of the chord length λ_Σ.

Properties 1.-4. put us in a position to prove (10.16). Consider (10.16) for an annulus $A_{R_1R_2}$ of inner radius R_1 and outer radius R_2 centered around the origin (Figure 34). First note that, since the disk D_{R_2} can be written as the union $D_{R_2}=D_{R_1}\cup A_{R_1R_2}$, additivity implies

$$V(A_{R_1R_2}) = V(D_{R_2})-V(D_{R_1}). \tag{10.25}$$

We already know that the volume formula holds for D_R, and this simple argument therefore extends it to annuli $A_{R_1R_2}$,

$$V(A_{R_1R_2}) = \mathrm{vol}(D_{R_2})-\mathrm{vol}(D_{R_1}) = \mathrm{vol}(A_{R_1R_2})\,. \tag{10.26}$$

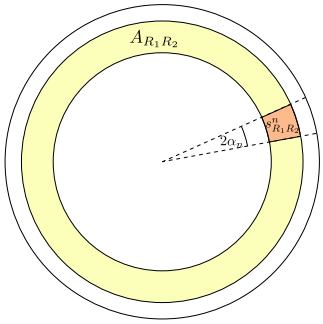

Figure 34: Annulus $A_{R_1R_2}$ of inner radius R_1 and outer radius R_2 and annulus segment $s^n_{R_1R_2}$ with opening angle α_n. Figure by Raimond Abt from [3].

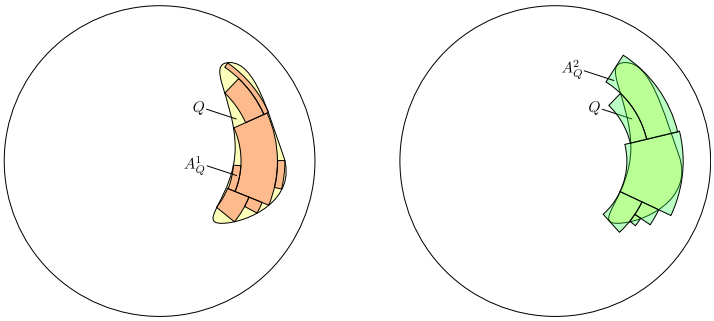

Figure 35: Approximation of an arbitrary set Q by annular arcs through Riemannian sums. The lower bound, $A^1_Q \subseteq Q$, is colored in red and the upper bound, $A^2_Q \supseteq Q$, is colored in green. Figure by Raimond Abt from [3].

The second step is to verify the proposal for a segment $s^n_{R_1R_2}$ of the annulus $A_{R_1R_2}$, as depicted in Figure 34, with opening angle

$$\alpha_n \equiv \frac{\pi}{n}\,, \qquad n \in \mathbb{N}\,. \tag{10.27}$$

Rotational invariance, additivity, and (10.26) together yield

$$V(s^n_{R_1R_2}) = \frac{1}{n}V(A_{R_1R_2}) = \frac{1}{n}\mathrm{vol}(A_{R_1R_2}) = \mathrm{vol}(s^n_{R_1R_2})\,. \tag{10.28}$$

So the proposal indeed holds for segments of annuli with opening angle α_n.

Finally, consider an arbitrary region Q. We can approximate $V(Q)$ arbitrarily well by filling Q with a disjoint union of sufficiently small annular arcs. Examples of such approximations strictly contained in Q (region A^1_Q) and strictly containing Q (region A^2_Q) are shown in Figure 35. Taking the limit where the arc size goes to zero proves the volume formula for arbitrary Q. Interested readers may find an additional proof for the Poincaré patch in [3].

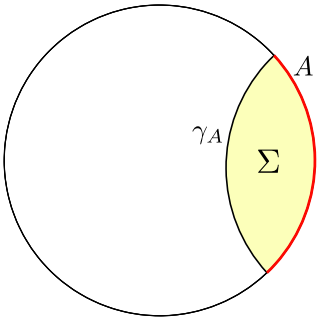

Figure 36: Subregion complexity of interval A in global AdS_3 is given by the volume of the region Σ. Figure by Raimond Abt from [3].

10.3 VACUUM SUBREGION COMPLEXITY

Given the volume formula (10.11), we are in a position to derive an expression for subregion complexity in a vacuum state in terms of entanglement entropy. Recall that the holographic subregion complexity of a CFT interval is defined to be $\frac{1}{8\pi G_N L}\text{vol}(\Sigma)$ [14], where Σ is the region contained beneath its RT surface. The situation differs slightly with respect to the previous chapter, because we deal with global AdS_3, see Figure 36. Using the kinematic space parametrization of entangling intervals of section 10.1, we denote the boundary interval by $(\theta_\Sigma, \alpha_\Sigma)$. The volume of Σ is easily computed, either directly [14, 50, 72] or by making use of the Gauss-Bonnet theorem [2] as we presented it in Chapter 9. Again we opt to compute the *topological complexity* $\mathcal{C}(\theta_\Sigma, \alpha_\Sigma)$ of the interval $(\theta_\Sigma, \alpha_\Sigma)$ via

$$\mathcal{C}(\theta_\Sigma, \alpha_\Sigma) = -\frac{1}{2}\int_\Sigma d\sigma\, \mathcal{R}\,. \tag{10.29}$$

We For constant $\mathcal{R}$ our definition (10.29) is proportional to the volume,

$$\mathcal{C}(\theta_\Sigma, \alpha_\Sigma) = -\frac{\mathcal{R}}{2}\text{vol}(\Sigma)\,, \tag{10.30}$$

and therefore to the subregion complexity of [14]. We will study this quantity with the normalization (10.30) of [2].

Let us emphasize that the volume formula (10.11) gives an integral expression for $\text{vol}(\Sigma)$ involving only entanglement entropies. Since entanglement entropy is a CFT quantity, this integral expression of the volume can be understood as a CFT formulation of the holographic subregion complexity. In the following we present the work of [2, 3], deriving explicitly the expression for $\text{vol}(\Sigma)$ in terms of entanglement entropies.

10.3.1 *Subregion Complexity in Terms of Entanglement Entropy*

In order to express $\mathrm{vol}(\Sigma)$ in terms of entanglement entropy alone, we apply the volume formula (10.11) to the region Σ lying below the geodesic $(\theta_\Sigma, \alpha_\Sigma)$,

$$\frac{\mathrm{vol}(\Sigma)}{4G_N} = \frac{1}{2\pi}\int_{\mathcal{K}} \lambda_\Sigma \omega\,. \tag{10.31}$$

Since we are considering vacuum states, the Crofton form ω depends only on entanglement entropies as evident from (10.6). The focus of our attention lies then on the chord length λ_Σ. For a given geodesic (θ, α), $\lambda_\Sigma(\theta, \alpha)$ is the length of the segment of (θ, α) which intersects Σ. We work with convex Σ. Then the chord length is simply the geodesic distance between the intersection points p, p' of the geodesic (θ, α) with the boundary of Σ, as exemplified in Figure 37. In (10.7) we gave an expression for the geodesic distance between two bulk points in terms of kinematic space quantities,

$$\frac{\lambda_\Sigma}{4G_N} = \frac{1}{4}\int_{\Delta_{pp'}} \omega\,. \tag{10.32}$$

The set $\Delta_{pp'}(\theta, \alpha) \subset \mathcal{K}$ is the region bounded by the two point curves corresponding to p and p' for fixed geodesic (θ, α) as can be seen in Figure 31. Of course, if (θ, α) does not intersect Σ then p, p' do not exist, and $\Delta_{pp'}$ is empty. In this case, (10.32) implies $\lambda_\Sigma(\theta, \alpha) = 0$ as required. Combining (10.31) and (10.32), we obtain an expression for $\mathrm{vol}(\Sigma)$ in terms of entanglement entropy,

$$\frac{\mathrm{vol}(\Sigma)}{4G_N^2} = \frac{1}{2\pi}\int_{\mathcal{K}} \omega\Big(\int_{\Delta_{pp'}} \omega\Big) = \frac{1}{8\pi}\int_{\mathcal{K}} d\theta d\alpha \int_{\Delta_{pp'}} d\theta' d\alpha' \partial_\alpha^2 S(\alpha)\partial_{\alpha'}^2 S(\alpha')\,. \tag{10.33}$$

Finally, applying (10.30) and inserting the relations $\mathcal{R} = -2/L^2$ and $G_N = 3L/2c$ gives an expression for the subregion complexity in terms of entanglement entropy:

$$\mathcal{C}(\theta_\Sigma, \alpha_\Sigma) = \frac{9}{8\pi c^2}\int_{\mathcal{K}} d\theta\, d\alpha \int_{\Delta_{pp'}} d\theta' d\alpha' \partial_\alpha^2 S(\alpha)\partial_{\alpha'}^2 S(\alpha')\,. \tag{10.34}$$

This expression the first main result of this chapter [3]: it defines a CFT quantity depending only on S and the integration region $\Delta_{pp'}$. To give a purely field theory expression for subregion complexity, if we can construct $\Delta_{pp'}$ purely within field theory. This is our next step.

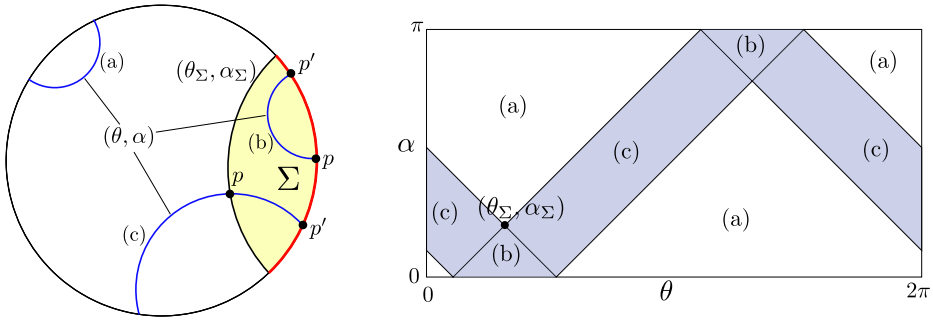

Figure 37: We distinguish three types of geodesics in the construction of $\Delta_{pp'}$ Type (a) geodesics do not intersect Σ at all. Type (b) geodesics lie entirely inside of Σ. Type (c) geodesics lie only partially inside of Σ. The intersection points p and p' of a geodesic with the boundary are interpreted as endpoints of entangling regions. On the LHS we show these three types in the bulk, while the RHS depicts the location of the three different types of geodesics in kinematic space. Figure by Raimond Abt from [3].

10.3.2 *Regions of Integration for Complexity*

The integrand on the right hand side of (10.34) contains only field theory quantities. We did, however, draw intuition from the bulk geometry to construct the region of integration $\Delta_{pp'}(\theta, \alpha)$ for each geodesic (θ, α). We now explain how to obtain the explicit form of $\Delta_{pp'}$ directly within CFT. Keep in mind that, as emphasized in Sec. 10.1, the geometry of kinematic space can be constructed from entanglement entropy. Therefore, if we can construct the $\Delta_{pp'}$ only in terms of the geometry of $\mathcal{K}$, we no longer reference the bulk in any way and hence compute subregion complexity in the field theory.

The regions $\Delta_{pp'}$ are bounded by point curves, which are space- or light-like geodesics in $\mathcal{K}$ [87]. So they are very natural objects in kinematic space. Thus the only thing left to do is to find a construction rule for the point curves of interest that can be formulated from the CFT perspective.

It is instructive to first examine these point curves from the bulk point of view and then translate our results into CFT language. We distinguish three types of geodesics, as depicted in Figure 37:

Type (a) geodesics are those (θ, α) that do not intersect Σ at all. Such geodesics have $\Delta_{pp'} = \emptyset$, and therefore $\lambda_\Sigma(\theta, \alpha) = 0$.

Type (b) geodesics are those (θ, α) that lie completely inside of Σ. In this situation, the intersection points p and p' are located on the conformal boundary, i.e. the constant time slice of the CFT. They are the endpoints of the entangling interval associated with (θ, α) and can be interpreted as points that lie on the boundary of $\mathcal{K}$. In particular they lie within the entangling interval corresponding to $(\theta_\Sigma, \alpha_\Sigma)$. Their corresponding point curves are null geodesics

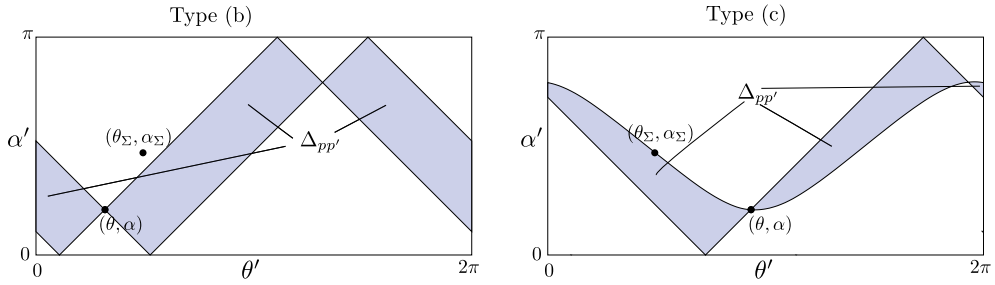

Figure 38: The regions of integration $\Delta_{pp'}(\theta, \alpha)$ for geodesics (θ, α) that are of type (b) and (c) w.r.t. $(\theta_\Sigma, \alpha_\Sigma)$. For type (b) geodesics $\Delta_{pp'}$ is bounded by light rays. For type (c) geodesics one boundary of $\Delta_{pp'}$ is the unique point curve that passes through $(\theta_\Sigma, \alpha_\Sigma)$ and (θ, α). Figure by Raimond Abt from [3].

[87] emitted from p and p'. Consequently, the region $\Delta_{pp'}$ enclosed by these light rays consists of causal diamonds in $\mathcal{K}$. An example of such a $\Delta_{pp'}$ is depicted in Figure 38.

Type (c) geodesics are those (θ, α) that lie only partially inside Σ. One of their intersection points p lies on the geodesic $(\theta_\Sigma, \alpha_\Sigma)$, while the other, p', lies on the boundary in the interval specified by $(\theta_\Sigma, \alpha_\Sigma)$. As for type (b), p' is one of the endpoints of the entangling region corresponding to (θ, α). Therefore, p' is a boundary point of $\mathcal{K}$ and the point curve of p' is once again a null geodesic emitted from p'. The point curve of p is a space-like geodesic in $\mathcal{K}$, as is explained in section 10.1. Noting that p lies on both geodesics $(\theta_\Sigma, \alpha_\Sigma)$ and (θ, α), the point curve of p is determined to be the unique geodesic in $\mathcal{K}$ containing both $(\theta_\Sigma, \alpha_\Sigma)$ and (θ, α). One example of such a $\Delta_{pp'}$ is depicted in Figure 38.

Observe that it is not possible for both p and p' to lie on the geodesic $(\theta_\Sigma, \alpha_\Sigma)$, since this would mean that the geodesic (θ, α) intersects $(\theta_\Sigma, \alpha_\Sigma)$ twice. Therefore, types (a)-(c) exhaust all possibilities. The right hand side of Figure 37 illustrates the location of different types of geodesics in kinematic space. Type (b) geodesics lie in the past of $(\theta_\Sigma, \alpha_\Sigma)$ and the future of $(\theta_\Sigma + \pi, \pi - \alpha_\Sigma)$, while type (c) geodesics are those enclosed by the light rays emitted from the endpoints of the entangling region associated to $(\theta_\Sigma, \alpha_\Sigma)$. All remaining geodesics are of type (a).

Now that we have constructed the region of integration $\Delta_{pp'}$ in terms of point curves, the next step is to recast this into field theoretic language. We now lay emphasis on the interpretation of $\mathcal{K}$ as the space of CFT intervals. This endows $\mathrm{vol}(\Sigma)$ with meaning without referencing the bulk geometry. When we treat (θ, α) and $(\theta_\Sigma, \alpha_\Sigma)$ as entangling intervals, the three types (a)-(c) distinguish where the endpoints of (θ, α) lie relative to $(\theta_\Sigma, \alpha_\Sigma)$ as presented in Figure 37: an entangling interval is of type (a) if none of its endpoints lie inside $(\theta_\Sigma, \alpha_\Sigma)$; the intervals

with both endpoints lying inside $(\theta_\Sigma, \alpha_\Sigma)$ are of type (b); of type (c) are the entangling regions with only one endpoint lying in $(\theta_\Sigma, \alpha_\Sigma)$.

We have therefore constructed $\Delta_{pp'}$ using only entangling regions and the geometry of $\mathcal{K}$:

- If (θ, α) is of type (a), we set $\Delta_{pp'}(\theta, \alpha) = \emptyset$.
- If (θ, α) is of type (b), $\Delta_{pp'}(\theta, \alpha)$ is the region bounded by the light rays emitted from both boundary points of (θ, α). (Fig. 38)
- If (θ, α) is of type (c), $\Delta_{pp'}(\theta, \alpha)$ is the region bounded by the light rays emitted from the endpoint of (θ, α) that lies inside of $(\theta_\Sigma, \alpha_\Sigma)$ and the space-like geodesic that intersects $(\theta_\Sigma, \alpha_\Sigma)$ and (θ, α). (Fig. 38)

Th volume formula is now specified by two components: the geometry of kinematic space, and the integration regions $\Delta_{pp'}$. The geometry of $\mathcal{K}$ is defined in terms of entanglement entropy, while we have shown that the form $\Delta_{pp'}$ is determined by this geometry. From our construction it is obvious that the resulting object (10.34) is actually defined for any CFT, regardless of whether it has a holographic dual or not. Nevertheless, when the CFT does possess a weakly curved holographic dual, this quantity coincides with the holographic subregion complexity (10.30).

It is clear that the only entangling intervals contributing to (10.34) have either one or both endpoints lying in the interval $(\theta_\Sigma, \alpha_\Sigma)$. In other words, only intervals of type (b) and (c) are present. For the outer integral (over θ, α) this is clear, simply because $\Delta_{pp'}(\theta, \alpha)$ is empty for intervals with no endpoint contained in $(\theta_\Sigma, \alpha_\Sigma)$. To see this for the integral computing chord lengths (over θ', α'), note that the region of integration $\Delta_{pp'}(\theta, \alpha)$ for type (b) and (c) is given by the set of geodesics passing through the chord of geodesic (θ, α) in Σ (see Section 10.1). As a result, the geodesics in $\Delta_{pp'}(\theta, \alpha)$ intersect Σ and must thus be of type (b) or (c) as well.

Let us briefly address the more general problem of evaluating the volume of an arbitrary bulk region Q. Attentive readers will have noticed that our ability to reconstruct the subregion complexity from the field theory relied crucially on the fact that Σ is defined by a geodesic. For arbitrary region Q it is rather opaque how to construct the integration regions in kinematic space without referencing the bulk. Nevertheless, we stress that it is possible to express arbitrary volumes in terms of entanglement entropies, in the same way that it is possible to express the length of an arbitrary curve as an integral over kinematic space.

10.3.3 *Subregion Complexity for Global AdS_3*

The last section explained how to construct the regions of integration in (10.34) from the field theory perspective. Now, we explicitely evaluate

(10.34) thereby computing the subregion complexity. In this section we consider global AdS_3 (10.12) and present the complexity for the cases where (1) the entangling interval $(\theta_\Sigma, \alpha_\Sigma)$ is the entire CFT circle, and (2) where it is half of this circle. General intervals for the Poincaré patch will be considered can be found in [3].

Consider equation (10.34) for the subregion complexity. The entanglement entropy S is found in (10.13). Note that $S \propto \mathsf{c}$ and thus we also have $\mathcal{C} \propto \mathsf{c}^0$. Of course, the complexity diverges, and must be regularized. The cutoff is the final subtlety we have to construct from the field theory. In the bulk, subregion complexity is defined as the volume below the RT surface and radial cutoffs are the natural choice We could translate this cutoff to kinematic space and use it for our computations. It does not come as a surprise that this regularization is not very natural from the kinematic space or CFT perspective. Once more we emphasize that we wish to compute complexity without using the bulk. We therefore opt for a different cutoff scheme: Introduce a minimal opening angle ξ and restrict to the part of kinematic space with opening angles $\alpha, \alpha' \in [\xi, \pi - \xi]$ as depicted in the LHS of Figure 39. This cutoff is in fact very natural from the CFT perspective as it filters out entangling intervals with an opening angle smaller than ξ. This cutoff scheme therefore naturally implements the usual UV cutoff chosen in the CFT.

As an example we take the entangling region to be the entire constant time slice In this case all entangling intervals (θ, α) are of type (b) (see Section 10.3.2), and therefore $\Delta_{pp'}(\theta, \alpha)$ consists of causal diamonds that now need to be cut off at $\alpha' = \xi$ and $\alpha' = \pi - \xi$. The resulting complexity of the entire CFT circle is thus [2, 3]

$$\mathcal{C}(\text{circle}) = \frac{9}{8\pi \mathsf{c}^2} \int_0^{2\pi} d\theta \int_\xi^{\pi-\xi} d\alpha \int_{\Delta^\xi_{pp'}} d\theta' d\alpha' \partial^2_\alpha S(\alpha) \partial^2_{\alpha'} S(\alpha') \,. \quad (10.35)$$

The region of integration $\Delta^\xi_{pp'}$ is depicted in the LHS of Figure 39. The inner integral easily evaluated,

$$\begin{aligned} \int_{\Delta^\xi_{pp'}} d\theta' d\alpha' \partial^2_{\alpha'} S(\alpha') &= -\frac{8\mathsf{c}}{3} \left(\log\left(\frac{\sin(\alpha)}{\sin(\xi)} \right) + \xi \cot(\xi) \right) \\ &= -\frac{8\mathsf{c}}{3} \left(\log\left(\frac{\sin(\alpha)}{\xi} \right) + \mathcal{O}(\xi^0) \right) . \end{aligned} \quad (10.36)$$

As $\xi \to 0$, this integral approaches -8 times the entanglement entropy of the boundary interval $[p, p']$, provided the CFT cutoff is identified with ξ appropriately. The integral (10.36) is proportional to the length of the geodesic connecting p and p' (see (10.7) and Figure 37) as it should be. The RT proposal relates this length to entanglement entropy. The expression (10.36) thus showcases the correct logarithmic divergence in our chosen cutoff scheme.

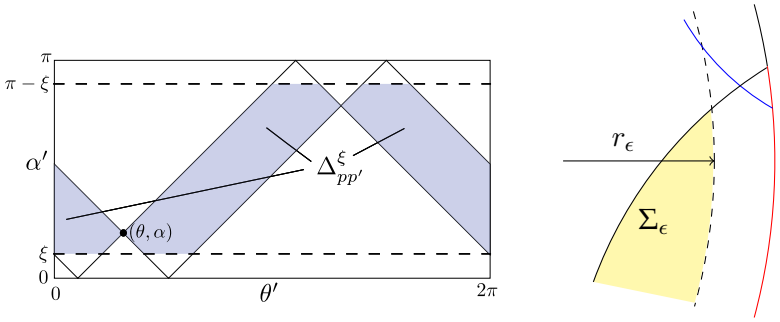

Figure 39: LHS: Cutoff scheme in kinematic space exemplified with type (b) geodesics. After introducing cutoffs at $\alpha' = \xi$ and $\alpha' = \pi - \xi$ the region of integration $\Delta_{pp'}(\theta, \alpha)$ reduces to $\Delta^{\xi}_{pp'}(\theta, \alpha)$. Figure by Raimond Abt from [3] RHS: Inequivalence of the radial cutoff and the kinematic space cutoff scheme.By choosing a cutoff at a fixed radial coordinate r_ϵ in the bulk (dashed line) we reduce Σ to a regularized region Σ_ϵ drawn in yellow.While the blue geodesic does not contribute to $\mathrm{vol}(\Sigma_\epsilon)$, it does contribute to the volume regularized with the kinematic space cutoff scheme, since its size is larger than ξ. Figure by Charles Melby-Thompson from [3].

By inserting (10.36) into (10.35) and performing the outer integral, we obtain [3]

$$\mathcal{C}(\text{circle}) = 4\left(\xi\cot^2(\xi) + \cot(\xi) + \xi - \frac{\pi}{2}\right) = \frac{8}{\xi} - 2\pi + \mathcal{O}(\xi^2)\,. \quad (10.37)$$

Had we chosen a radial cutoff $r_\epsilon = Ll_{\mathrm{CFT}}/\epsilon$, as was done in [2] and Chapter 9, we could relate the results via setting $\xi = 4\epsilon/\pi l_{\mathrm{CFT}}$. Note that, just as in the previous chapter we find a constant piece -2π.

We note that our kinematic space cutoff scheme is not equivalent to any sharp geometric cutoff in the bulk. To see this explicitly, we consider the region Σ_ϵ obtained by regulating Σ at the radial cutoff r_ϵ, as shown in the RHS of Figure 39. When computing the regularized subregion complexity in the kinematic space prescription with a cutoff at fixed ξ, however, the result receives contributions from geodesics – like the blue geodesic of the figure – that have an opening angle larger than ξ and yet do not intersect the bulk region Σ_ϵ.

The fact that the constant coefficient in the subregion complexity is the same in both cutoff schemes supports the idea that it is indeed universal [2, 14]. This statement is corroborated by the result for the complexity of one half of the CFT circle, computed in the Appendix of [3]. We find

$$\mathcal{C}(\text{semicircle}) = 2\xi\cot^2(\xi) + 2\cot(\xi) + 2\xi - \pi = \frac{4}{\xi} - \pi + \mathcal{O}(\xi^2)\,. \quad (10.38)$$

The constant and divergent parts of the complexity match the general results of the previous chapter, which showcased in [2], provided we

identify $\xi = 4\epsilon/\pi l_{\text{CFT}}$. In that paper one also finds the explicit evaluation for an arbitrary subregion complexity in the Poincaré patch. Moreover, in that case it is possible to relate the subregion complexity to *mutual information*.

10.4 EXCITED STATES

It is time to apply what we have learned to excited states. It turns out that the same tools we used to study the vacuum can be applied to quotients of AdS_3 by discrete groups of isometries. This is ultimately the case, because the kinematic spaces for these geometries are themselves a quotient of the AdS_3 kinematic space.

Our focus lies on the *conical defect* and (static) *BTZ black hole* geometries. In the CFT, these are dual to light primary excitations and finite temperature states, respectively. Because the kinematic spaces of these geometries are quotients of the vacuum kinematic space, it follows that the volume formula derived above for vacuum AdS still applies, with the measure ω inherited from the quotienting procedure.

Nevertheless there are several important disctinctions to be made with the vacuum case. The most important difference is perhaps that a given boundary interval may now have multiple geodesics terminating on its endpoints, and only the shortest of *minimal* geodesic carries the interpretation of entanglement entropy through the RT proposal. Non-minimal geodesics come in two classes. The first are those anchored at the endpoints of a boundary interval, but are not minimal; these we call *winding geodesics*. The second are those with only one endpoint lying on the boundary; these occure only for thermal states, as we will see.

In general, the bulk contains regions that are not penetrated minimal geodesics. Such regions untouched by entanglement entropy go by the name *entanglement shadow*. Fortunately, the entanglement shadow is probed by non-minimal geodesics, which are naturally described within the quotient kinematic spaces. In the literature, non-minimal geodesics constitute the building blocks of an observable called *entwinement* [38], and were conjectured to measure correlations between internal degrees of freedom. For symmetric orbifold theories, an expression for entwinement with the correct properties was proposed in [35].

The non-uniqueness of geodesics implies that the kinematic space measure ω is no longer given purely by entanglement entropy. This is plausible once one recalls that at large c the entropy is sensitive only to the shortest geodesic. In order to express the subregion complexity in terms of CFT quantities, we would therefore need to compute the lengths of non-minimal geodesics by alternate means, something that remains impossible with the present tools. In contrast to the conical defect, thermal states also possess geodesics that pass through the black hole horizon. These contributions have been considered for the first time

in [3] and we expect them to be associated to the thermal part of the reduced density matrix. This is discussed below.

We begin this section by studying volumes first in conical defect geometries, followed by the BTZ black hole. We end by examining the decomposition of subregion complexity into contributions from entanglement entropy and from non-minimal geodesics, and a discussion of its physical significance.

10.4.1 *Primary States: The Conical Defect $\mathcal{CD}_N$*

The metric of the conical defect geometry $\mathcal{CD}_N$ takes the same form as the AdS_3 geometry (10.12), except that the periodicity of ϕ is shortened by the quotient to $\phi \sim \phi + 2\pi/N$ $(N \in \mathbb{N})$. More concretely, it can be thought of as a quotient of pure AdS_3,

$$\mathcal{CD}_N = \frac{\mathrm{AdS}_3}{\mathbb{Z}_N}\,. \tag{10.39}$$

The kinematic space metric of the conical defect has been worked out in [81]. It takes the same form (10.6) as in the vacuum,

$$ds^2_{\mathcal{K}} = -\frac{1}{2}\partial^2_\alpha S(-d\alpha^2 + d\theta^2)\,, \quad \omega = -\frac{1}{2}\partial^2_\alpha S d\theta \wedge d\alpha\,, \tag{10.40}$$

the difference being again that now $\theta \sim \theta + 2\pi/N$. As a result, some geodesics have lengths computed by entanglement entropy, while others are non-minimal geodesics, winding multiple times around the singularity. The fundamental region is divided into sectors $\alpha \in \mathcal{W}_n^{\pm}$ specified by

$$\mathcal{W}_n^{+} = \left(\frac{n\pi}{2N}, \frac{(n+1)\pi}{2N}\right], \tag{10.41}$$

$$\mathcal{W}_n^{-} = \left[\frac{(2N-n-1)\pi}{2N}, \frac{(2N-n)\pi}{2N}\right), \tag{10.42}$$

with $n \in \{0, ..., N-1\}$. $\mathcal{W}_n^{\pm}$ describes the geodesics with winding number n and orientation $\pm$. Minimal geodesics, i.e. entanglement entropy, lie in the sector $n = 0$, while geodesics with $n \neq 0$ are non-minimal. An illustration of these sectors is given in Figure 40 for the case $N = 3$.

We can now explicitely very that non-minimal geodesics are necessary and sufficient to compute the volume of the constant times slice of the conical defect,

$$\begin{aligned}\mathcal{C}(\mathcal{CD}_N) &= \frac{9}{8\pi \mathsf{c}^2}\underbrace{\int_0^{2\pi/N} d\theta}_{2\pi/N}\underbrace{\int_\xi^{\pi-\xi} d\alpha \int_{\Delta^\xi_{pp'}} d\theta' d\alpha' \partial^2_\alpha S(\alpha)\partial^2_{\alpha'} S(\alpha')}_{\text{cf. (10.35)}} \\ &= \frac{1}{N}\mathcal{C}(\text{circle})\,.\end{aligned} \tag{10.43}$$

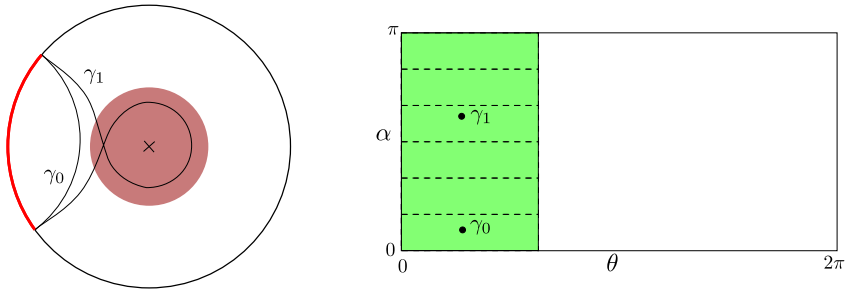

Figure 40: Left: Conical defect with $N = 3$. A minimal (γ_0) and a non-minimal (γ_1) geodesic are depicted. The latter reaches into the entanglement shadow, drawn in red. Right: kinematic space for $N = 3$. Minimal geodesics correspond to the lowest and upmost ($n = 0$) sectors. The rest correspond to non-minimal geodesics such as γ_1. Figure by Raimond Abt from [3].

Neglecting contributions from non-minimal geodesics, on the other hand, leads to expressions with the wrong divergence structure. In other words, using only entanglement entropy in excited states to compute subregion complexity is not even meaningful. Indeed, if we evaluate the outer integral in (10.43) over minimal geodesics alone, we obtain

$$-\frac{1}{2}\int_0^{\frac{2\pi}{N}} d\theta \left[\int_\xi^{\frac{\pi}{2N}} d\alpha + \int_{\frac{(2N-1)\pi}{2N}}^{\pi-\xi} d\alpha\right] \underbrace{\int_{\Delta^\xi_{pp'}} d\theta' d\alpha' \partial^2_{\alpha'} S(\alpha')}_{\text{cf. (10.36)}} \partial^2_\alpha S(\alpha)$$
$$= \frac{\text{vol}(\text{AdS}_3)}{N} - \frac{\pi}{N}\left(2\cot\left(\frac{\pi}{2N}\right)\log\left(\frac{\sin(\pi/2N)}{\xi}\right) - \frac{\pi}{N}(N-1)\right) + \mathcal{O}(\xi^2)\,. \tag{10.44}$$

Here, $\text{vol}(\text{AdS}_3)$ is the volume (10.37) of a constant time slice of AdS_3. Only by setting $N = 1$, i.e. the vacuum, does this produce a sensible answer and coincides with (10.43). In fact, away from $N = 1$ the logarithmic dependence on the cutoff is not even consistent with a volume in an asymptotically AdS_3 spacetime, which should exhibit as its sole singularity a term scaling as ξ^{-1} [2]. By comparison with (10.43), we see that the problematic logarithm of (10.44) drops out when we include non-minimal geodesics.

Finally, we emphasize that non-minimal geodesics are required not only to compute volumes in the entanglement shadow, but also for regions outside of it, as is evident from Figure 40.

10.4.2 *Subregion Complexity at Finite Temperatures*

Our last application of the volume formula treats BTZ black hole geometries [39]. For simplicity we restrict ourselves to the spinless solution ($J = 0$), whose metric is

$$ds^2 = -\frac{r^2 - r_0^2}{L^2} dt^2 + \frac{L^2}{r^2 - r_0^2} dr^2 + r^2 d\phi^2 \,, \qquad \phi \sim \phi + 2\pi \,. \tag{10.45}$$

The first step is to set up the BTZ kinematic space[2] and subsequently we can generalize the volume formula (10.11) to this case. We then compute the BTZ subregion complexity through this formula. It is written simplest in terms of the Poincaré patch measure of [2].

Kinematic Space of the BTZ Black Hole

The BTZ black hole geometry (10.45) is obtained from AdS_3 by quotienting by a discrete group of isometries with a particularly simple form in Poincaré patch coordinates. Consider first the Poincaré patch metric in the form

$$ds^2 = L^2 \frac{-(dx^0)^2 + (dx^1)^2 + dz^2}{z^2} = L^2 \frac{dx^+ dx^- + dz^2}{z^2} \,, \tag{10.46}$$

with $x^\pm = x^1 \pm x^0$. The map

$$x^\pm = \left(1 - \frac{r_0^2}{r^2}\right)^{1/2} e^{\frac{r_0}{L}(\phi \pm t/L)} \,, \qquad z = \frac{r_0}{r} e^{\frac{r_0}{L}\phi} \,, \tag{10.47}$$

is a local isometry of (10.45). The periodicity $\phi \sim \phi + 2\pi$ of the BTZ coordinates is mirrored in the equivalence relation

$$(x^0, x^1, z) \sim e^{2\pi r_0/L} (x^0, x^1, z) \,. \tag{10.48}$$

This identification generates a group of infinite order, and the quotient of the Poincaré patch by it is isometric to a region in the maximally extended BTZ geometry of mass $M = r_0^2/L^2$.

Observe that $x^0 = 0$ is a fixed point of the identification (10.48). As a consequence the spatial slice of constant time $t = 0$ of the black hole geometry is the image of the spatial slice $x^0 = 0$ of the Poincaré patch,

$$ds^2 = L^2 \frac{(dx^1)^2 + dz^2}{z^2} \,. \tag{10.49}$$

2 Two versions of BTZ kinematic space have appeared in the literature: quotient kinematic spaces of the type used here also appeared in [85, 235], whereas the kinematic space of [21] contained only minimal geodesics.

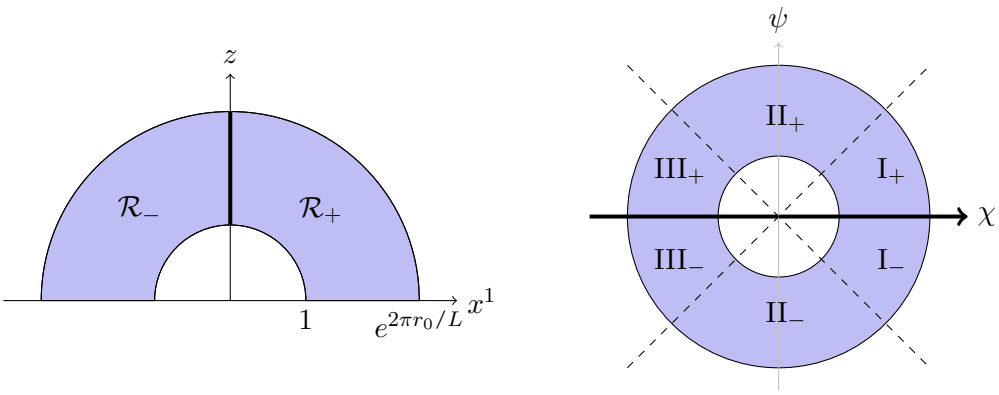

Figure 41: Figure on left: Fundamental region for the spatial slice of the 2-sided black hole in Poincaré patch coordinates (10.52). The horizon (thick line) separates the two asymptotic regions $\mathcal{R}_+$ and $\mathcal{R}_-$. Figure on right: The black hole's kinematic space is divided into six fundamental domains in (χ, ψ) coordinates. The ratio of the outer and inner radii is $e^{2\pi r_0/L}$. The metric diverges as one approaches the thick line $\psi = 0$. Figure by Charles Melby-Thompson from [3].

The quotient space of this slice is, in fact, globally equivalent to the spatial slice of the two-sided BTZ black hole. For our purposes the most convenient fundamental domain is

$$1 \leq (x^1)^2 + z^2 < e^{4\pi r_0/L} \tag{10.50}$$

All fundamental domains of the BTZ kinematic space are depicted in Figure 41. Note each geodesic in the slice is mapped to a geodesic, modulo the identification (10.48), which acts simultaneously on both endpoints. This confirms that kinematic space of BTZ is again a quotient of the kinematic space of AdS_3. As in section 4.4. of [3], spatial geodesics in the Poincaré patch ending at $x^1 = u, v$ can be written as $u = \chi - \psi$, $v = \chi + \psi$. This parametrization hands us the kinematic space of BTZ as the quotient manifold

$$ds^2_{\mathcal{K}_{\mathrm{BTZ}}} = \frac{\mathsf{c}}{6}\frac{d\chi^2 - d\psi^2}{\psi^2}\,, \qquad (\chi, \psi) \sim e^{2\pi r_0/L}(\chi, \psi)\,. \tag{10.51}$$

The horizon corresponds to the line $x^0 = x^1 = 0$ in the Poincaré patch geometry.

Both sides of the black hole are separated by the horizon, which is drawn as dark line on the LHS of Figure 41. BTZ kinematic space naturally separates into six families. In terms of the covering space coordinates (u, v), we associate region I_+ with $0 < u < v$, region II_+ with $u < 0 < v$ and region III_+ with $u < v < 0$. The corresponding orientation reversals, region I_-, II_- III_- are found through $(u \leftrightarrow v)$ of the prior sets. Each region has a convenient coordinate system. For instance I_+, which are the geodesics contained entirely in the positive

asymptotic region with $0 < u < v$ (see Figure 41) is appropriately parametrized by

$$v = e^{\frac{r_0}{L}(\theta+\alpha)}\,, \qquad u = e^{\frac{r_0}{L}(\theta-\alpha)}\,, \tag{10.52}$$

This yields

$$ds^2_{\mathrm{I}_+} = \frac{r_0^2}{L}\frac{d\theta^2 - d\alpha^2}{\sinh^2(\frac{r_0\alpha}{L})}\,, \qquad \theta \sim \theta + 2\pi\,,\ \alpha \in \mathbb{R}\,. \tag{10.53}$$

Observe $ds^2_{\mathrm{I}_+}$ behaves exactly as the vacuum kinematic space metric (10.14) in the limit $\alpha \to 0$, as it should. Geodesics are classified into sectors through their opening angle $\alpha \in \mathcal{V}_n$,

$$\mathcal{V}_n = [2\pi n, 2\pi(n+1))\,. \tag{10.54}$$

Sector $\mathcal{V}_n$ is said to have winding number n, similar to the conical defect kinematic space of the previous section. Here we encounter a new set of geodesics, namely geodesics passing through the horizon corresponding to $u < 0 < v$. We set

$$v = e^{\frac{r_0}{L}(\tilde\theta+\tilde\alpha)} \qquad u = -e^{\frac{r_0}{L}(\tilde\theta-\tilde\alpha)}\,, \tag{10.55}$$

leading to the geometry

$$ds^2_{\mathrm{II}_+} = \frac{r_0^2}{L}\frac{d\tilde\alpha^2 - d\tilde\theta^2}{\sinh^2(\frac{r_0\tilde\alpha}{L})}\,, \qquad \tilde\theta \sim \tilde\theta + 2\pi\,,\ \tilde\alpha \in \mathbb{R}\,. \tag{10.56}$$

The other four patches are related to (10.53) and (10.56) by sign changes. I_+, II_+, and III_+ all meet at a cuspoidal point, the (positively oriented) horizon geodesic, which corresponds in the two coordinate systems above to $\alpha \to \infty$ and $\tilde\alpha \to \infty$, respectively.

Volume Formula at Finite Temperature

We are finally in a position to compute volumes in the BTZ black hole geometry through the volume formula (10.11). The quotient construction provides a recipe applying the volume formula: given a volume in BTZ, we first lift it to the fundamental domain (10.50) where we are free to employ (10.11). It is a fact of life in black hole geometries that one always requires contributions from geodesics passing through the horizon, even for regions Q located entirely outside the black hole. Pulling the resulting quantities back to BTZ kinematic space, the volume becomes

$$\frac{\mathrm{vol}(Q)}{4G_N} = \frac{1}{2\pi}\sum_{\mathcal{D}}\int \lambda_Q \omega_{\mathcal{D}}\,, \tag{10.57}$$

with $\mathcal{D}$ running over the domains $\mathrm{I}_\pm$, $\mathrm{II}_\pm$, and $\mathrm{III}_\pm$ of Figure 41. Note that contributions from region $\mathrm{III}_\pm$ trivially vanish when Q lies outside

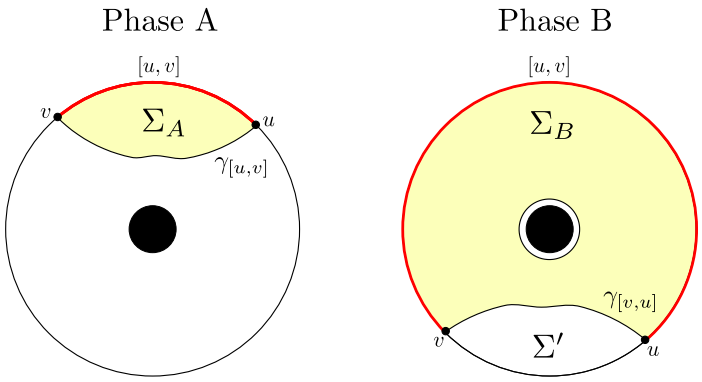

Figure 42: Entanglement phase transition for BTZ black hole. If the entangling interval $[u,v]$ is too large, the RT surface is no longer the geodesic $\gamma_{[u,v]}$ lying on the same side of the black hole as $[u,v]$ (Phase A), but composes of the black hole horizon and the geodesic $\gamma_{[v,u]}$ lying on the opposite side of the black hole (Phase B). At the the phase transition the volume below the RT surface jumps from $\mathrm{vol}(\Sigma_A)$ to $\mathrm{vol}(\Sigma_B)$. Figure by Raimond Abt from [3].

the horizon. Finally, we give the Crofton form in the coordinates (10.52) and (10.55):

$$\omega_{\mathrm{I,III}} = \frac{\mathsf{c}}{6}\frac{d\theta \wedge d\alpha}{\sinh^2(\frac{r_0}{L}\alpha)} \qquad \omega_{\mathrm{II}} = -\frac{\mathsf{c}}{6}\frac{d\tilde{\theta} \wedge d\tilde{\alpha}}{\sinh^2(\frac{r_0}{L}\alpha)}\,. \tag{10.58}$$

Note that the contributions from the "$-$" regions equals that from the "$+$" regions and thus we are free to omit the former in exchange for an overall factor of 2 on the contributions of the latter.

In practice, the simplest way to perform computations is to work directly with a fundamental region in Poincaré patch. We now turn to the application of this method to evaluating the holographic subregion complexity in BTZ.

Subregion Complexity and the Phase Transition

It is time to address the topological jump of Chapter 9. For convenience we briefly recall the situation outlined in detail in Section 9.1.2. The entanglement entropy of an interval (u,v) is the minimal curve homologous to that interval [161] and the subregion complexity is the volume of the region subtended by it. Depending on the size of the interval, there are two such curves, corresponding to distinct phases[3] A and B (see Figure 42). In phase A, the minimal curve is simply the curve in $\mathcal{V}_0$ ending on (u,v). In phase B, it is the union of the curve in $\mathcal{V}_{-1}$ and the curve ending on (v,u) (orientation reversal!) and the horizon geodesic. The dominant phase is picked out by having the shortest length. We

3 Since we used the letters a, b, c to indicate geodesic types we call the phases A, B here instead of a, b and in the previous chapter.

saw in Section 9.1.2 that under the transition from phase A to phase B, affects the topological complexity (10.29) by an increase of 2π.

We compute the subregion complexity by applying the Poincaré patch volume formula of [3] to a fundamental region. For comparison with the results of Section 9.1.2, we employ the bulk cutoff regularization. The correct domain of integration depends on the cutoff surface and differs from that in the Poincaré patch. The cutoff in the BTZ geometry lies at $r_\epsilon = L l_{\mathrm{CFT}}/\epsilon$, corresponding in the Poincaré patch to the x^1-dependent cutoff

$$\epsilon(x) = \left(\frac{r_\epsilon}{r_0} - 1\right)^{-1/2} |x^1| \,. \tag{10.59}$$

We quote the final result for the volume in phase A from [3]

$$\begin{aligned} \mathrm{vol}(\Sigma_A) &= L^2 \left(\left(\frac{r_\epsilon}{r_0} - 1\right)^{1/2} \log\left(\frac{v}{u}\right) - \pi \right) + \mathcal{O}(\epsilon) \\ &= L^2 \left(\frac{x}{\epsilon} - \pi\right) + \mathcal{O}(\epsilon) \,. \end{aligned} \tag{10.60}$$

Here $x = 2 l_{\mathrm{CFT}} \alpha$ is the length of the entangling interval in BTZ coordinates.

In phase B, the integration region of the volume formula reaches from the outside of the complementary geodesic up to the black hole horizon. Thus, the volume is evaluated by calculating the volume between boundary and horizon, and subsequently subtracting the volume subtended by the geodesic of the complementary interval $[v, u]$. We again quote the result from [3]

$$\begin{aligned} \mathrm{vol}(\Sigma_B) &= \mathrm{vol}(\text{outside horizon}) - \mathrm{vol}(\Sigma') \\ &= L^2 \left(\frac{x}{\epsilon} + \pi\right) , \end{aligned} \tag{10.61}$$

Here Σ' is region beneath $\gamma_{[v,u]}$ and x is the length of the boundary interval. The situation is depicted in Figure 42. The volume of the outside horizon region is computed in kinematic space by taking the integral over all geodesics, cut off at the horizon for those that fall into the black hole, weighted with the Crofton form. Comparing with (10.60) gives the expected jump in complexity of 2π. We note that the topological origin of the jump is completely blurred in the field theory, while it was handed to us on a silver platter on the gravity side by the Gauss-Bonnet theorem.

10.4.3 *A Bound on Subregion Complexity from Entanglement Entropy*

The above examples clarify that subregion complexity generally contains contributions other than entanglement entropy; only in the vac-

uum case do the latter suffice we have seen in Section 10.3. These extra contribution stem from non-minimal geodesics. Here we present an argument for isolating the contributions coming solely from the entanglement entropies.

We begin with the simpler case: the conical defect. Here, the only extra contributions to subregion complexity stem from winding geodesics. The first consequence is the violation of the one-to-one correspondence between geodesics and entangling intervals. Nevertheless, we can find equivalence classes of geodesics by associating all geodesics with the same pair of endpoints to the same entangling interval. It is therefore sensible to organize the expression (10.34) for the subregion complexity of a boundary interval A in the form

$$\mathcal{C}(A) = \int d\hat{\theta}\, d\hat{\alpha} \left(F_A^{CD} + G_A^{CD} \right), \tag{10.62}$$

where $\hat{\theta}$ and $\hat{\alpha}$ parametrize the set of boundary intervals as in the vacuum kinematic space (10.14). We have split the contributions to the subregion complexity into two pieces. The first is F_A^{CD}, which denotes the part containing only entanglement entropies. In other words, the subregions of $\mathcal{K}$ and $\Delta_{pp'}$ in the integral expression (10.34) due to minimal geodesics. The second piece, G_A^{CD}, contains all contributions from non-minimal geodesics winding around the singularity.

Let us repeat the same game with the BTZ black hole. It also has winding geodesics Additionally, black holes have a new class of geodesics contributing to subregion complexity, namely those that pass through the black hole horizon $r = r_0$. Because they are occure only at finite temperature, we dub them 'thermal contributions'. The subregion complexity splits into

$$\mathcal{C}(A) = \int d\hat{\theta} d\hat{\alpha} \left(F_A^{BTZ} + G_A^{BTZ} \right) + \text{thermal contributions}\,, \tag{10.63}$$

where F_A^{BTZ} denotes those contributions from entanglement entropies alone, and G_A^{BTZ} represents contributions of winding geodesics. The thermal contributions cannot be associated to a single entangling interval, since only one of their endpoints is anchored at the boundary, the other endpoint vanishes into the horizon. Therefore we have not included them into the integral in (10.63).

We have already noted that the contributions from entanglement entropy do not suffice to compute the subregion complexity. Nevertheless, these contributions, $\int F$, place a lower bound on the holographic subregion complexity, because all other contributions in (10.63) are non-negative.

SUMMARY

A major motivation for the work presented in this chapter was the complexity=volume conjecture. For our purposes a version of this proposal was more accesible: Alishahiha's conjecture that the volume subtended by an RT surface is dual to the complexity of the corresponding reduced density matrix [14]. Both proposals are difficult to test, since no satisfactory notion of complexity exists at present in the field theory. Yet, we can approach the problem from a complimentary point of view: Is it possible to compute Alishahiha's bulk geometric quantity purely through access of the field theory side? As shown in this chapter the answer is affirmative, at least in the vacuum of a large-N CFT.

Evidently, our answer, (10.34), aligns beautifully with the motto "entanglement builds geometry" [228] in case of the vacuum, since entanglement suffices solely to compute the volume. Yet, already for primary states or thermal states we require additional contributions. For the former we need non-minimal winding geodesics related to entwinement, while in the latter we furthermore need geodesics starting at the boundary and falling into the horizon. These geodesics have no clear interpretation in the field theory. Nevertheless, since they occur only for thermal states, because of the presence of an event horizon, they must carry important information of the thermal density matrix corresponding to the traced out state.

Susskind's catchphrase "entanglement is not enough" fits quite well, even though we take it slightly out of context.

Let us now consider the implications of our results under the premise that Alishahiha's proposal is valid [3]. The first is that in the vacuum state, subregion complexity depends purely on entanglement entropy, suggesting that vacuum subregion complexity is encoded in the spectrum of single-interval entanglement, at least in the large-N limit. This ceases to hold in non-vacuum geometries, where entwinement and thermal contributions become relevant. Yet, there is still a part of the complexity in each geometry we considered, which was sourced by entanglement entropies alone, as expressed in (10.62) and (10.63). In particular, we could show that these entanglement contributions provide a lower bound on Alishahiha's subregion complexity.

Our construction reveals that subregion complexity, in Alishahiha's sense, is universal in the vacuum and thermal states in that it depends solely on the central charge of the field theory. Current field theory proposals for complexity [149, 163] do not satisfy this property, because they show varying behavior for bosons and fermions. We should stress at this point though that these proposals are concerned with Gaussian states, while our construction is valid only for complexities in strongly interacting theories in the large-N limit. Nevertheless, this universality constitutes a strong test for any future candidate for subregion complexity in the field theory.

This ends our discussion on the borderline of gauge/gravity and quantum information. An outlook is found in Chapter 11.

11 CONCLUSION AND OUTLOOK

In this thesis we pursued two topics at the forefront of research in the field of gauge/gravity duality. The first was motivated by the connection of condensed matter with holography and the study of CFTs in general; we give a summary and outlook on our holographic Kondo flows in Section 11.1. The second topic was concerned with the relation of geometry to quantum information. Its summary and outlook is given in Section 11.2. Both of these two conclusion sections are dedicated solely to the topic in question. However, there are many important and interesting overlaps between interfaces and quantum information. We give an outlook concerning future work on that intersection in Section 11.3.

11.1 HOLOGRAPHIC KONDO RG FLOWS

Let us briefly summarize all findings in Part ii before giving an outlook.

We began with the formal WZW description of the Kondo effect in terms of conformal boundary conditions: a stack of pointlike branes condense into a single spherically extended brane, while sliding down on an S^3. This motivated us to look for similar flows in holography. The ideal stage was the F1/NS5 (D1/D5) system since it gives rise to string theory on $\mathrm{AdS}_3 \times S^3 \times T^4$ with S^3 described by an $\hat{\mathfrak{su}}(2)_k$ model, similar to the Kondo model.

Probe Branes, Chapter 5

We profited from existing literature [31, 64], with which we pinned down the IR fixed point of the Kondo flow as supersymmetric D3-brane with dissolved F1 and D1 charges. Moreover, for the case of pure D1 charge, we determined the flow profile of the polar angle θ on the S^3 away from the UV fixed point. It saturates at fixed value θ_p, thereby confirming a non-trivial IR fixed point, see Figure 12. When contemplating the UV fixed point we resorted to the non-abelian brane description of the stack of D1-branes. Evaluating the non-abelian DBI action is a difficult task in general. For us it sufficed to show that the flows were indeed tripped, which we were able to show by demonstrating that the tripping operator is marginally relevant. This is in fact identical to the original Kondo problem! Alltogether, this establishes the existence of the sought after Kondo flows, at least so long as the interfaces do not backreact. The next chapter amended this circumstance.

Backreacted Supergravity Solutions, Chapter 6

The probe brane description is inherently limited since many quantities of interest rely on backreaction, such as correlators in the CFT or the g-factors. We therefore compute the fully backreacted supergravity solutions dual to the UV and IR fixed points of our Kondo flow in the F1/NS5 and D1/D5 duality frame. The existence of the fixed points of the probe brane flows even for strong backreaction is confirmed. In particular, we can detect critical screening, which follows the same pattern as in the original Kondo effect.

Boundary Entropies, Chapter 7

We computed the g-factors for the fixed points of the flow holographically and confirmed the g-theorem. This fully legitimates the existence of our Kondo flows! Again, for critical screening the g-factors vanish in the IR, just as for the original Kondo model. Crucially, our g-factors contain important information, which is encoded in the backreaction of the gravity dual and cannot be reproduced by the probe brane limit. We concluded with a brief outline of the field theory side.

Outlook

One shortcoming of our discussion here is that we do not discuss the flow profiles for interfaces with extra F1 charge. This is more handily done in the D1/D5 frame and will appear in an upcoming publication [112]. Besides the many similarities with the original Kondo problem that we discovered, such as being tripped by a marginally relevant pertubation or critical screening, we mention one noteworthy difference here. When working with the field theory the impurity is valued in $\mathrm{SU}(N_5)$ (with N_5 the number of five-branes), in contrast to the original Kondo problem, where the impurity is valued in $\mathrm{SU}(2)$. This renders our impurity more in tune with the multichannel Kondo model, which obeys an $\mathrm{SU}(N_5)$ symmetry. However, it is not quite analogous to that model either, because the flows still happen on an $S^3 \simeq \mathrm{SU}(2)$. In that sense our model is a hybrid. This behavior is ultimately traced back to the fact that the D1/D5 system gives rise to a $\mathrm{U}(5)$ gauge theory that still has access to Kondo-like flows, because the S^3 inside $\mathrm{AdS}_3 \times S^3 \times T^4$ has a description as $\mathfrak{su}(2)_k$ WZW model.

Interesting work for the future would be for instance to look for brane annihilation processes. In the UV we place one stack of pointlike branes at both, the north and south pole, with opposite charge. The absolute value of the charges should be large enough so as to have the puffed up branes meet somewhere on the three-sphere along the RG flow. Also, it would be interesting to compute the reflection and transmission coefficients of these interfaces [184, 205] or one point functions. More in tune

with the original Kondo problem, one future direction is to work out the influence of temperature on the story outlined here. This involves extra black holes in the gravity dual.

Of course, the obvious question regards the field theory, which we only sketched in this thesis, because the details are still under inspection as of this writing. In the upcoming publication [112] we present a description of the interface quantum mechanics in terms of the gauge instanton description of the D1/D5 system [225–227]. While we have a good understanding of the interface in the IR in terms of Wilson operators of the type presented in [140, 141], the UV interfaces are elusive. Our approach is to determine the correct lagrangian of the system and pin down all possible boundary conditions with the appropriate symmetries. Future work here would be for instance to compute the g-factors in the field theory using supersymmetric localization [158, 159]. Moreover, from a mathematical perspective, the interfaces provide maps between two distinct D1/D5 CFTs. The RG flow itself then changes this mapping into another mapping. Therefore the flow provides a map between interface maps. It is interesting to investigate these connections from a category theoretic point of view in order to see what mappings are possible and to use this to study boundary RG flows in general.

We mentioned in the introduction that the Kondo model provided necessary insights into the construction of a host of boundary RG flows in BCFT [128, 130]. The flows that we studied here bear great resemblance with the flows investigated in [150]. This begs the question to what extend one can generalize our flows to other brane systems. Given the stable energy minima of brane configurations in [64], it certainly should be possible to extend the flows to holographic systems susceptible to these brane configurations. It is also desirable to find a representation theoretic explanation for these flows, possibly even similar to the "absorbtion of boundary spin" rule of [128, 130]. Fortunately, a great class of supersymmetric boundary conditions has already been classified in [135] and it remains to see if the appropriate ones for our flows are amongst these. In that case one can implement combinations of T- and S-dualities to find flows in different systems on the spot. A different route in this vein starts by noting that all these flows have a compact manifold in common, a sphere. One might wonder if one can also exend these flows to compact manifolds with multiple cycles.

One idea that motivated us to begin this project was the hope of finding interface-boundary fusion [33], which can be explicitely studied in the gravity dual. In particular we were interested in how the representation theoretic data was encoded in gravity. Unfortunately, our interfaces are not chiral [112] and therefore the desired fusion processes cannot be observed. The way out is to repeat our analysis in a different string theory background based on AdS_3, which have seen remarkable progress recently [88, 91, 93–102]. A natural candidate is $AdS_3 \times S^3 \times S^3 \times S^1$, because it features three-spheres on which to stage the same Kondo

flow as ours. Also, its symmetry algebra is related to the symmetry algebra of $AdS_3 \times S^3 \times T^4$. While the latter has *small* $\mathcal{N} = (4,4)$ superconformal symmetry, the former has *large* $\mathcal{N} = (4,4)$ superconformal symmetry. The main advantage of $AdS_3 \times S^3 \times S^3 \times S^1$ is however that it has points in moduli space, where the CFT is described by cosets. This extended symmetry structure raises the possibility of finding chiral interfaces considerably, and thus also the change of finding fusion processes gravitationally.

11.2 VOLUMES IN GRAVITY AND QUANTUM INFORMATION

Again, we briefly summarize all results relevant to this topic, which are found in Part iii before giving an outlook.

Topological Complexity, Chapter 9

We computed subregion complexity in AdS_3, i.e. the vacuum state, for multiple intervals via the Gauss-Bonnet theorem. We found multiple phases, for which the subregion complexity is distinguished solely by topology. In particular, the difference between phases is given by a multiple of the euler characteristic χ. We move on to study subregion complexity in for a single interval in the BTZ geometry. Again we find a phase transition, this time controlled by the mass of the black hole. The difference in subregion complexity between the phases is again determined by topology. In particular, there is no temperature dependence. When the RT surface does not engulf the black hole, the subregion complexity assumes the same value as in the vacuum. The subregion complexity of the conical defect geometry then interpolates between the two phases of the black hole, see Figure 29.

Volumes in Field Theory, Chapter 10

We provide and proof a formula, which computes subregion complexities without referencing the bulk. The subregion complexities of the vacuum AdS_3, the conical defect and the BTZ black hole are treated. The framework of choice is kinematic space. For the BTZ black hole we had to construct the kinematic space first. Our formula shows how the geometry is encoded in the field theory. In particular, the properties of the phase transitions are completely blurred in the process. Subregion complexities depend on three contributions in general: entanglement entropy, entwinement and thermal contributions ("Entanglement is not enough"). These are used to argue in favor of a lower bound for subregion complexity.

Outlook

What about Susskind's "complexity equals volume" proposal using our volume formula? We have already investigated a black hole. As is evident from Figure 41 the kinematic space of the BTZ black hole captures its two-sidedness. The success of computing volumes of black hole interiors via our formula hinges on whether volumes detached from the boundary can be computed solely through access of field theory data. This question can already be investigated using our setup. Should the answer be positive, we can move on to the next obstacle, which is to implement the time-dependence into kinematic space. Fortunately, first advances in that direction appeared recently in [82]. What remains is to implement this formalism for the appropriate geometries and to check what generalizations our volume formula requires in this framework. In the end, it is likely that this procedure will again only give insight into what contributes to the volume from the field theory, not tell us immediately what the field theory dual is. As we have demonstrated however, this suffices to find constraints on the candidates for field theory duals, which allow for further investigation. Most important for the characterization of these volumes in the CFT, is to understand the thermal contributions, which penetrate the black hole horizon.

11.3 OUTLOOK ON INTERFACES & QUANTUM INFORMATION

We have largely treated the study of interfaces and quantum information separately, simply because our motivations to dive into those branches of research were rooted in different frontiers of the gauge/-gravity duality. However, both notions are sufficiently general so that they can be combined in intriguing ways. Indeed, interfaces have been succesfully put to the test in quantum information already.

For instance, the influence of interfaces on entanglement entropy has been investigated in [57, 58, 145]. Even though, we did not phrase it this way, our discussion in Chapter 7 also investigates entanglement entropy in interface solutions for intervals placed symmetrically about the interface. CFT junctions have also been treated [147]. All these papers touch upon entanglement through interfaces in rational CFTs. However, also holographic scenarios have been discussed. One example, found in [146], treats the Janus interfaces of [79] and is therefore similar in spirit to our interfaces. In contrast to our scenario in Chapter 7, they study entangling intervals which lie entirely on one side of the interface. Similar to our findings, this produces an additive boundary term. More interestingly, the entanglement entropy is no longer universal but depends on features of the interface. It is likely that the entanglement entropy in our case follows the same pattern.

The first question that arises in light of our Kondo flows, is how this interface entanglement entropy changes along the RG flow. Another

intriguing question regards the possible "extensiveness" of this entanglement entropy. That is, given multiple interfaces, of the same type say, how do they individually contribute to the entanglement entropy? Do their contribtutions add? A first step is to construct the interface solutions in question, which is readily done, since it amounts to placing more singularities of type (6.44) or (6.71) on the open Riemann surface Σ. Then one can repeat the analysis of [146].

Interfaces have also provided insight into the study of complexity recently [75], where they discerned the "complexity equals volume" proposal from the "complexity equals action" proposal. Moving towards our work, once entanglement entropy is under good control in our interface solutions, we can consider subregion complexity extensively. Beginning with a single interval placed symmetrically around the interface, we can ask how the interface affects subregion complexity. Thereafter, it is interesting to see whether the topological properties of entanglement entropy persist in the presence of the interface. For this we first need to investigate the entanglement plateaux of the system. To that end we can compute the entanglement entropy for two intervals, one to either side of the interface. Upon tuning the distance of the entangling regions to one another, the entanglement phase transition should take place. It is likely that the interface drags other conformal blocks than that of the unit field into the computation, because of the non-universality of entanglement entropy. Thus our expectation is that the phase transition is highly dependent on the interface in use. In any event, it is interesting to consider subregion complexity for this case. Even though we think that the topological contributions are not the only contribution to the difference in subregion complexities, they should still be visible.

Recall that the entanglement phase transition is controlled in the CFT solely by the conformal block of the unit field.

To round things up, let us mention a last connection involving interfaces in quantum information, albeit unrelated to our Kondo setup. An important role in linking geometry with entanglement is played by the modular Hamiltonian, for which there are a number of results in the single interval case. However, the case of multiple intervals could only be addressed in the very special case of free fermions [74]. In [69] the groundwork for systematically deducing modular Hamiltonians was laid out for two-dimensional CFTs. Again, it works only for single intervals, but the authors also give a prescription for two intervals (eq. (75) in that paper) reminiscent of interfaces [198]. It makes use of mappings $X : \mathcal{H}_A \to \mathcal{H}_{\bar{A}}$, where A is the entangling interval and $\bar{A}$ its complement. It remains to be seen, whether these operators, X, are interfaces per se, and if they are, what kind are they? A first step is to investigate how these operators transform under the symmetries of a CFT. In any event, it should be possible to highly constrain these operators using the symmetries and structure of a CFT, thereby, shedding new light on the entanglement structure of disconnected intervals.

Part IV

APPENDIX

A

THE VERY BASICS OF SUPERSYMMETRY AND SUPERGRAVITY

This appendix contains introductory material on supersymmetry and supergravity. The first part, Section A.1, is concerned with supersymmetry and is truly a soft introduction as it is aimed at readers unfamiliar with the concepts. The second part, Section A.2 is concerned with supergravity. It is a little steeper in character, but still only introduces basic building blocks.

A.1 SUPERSYMMETRY

In this thesis it is important to understand a few basic features on how states are organized in a supersymmetric theory. This first section of our appendix is therefore concerned with the structure of representations of the supersymmetry algebra. We follow the classic books [230], [199] and the review [17]. For complementary information the reader is referred to these sources. For simplicity we restrict to four spacetime dimensions in the beginning and only toward the end, in Section A.1.3, we present relevant facts in other dimensions. The goal of this section is to introduce the terminology "BPS" and to explain how supersymmetries are counted.

A.1.1 *The supersymmetry algebra without central charges*

Whenever we are dealing with a theory, which contains both bosons and fermions we might wonder, if we could transform them into each other such that the corresponding action remains invariant. If this is possible, we obviously have a symmetry at hand. It is called *supersymmetry*. They are continuous symmetries for which we are free to construct conserved currents and conserved charges via Noether's theorem; the *supercurrents* and *supercharges* Q^I respectively. I is an internal index running from 1 to $\mathcal{N}$, where $\mathcal{N}$ may take the values 1,2 or 4. For now, we just note that it quantifies how supersymmetric our theory is and leave the details for the end of the supersymmetry section.

We consider relativistic quantum field theories, which obey the Poincaré algebra composed of the momentum generator P_μ and the Lorentz generator $M_{\mu\nu}$ $(\mu, \nu = 0, \ldots, 3)$. Together with the supercharges Q^I_a and

their hermitian conjugates $Q_{\dot{a}}^{I\dagger} = (Q_a^I)^\dagger$ – we discuss the subscripts momentarily – they form the *Super-Poincaré* algebra,

$$[Q_a^I, P_\mu] = 0 \tag{A.1a}$$
$$[Q_{\dot{a}}^{I\dagger}, P_\mu] = 0 \tag{A.1b}$$
$$[Q_a^I, M^{\mu\nu}] = (S_{\mathrm{L}}^{\mu\nu})_a{}^c Q_c^I \tag{A.1c}$$
$$[Q_{\dot{a}}^{I\dagger}, M^{\mu\nu}] = (S_{\mathrm{R}}^{\mu\nu})_{\dot{a}}{}^{\dot{c}} Q_{\dot{c}}^{I\dagger} \tag{A.1d}$$
$$\{Q_a^I, Q_{\dot{a}}^{J\dagger}\} = 2\sigma_{a\dot{a}}^\mu P_\mu \delta^{IJ} \tag{A.1e}$$
$$\{Q_a^I, Q_b^J\} = 0 = \{Q_{\dot{a}}^{I\dagger}, Q_{\dot{b}}^{J\dagger}\} \tag{A.1f}$$

The supercharges transform in the spin-$\frac{1}{2}$ representation of the Lorentz group.

The first two equations confirm that the supercharges are indeed conserved. The matrices $S_{\mathrm{L}}^{\mu\nu}$ and $S_{\mathrm{R}}^{\mu\nu}$ implement the action of the Lorentz group in its left-handed and right-handed spinor representation. Thus (A.1c) and (A.1d) mean that Q_a is a left-handed spinor with $a = 1, 2$ and $Q_{\dot{a}}^\dagger$ is a right-handed spinor with $\dot{a} = \dot{1}, \dot{2}$.

It is the last three equations, (A.1e) and (A.1f), which are usually referred to as the *supersymmetry algebra*. Equation (A.1e) informs us that two supersymmetry transformations amount to a translation. The matrices $\sigma^\mu = (-\mathbb{1}, \vec{\sigma})$ includes the 2×2 identity matrix and the Pauli-matrix vector. The last two equations (A.1f) are not yet in their most general form, but we will get to that soon enough. Observe that the supercharges are fermionic and thus they "talk to each other" through anti-commutators rather than commutators.

Linear combinations of the supercharges may be used as raising and lowering operator in representations of the supersymmetry algebra; we will become more explicit momentarily. Before that two comments are in order. (a) It can be shown quite straightforwardly using (A.1e) that every finite dimensional representation of the supersymmetry algebra has the same amount of bosons and fermions; they each come in pairs [230]. (b) Equations (A.1a) and (A.1b) imply that the supercharges also commute with the mass operator P^2, which in turn implies that all states in a given representation have the same mass M.

Massive Irreducible Representations

For massive states we can always boost to the rest frame $P_\mu = (M, 0, 0, 0)$ after which the supersymmetry algebra, (A.1e) and (A.1f), becomes ($\eta_{\mu\nu} = \mathrm{diag}(+, -, -, -)$)

$$\{Q_a^I, Q_{\dot{a}}^{J\dagger}\} = 2M\delta_{a\dot{a}}\delta^{IJ}, \tag{A.2a}$$
$$\{Q_a^I, Q_b^J\} = 0 = \{Q_{\dot{a}}^{I\dagger}, Q_{\dot{b}}^{J\dagger}\}. \tag{A.2b}$$

We can rescale the supercharges

$$\alpha_a^I = \frac{1}{\sqrt{M}} Q_a^I, \qquad (\alpha_a^I)^\dagger = \frac{1}{\sqrt{M}} Q_{\dot{a}}^{I\dagger} \tag{A.3}$$

in terms of which (A.2) becomes

$$\{\alpha_a^I, (\alpha_b^J)^\dagger\} = \delta_{ab}\delta^{IJ}, \tag{A.4a}$$
$$\{\alpha_a^I, \alpha_b^J\} = 0 = \{(\alpha_a^I)^\dagger, (\alpha_b^J)^\dagger\}. \tag{A.4b}$$

This is nothing but the algebra of $2\mathcal{N}$ fermionic creation and annihilation operators. Define a Clifford $|\Omega\rangle$ "vacuum" via

$$\alpha_a^I|\Omega\rangle = 0. \tag{A.5}$$

Any state in the representation is built through application of the creation operators $(\alpha_a^I)^\dagger$ to the vacuum $|\Omega\rangle$. This representation can be shown to be $2^{2\mathcal{N}}$-dimensional, $2^{2\mathcal{N}-1}$ bosonic states and $2^{2\mathcal{N}-1}$ fermionic states [230].

Massless Irreducible Representations

We boost to $P_\mu = (-E, 0, 0, E)$ then the supersymmetry algebra, (A.1e) and (A.1f), becomes

$$\{Q_a^I, Q_{\dot{a}}^{J\dagger}\} = \begin{pmatrix} 4E & 0 \\ 0 & 0 \end{pmatrix} \delta^{IJ}, \tag{A.6}$$
$$\{Q_a^I, Q_b^J\} = 0 = \{Q_{\dot{a}}^{I\dagger}, Q_{\dot{b}}^{J\dagger}\}. \tag{A.7}$$

Since Q_2^I and $Q_{\dot{2}}^{J\dagger}$ are conjugate to each other, (A.6) implies that both are represented trivially. Indeed, introduce the Clifford vacuum $|\Omega\rangle$, which is satisfies $Q_2^I|\Omega\rangle = 0$. Now consider the norm of the state, where the creator acts on it,

$$||Q_{\dot{2}}^{J\dagger}|\Omega\rangle||^2 = \langle\Omega|Q_2^I\, Q_{\dot{2}}^{J\dagger}|\Omega\rangle = \langle\Omega|\{Q_2^I,\, Q_{\dot{2}}^{J\dagger}\}|\Omega\rangle = 0 \tag{A.8}$$

Hence any state created via $Q_{\dot{2}}^{J\dagger}$ is null and decouples from the theory. We can therefore safely set $Q_2^I = Q_{\dot{2}}^{J\dagger} = 0$. We then only introduce one set of rescaled modes

$$\alpha^I = \frac{1}{\sqrt{M}} Q_1^I, \qquad (\alpha^I)^\dagger = \frac{1}{\sqrt{M}} Q_{\dot{1}}^{I\dagger}. \tag{A.9}$$

and the supersymmetry algebra, (A.1e) and (A.1f), becomes

$$\{\alpha^I, (\alpha^J)^\dagger\} = \delta^{IJ}, \tag{A.10a}$$
$$\{\alpha^I, \alpha^J\} = 0 = \{(\alpha^I)^\dagger, (\alpha^J)^\dagger\}. \tag{A.10b}$$

In contrast to the massive case, we have only $\mathcal{N}$ fermionic creation and annihilation modes at our disposal. The representation is then only half as large with dimension $2^{2\mathcal{N}-1}$, $2^{2\mathcal{N}-2}$ bosonic states and $2^{2\mathcal{N}-2}$ fermionic states.

A.1.2 *The supersymmetry algebra with central charges*

We mentioned that the supersymmetry algebra, (A.1e) and (A.1f), was not in its most general form. It is time to amend that following [17]. It was shown in [148] that the supersymmetry algebra can be enhanced by *central charges*. These are operators Z which commute with any other operator of the algebra. The extended supersymmetry algebra is then

$$\{Q^I_a, Q^{J\dagger}_{\dot a}\} = 2\sigma^\mu_{a\dot a} P_\mu \delta^{IJ} \tag{A.11a}$$
$$\{Q^I_a, Q^J_b\} = 2\sqrt{2}\epsilon_{ab} Z^{IJ} \tag{A.11b}$$
$$\{Q^\dagger_{I\dot a}, Q^\dagger_{J\dot b}\} = 2\sqrt{2}\epsilon_{ab} Z^*_{IJ} \tag{A.11c}$$

Note that Z and Z^* must be antisymmetric in I, J. For our purposes it is sufficient to consider the case $\mathcal{N} = 2$. We then get

$$\{Q^I_a, Q^{J\dagger}_{\dot a}\} = 2\sigma^\mu_{a\dot a} P_\mu \delta^{IJ} \tag{A.12a}$$
$$\{Q^I_a, Q^J_b\} = 2\sqrt{2}\epsilon_{ab} \epsilon^{IJ} Z \tag{A.12b}$$
$$\{Q^\dagger_{I\dot a}, Q^\dagger_{J\dot b}\} = 2\sqrt{2}\epsilon_{ab} \epsilon_{IJ} Z \tag{A.12c}$$

Z commutes with all generators and thus, in a given irreducible representation, it will always act as $q\mathbb{1}$, where $q \in \mathbb{R}$ is its eigenvalue in that representation. Again we define fermionic modes

$$\alpha_a = \frac{1}{2}\left(Q^1_a + \epsilon_{ab}(Q^2_b)^\dagger\right), \quad \beta_a = \frac{1}{2}\left(Q^1_a - \epsilon_{ab}(Q^2_b)^\dagger\right) \tag{A.13}$$

in terms of which (A.12) becomes (we consider massive representations)

$$\{\alpha_a, \alpha^\dagger_b\} = \delta_{ab}(M + \sqrt{2}q), \quad \{\beta_a, \beta^\dagger_b\} = \delta_{ab}(M - \sqrt{2}q) \tag{A.14}$$

Arguments similar to (A.8) then imply the bound $M \geq \sqrt{2}|q|$ for massive states. When the bound is saturated, either the modes α or β decouple and the massive representation is only half as large as in the case without central charge. Even though we restricted to $\mathcal{N} = 2$ this is true for any even $\mathcal{N}$ [17]. Such representations, with $M = \sqrt{2}|q|$ are called *short multiplets* and have dimension $2^{2\mathcal{N}-1}$. Representations with $M > \sqrt{2}|q|$ are called *long multiplets* and have dimension $2^{2\mathcal{N}}$.

States in short multiplets are called Bogomol'nyi–Prasad–Sommerfield (BPS) states and (A.14) implies that one half of the supersymmetry generators annihilates these states. Or in the words that we will most frequently use, BPS states only preserve one half of the full supersymmetry of the theory. We anticipate that branes, the protagonists of the AdS/CFT correspondence, are BPS states of string theory. Unfortunately, we will not have space in this text to argue this in full detail. Instead, we will contend ourselves with heuristic arguments and standard lore to cement this fact.

It is also possible to encounter states, which preserve only one quarter or one eighth of the supersymmetry of the full theory. These are also BPS, but it pays off to indicate to what "degree". We then write $\frac{1}{4}$-BPS or $\frac{1}{8}$-BPS and so on. The previous BPS states are then called $\frac{1}{2}$-BPS.

A.1.3 *Counting Supersymmetries*

We now pick up an unanswered question from above: what is $\mathcal{N}$? To answer this, we discuss reperesenations of the Clifford algebra. Mostly, this is standard material and we will be brief, following appendix B of [199], where the reader can find an extensive discussion.

Consider the supercharges Q_a^I from above and fix $\mathcal{N} = 1$ so that I can only be 1 and hence we drop this label. We observed that $a = 1, 2$ is a *spinorial* index of the Lorentz group. Since Q_a is complex this makes up four real components and thus a theory with $\mathcal{N} = 1$ in four spacetime dimensions has four supercharges. Now reinstate the superscript $I = 1, \ldots, \mathcal{N}$ and recall that in four spacetime dimensions we can have $\mathcal{N} = 1, 2, 4$ only. The theory with $\mathcal{N} = 2$ in has eight supercharges and a theory with $\mathcal{N} = 4$ has sixteen.

The way to think about about this is that the supercharges organize themselves into the smallest available spinor representation of the Lorentz algebra, each labelled by a fixed I. $\mathcal{N}$ then simply counts how many such smallest representations we need to accomodate all supercharges of the theory. Therefore we briefly review spinor representations.

Clifford, Dirac and Lorentz

Recall the Clifford algebra

$$\{\Gamma^\mu, \Gamma^\nu\} = 2\eta^{\mu\nu}, \tag{A.15}$$

where Γ^μ are Dirac matrices and $\mu = 0, d-1$. The flat metric has signature $\eta^{\mu\nu} = \text{diag}(-, +, \ldots, +)$.

For even $d = 2k + 2$, we can group the Dirac matrices into pairs

$$\Gamma^{0\pm} = \frac{1}{2}(\pm\Gamma^0 + \Gamma^1), \tag{A.16a}$$

$$\Gamma^{0\pm} = \frac{1}{2}(\pm\Gamma^{2m} \pm i\Gamma^{2m+1}), \quad m = 1, \ldots, k\,, \tag{A.16b}$$

in terms of which the (A.15) reads

$$\{\Gamma^{m+}, \Gamma^{n-}\} = \delta^{mn}, \tag{A.17a}$$

$$\{\Gamma^{m+}, \Gamma^{n+}\} = 0 = \{\Gamma^{m-}, \Gamma^{n-}\}. \tag{A.17b}$$

Note that $(\Gamma^{m\pm})^2 = 0$ and so, in a given representation we may apply each Γ^{m+} only once. Starting with a state ζ, which is annihilated by all Γ^{m-},

$$\Gamma^{m-}\zeta = 0 \text{ for all } m, \tag{A.18}$$

we may construct a $2^{k+1} = 2^{d/2}$-(complex)-dimensional representation by acting with the Γ^{m+} on ζ. Its states are

$$\zeta^{\mathbf{s}} = (\Gamma^{k+})^{s_k+1/2} \dots (\Gamma^{k+})^{s_0+1/2}\zeta, \tag{A.19}$$

where $\mathbf{s} = (s_0, s_1, \dots, s_k)$ and $s_m = \pm 1/2$. Now recall the well known fact that the Dirac matrices can be combined into generators

$$\Sigma^{\mu\nu} = -\frac{i}{4}[\Gamma^\mu, \Gamma^\nu] \tag{A.20}$$

of the Lorentz group $SO(d-1,1)$,

$$i[\Sigma^{\mu\nu}, \Sigma^{\sigma\rho}] = \eta^{\nu\sigma}\Sigma^{\mu\rho} + \eta^{\mu\rho}\Sigma^{\nu\sigma} - \eta^{\nu\rho}\Sigma^{\mu\sigma} - \eta^{\mu\sigma}\Sigma^{\nu\rho}\,. \tag{A.21}$$

As usual in representation theory it is useful to use commuting generators, which are just $\Sigma^{2m,2m+1}$. They can be simultaneously diagonalized. In terms of the raising and lowering operators we write

$$S_m = i^{\delta_{m,0}}\Sigma^{2m,2m+1} = \Gamma^{m+}\Gamma^{m-} - \frac{1}{2}. \tag{A.22}$$

These have the half-integer eigenvalues s_m, informing us that the S_m act in a spinor representation. Then the states (A.19) are spinors and the representation is called the *Dirac* representation.

Weyl and Majorana

The Dirac representation is irreducible as representation of the Clifford algebra. However, as representation of the Lorentz algebra it is reducible. Indeed, since the $\Sigma^{\mu\nu}$ are quadratic in Γ they cannot transform a spinor $\zeta^{\mathbf{s}}$ with an odd number of $-\frac{1}{2}$ into one with an even number thereof. To project onto these sectors, we define the *chirality matrix* $\Gamma = i^{-k}\Gamma^0\Gamma^1, \dots \Gamma^{d-1}$ with

$$\Gamma^2 = 0, \quad \{\Gamma, \Gamma^\mu\} = 0, \quad [\Gamma, \Sigma^{\mu\nu}] = 0, \tag{A.23}$$

and the projector

$$P_\pm = \frac{1}{2}(1 \pm \Gamma). \tag{A.24}$$

The image under these projectors are called *Weyl* representations and they are irreducible under the Lorentz algebra. Choosing P_+ returns the Weyl representation of positive chirality and P_- onto that of neg-

d	Majorana	Weyl	Majorana-Weyl	d_s
2	yes	yes	yes	1
3	yes	no	no	2
4	yes	yes	no	4
5	no	no	no	8
6	no	yes	no	8
7	no	no	no	16
8	yes	yes	no	16
9	yes	no	no	16
10	yes	yes	yes	16

Table 7: Spinor conditions in dimensions $d = 2, \ldots, 10$. The last column indicates the real dimension d_s of the smallest spinor representation in the respective spacetime dimension .

ative chirality. Both representations have complex dimension 2^k. Another way to construct representations with half the size of the Dirac representation is to first realize that the matrices $\Gamma^{\mu *}$ and $-\Gamma^{\mu *}$ also satisfy the Clifford algebra, (A.15). Hence they must be related to Γ^μ by a similarity transformation[1]

$$B_\pm \Gamma^\mu B_\pm^{-1} = \pm \Gamma^{\mu *}. \tag{A.25}$$

These matrices may be used to impose a *Majorana* condition

$$\zeta^* = B_\pm \zeta \tag{A.26}$$

It is a reality condition in the sense that it relates ζ to its complex conjugate. It removes one half of the degrees of freedom in the representation, leaving us with 2^k complex states. These representations are called *Majorana* representations. Explicit expressions for $B_\pm$ can be found in appendix B of [199].

Majorana and Weyl conditions are not accessible in every spacetime dimension. In dimensions $d = 2 \bmod 8$, however, we can actually impose both simultaneously, thereby reducing the dimensionality of the Dirac representation by a factor of four. In Table 7, which is taken from [199], we collect what conditions are applicable in spacetime dimensions up to ten and list the real (not complex) dimension d_s of the smallest spinor representation.

At long last we return to the complex supercharges Q_a^I, but now for arbitrary spacetime dimension d. They are organized in terms of the smallest spinor representations. Recall that a labels complex components and so it runs through $a = 1, \ldots, d_2/2$. In $d = 4$ we have $d_s = 4$ implying $a = 1, 2$ as required. Sometimes we will prefer to have a run

1 We are being very schematic here, since we assume familiarity with Majorana conditions. Interested readers are advised to consult [199]

over the real components, $a = 1, 2, 3, 4$. The superscript $I = 1, \ldots, \mathcal{N}$ then simply labels how many of such smallest spinors we have in the theory. Consider now $\mathcal{N} = 4$, $d = 4$ for instance. It has four spinors of smallest size making up a total of sixteen real supercharges. This is the same amount of supercharges as $\mathcal{N} = 1$ in $d = 10$. From now on, whenever we count supercharges, we will always mean real supercharges, as is done in the literature. Important examples are type II string theory and type II supergravity. Both feature $\mathcal{N} = 2$ in $d = 10$ giving a total of 32 supercharges in either theory.

One last remark is in order. When *superconformal* symmetry is at play the amount of supersymmetry is actually doubled, due to the presence of extra superconformal charges S^I_a. Its indices span the same range as those of Q. The infamous $\mathcal{N} = 4$ SYM theory in $d = 4$, which we need in the AdS/CFT correspondence, is superconformal. It has sixteen ordinary supercharges Q and another sixteen superconformal charges S; together the theory possesses thirty-two supercharges.

A.2 SUPERGRAVITY

The final section of this appendix is dedicated to a quick survey of supergravity, with the purpose of introducing S-duality. We will by no means be complete, because supergravity is a vast subject of its own. The material covered here is taken from [54] and the reader is referred to chapter 16 and 18 thereof for further details.

Type II supergravity arises as low-energy effective theory of type II string theory; the latter being UV completion of the former. Hence we consider theories of gravity in ten-dimensional spacetime with $\mathcal{N} = 2$ supersymmetry. So, we have a total of 32 supersymmetries. Indeed, a Dirac spinor in ten dimensions has 32 complex components. In $d = 10$ we may apply a Weyl and Majorana condition simultaneously leaving onyl 16 *real* degrees of freedom. $\mathcal{N} = 2$ means that all supersymmetries are organized into two such spinors of smallest size. Because the spinors are Weyl, the chirality of these spinors is important. So much so that we distinguish two kinds of type II supergravity depending on these chiralities: When their chiralities coincide we have IIA supergravity, when they differ we have IIB supergravity.

The massless bosonic spectrum of type II string theory falls into two classes: the NS-NS sector and the R-R sector. The former gives rise to the metric, antisymmetric NS-NS two form B_{MN} and the Dilaton

$$\text{NS-NS}: \qquad G_{MN},\ B_{MN},\ \phi. \tag{A.27}$$

Capital latin letters run from zero to nine and label ten-dimensional spacetime. The content of the second sector are the RR gauge potentials C_p (we sometimes just refer to them as RR fields)

$$\text{R-R}: \begin{cases} (C_1)_M,\ (C_3)_{MNR}, & \text{IIA}, \\ C_0,\ (C_2)_{MN},\ (C_4)_{MNRS} & \text{IIB}. \end{cases} \tag{A.28}$$

These are the same gauge fields that couple to the Dp-branes and this confirms that IIA has only p odd, while IIB has p even. C_4 obeys a self-duality constraint, which is employed at the level of equations of motion; otherwise it contains twice as many components as available in the massless spectrum of the string theory. From now on we restrict to type IIB supergravity since type IIA is irrelevant for this thesis.

The action of IIB supergravity consists of three pieces

$$S_{IIB} = \frac{1}{2\tilde{\kappa}_{10}^2}\Big(S_{\text{NSNS}} + S_{\text{RR}} + S_{\text{CS}}\Big) \tag{A.29}$$

The gravitational coupling is expressed through $2\tilde{\kappa}_{10}^2 = (2\pi)^7\alpha'^4 = (2\pi)^7 l_s^8$. The individual actions read

The gravitational coupling here differs from the gravitational constant in Chapter 3 via $\kappa_{10} = \tilde{\kappa}_{10}\, g_s$. Hence it carries a twiddle.

$$S_{\text{NSNS}} = \int d^{10}x\sqrt{-G}e^{-2\phi}\left(R + 4(\nabla\phi)^2 - \frac{1}{2}|H^2|\right), \tag{A.30a}$$

$$S_{\text{RR}} = -\frac{1}{2}\int d^{10}x\sqrt{-G}\left(|F_1^2| + |F_3^2| + \frac{1}{2}|F_5^2|\right), \tag{A.30b}$$

$$S_{\text{CS}} = -\frac{1}{2}\int d^{10}x\, C_4 \wedge H_3 \wedge F_3. \tag{A.30c}$$

The latter is a Chern-Simons term since it is independent of the metric. It is not to be confused with the Chern-Simons terms of the previous sections. H is the field strength of the NS-NS two-form,

$$H = dB, \qquad H_{MNR} = 3\partial_{[M}B_{NR]}. \tag{A.31}$$

The squares of all forms in (A.30) are defined through

$$|F_{p+1}| = \frac{1}{(p+1)!}F_{M_1\ldots M_{p+1}}F^{M_1\ldots M_{p+1}} \tag{A.32}$$

valid also for H with $p = 2$. The field strengths are

$$F_1 = dC_0, \tag{A.33a}$$

$$F_3 = dC_2 - C_0\, dB, \tag{A.33b}$$

$$F_5 = dC_4 - \frac{1}{2}C_2 \wedge dB + \frac{1}{2}B \wedge dC_2 \tag{A.33c}$$

The self-duality constraint $F_5 = \star F_5$ must be enforced in the equations of motion. No closed form where this is implemented at the level of a covariant action is known.

All field strengths enjoy invariance under the gauge transformations,

$$\delta B = d\zeta_0, \tag{A.34a}$$
$$\delta C_0 = 0, \tag{A.34b}$$
$$\delta C_2 = d\Lambda_1 \tag{A.34c}$$
$$\delta C_4 = d\Lambda_3 - \frac{1}{2} dB \wedge \Lambda_1 + \frac{1}{2} dC_2 \wedge \zeta_0. \tag{A.34d}$$

Subscripts indicate the form-degree.

IIB supergravity has a hidden $SL(2,\mathbb{R})$ symmetry, which is highlighted when going to *Einstein frame* by rescaling the metric,

$$G^E_{MN} = e^{-\phi/2} G_{MN}. \tag{A.35}$$

Additionally we define a complex scalar and a combined three-form

$$\tau = C_0 + ie{-\phi}, \qquad G_3 = F_3 - ie^{-\phi} H = dC_2 - \tau dB \tag{A.36}$$

These definitions rephrase the action to

$$\begin{aligned} S_{IIB} =& \frac{1}{2\tilde{\kappa}_{10}^2} \int \sqrt{-G} \left[R - \frac{\partial_M \tau \partial^M \bar{\tau}}{2(\Im \tau)^2} - \frac{1}{4} |F_5|^2 \right] \\ &+ \frac{1}{8i\tilde{\kappa}_{10}^2} \int \frac{1}{\Im \tau} C_4 \wedge G_3 \wedge \bar{G}_3. \end{aligned} \tag{A.37}$$

It is called Einstein frame, because here the Ricci scalar appears in the form that it does in the Einstein-Hilbert action.

This form of the action is manifestly invariant under an $SL(2,R)$ symmetry, which acts as

$$\tau \to \frac{a\tau + b}{c\tau + d}, \quad \begin{pmatrix} C_2 \\ B \end{pmatrix} \to \begin{pmatrix} a & b \\ c & d \end{pmatrix} \begin{pmatrix} C_2 \\ B \end{pmatrix}, \quad ad - bc = 1, \tag{A.38}$$

while leaving C_4 invariant. This implies that a D3-brane always remains D3-brane, while D1- and F1-branes are mixed into bound states. Similarly the fivebranes, which are magnetically charged under C_2 and B are also mixed into bound states. These are the (p,q)-strings and (p,q)-fivebranes we discussed at the end of Section 2.1.1.

S-Duality

In the main text we make use of S-duality, which is nothing but the specific $SL(2,R)$ transformation

$$\begin{pmatrix} a & b \\ c & d \end{pmatrix} = \begin{pmatrix} 0 & 1 \\ -1 & 0 \end{pmatrix}. \tag{A.39}$$

In the cases of interest to us we always have $C_0 = 0$ and so we get $\tau' = -1/\tau$ implying $e^{\phi} \to e^{-\phi}$. In particular this inverts the string coupling $g_s \to g_s^{-1}$. It is an example of a strong weak duality. Furthermore, this transformation exchanges C_2 and B. Hence fundamental strings are turned into D-strings and vice versa. The same holds true for D5- and F5-branes. As consequence the D1/D5 and F1/F5 supergravity solutions of the main text are turned into each other under S-duality.

BIBLIOGRAPHY

[1] B. P. Abbott et al. "Observation of Gravitational Waves from a Binary Black Hole Merger." In: *Phys. Rev. Lett.* 116.6 (2016), p. 061102. DOI: 10.1103/PhysRevLett.116.061102. arXiv: 1602.03837 [gr-qc].

[2] Raimond Abt, Johanna Erdmenger, Haye Hinrichsen, Charles M. Melby-Thompson, Rene Meyer, Christian Northe, and Ignacio A. Reyes. "Topological Complexity in AdS3/CFT2." In: (2017). arXiv: 1710.01327 [hep-th].

[3] Raimond Abt, Johanna Erdmenger, Marius Gerbershagen, Charles M. Melby-Thompson, and Christian Northe. "Holographic Subregion Complexity from Kinematic Space." In: *JHEP* 01 (2019), p. 012. DOI: 10.1007/JHEP01(2019)012. arXiv: 1805.10298 [hep-th].

[4] Ian Affleck. "A Current Algebra Approach to the Kondo Effect." In: *Nucl. Phys.* B336 (1990), pp. 517–532. DOI: 10.1016/0550-3213(90)90440-O.

[5] Ian Affleck. "Conformal field theory approach to the Kondo effect." In: *Acta Phys. Polon.* B26 (1995), pp. 1869–1932. arXiv: cond-mat/9512099 [cond-mat].

[6] Ian Affleck and Andreas W. W. Ludwig. "Critical theory of overscreened Kondo fixed points." In: *Nucl. Phys.* B360 (1991), pp. 641–696. DOI: 10.1016/0550-3213(91)90419-X.

[7] Ian Affleck and Andreas W. W. Ludwig. "Universal noninteger 'ground state degeneracy' in critical quantum systems." In: *Phys. Rev. Lett.* 67 (1991), pp. 161–164. DOI: 10.1103/PhysRevLett.67.161.

[8] Ian Affleck and Andreas W. W. Ludwig. "Exact conformal-field-theory results on the multichannel Kondo effect: Single-fermion Green's function, self-energy, and resistivity." In: *Phys. Rev. B* 48 (10 1993), pp. 7297–7321. DOI: 10.1103/PhysRevB.48.7297. URL: https://link.aps.org/doi/10.1103/PhysRevB.48.7297.

[9] Ian Affleck and Andreas W.W. Ludwig. "Critical theory of overscreened Kondo fixed points." In: *Nuclear Physics B* 360.2 (1991), pp. 641 –696. ISSN: 0550-3213. DOI: https://doi.org/10.1016/0550-3213(91)90419-X. URL: http://www.sciencedirect.com/science/article/pii/055032139190419X.

[10] Ian Affleck and Andreas W.W. Ludwig. "The Kondo effect, conformal field theory and fusion rules." In: *Nuclear Physics B* 352.3 (1991), pp. 849 –862. ISSN: 0550-3213. DOI: https://doi.org/10.1016/0550-3213(91)90109-B. URL: http://www.sciencedirect.com/science/article/pii/055032139190109B.

[11] Ofer Aharony, Oliver DeWolfe, Daniel Z. Freedman, and Andreas Karch. "Defect conformal field theory and locally localized gravity." In: *JHEP* 07 (2003), p. 030. DOI: 10.1088/1126-6708/2003/07/030. arXiv: hep-th/0303249 [hep-th].

[12] Kazunori Akiyama et al. "First M87 Event Horizon Telescope Results. VI. The Shadow and Mass of the Central Black Hole." In: *Astrophys. J.* 875.1 (2019), p. L6. DOI: 10.3847/2041-8213/ab1141. arXiv: 1906.11243 [astro-ph.GA].

[13] Anton Yu. Alekseev, Stefan Fredenhagen, Thomas Quella, and Volker Schomerus. "Noncommutative gauge theory of twisted D-branes." In: *Nucl. Phys.* B646 (2002), pp. 127–157. DOI: 10.1016/S0550-3213(02)00873-8. arXiv: hep-th/0205123 [hep-th].

[14] Mohsen Alishahiha. "Holographic Complexity." In: *Phys. Rev.* D92.12 (2015), p. 126009. DOI: 10.1103/PhysRevD.92.126009. arXiv: 1509.06614 [hep-th].

[15] Mohsen Alishahiha and Amin Faraji Astaneh. "Holographic Fidelity Susceptibility." In: (2017). arXiv: 1705.01834 [hep-th].

[16] Andrea Allais and Subir Sachdev. "Spectral function of a localized fermion coupled to the Wilson-Fisher conformal field theory." In: *Phys. Rev.* B90.3 (2014), p. 035131. DOI: 10.1103/PhysRevB.90.035131. arXiv: 1406.3022 [cond-mat.str-el].

[17] Luis Alvarez-Gaume and S. F. Hassan. "Introduction to S duality in N=2 supersymmetric gauge theories: A Pedagogical review of the work of Seiberg and Witten." In: *Fortsch. Phys.* 45 (1997), pp. 159–236. DOI: 10.1002/prop.2190450302. arXiv: hep-th/9701069 [hep-th].

[18] Martin Ammon and Johanna Erdmenger. *Gauge/gravity duality.* Cambridge: Cambridge University Press, 2015. ISBN: 9781107010345, 9781316235942. URL: http://www.cambridge.org/de/academic/subjects/physics/theoretical-physics-and-mathematical-physics/gaugegravity-duality-foundations-and-applications.

[19] N. Andrei. "Diagonalization of the Kondo Hamiltonian." In: *Phys. Rev. Lett.* 45 (1980), p. 379. DOI: 10.1103/PhysRevLett.45.379.

[20] N. Andrei and C. Destri. "Solution of the Multichannel Kondo Problem." In: *Phys. Rev. Lett.* 52 (1984), pp. 364–367. DOI: 10.1103/PhysRevLett.52.364.

[21] Curtis T. Asplund, Nele Callebaut, and Claire Zukowski. "Equivalence of Emergent de Sitter Spaces from Conformal Field Theory." In: *JHEP* 09 (2016), p. 154. DOI: 10.1007/JHEP09(2016)154. arXiv: 1604.02687 [hep-th].

[22] Steven G. Avery. "Using the D1D5 CFT to Understand Black Holes." PhD thesis. Ohio State U., 2010. arXiv: 1012.0072 [hep-th].

[23] Steven G. Avery and Borun D. Chowdhury. "Emission from the D1D5 CFT: Higher Twists." In: *JHEP* 01 (2010), p. 087. DOI: 10.1007/JHEP01(2010)087. arXiv: 0907.1663 [hep-th].

[24] Steven G. Avery and Borun D. Chowdhury. "Intertwining Relations for the Deformed D1D5 CFT." In: *JHEP* 05 (2011), p. 025. DOI: 10.1007/JHEP05(2011)025. arXiv: 1007.2202 [hep-th].

[25] Steven G. Avery, Borun D. Chowdhury, and Samir D. Mathur. "Emission from the D1D5 CFT." In: *JHEP* 10 (2009), p. 065. DOI: 10.1088/1126-6708/2009/10/065. arXiv: 0906.2015 [hep-th].

[26] Steven G. Avery, Borun D. Chowdhury, and Samir D. Mathur. "Deforming the D1D5 CFT away from the orbifold point." In: *JHEP* 06 (2010), p. 031. DOI: 10.1007/JHEP06(2010)031. arXiv: 1002.3132 [hep-th].

[27] Steven G. Avery, Borun D. Chowdhury, and Samir D. Mathur. "Excitations in the deformed D1D5 CFT." In: *JHEP* 06 (2010), p. 032. DOI: 10.1007/JHEP06(2010)032. arXiv: 1003.2746 [hep-th].

[28] Steven G. Avery and Jeremy Michelson. "Mechanics and Quantum Supermechanics of a Monopole Probe Including a Coulomb Potential." In: *Phys. Rev.* D77 (2008), p. 085001. DOI: 10.1103/PhysRevD.77.085001. arXiv: 0712.0341 [hep-th].

[29] C. Bachas, I. Brunner, and D. Roggenkamp. "Fusion of Critical Defect Lines in the 2D Ising Model." In: *J. Stat. Mech.* 1308 (2013), P08008. DOI: 10.1088/1742-5468/2013/08/P08008. arXiv: 1303.3616 [cond-mat.stat-mech].

[30] C. Bachas, Michael R. Douglas, and C. Schweigert. "Flux stabilization of D-branes." In: *JHEP* 05 (2000), p. 048. DOI: 10.1088/1126-6708/2000/05/048. arXiv: hep-th/0003037 [hep-th].

[31] C. Bachas and M. Petropoulos. "Anti-de Sitter D-branes." In: *JHEP* 02 (2001), p. 025. DOI: 10.1088/1126-6708/2001/02/025. arXiv: hep-th/0012234 [hep-th].

[32] C. Bachas, J. de Boer, R. Dijkgraaf, and H. Ooguri. "Permeable conformal walls and holography." In: *JHEP* 06 (2002), p. 027. DOI: 10.1088/1126-6708/2002/06/027. arXiv: hep-th/0111210 [hep-th].

[33] Constantin Bachas and Matthias Gaberdiel. "Loop operators and the Kondo problem." In: *JHEP* 11 (2004), p. 065. DOI: 10.1088/1126-6708/2004/11/065. arXiv: hep-th/0411067 [hep-th].

[34] Elaheh Bakhshaei, Ali Mollabashi, and Ahmad Shirzad. "Holographic Subregion Complexity for Singular Surfaces." In: (2017). arXiv: 1703.03469 [hep-th].

[35] V. Balasubramanian, A. Bernamonti, B. Craps, T. De Jonckheere, and F. Galli. "Entwinement in discretely gauged theories." In: *JHEP* 12 (2016), p. 094. DOI: 10.1007/JHEP12(2016)094. arXiv: 1609.03991 [hep-th].

[36] Vijay Balasubramanian, Per Kraus, and Masaki Shigemori. "Massless black holes and black rings as effective geometries of the D1-D5 system." In: *Class. Quant. Grav.* 22 (2005), pp. 4803–4838. DOI: 10.1088/0264-9381/22/22/010. arXiv: hep-th/0508110 [hep-th].

[37] Vijay Balasubramanian, Borun D. Chowdhury, Bartlomiej Czech, Jan de Boer, and Michal P. Heller. "Bulk curves from boundary data in holography." In: *Phys. Rev.* D89.8 (2014), p. 086004. DOI: 10.1103/PhysRevD.89.086004. arXiv: 1310.4204 [hep-th].

[38] Vijay Balasubramanian, Borun D. Chowdhury, Bartlomiej Czech, and Jan de Boer. "Entwinement and the emergence of spacetime." In: *JHEP* 01 (2015), p. 048. DOI: 10.1007/JHEP01(2015)048. arXiv: 1406.5859 [hep-th].

[39] Maximo Banados, Claudio Teitelboim, and Jorge Zanelli. "The Black hole in three-dimensional space-time." In: *Phys. Rev. Lett.* 69 (1992), pp. 1849–1851. DOI: 10.1103/PhysRevLett.69.1849. arXiv: hep-th/9204099 [hep-th].

[40] Souvik Banerjee, Johanna Erdmenger, and Debajyoti Sarkar. "Connecting Fisher information to bulk entanglement in holography." In: (2017). arXiv: 1701.02319 [hep-th].

[41] Ning Bao, Jason Pollack, and Grant N. Remmen. "Splitting Spacetime and Cloning Qubits: Linking No-Go Theorems across the ER=EPR Duality." In: *Fortsch. Phys.* 63 (2015), pp. 705–710. DOI: 10.1002/prop.201500053. arXiv: 1506.08203 [hep-th].

[42] K. Becker, M. Becker, and J. H. Schwarz. *String theory and M-theory: A modern introduction*. Cambridge University Press, 2006. ISBN: 9780511254864, 9780521860697.

[43] Roger E. Behrend, Paul A. Pearce, Valentina B. Petkova, and Jean-Bernard Zuber. "Boundary conditions in rational conformal field theories." In: *Nucl. Phys.* B570 (2000). [Nucl. Phys.B579,707(2000)], pp. 525–589. DOI: 10.1016/S0550-3213(99)00592-1, 10.1016/S0550-3213(00)00225-X. arXiv: hep-th/9908036 [hep-th].

[44] J. D. Bekenstein. "Black holes and the second law." In: *Lett. Nuovo Cim.* 4 (1972), pp. 737–740. DOI: 10.1007/BF02757029.

[45] Jacob D. Bekenstein. "Black holes and entropy." In: *Phys. Rev.* D7 (1973), pp. 2333–2346. DOI: 10.1103/PhysRevD.7.2333.

[46] Jacob D. Bekenstein. "Generalized second law of thermodynamics in black hole physics." In: *Phys. Rev.* D9 (1974), pp. 3292–3300. DOI: 10.1103/PhysRevD.9.3292.

[47] Jacob D. Bekenstein. "A Universal Upper Bound on the Entropy to Energy Ratio for Bounded Systems." In: *Phys. Rev.* D23 (1981), p. 287. DOI: 10.1103/PhysRevD.23.287.

[48] J. S. Bell. "On the Einstein-Podolsky-Rosen paradox." In: *Physics Physique Fizika* 1 (1964), pp. 195–200. DOI: 10.1103/PhysicsPhysiqueFizika.1.195.

[49] Omer Ben-Ami and Dean Carmi. "On Volumes of Subregions in Holography and Complexity." In: *JHEP* 11 (2016), p. 129. DOI: 10.1007/JHEP11(2016)129. arXiv: 1609.02514 [hep-th].

[50] Omer Ben-Ami and Dean Carmi. "On Volumes of Subregions in Holography and Complexity." In: *JHEP* 11 (2016), p. 129. DOI: 10.1007/JHEP11(2016)129. arXiv: 1609.02514 [hep-th].

[51] Lorenzo Bianchi, Marco Meineri, Robert C. Myers, and Michael Smolkin. "Rényi entropy and conformal defects." In: *JHEP* 07 (2016), p. 076. DOI: 10.1007/JHEP07(2016)076. arXiv: 1511.06713 [hep-th].

[52] N. E. Bickers. "Review of techniques in the large-N expansion for dilute magnetic alloys." In: *Rev. Mod. Phys.* 59 (1987), pp. 845–939. DOI: 10.1103/RevModPhys.59.845.

[53] Marco Billò, Vasco Gonçalves, Edoardo Lauria, and Marco Meineri. "Defects in conformal field theory." In: *JHEP* 04 (2016), p. 091. DOI: 10.1007/JHEP04(2016)091. arXiv: 1601.02883 [hep-th].

[54] Ralph Blumenhagen, Dieter Lüst, and Stefan Theisen. *Basic concepts of string theory*. Theoretical and Mathematical Physics. Heidelberg, Germany: Springer, 2013. ISBN: 9783642294969. DOI: 10.1007/978-3-642-29497-6. URL: http://www.springer.com/physics/theoretical%2C+mathematical+%26+computational+physics/book/978-3-642-29496-9.

[55] Ralph Blumenhagen and Erik Plauschinn. *Introduction to Conformal Field Theory: With Applications to String Theory*. Lecture Notes in Physics 779. Berlin Heidelberg: Springer, 2009. ISBN: 978-3-642-00450-6. URL: http://www.springer.com/us/book/9783642004490.

[56] Jan de Boer, Felix M. Haehl, Michal P. Heller, and Robert C. Myers. "Entanglement, holography and causal diamonds." In: *JHEP* 08 (2016), p. 162. DOI: 10.1007/JHEP08(2016)162. arXiv: 1606.03307 [hep-th].

[57] Enrico M. Brehm and Ilka Brunner. "Entanglement entropy through conformal interfaces in the 2D Ising model." In: *JHEP* 09 (2015), p. 080. DOI: 10.1007/JHEP09(2015)080. arXiv: 1505.02647 [hep-th].

[58] Enrico M. Brehm, Ilka Brunner, Daniel Jaud, and Cornelius Schmidt-Colinet. "Entanglement and topological interfaces." In: *Fortsch. Phys.* 64.6-7 (2016), pp. 516–535. DOI: 10.1002/prop.201600024. arXiv: 1512.05945 [hep-th].

[59] Adam R. Brown and Leonard Susskind. "The Second Law of Quantum Complexity." In: (2017). arXiv: 1701.01107 [hep-th].

[60] J. David Brown and M. Henneaux. "Central Charges in the Canonical Realization of Asymptotic Symmetries: An Example from Three-Dimensional Gravity." In: *Commun. Math. Phys.* 104 (1986), pp. 207–226. DOI: 10.1007/BF01211590.

[61] Ilka Brunner, Nils Carqueville, and Daniel Plencner. "A quick guide to defect orbifolds." In: *Proc. Symp. Pure Math.* 88 (2014), pp. 231–242. DOI: 10.1090/pspum/088/01456. arXiv: 1310.0062 [hep-th].

[62] Pasquale Calabrese and John Cardy. "Entanglement entropy and quantum field theory." In: *Journal of Statistical Mechanics: Theory and Experiment* 2004.06 (2004), P06002. DOI: 10.1088/1742-5468/2004/06/p06002. URL: https://doi.org/10.1088%2F1742-5468%2F2004%2F06%2Fp06002.

[63] Pasquale Calabrese and John Cardy. "Entanglement entropy and conformal field theory." In: *J. Phys.* A42 (2009), p. 504005. DOI: 10.1088/1751-8113/42/50/504005. arXiv: 0905.4013 [cond-mat.stat-mech].

[64] J. M. Camino, Angel Paredes, and A. V. Ramallo. "Stable wrapped branes." In: *JHEP* 05 (2001), p. 011. DOI: 10.1088/1126-6708/2001/05/011. arXiv: hep-th/0104082 [hep-th].

[65] Pawel Caputa, Nilay Kundu, Masamichi Miyaji, Tadashi Takayanagi, and Kento Watanabe. "Anti-de Sitter Space from Optimization of Path Integrals in Conformal Field Theories." In: *Phys. Rev. Lett.* 119.7 (2017), p. 071602. DOI: 10.1103/PhysRevLett.119.071602. arXiv: 1703.00456 [hep-th].

[66] Pawel Caputa, Nilay Kundu, Masamichi Miyaji, Tadashi Takayanagi, and Kento Watanabe. "Liouville Action as Path-Integral Complexity: From Continuous Tensor Networks to AdS/CFT." In: (2017). arXiv: 1706.07056 [hep-th].

[67] John L. Cardy. "Boundary Conditions, Fusion Rules and the Verlinde Formula." In: *Nucl. Phys.* B324 (1989), pp. 581–596. DOI: 10.1016/0550-3213(89)90521-X.

[68] John L. Cardy. "CONFORMAL INVARIANCE AND STATISTICAL MECHANICS." In: *Les Houches Summer School in Theoretical Physics: Fields, Strings, Critical Phenomena Les Houches, France, June 28-August 5, 1988*. 1989, pp. 0169–246.

[69] John Cardy and Erik Tonni. "Entanglement hamiltonians in two-dimensional conformal field theory." In: *J. Stat. Mech.* 1612.12 (2016), p. 123103. DOI: 10.1088/1742-5468/2016/12/123103. arXiv: 1608.01283 [cond-mat.stat-mech].

[70] Dean Carmi. "More on Holographic Volumes, Entanglement, and Complexity." In: (2017). arXiv: 1709.10463 [hep-th].

[71] Dean Carmi, Robert C. Myers, and Pratik Rath. "Comments on Holographic Complexity." In: *JHEP* 03 (2017), p. 118. DOI: 10.1007/JHEP03(2017)118. arXiv: 1612.00433 [hep-th].

[72] Dean Carmi, Shira Chapman, Hugo Marrochio, Robert C. Myers, and Sotaro Sugishita. "On the Time Dependence of Holographic Complexity." In: (2017). arXiv: 1709.10184 [hep-th].

[73] Jorge Casalderrey-Solana, Hong Liu, David Mateos, Krishna Rajagopal, and Urs Achim Wiedemann. "Gauge/String Duality, Hot QCD and Heavy Ion Collisions." In: (2011). DOI: 10.1017/CBO9781139136747. arXiv: 1101.0618 [hep-th].

[74] H. Casini and M. Huerta. "Reduced density matrix and internal dynamics for multicomponent regions." In: *Class. Quant. Grav.* 26 (2009), p. 185005. DOI: 10.1088/0264-9381/26/18/185005. arXiv: 0903.5284 [hep-th].

[75] Shira Chapman, Dongsheng Ge, and Giuseppe Policastro. "Holographic Complexity for Defects Distinguishes Action from Volume." In: *JHEP* 05 (2019), p. 049. DOI: 10.1007/JHEP05(2019)049. arXiv: 1811.12549 [hep-th].

[76] Shira Chapman, Michal P. Heller, Hugo Marrochio, and Fernando Pastawski. "Towards Complexity for Quantum Field Theory States." In: (2017). arXiv: 1707.08582 [hep-th].

[77] Shira Chapman, Jens Eisert, Lucas Hackl, Michal P. Heller, Ro Jefferson, Hugo Marrochio, and Robert C. Myers. "Complexity and entanglement for thermofield double states." In: *SciPost Phys.* 6.3 (2019), p. 034. DOI: 10.21468/SciPostPhys.6.3.034. arXiv: 1810.05151 [hep-th].

[78] Marco Chiodaroli, Michael Gutperle, and Ling-Yan Hung. "Boundary entropy of supersymmetric Janus solutions." In: *JHEP* 09 (2010), p. 082. DOI: 10.1007/JHEP09(2010)082. arXiv: 1005.4433 [hep-th].

[79] Marco Chiodaroli, Michael Gutperle, and Darya Krym. "Half-BPS Solutions locally asymptotic to $AdS_3 \times S^3$ and interface conformal field theories." In: *JHEP* 02 (2010), p. 066. DOI: 10.1007/JHEP02(2010)066. arXiv: 0910.0466 [hep-th].

[80] Marco Chiodaroli, Michael Gutperle, Ling-Yan Hung, and Darya Krym. "String Junctions and Holographic Interfaces." In: *Phys. Rev.* D83 (2011), p. 026003. DOI: 10.1103/PhysRevD.83.026003. arXiv: 1010.2758 [hep-th].

[81] Jesse C. Cresswell and Amanda W. Peet. "Kinematic Space for Conical Defects." In: (2017). arXiv: 1708.09838 [hep-th].

[82] Bartlomiej Czech, Yaithd D. Olivas, and Zi-zhi Wang. "Holographic integral geometry with time dependence." In: (2019). arXiv: 1905.07413 [hep-th].

[83] Bartlomiej Czech, Lampros Lamprou, Samuel McCandlish, and James Sully. "Integral Geometry and Holography." In: *JHEP* 10 (2015), p. 175. DOI: 10.1007/JHEP10(2015)175. arXiv: 1505.05515 [hep-th].

[84] Bartlomiej Czech, Lampros Lamprou, Samuel McCandlish, Benjamin Mosk, and James Sully. "A Stereoscopic Look into the Bulk." In: *JHEP* 07 (2016), p. 129. DOI: 10.1007/JHEP07(2016)129. arXiv: 1604.03110 [hep-th].

[85] Bartlomiej Czech, Lampros Lamprou, Samuel McCandlish, and James Sully. "Tensor Networks from Kinematic Space." In: *JHEP* 07 (2016), p. 100. DOI: 10.1007/JHEP07(2016)100. arXiv: 1512.01548 [hep-th].

[86] Bartlomiej Czech, Lampros Lamprou, Samuel McCandlish, Benjamin Mosk, and James Sully. "Equivalent Equations of Motion for Gravity and Entropy." In: *JHEP* 02 (2017), p. 004. DOI: 10.1007/JHEP02(2017)004. arXiv: 1608.06282 [hep-th].

[87] Bartłomiej Czech and Lampros Lamprou. "Holographic definition of points and distances." In: *Phys. Rev.* D90 (2014), p. 106005. DOI: 10.1103/PhysRevD.90.106005. arXiv: 1409.4473 [hep-th].

[88] Shouvik Datta, Lorenz Eberhardt, and Matthias R. Gaberdiel. "Stringy $\mathcal{N} = (2, 2)$ holography for AdS_3." In: *JHEP* 01 (2018), p. 146. DOI: 10.1007/JHEP01(2018)146. arXiv: 1709.06393 [hep-th].

[89] Justin R. David, Gautam Mandal, and Spenta R. Wadia. "Microscopic formulation of black holes in string theory." In: *Phys. Rept.* 369 (2002), pp. 549–686. DOI: 10.1016/S0370-1573(02)00271-5. arXiv: hep-th/0203048 [hep-th].

[90] Oliver DeWolfe, Daniel Z. Freedman, and Hirosi Ooguri. "Holography and defect conformal field theories." In: *Phys. Rev.* D66 (2002), p. 025009. DOI: 10.1103/PhysRevD.66.025009. arXiv: hep-th/0111135 [hep-th].

[91] Andrea Dei, Lorenz Eberhardt, and Matthias R. Gaberdiel. "Three-point functions in AdS_3/CFT_2 holography." In: (2019). arXiv: 1907.13144 [hep-th].

[92] P. Di Francesco, P. Mathieu, and D. Senechal. *Conformal Field Theory*. Graduate Texts in Contemporary Physics. New York: Springer-Verlag, 1997. ISBN: 9780387947853, 9781461274759. DOI: 10.1007/978-1-4612-2256-9. URL: http://www-spires.fnal.gov/spires/find/books/www?cl=QC174.52.C66D5::1997.

[93] Lorenz Eberhardt. "Supersymmetric AdS_3 supergravity backgrounds and holography." In: *JHEP* 02 (2018), p. 087. DOI: 10.1007/JHEP02(2018)087. arXiv: 1710.09826 [hep-th].

[94] Lorenz Eberhardt and Kevin Ferreira. "The plane-wave spectrum from the worldsheet." In: *JHEP* 10 (2018), p. 109. DOI: 10.1007/JHEP10(2018)109. arXiv: 1805.12155 [hep-th].

[95] Lorenz Eberhardt and Kevin Ferreira. "Long strings and chiral primaries in the hybrid formalism." In: *JHEP* 02 (2019), p. 098. DOI: 10.1007/JHEP02(2019)098. arXiv: 1810.08621 [hep-th].

[96] Lorenz Eberhardt and Matthias R. Gaberdiel. "String theory on $AdS_{\mathbf{3}}$ and the symmetric orbifold of Liouville theory." In: (2019). arXiv: 1903.00421 [hep-th].

[97] Lorenz Eberhardt and Matthias R. Gaberdiel. "Strings on $AdS_3 \times S^3 \times S^3 \times S^1$." In: *JHEP* 06 (2019), p. 035. DOI: 10.1007/JHEP06(2019)035. arXiv: 1904.01585 [hep-th].

[98] Lorenz Eberhardt, Matthias R. Gaberdiel, and Rajesh Gopakumar. "The Worldsheet Dual of the Symmetric Product CFT." In: *JHEP* 04 (2019), p. 103. DOI: 10.1007/JHEP04(2019)103. arXiv: 1812.01007 [hep-th].

[99] Lorenz Eberhardt, Matthias R. Gaberdiel, and Wei Li. "A holographic dual for string theory on $AdS_3 \times S^3 \times S^3 \times S^1$." In: *JHEP* 08 (2017), p. 111. DOI: 10.1007/JHEP08(2017)111. arXiv: 1707.02705 [hep-th].

[100] Lorenz Eberhardt, Matthias R. Gaberdiel, and Ingo Rienacker. "Higher spin algebras and large $\mathcal{N} = 4$ holography." In: *JHEP* 03 (2018), p. 097. DOI: 10.1007/JHEP03(2018)097. arXiv: 1801.00806 [hep-th].

[101] Lorenz Eberhardt and Ida G. Zadeh. "$\mathcal{N} = (3,3)$ holography on $AdS_3 \times (S^3 \times S^3 \times S^1)/\mathbb{Z}_2$." In: *JHEP* 07 (2018), p. 143. DOI: 10.1007/JHEP07(2018)143. arXiv: 1805.09832 [hep-th].

[102] Lorenz Eberhardt, Matthias R. Gaberdiel, Rajesh Gopakumar, and Wei Li. "BPS spectrum on $AdS_3 \times S^3 \times S^3 \times S^1$." In: *JHEP* 03 (2017), p. 124. DOI: 10.1007/JHEP03(2017)124. arXiv: 1701.03552 [hep-th].

[103] Albert Einstein. "The Field Equations of Gravitation." In: *Sitzungsber. Preuss. Akad. Wiss. Berlin (Math. Phys.)* 1915 (1915), pp. 844–847.

[104] Albert Einstein. "Approximative Integration of the Field Equations of Gravitation." In: *Sitzungsber. Preuss. Akad. Wiss. Berlin (Math. Phys.)* 1916 (1916), pp. 688–696.

[105] Albert Einstein. "Die Grundlage der allgemeinen Relativitätstheorie." In: *Annalen Phys.* 49.7 (1916). [Annalen Phys.354,no.7,769(1916)], pp. 769–822. DOI: 10.1002/andp.200590044,10.1002/andp.19163540702.

[106] Albert Einstein. "Über Gravitationswellen." In: *Sitzungsber. Preuss. Akad. Wiss. Berlin (Math. Phys.)* 1918 (1918), pp. 154–167.

[107] Albert Einstein, Boris Podolsky, and Nathan Rosen. "Can quantum mechanical description of physical reality be considered complete?" In: *Phys. Rev.* 47 (1935), pp. 777–780. DOI: 10.1103/PhysRev.47.777.

[108] Dalit Engelhardt, Ben Freivogel, and Nabil Iqbal. "Electric fields and quantum wormholes." In: *Phys. Rev.* D92.6 (2015), p. 064050. DOI: 10.1103/PhysRevD.92.064050. arXiv: 1504.06336 [hep-th].

[109] J. Erdmenger, M. Flory, C. Hoyos, M-N. Newrzella, A. O'Bannon, and J. Wu. "Holographic impurities and Kondo effect." In: *Fortsch. Phys.* 64 (2016), pp. 322–329. DOI: 10.1002/prop.201500079. arXiv: 1511.09362 [hep-th].

[110] Johanna Erdmenger, Mario Flory, and Max-Niklas Newrzella. "Bending branes for DCFT in two dimensions." In: *JHEP* 01 (2015), p. 058. DOI: 10.1007/JHEP01(2015)058. arXiv: 1410.7811 [hep-th].

[111] Johanna Erdmenger, Zachary Guralnik, and Ingo Kirsch. "Four-dimensional superconformal theories with interacting boundaries or defects." In: *Phys. Rev.* D66 (2002), p. 025020. DOI: 10.1103/PhysRevD.66.025020. arXiv: hep-th/0203020 [hep-th].

[112] Johanna Erdmenger, Charles M. Melby-Thompson, and Christian Northe. "Kondo RG-flows in AdS_3/CFT_2." In: (2018). 19**.****, in progress.

[113] Johanna Erdmenger, Carlos Hoyos, Andy O'Bannon, and Jackson Wu. "A Holographic Model of the Kondo Effect." In: *JHEP* 12 (2013), p. 086. DOI: 10.1007/JHEP12(2013)086. arXiv: 1310.3271 [hep-th].

[114] Johanna Erdmenger, Mario Flory, Carlos Hoyos, Max-Niklas Newrzella, and Jackson M. S. Wu. "Entanglement Entropy in a Holographic Kondo Model." In: *Fortsch. Phys.* 64 (2016), pp. 109–130. DOI: 10.1002/prop.201500099. arXiv: 1511.03666 [hep-th].

[115] Johanna Erdmenger, Carlos Hoyos, Andy O'Bannon, Ioannis Papadimitriou, Jonas Probst, and Jackson M. S. Wu. "Holographic Kondo and Fano Resonances." In: *Phys. Rev.* D96.2 (2017), p. 021901. DOI: 10.1103/PhysRevD.96.021901. arXiv: 1611.09368 [hep-th].

[116] Johanna Erdmenger, Mario Flory, Max-Niklas Newrzella, Migael Strydom, and Jackson M. S. Wu. "Quantum Quenches in a Holographic Kondo Model." In: *JHEP* 04 (2017), p. 045. DOI: 10.1007/JHEP04(2017)045. arXiv: 1612.06860 [hep-th].

[117] Johanna Erdmenger, Carlos Hoyos, Andy O'Bannon, Ioannis Papadimitriou, Jonas Probst, and Jackson M. S. Wu. "Two-point Functions in a Holographic Kondo Model." In: *JHEP* 03 (2017), p. 039. DOI: 10.1007/JHEP03(2017)039. arXiv: 1612.02005 [hep-th].

[118] Thomas Faulkner. "The Entanglement Renyi Entropies of Disjoint Intervals in AdS/CFT." In: (2013). arXiv: 1303.7221 [hep-th].

[119] Thomas Faulkner, Monica Guica, Thomas Hartman, Robert C. Myers, and Mark Van Raamsdonk. "Gravitation from Entanglement in Holographic CFTs." In: *JHEP* 03 (2014), p. 051. DOI: 10.1007/JHEP03(2014)051. arXiv: 1312.7856 [hep-th].

[120] Mario Flory. "A complexity/fidelity susceptibility g-theorem for $AdS_3/BCFT_2$." In: *JHEP* 06 (2017), p. 131. DOI: 10.1007/JHEP06(2017)131. arXiv: 1702.06386 [hep-th].

[121] Mario Flory. "WdW-patches in AdS_3 and complexity change under conformal transformations II." In: *JHEP* 05 (2019), p. 086. DOI: 10.1007/JHEP05(2019)086. arXiv: 1902.06499 [hep-th].

[122] Mario Flory and Nina Miekley. "Complexity change under conformal transformations in AdS_3/CFT_2." In: *JHEP* 05 (2019), p. 003. DOI: 10.1007/JHEP05(2019)003. arXiv: 1806.08376 [hep-th].

[123] Stefan Fredenhagen. "Organizing boundary RG flows." In: *Nucl. Phys.* B660 (2003), pp. 436–472. DOI: 10.1016/S0550-3213(03)00226-8. arXiv: hep-th/0301229 [hep-th].

[124] Stefan Fredenhagen and Cosimo Restuccia. "The geometry of the limit of N=2 minimal models." In: *J. Phys.* A46 (2013), p. 045402. DOI: 10.1088/1751-8113/46/4/045402. arXiv: 1208.6136 [hep-th].

[125] Stefan Fredenhagen and Cosimo Restuccia. "The large level limit of Kazama-Suzuki models." In: *JHEP* 04 (2015), p. 015. DOI: 10.1007/JHEP04(2015)015. arXiv: 1408.0416 [hep-th].

[126] Stefan Fredenhagen, Cosimo Restuccia, and Rui Sun. "The limit of N=(2,2) superconformal minimal models." In: *JHEP* 10 (2012), p. 141. DOI: 10.1007/JHEP10(2012)141. arXiv: 1204.0446 [hep-th].

[127] Stefan Fredenhagen and Volker Schomerus. "Brane dynamics in CFT backgrounds." In: *Strings 2001: International Conference Mumbai, India, January 5-10, 2001*. 2001. arXiv: hep-th/0104043 [hep-th].

[128] Stefan Fredenhagen and Volker Schomerus. "Branes on group manifolds, gluon condensates, and twisted K theory." In: *JHEP* 04 (2001), p. 007. DOI: 10.1088/1126-6708/2001/04/007. arXiv: hep-th/0012164 [hep-th].

[129] Stefan Fredenhagen and Volker Schomerus. "D-branes in coset models." In: *JHEP* 02 (2002), p. 005. DOI: 10.1088/1126-6708/2002/02/005. arXiv: hep-th/0111189 [hep-th].

[130] Stefan Fredenhagen and Volker Schomerus. "On boundary RG flows in coset conformal field theories." In: *Phys. Rev.* D67 (2003), p. 085001. DOI: 10.1103/PhysRevD.67.085001. arXiv: hep-th/0205011 [hep-th].

[131] Daniel Friedan and Anatoly Konechny. "On the boundary entropy of one-dimensional quantum systems at low temperature." In: *Phys. Rev. Lett.* 93 (2004), p. 030402. DOI: 10.1103/PhysRevLett.93.030402. arXiv: hep-th/0312197 [hep-th].

[132] Jurg Frohlich, Jurgen Fuchs, Ingo Runkel, and Christoph Schweigert. "Duality and defects in rational conformal field theory." In: *Nucl. Phys.* B763 (2007), pp. 354–430. DOI: 10.1016/j.nuclphysb.2006.11.017. arXiv: hep-th/0607247 [hep-th].

[133] Matthias Gaberdiel. "Fusion in conformal field theory as the tensor product of the symmetry algebra." In: *Int. J. Mod. Phys.* A9 (1994), pp. 4619–4636. DOI: 10.1142/S0217751X94001849. arXiv: hep-th/9307183 [hep-th].

[134] Matthias Gaberdiel. "Boundary conformal field theory and D-branes." In: (Aug. 2003).

[135] Davide Gaiotto and Edward Witten. "Supersymmetric Boundary Conditions in N=4 Super Yang-Mills Theory." In: *J. Statist. Phys.* 135 (2009), pp. 789–855. DOI: 10.1007/s10955-009-9687-3. arXiv: 0804.2902 [hep-th].

[136] Wen-Cong Gan and Fu-Wen Shu. "Holographic complexity: A tool to probe the property of reduced fidelity susceptibility." In: *Phys. Rev.* D96.2 (2017), p. 026008. DOI: 10.1103/PhysRevD.96.026008. arXiv: 1702.07471 [hep-th].

[137] Krzysztof Gawedzki. "Conformal field theory: A Case study." In: (1999). arXiv: hep-th/9904145 [hep-th].

[138] Paul H. Ginsparg. "Applied Conformal Field Theory." In: *Les Houches Summer School in Theoretical Physics: Fields, Strings, Critical Phenomena Les Houches, France, June 28-August 5, 1988*. 1988, pp. 1–168. arXiv: hep-th/9108028 [hep-th].

[139] Johann Wolfgang von Goethe. *Faust, der Tragödie Erster Teil.* 1808.

[140] Jaume Gomis and Filippo Passerini. "Holographic Wilson Loops." In: *JHEP* 08 (2006), p. 074. DOI: 10.1088/1126-6708/2006/08/074. arXiv: hep-th/0604007 [hep-th].

[141] Jaume Gomis and Filippo Passerini. "Wilson Loops as D3-Branes." In: *JHEP* 01 (2007), p. 097. DOI: 10.1088/1126-6708/2007/01/097. arXiv: hep-th/0612022 [hep-th].

[142] K. Graham, I. Runkel, and G. M. T. Watts. "Renormalization group flows of boundary theories." In: *PoS* tmr2000 (2000), p. 040. DOI: 10.22323/1.006.0040. arXiv: hep-th/0010082 [hep-th].

[143] K. Graham and G. M. T. Watts. "Defect lines and boundary flows." In: *JHEP* 04 (2004), p. 019. DOI: 10.1088/1126-6708/2004/04/019. arXiv: hep-th/0306167 [hep-th].

[144] M. Gunaydin, G. Sierra, and P. K. Townsend. "The Unitary Supermultiplets of $d = 3$ Anti-de Sitter and $d = 2$ Conformal Superalgebras." In: *Nucl. Phys.* B274 (1986), pp. 429–447. DOI: 10.1016/0550-3213(86)90293-2.

[145] Michael Gutperle and John D. Miller. "A note on entanglement entropy for topological interfaces in RCFTs." In: *JHEP* 04 (2016), p. 176. DOI: 10.1007/JHEP04(2016)176. arXiv: 1512.07241 [hep-th].

[146] Michael Gutperle and John D. Miller. "Entanglement entropy at holographic interfaces." In: *Phys. Rev.* D93.2 (2016), p. 026006. DOI: 10.1103/PhysRevD.93.026006. arXiv: 1511.08955 [hep-th].

[147] Michael Gutperle and John D. Miller. "Entanglement entropy at CFT junctions." In: *Phys. Rev.* D95.10 (2017), p. 106008. DOI: 10.1103/PhysRevD.95.106008. arXiv: 1701.08856 [hep-th].

[148] Rudolf Haag, Jan T. Lopuszanski, and Martin Sohnius. "All Possible Generators of Supersymmetries of the s Matrix." In: *Nucl. Phys.* B88 (1975). [,257(1974)], p. 257. DOI: 10.1016/0550-3213(75)90279-5.

[149] Lucas Hackl and Robert C. Myers. "Circuit complexity for free fermions." In: (2018). arXiv: 1803.10638 [hep-th].

[150] Sarah Harrison, Shamit Kachru, and Gonzalo Torroba. "A maximally supersymmetric Kondo model." In: *Class. Quant. Grav.* 29 (2012), p. 194005. DOI: 10.1088/0264-9381/29/19/194005. arXiv: 1110.5325 [hep-th].

[151] Thomas Hartman. "Entanglement Entropy at Large Central Charge." In: (2013). arXiv: 1303.6955 [hep-th].

[152] Thomas Hartman and Juan Maldacena. "Time Evolution of Entanglement Entropy from Black Hole Interiors." In: *JHEP* 05 (2013), p. 014. DOI: 10.1007/JHEP05(2013)014. arXiv: 1303.1080 [hep-th].

[153] S. W. Hawking. "Particle Creation by Black Holes." In: *Commun. Math. Phys.* 43 (1975). [,167(1975)], pp. 199–220. DOI: 10.1007/BF02345020,10.1007/BF01608497.

[154] Stephen Hawking, John Preskill, and Kip Thorne. *Wager on the black hole information paradox.* http://www.theory.caltech.edu/~preskill/info_bet.html.

[155] Patrick Hayden and John Preskill. "Black holes as mirrors: Quantum information in random subsystems." In: *JHEP* 09 (2007), p. 120. DOI: 10.1088/1126-6708/2007/09/120. arXiv: 0708.4025 [hep-th].

[156] Gerard 't Hooft. "Dimensional reduction in quantum gravity." In: *Conf. Proc.* C930308 (1993), pp. 284–296. arXiv: gr-qc/9310026 [gr-qc].

[157] Gerard 't Hooft. "The Holographic principle: Opening lecture." In: *Subnucl. Ser.* 37 (2001), pp. 72–100. DOI: 10.1142/9789812811585_0005. arXiv: hep-th/0003004 [hep-th].

[158] K. Hori, S. Katz, A. Klemm, R. Pandharipande, R. Thomas, C. Vafa, R. Vakil, and E. Zaslow. *Mirror symmetry.* Vol. 1. Clay mathematics monographs. Providence, USA: AMS, 2003. URL: http://www.claymath.org/library/monographs/cmim01.pdf.

[159] Kentaro Hori and Mauricio Romo. "Exact Results In Two-Dimensional (2,2) Supersymmetric Gauge Theories With Boundary." In: (2013). arXiv: 1308.2438 [hep-th].

[160] Veronika E. Hubeny, Mukund Rangamani, and Tadashi Takayanagi. "A Covariant holographic entanglement entropy proposal." In: *JHEP* 07 (2007), p. 062. DOI: 10.1088/1126-6708/2007/07/062. arXiv: 0705.0016 [hep-th].

[161] Veronika E. Hubeny, Henry Maxfield, Mukund Rangamani, and Erik Tonni. "Holographic entanglement plateaux." In: *JHEP* 08 (2013), p. 092. DOI: 10.1007/JHEP08(2013)092. arXiv: 1306.4004 [hep-th].

[162] Nobuyuki Ishibashi. "The Boundary and Crosscap States in Conformal Field Theories." In: *Mod. Phys. Lett.* A4 (1989), p. 251. DOI: 10.1142/S0217732389000320.

[163] Robert A. Jefferson and Robert C. Myers. "Circuit complexity in quantum field theory." In: (2017). arXiv: 1707.08570 [hep-th].

[164] Kristan Jensen and Andreas Karch. "Holographic Dual of an Einstein-Podolsky-Rosen Pair has a Wormhole." In: *Phys. Rev. Lett.* 111.21 (2013), p. 211602. DOI: 10.1103/PhysRevLett.111.211602. arXiv: 1307.1132 [hep-th].

[165] Kristan Jensen and Julian Sonner. "Wormholes and entanglement in holography." In: *Int. J. Mod. Phys.* D23.12 (2014), p. 1442003. DOI: 10.1142/S0218271814420036. arXiv: 1405.4817 [hep-th].

[166] Clifford V. Johnson. *D-branes*. Cambridge Monographs on Mathematical Physics. Cambridge University Press, 2005. ISBN: 9780511057694, 9780521030052, 9780521809122, 9780511606540. DOI: 10.1017/CBO9780511606540. URL: http://books.cambridge.org/0521809126.htm.

[167] Andreas Karch and Lisa Randall. "Open and closed string interpretation of SUSY CFT's on branes with boundaries." In: *JHEP* 06 (2001), p. 063. DOI: 10.1088/1126-6708/2001/06/063. arXiv: hep-th/0105132 [hep-th].

[168] Andreas Karch, James Sully, Christoph F. Uhlemann, and Devin G. E. Walker. "Boundary Kinematic Space." In: *JHEP* 08 (2017), p. 039. DOI: 10.1007/JHEP08(2017)039. arXiv: 1703.02990 [hep-th].

[169] Keun-Young Kim, Chao Niu, Run-Qiu Yang, and Cheng-Yong Zhang. "Check proposals of complexity by time dependent thermofield double states." In: (2017). arXiv: 1710.00600 [hep-th].

[170] Alexei Kolezhuk, Subir Sachdev, Rudro R. Biswas, and Peiqiu Chen. "Theory of quantum impurities in spin liquids." In: *Physical Review B* 74.16, 165114 (2006), p. 165114. DOI: 10.1103/PhysRevB.74.165114. arXiv: cond-mat/0606385 [cond-mat.str-el].

[171] Jun Kondo. "Resistance Minimum in Dilute Magnetic Alloys." In: *Progress of Theoretical Physics* 32.1 (July 1964), pp. 37–49. ISSN: 0033-068X. DOI: 10.1143/PTP.32.37. eprint: http://oup.prod.sis.lan/ptp/article-pdf/32/1/37/5193092/32-1-37.pdf. URL: https://doi.org/10.1143/PTP.32.37.

[172] Jun Kondo. "Sticking to My Bush." In: *Journal of the Physical Society of Japan* 74.1 (2005), pp. 1–3. DOI: 10.1143/JPSJ.74.1. eprint: https://doi.org/10.1143/JPSJ.74.1. URL: https://doi.org/10.1143/JPSJ.74.1.

[173] Marton Kormos, Ingo Runkel, and Gerard M. T. Watts. "Defect flows in minimal models." In: *JHEP* 11 (2009), p. 057. DOI: 10.1088/1126-6708/2009/11/057. arXiv: 0907.1497 [hep-th].

[174] Leo Kouwenhoven and Leonid Glazman. "Revival of the Kondo effect." In: *arXiv e-prints*, cond-mat/0104100 (2001), cond–mat/0104100. arXiv: cond-mat/0104100 [cond-mat.mes-hall].

[175] P. Kovtun, Dan T. Son, and Andrei O. Starinets. "Viscosity in strongly interacting quantum field theories from black hole physics." In: *Phys. Rev. Lett.* 94 (2005), p. 111601. DOI: 10.1103/PhysRevLett.94.111601. arXiv: hep-th/0405231 [hep-th].

[176] Aitor Lewkowycz and Juan Maldacena. "Generalized gravitational entropy." In: *JHEP* 08 (2013), p. 090. DOI: 10.1007/JHEP08(2013)090. arXiv: 1304.4926 [hep-th].

[177] David A. Lowe and Larus Thorlacius. "AdS / CFT and the information paradox." In: *Phys. Rev.* D60 (1999), p. 104012. DOI: 10.1103/PhysRevD.60.104012. arXiv: hep-th/9903237 [hep-th].

[178] Matthew Luzum and Paul Romatschke. "Conformal Relativistic Viscous Hydrodynamics: Applications to RHIC results at s(NN)**(1/2) = 200-GeV." In: *Phys. Rev.* C78 (2008). [Erratum: Phys. Rev.C79,039903(2009)], p. 034915. DOI: 10.1103/PhysRevC.78.034915,10.1103/PhysRevC.79.039903. arXiv: 0804.4015 [nucl-th].

[179] Juan Martin Maldacena. "The Large N limit of superconformal field theories and supergravity." In: *Int. J. Theor. Phys.* 38 (1999). [Adv. Theor. Math. Phys.2,231(1998)], pp. 1113–1133. DOI: 10.1023/A:1026654312961,10.4310/ATMP.1998.v2.n2.a1. arXiv: hep-th/9711200 [hep-th].

[180] Juan Martin Maldacena and Andrew Strominger. "AdS(3) black holes and a stringy exclusion principle." In: *JHEP* 12 (1998), p. 005. DOI: 10.1088/1126-6708/1998/12/005. arXiv: hep-th/9804085 [hep-th].

[181] Juan Maldacena and Leonard Susskind. "Cool horizons for entangled black holes." In: *Fortsch. Phys.* 61 (2013), pp. 781–811. DOI: 10.1002/prop.201300020. arXiv: 1306.0533 [hep-th].

[182] Donald Marolf. "Chern-Simons terms and the three notions of charge." In: *Quantization, gauge theory, and strings. Proceedings, International Conference dedicated to the memory of Professor Efim Fradkin, Moscow, Russia, June 5-10, 2000. Vol. 1+2.* 2000, pp. 312–320. arXiv: hep-th/0006117 [hep-th].

[183] Donald Marolf. "The Black Hole information problem: past, present, and future." In: *Rept. Prog. Phys.* 80.9 (2017), p. 092001. DOI: 10.1088/1361-6633/aa77cc. arXiv: 1703.02143 [gr-qc].

[184] Marco Meineri, Joao Penedones, and Antonin Rousset. "Colliders and conformal interfaces." In: (2019). arXiv: 1904.10974 [hep-th].

[185] Charles Melby-Thompson and Cornelius Schmidt-Colinet. "Double Trace Interfaces." In: *JHEP* 11 (2017), p. 110. DOI: 10.1007/JHEP11(2017)110. arXiv: 1707.03418 [hep-th].

[186] Max A. Metlitski and Subir Sachdev. "Valence bond solid order near impurities in two-dimensional quantum antiferromagnets." In: *Physical Review B* 77.5, 054411 (2008), p. 054411. DOI: 10.1103/PhysRevB.77.054411. arXiv: 0710.0626 [cond-mat.str-el].

[187] Masamichi Miyaji, Tadashi Takayanagi, and Kento Watanabe. "From path integrals to tensor networks for the AdS/CFT correspondence." In: *Phys. Rev.* D95.6 (2017), p. 066004. DOI: 10.1103/PhysRevD.95.066004. arXiv: 1609.04645 [hep-th].

[188] Masamichi Miyaji, Tokiro Numasawa, Noburo Shiba, Tadashi Takayanagi, and Kento Watanabe. "Distance between Quantum States and Gauge-Gravity Duality." In: *Phys. Rev. Lett.* 115.26 (2015), p. 261602. DOI: 10.1103/PhysRevLett.115.261602. arXiv: 1507.07555 [hep-th].

[189] Gregory W. Moore and Nathan Seiberg. "Polynomial Equations for Rational Conformal Field Theories." In: *Phys. Lett.* B212 (1988), pp. 451–460. DOI: 10.1016/0370-2693(88)91796-0.

[190] Robert C. Myers. "Dielectric branes." In: *JHEP* 12 (1999), p. 022. DOI: 10.1088/1126-6708/1999/12/022. arXiv: hep-th/9910053 [hep-th].

[191] M. Nakahara. *Geometry, topology and physics*. 2003.

[192] M. A. Nielsen. "A geometric approach to quantum circuit lower bounds." In: *Quantum Information and Computation* 6 (3 2006), pp. 213–262. eprint: quant-ph/0502070.

[193] P Nozières. "A "Fermi Liquid" description of the Kondo problem at low tempertures." In: *Journal of Low Temperature Physics* 17 (Oct. 1974), pp. 31–42. DOI: 10.1007/BF00654541.

[194] Andy O'Bannon, Ioannis Papadimitriou, and Jonas Probst. "A Holographic Two-Impurity Kondo Model." In: *JHEP* 01 (2016), p. 103. DOI: 10.1007/JHEP01(2016)103. arXiv: 1510.08123 [hep-th].

[195] Tetsuya Onogi and Nobuyuki Ishibashi. "Conformal Field Theories on Surfaces With Boundaries and Crosscaps." In: *Mod. Phys. Lett.* A4 (1989). [Erratum: Mod. Phys. Lett.A4,885(1989)], p. 161. DOI: 10.1142/S0217732389000228.

[196] C. M. Papadimitriou. *Computational complexity*. Reading, Massachusetts: Addison-Wesley, 1994.

[197] Kyriakos Papadodimas and Suvrat Raju. "Black Hole Interior in the Holographic Correspondence and the Information Paradox." In: *Phys. Rev. Lett.* 112.5 (2014), p. 051301. DOI: 10.1103/PhysRevLett.112.051301. arXiv: 1310.6334 [hep-th].

[198] V. B. Petkova and J. B. Zuber. "Generalized twisted partition functions." In: *Phys. Lett.* B504 (2001), pp. 157–164. DOI: 10.1016/S0370-2693(01)00276-3. arXiv: hep-th/0011021 [hep-th].

[199] J. Polchinski. *String theory. Vol. 2: Superstring theory and beyond*. Cambridge Monographs on Mathematical Physics. Cambridge University Press, 2007. ISBN: 9780511252280, 9780521633048, 9780521672283. DOI: 10.1017/CBO9780511618123.

[200] Joseph Polchinski. "Dirichlet Branes and Ramond-Ramond charges." In: *Phys. Rev. Lett.* 75 (1995), pp. 4724–4727. DOI: 10.1103/PhysRevLett.75.4724. arXiv: hep-th/9510017 [hep-th].

[201] Joseph Polchinski. "The Black Hole Information Problem." In: *Proceedings, Theoretical Advanced Study Institute in Elementary Particle Physics: New Frontiers in Fields and Strings (TASI 2015): Boulder, CO, USA, June 1-26, 2015*. 2017, pp. 353–397. DOI: 10.1142/9789813149441_0006. arXiv: 1609.04036 [hep-th].

[202] Stephen Powell and Subir Sachdev. "Excited-state spectra at the superfluid-insulator transition out of paired condensates." In: *Physical Review A* 75.3, 031601 (2007), p. 031601. DOI: 10.1103/PhysRevA.75.031601. arXiv: cond-mat/0608611 [cond-mat.str-el].

[203] Stephen Powell and Subir Sachdev. "Spin dynamics across the superfluid-insulator transition of spinful bosons." In: *Physical Review A* 76.3, 033612 (2007), p. 033612. DOI: 10.1103/PhysRevA.76.033612. arXiv: cond-mat/0703011 [cond-mat.str-el].

[204] John Preskill. *On Hawking's concession*. http://www.theory.caltech.edu/~preskill/jp_24jul04.html.

[205] Thomas Quella, Ingo Runkel, and Gerard M. T. Watts. "Reflection and transmission for conformal defects." In: *JHEP* 04 (2007), p. 095. DOI: 10.1088/1126-6708/2007/04/095. arXiv: hep-th/0611296 [hep-th].

[206] Mukund Rangamani and Tadashi Takayanagi. "Holographic Entanglement Entropy." In: *Lect. Notes Phys.* 931 (2017), pp.–. DOI: 10.1007/978-3-319-52573-0. arXiv: 1609.01287 [hep-th].

[207] Andreas Recknagel and Volker Schomerus. *Boundary Conformal Field Theory and the Worldsheet Approach to D-Branes*. Cambridge Monographs on Mathematical Physics. Cambridge University Press, 2013. ISBN: 9780521832236, 9780521832236, 9781107496125. DOI: 10.1017/CBO9780511806476. URL: http://www.cambridge.org/9780521832236.

[208] Cosimo Restuccia. "Limit theories and continuous orbifolds." PhD thesis. Humboldt U., Berlin (main), 2013. arXiv: 1310.6857 [hep-th].

[209] Sylvain Ribault. "On 2d CFTs that interpolate between minimal models." In: *SciPost Phys.* 6 (2019), p. 075. DOI: 10.21468/SciPostPhys.6.6.075. arXiv: 1809.03722 [hep-th].

[210] Sylvain Ribault and Raoul Santachiara. "Liouville theory with a central charge less than one." In: *JHEP* 08 (2015), p. 109. DOI: 10.1007/JHEP08(2015)109. arXiv: 1503.02067 [hep-th].

[211] Pratim Roy and Tapobrata Sarkar. "On subregion holographic complexity and renormalization group flows." In: (2017). arXiv: 1708.05313 [hep-th].

[212] S. Ryu and T. Takayanagi. "Holographic Derivation of Entanglement Entropy from the anti de Sitter Space/Conformal Field Theory Correspondence." In: *Physical Review Letters* 96.18, 181602 (May 2006), p. 181602. DOI: 10.1103/PhysRevLett.96.181602. eprint: hep-th/0603001.

[213] Shinsei Ryu and Tadashi Takayanagi. "Holographic derivation of entanglement entropy from AdS/CFT." In: *Phys. Rev. Lett.* 96 (2006), p. 181602. DOI: 10.1103/PhysRevLett.96.181602. arXiv: hep-th/0603001 [hep-th].

[214] Subir Sachdev, Chiranjeeb Buragohain, and Matthias Vojta. "Quantum Impurity in a Nearly Critical Two Dimensional Antiferromagnet." In: *arXiv e-prints*, cond-mat/0004156 (2000), cond–mat/0004156. arXiv: cond-mat/0004156 [cond-mat.str-el].

[215] Luis A. Santaló. *Integral Geometry and Geometric Probability*. Massachusetts: Addison-Wesley Publishing Company, 1976.

[216] Gordon W. Semenoff. "Lectures on the holographic duality of gauge fields and strings." In: *Les Houches Summer School: Integrability: From Statistical Systems to Gauge Theory Les Houches, France, June 6-July 1, 2016*. 2018. arXiv: 1808.04074 [hep-th].

[217] Assaf Shomer. "A Pedagogical explanation for the non-renormalizability of gravity." In: (2007). arXiv: 0709.3555 [hep-th].

[218] Miguel A. Sierra, Rosa López, and Jong Soo Lim. "Thermally Driven Out-of-Equilibrium Two-Impurity Kondo System." In: *Phys. Rev. Lett.* 121 (9 2018), p. 096801. DOI: 10.1103/PhysRevLett.121.096801. URL: https://link.aps.org/doi/10.1103/PhysRevLett.121.096801.

[219] Miguel A. Sierra and David Sánchez. "Heat current through an artificial Kondo impurity beyond linear response." In: *Journal of Physics: Conference Series* 969 (2018), p. 012144. DOI: 10.1088/1742-6596/969/1/012144. URL: https://doi.org/10.1088%2F1742-6596%2F969%2F1%2F012144.

[220] Dam T. Son and Andrei O. Starinets. "Viscosity, Black Holes, and Quantum Field Theory." In: *Ann. Rev. Nucl. Part. Sci.* 57 (2007), pp. 95–118. DOI: 10.1146/annurev.nucl.57.090506.123120. arXiv: 0704.0240 [hep-th].

[221] Andrew Strominger and Cumrun Vafa. "Microscopic origin of the Bekenstein-Hawking entropy." In: *Phys. Lett.* B379 (1996), pp. 99–104. DOI: 10.1016/0370-2693(96)00345-0. arXiv: hep-th/9601029 [hep-th].

[222] Leonard Susskind. "The World as a hologram." In: *J. Math. Phys.* 36 (1995), pp. 6377–6396. DOI: 10.1063/1.531249. arXiv: hep-th/9409089 [hep-th].

[223] Leonard Susskind. "Computational Complexity and Black Hole Horizons." In: *Fortsch. Phys.* 64 (2016), pp. 24–43. DOI: 10.1002/prop.201500092. arXiv: 1403.5695 [hep-th].

[224] Leonard Susskind. "Entanglement is not enough." In: *Fortsch. Phys.* 64 (2016), pp. 49–71. DOI: 10.1002/prop.201500095. arXiv: 1411.0690 [hep-th].

[225] David Tong. "TASI lectures on solitons: Instantons, monopoles, vortices and kinks." In: *Theoretical Advanced Study Institute in Elementary Particle Physics: Many Dimensions of String Theory (TASI 2005) Boulder, Colorado, June 5-July 1, 2005*. 2005. arXiv: hep-th/0509216 [hep-th].

[226] David Tong. "The holographic dual of $AdS_3 \times S^3 \times S^3 \times S^1$." In: *JHEP* 04 (2014), p. 193. DOI: 10.1007/JHEP04(2014)193. arXiv: 1402.5135 [hep-th].

[227] David Tong and Kenny Wong. "Instantons, Wilson lines, and D-branes." In: *Phys. Rev.* D91.2 (2015), p. 026007. DOI: 10.1103/PhysRevD.91.026007. arXiv: 1410.8523 [hep-th].

[228] Mark Van Raamsdonk. "Building up spacetime with quantum entanglement." In: *Gen. Rel. Grav.* 42 (2010). [Int. J. Mod. Phys.D19,2429(2010)], pp. 2323–2329. DOI: 10.1007/s10714-010-1034-0,10.1142/S0218271810018529. arXiv: 1005.3035 [hep-th].

[229] Mark Van Raamsdonk. "Lectures on Gravity and Entanglement." In: *Proceedings, Theoretical Advanced Study Institute in Elementary Particle Physics: New Frontiers in Fields and Strings (TASI 2015): Boulder, CO, USA, June 1-26, 2015*. 2017, pp. 297–351. DOI: 10.1142/9789813149441_0005. arXiv: 1609.00026 [hep-th].

[230] J. Wess and J. Bagger. *Supersymmetry and supergravity*. Princeton, NJ, USA: Princeton University Press, 1992. ISBN: 9780691025308.

[231] Kenneth G. Wilson. "The Renormalization Group: Critical Phenomena and the Kondo Problem." In: *Rev. Mod. Phys.* 47 (1975), p. 773. DOI: 10.1103/RevModPhys.47.773.

[232] Edward Witten. "Nonabelian Bosonization in Two-Dimensions." In: *Commun. Math. Phys.* 92 (1984). [,201(1983)], pp. 455–472. DOI: 10.1007/BF01215276.

[233] Ying-Hai Wu and Hong-Hao Tu. "Quantum impurity models from conformal field theory." In: (2019). arXiv: 1906.03464 [hep-th].

[234] Bei Zeng, Xie Chen, Duanlu Zhou, and Xiao-Gang Wen. "Quantum Information Meets Quantum Matter – From Quantum Entanglement to Topological Phase in Many-Body Systems." In: (Aug. 2015).

[235] Jian-dong Zhang and Bin Chen. "Kinematic Space and Wormholes." In: *JHEP* 01 (2017), p. 092. DOI: 10.1007/JHEP01(2017)092. arXiv: 1610.07134 [hep-th].

ACKNOWLEDGEMENTS

First and foremost I thank my supervisor *Johanna Erdmenger* for giving me the opportunity to embark on three years within the marvel that is holography. In only three years Johanna has crafted an intriguing and ever-changing working environment[2], in which I could explore and test my interests. Moreover, she has demonstrated extraordinary patience in teaching me how to present new ideas or finished work, and I can only hope to keep refining these treats with her council in mind.

I am grateful to René Meyer, who is a defining character of the group and has given me the opportunity to learn and teach string theory at his side. He is always up for a good time and is on the look-out for the members of the group. I rarely know when to stop working and I remember a stressed afternoon, where René came into my office and convinced me to take the break that I desperately needed. In a small group we went to Burger & Bier, where I had a relaxing time and one of the best burgers in Wuerzburg.

I thank my office mates Marius Gerbershagen and Ignacio Reyes for a pleasant and cheerful working environment, who were always up for an enlightning conversation, satirycal comment or a good laugh! I will certainly miss office M1.2.019. Next up are the guys next door, Raimond Abt and Yiqiang Du, whom I thank for carefully dissecting parts of Nakahara's book with me and for the many cheerful and insightful conversations on the corridor. Of course, there are the guys from the upper floor, Pascal Fries, Ioannis Matthaiakakis, David Rodriguez, whose contageous fascination for physics motivated me to keep going in hard times. I owe special gratitude to Nina Miekley, who patiently smoothed away my difficulties with almost any digital device in my way. Moreover, she always had time to discuss some physics or other geeky stuff and share a good time.

I thank Nelly Meyer, for taking care of all the administrative stuff that would have driven me crazy and for all the cheerful conversations.

My time in TP3 had not been as rewarding had it not also been for the presence of all its remaining members, whom I thank: Haye Hinrichsen, Manuel Schrauth, Max Weber, Theresa Christ, Oliver Niggemann, Max Wagner, Kevin Grosvenor, Arash Jakfar and the many others that I didn't mean to forget.

I am indebted to Fernando Dominguez and Christian Simon for carefully reading parts of the draft.

2 This is more impressive given that there was no prior string theory group present in Wuerzburg before her's.

Last but not least I thank Charles Melby-Thompson, who has guided me into the realm of interfaces, branes and supersymmetric gauge theory. To whatever question I could muster, he always had an answer, and, more often than not, with a tweak he transformed my troubles into strikingly simple problems. His calm and witty council has transformed my approach to physics and will accompany me down the road. Moreover, his kind and cheerful personality made hanging around with him exceptionally pleasant and I am proud to have found a new friend in him.